VNIVERSITAT DE VALÈNCIA

Facultat de Medicina i Odontologia
Departamento de Farmacología

Programa de Doctorado en Biomedicina y Farmacia

EFFECT OF RXR/PPAR INTERACTION IN ANGIOTENSIN II-INDUCED VASCULAR INFLAMMATION AND ANGIOGENESIS.

ROLE OF CXCL16/CXCR6 AXIS IN ANGIOTENSIN II OR CIGARETTE SMOKE-INDUCED VASCULAR INFLAMMATION.

TESIS DOCTORAL

PRESENTADA POR:

PAULA ESCUDERO DÍAZ

DIRECTORES:

María Jesús Sanz Ferrando
Laura Piqueras ruiz

VALENCIA, Mayo 2016

VNIVERSITAT DE VALÈNCIA Facultat de Medicina i Odontologia

Dña. María Jesús Sanz Ferrando, Catedrática del Departamento de Farmacología de la Universidad de Valencia y **Laura Piqueras Ruiz**, Investigadora adscrita al Instituto de Investigación Sanitaria Incliva

HACEN CONSTAR:

Que el trabajo, titulado "Effect of RXR/PPAR interaction in angiotensin II-induced vascular inflammation and angiogenesis. Role of CXCL16/CXCR6 axis in angiotensin II or cigarette smoke-induced vascular inflammation", presentado por la Lda. **Paula Escudero Díaz** para obtener el grado de doctor, ha sido realizado en el Departamento de Farmacología de la Facultad de Medicina y Odontología de la Universidad de Valencia, bajo nuestra dirección.

Concluido el trabajo experimental y bibliográfico, autorizamos la presentación y la defensa de esta Tesis Doctoral.

Valencia, 6 de mayo de 2016

Fdo. Dra. María Jesús Sanz Ferrando

Fdo. Laura Piqueras Ruiz

La presente Tesis Doctoral ha sido financiada por las siguientes becas y proyectos:

- Beca del Programa Vali+d concedida por la Conselleria de Educación de la Generalitat Valenciana. ACIF/2011/109. Junio 2011-Enero 2012
- Beca del Programa de Formación del Profesorado Universitario (FPU) concedida por el Ministerio de Educación. AP2010-1987. Enero 2012-Junio 2015.
- Ayudas del Programa de Formación del Profesorado Universitario (FPU). Convocatoria 2013. Estancias Breves. EST13/00613. Julio 2014-Octubre 2014.
- "Estudio de los mecanismos celulares y moleculares implicados en la inflamación vascular causada por ciertos factores de riesgo de aterosclerosis. Búsqueda de nuevas dianas terapéuticas". IP: María Jesús Sanz Ferrando. SAF2008-03477. Entidad financiadora: Ministerio de Ciencia e Innovación. 2008-2011.
- "Estudio de nuevas dianas farmacológicas para el tratamiento de la enfermedad pulmonar obstructiva crónica en paradigmas experimentales de células humanas aisladas y modelos animales in vivo". IP: Esteban J Morcillo Sánchez. PROMETEO/2008/045. Entidad financiadora: Conselleria de Educación. Generalitat Valenciana. 2008-2012.
- "Red de Inflamación y enfermedades reumáticas". IP: María Jesús Sanz Ferrando. RD08/0075/0016. Entidad financiadora: Instituto de Salud Carlos III. Ministerio de Sanidad. 2009-2013.
- "Estudio de los mecanismos moleculares y celulares en la disfunción endotelial asociada a enfermedades con inflamación sistémica que podrían inducir desórdenes cardiovasculares". IP: María Jesús Sanz Ferrando. SAF2011-23777. Entidad financiadora: Ministerio de Economía y Competitividad. 2011-2015.
- "Estudio de los mecanismos moleculares y celulares en la disfunción endotelial asociada a enfermedades con inflamación sistémica que podrían inducir desórdenes cardiovasculares". IP: María Jesús Sanz Ferrando. GVACOMP2013-015. Entidad financiadora: Conselleria de Educación, Dirección General de Política Científica. Generalitat Valenciana. 2013-2013.
- "Estudio de nuevos marcadores inflamatorios en la disfunción endotelial: Papel modulador de ligandos de PPAR y RXR". IP: Laura Piqueras Ruiz. PI12/01271. Entidad financiadora: Instituto de Salud Carlos III/ FIS/ cofinanciado Fondos FEDER. 2013-2015.

- “Nuevas dianas farmacológicas para el tratamiento de la EPOC y sus comorbilidades vasculares”. IP: Esteban J Morcillo Sánchez. PROMETEO II/2013/ 014. Entidad financiadora: Conselleria de Educación. Generalitat Valenciana. 2013-2016.
- “Estudio de los mecanismos moleculares y celulares en la disfunción endotelial asociada a enfermedades con inflamación sistémica que podrían inducir desórdenes cardiovasculares”. IP: María Jesús Sanz Ferrando. GVACOMP2014-006. Entidad financiadora: Conselleria de Educación, Dirección General de Política Científica. Generalitat Valenciana. 2014-2014.
- “Modulación Inmunofarmacológica de la Inflamación Sistémica asociada a Desordenes Metabólicos. Búsqueda de nuevas dianas terapéuticas y síntesis de fármacos novedosos”. IP: Jesús Sanz Ferrando y Juan Ascaso Gimilio. SAF2014-57845-R. Entidad financiadora: Ministerio de Economía y Competitividad. 2015-2018.
- “Estudio de nuevos mecanismos inflamatorios y angiogénicos asociados a la obesidad grave mórbida; Papel del eje CXCR3 y los receptores nucleares ROR”. IP: Laura Piqueras Ruiz. PI15/00082. Entidad financiadora: Instituto de Salud Carlos III/ FIS/ cofinanciado Fondos FEDER. 2016-2018.
- “A multidisciplinary project to advance in basic mechanisms, diagnosis, prediction, and prevention of cardiac damage in reperfused acute myocardial infarction”. IP: Vicente Bodi Investigador principal de grupo: Dra Laura Piqueras, INCLIVA. PIE15/00013. Entidad financiadora: Instituto de Salud Carlos III/ FIS/ cofinanciado Fondos FEDER. 2016-2018.

AGRADECIMIENTOS

Deseo expresar mi agradecimiento a todas aquellas personas que han hecho posible la realización de esta tesis doctoral:

A mis directoras de tesis, María Jesús y Laura, por acogerme en su grupo de investigación, confiar en mí para la realización de este trabajo y enseñarme el camino.

Al profesor Andreas Ludwig y su equipo por acogerme en su laboratorio, hacerme sentir parte del equipo y el inmenso apoyo que siempre me brindan.

Al personal de los servicios de Citometría y Animalario; Guadalupe, Ana, Eva e Inma, sin vuestra ayuda partes de esta tesis no habrían sido posibles o al menos habrían sido infinitamente más difíciles, gracias por estar dispuestas a ayudar y siempre con una sonrisa.

A mis compañeros del laboratorio, a los que estáis y a los que ya no, con los que he aprendido y compartido mucho.

Al personal técnico y clínico que ha hecho posible la recogida de muestras para la realización de esta tesis doctoral.

A mis padres y familia por su amor, ilusión incondicional y su apoyo en todas mis decisiones.

A Joaquín, porque incluso cuando no es fácil, lo haces posible. Esta tesis y todo.

GRACIAS.

RESUMEN

Aumentos en los niveles circulantes de mediadores, incluyendo angiotensina II (Ang-II) y citoquinas, han sido detectados en enfermedades cardiovasculares y cardiometabólicas como la hipertensión, la obesidad y la diabetes, y parecen ejercer efectos negativos sobre la función endotelial (Granger *et al.*, 2004; Marinou *et al.*, 2010). Estos agentes inician una cascada inflamatoria de señalización que promueve la generación de especies reactivas del oxígeno, aumento en la superficie celular de la expresión de moléculas de adhesión y mayor adhesividad de leucocitos a las células endoteliales (Libby, 2002; Granger *et al.*, 2004). Estas respuestas están asociadas con la disfunción endotelial, un estado pro-trombótico y pro-inflamatoria del endotelio (Landmesser *et al.*, 2004) que juega un papel importante a las primeras etapas de la aterogénesis (Libby, 2002; Landmesser *et al.*, 2004; Galkina *et al.*, 2009).

Rosuvastatina (Rosu) y Bexaroteno (Bex) son fármacos comúnmente prescritos para tratar la hipercolesterolemia y el linfoma de células T, respectivamente, que además han demostrado inhibir la inflamación vascular (Mira *et al.*, 2009; Farol *et al.*, 2004; Sanz *et al.*, 2012) y que, a pesar de su actividad antiinflamatoria, producen graves efectos adversos relacionados con dosis. Aunque generalmente bien toleradas, las estatinas se asocian con miopatías y fallo renal agudo (Golomb *et al.*, 2008; Hoffman *et al.*, 2012; Dormuth *et al.*, 2013). Así mismo, el tratamiento con Bex se asocia con efectos secundarios inevitables y que limitan la dosis administrada, en particular, hipertrigliceridemia, hipercolesterolemia y en menor medida hipotiroidismo (de Vries-van der Weij *et al.*, 2009; Vakeva *et al.*, 2012). Sin embargo, la administración de Rosu reduce los niveles de triglicéridos (Florentin *et al.*, 2013), por ello en las guías clínicas sobre la prescripción segura de Bex se recomienda el uso conjunto con estatinas con el fin de prevenir los efectos dislipémicos (Scarisbrick *et al.*, 2013). Por consiguiente, debido a la necesidad de estrategias más eficaces y seguras para prevenir y tratar la aterosclerosis, en la presente tesis evaluamos el efecto de la coadministración de Rosu y Bex en la inflamación vascular causada por Ang-II.

Para ello, células endoteliales de arteria de cordón umbilical humano (HUAEC) fueron tratadas con vehículo, Rosu (10-30 nM), Bexa (0,3-1 μM) o una combinación de ambos, 20 h antes de la estimulación con Ang-II 1 μM durante 4h. Sorprendentemente, la combinación de Rosu (10 nM) + Bex (0,3 μM), que no ejercieron efecto sobre el reclutamiento de células mononucleares inducido por Ang-II cuando ambos fármacos

fueron estudiados por separado, significativamente redujo esta respuesta. Este efecto fue acompañado por una disminución de la expresión en el endotelio de ICAM-1, VCAM-1 y CX_3CL1 así como de la producción de CXCL1, CXCL8, CCL2 y CCL5 inducida por Ang II. La preincubación de HUAECs con Rosu y Bex inhibió la expresión Nox5 y la consecuente activación de RhoA inducida por Ang-II a través de una mayor expresión RXRα, PPARα y PPARγ, además del aumento de las interacciones RXRα/PPARα y RXRα/PPARγ.

In vivo, la combinación, pero no la administración por separado, de Rosu (1,25 mg/kg/día) y Bex (10 mg/kg/día), disminuyó significativamente la adhesión de leucocitos a la microcirculación cremastérica arteriolar causada por Ang-II en ratones C57BL/6 y la formación de la lesión aterosclerótica en ratones deficientes en la apolipoproteína E ($apoE^{-/-}$) sometidos a una dieta aterogénica.

Por todo lo anteriormente expuesto podemos concluir que la administración conjunta de Rosu y Bex a dosis subóptimas podría constituir una nueva y eficaz alternativa de tratamiento en el control de la inflamación vascular asociada a desordenes cardiometabólicos debido a que la sinergia en su actividad antiinflamatoria podría contrarrestar sus reacciones adversas.

El aneurisma aórtico abdominal (AAA) es una importante causa de muerte en los países desarrollados. A pesar de ello, existe un gran desconocimiento de los mecanismos responsables de la iniciación, propagación y ruptura del AAA. Los estudios realizados demuestran que el sistema renina angiotensina y la angiogénesis juegan un papel fundamental en el desarrollo de esta patología. De hecho, la formación de nuevos microvasos está relacionada con el riesgo de ruptura y las complicaciones que causan la alta tasa de mortalidad asociada a este estado patológico.

El Bex es un fármaco agonista del Receptor del Retinoide X (RXR) con actividad antiangiogénica. Dicho receptor forma heterodímeros permisivos con los Receptores Activadores de la Proliferación Peroxisomal (PPAR). A su vez, las estatinas son capaces de activar los receptores PPAR.

Dado que nuevos estudios indican que un solo fármaco antiangiogénico puede no ser suficiente para combatir la amplia gama de factores angiogénicos producidos y las vías implicadas en el proceso angiogénico, es importante encontrar nuevos enfoques

farmacológicos para detener su la formación y progresión de la lesión. Por lo tanto, en la presente tesis doctoral se investigó el efecto del tratamiento combinado de Rosu y Bex en el AAA inducido por Ang-II así como el proceso angiogénico y los mecanismos subyacentes implicados.

Para ello, se administraron durante 28 días ambos fármacos, en un modelo animal de AAA en ratones apoE$^{-/-}$ inducido por Ang-II y dieta grasa. El tratamiento combinado de Rosu y Bex a dosis de 10 mg/kg/día redujo significativamente la incidencia de AAA. Además, dicha terapia combinada disminuyó la neovascularización, la infiltración de macrófagos y los niveles de expresión de ARNm de las quimiocinas KC/CXCL1, MCP-1/CCL2, RANTES/CCL5 y el factor de crecimiento vascular, VEGF, disminución que parece estar mediada por la activación de las interacciones RXRα/PPARα y RXRα/PPARγ. Estas respuestas fueron acompañadas de una menor activación de la ruta de señalización AKT/mTOR/p70S6K1. En conjunto, estos resultados sugieren que la combinación a dosis subóptimas de un agonista de RXR y una estatina interfiere sinérgicamente con los mecanismos de señalización que modulan la angiogénesis, así como la inflamación asociada a la misma, pudiendo constituir una nueva herramienta terapéutica para la prevención del desarrollo del AAA.

CXCL16 es una quimiocina transmembrana que, debido a su doble función como sustancia quimioatrayente y molécula de adhesión de monocitos y linfocitos, así como su presencia en la pared vascular, hace que sea un candidato atractivo para jugar un papel fundamental en el proceso inflamatorio vascular. Sin embargo, hasta la fecha su papel en AAA y la inflamación vascular inducida por Ang- II no ha sido caracterizado. Por lo tanto, en la presente tesis doctoral se ha investigado la potencial implicación del eje CXCR6/CXCL16 en la inflamación vascular inducida por Ang-II así como los mecanismos relacionados en este proceso.

Mediante estudios *in vivo,* observamos que el tratamiento con Ang-II durante 15 días produjo un aumento en la expresión de CXCL16 en las arteriolas cremastericas del ratón que se correlacionó con un aumento en la adhesión de los leucocitos al endotelio arteriolar.

A continuación nos planteamos trasladar estas observaciones a un modelo patológico. Por ello, evaluamos el efecto de un antagonista del receptor AT_1 de Ang-II,

losartán, y la posible implicación de CXCL16, en un modelo experimental de AAA. Ratones deficientes en apo E $^{-/-}$ fueron sometidos a una dieta rica en grasa y estimulados durante 28 días con Ang-II (500 ng/kg/min). Algunos animales fueron tratados con losartán a dos dosis: 10 y 30 mg/kg/día. Los animales no tratados pero sí estimulados con Ang-II mostraron mayor incidencia de AAA, incremento de la infiltración de macrófagos, linfocitos $CD3^{+}$, células $CXCR6^{+}$ y neovascularización. Estos efectos fueron acompañados de un incremento en la lesión de la expresión de ARNm de MCP-1/CCL2, CXCL16, CXCR6 y del factor de crecimiento vascular VEGF. Losartán a una dosis de 30 mg/kg/día, logró reducir todos estos eventos.

Mediante estudios *in vitro* se detectó un aumento en la expresión de CXCL16 cuando las HUAECs fueron estimuladas con Ang-II 1 μM, la neutralización de su actividad inhibió significativamente la interacción de leucocitos mononucleares a HUAEC inducida por Ang-II. El aumento de la expresión de CXCL16 inducida por Ang-II fue dependiente de la expresión de Nox5, la generación de radicales libres y la subsiguiente activación de RhoA/p38-MAPK/NFκB.

Estos resultados sugieren que el eje CXCL16/CXCR6 podría constituir una nueva estrategia terapéutica en el tratamiento de enfermedades cardiovasculares asociadas a la activación del sistema renina-angiotensina.

La enfermedad pulmonar obstructiva crónica (EPOC) es una enfermedad inflamatoria crónica del tracto respiratorio muy compleja, que involucra diferentes tipos de células inflamatorias y estructurales, las cuales a su vez tienen la capacidad de liberar múltiples mediadores inflamatorios locales y sistémicos. La enfermedad es una respuesta inflamatoria anormal de los pulmones, principalmente al humo del cigarro (también gases y partículas nocivas) que conduce a una disminución lenta, progresiva e irreversible de la ventilación pulmonar.

Las enfermedades cardiovasculares son unas de las comorbilidades más frecuentemente asociadas a la EPOC, aunque los mecanismos implicados en su desarrollo son aún desconocidos.

En este estudio hemos investigado la posible relación entre el eje CXCR6/CXCL16 y la disfunción endotelial asociada a la EPOC.

La citometría de flujo se utilizó para comparar la expresión de marcadores

activación plaquetaria, expresión de CXCL16/CXCR6 en plaquetas y la expresión de CXCR6 en leucocitos de pacientes de EPOC versus controles sanos. Estos estudios revelaron que los pacientes de EPOC presentan mayor número de plaquetas activadas ($PAC\text{-}1^{+}$) con mayor expresión de P-selectina, CXCL16 y CXCR6 además de un incremento en la adhesión leucocito-plaqueta comparado con los controles. Estos pacientes también presentaron mayor expresión de CXCR6 en leucocitos mononucleares.

Basándonos en estos resultados procedimos a ampliar el estudio trasladando los resultados obtenidos a estudios *in vitro* en células humanas. En primer lugar, en condiciones fisiológicas de flujo, se observó que los leucocitos mononucleares procedentes de pacientes de EPOC presentaban mayor adhesividad al endotelio arterial estimulado con humo de tabaco.

A continuación, se observó que la estimulación con extracto de humo de tabaco (EHT) promueve un aumento en la expresión arterial de CXCL16 tanto a nivel de ARNm y como de proteína en HUAECs.

En condiciones fisiológicas de flujo, CXCL16 medió la adhesión de leucocitos mononucleares al endotelio arteriolar estimulado con EHT, dicho aumento en la adhesión fue significativamente inhibido mediante el bloqueo de la actividad de CXCL16. El aumento de la expresión de CXCL16 inducida por EHT fue dependiente de la expresión de Nox5 y la subsiguiente activación de la vía RhoA/p38-MAPK/NFκB.

Mediante microscopia intravital, el reclutamiento leucocitario en animales expuestos a HT durante 3 días fue evaluado. Nuestros resultados indican que el humo de tabaco produjo inflamación pulmonar y además incrementó las interacciones leucocito-endotelio en el cremaster de ratón, poniendo de manifiesto una mayor inflamación sistémica. Cabe destacar que estas respuestas fueron significativamente reducidas en ratones deficientes en el receptor de CXCL16 (CXCR6).

En este estudio se presentan las primeras evidencia de aumento de expresión de CXCR6 en plaquetas y leucocitos circulantes con pacientes de EPOC, lo que puede constituir un nuevo marcador pronóstico de enfermedades cardiovasculares asociadas a esta patología. Además el bloqueo del eje CXCL16/CXCR6 podría constituir una nueva diana terapéutica en la prevención y tratamiento de las enfermedades cardiovasculares asociadas a la EPOC.

Parte de estos resultados vienen recogidos en las siguientes publicaciones:

- **Escudero P**, Navarro A, Ferrando C, Furió E, González Navarro H, Juez M, Sanz MJ, Piqueras L. Combined treatment with Bexarotene and Rosuvastatin reduces angiotensin-II-induced abdominal aortic aneurysm in apoE-/- mice and angiogenesis. Br J Pharmacol. 172(12):2946-60 (2015).
- **Escudero P**, Martínez de Marañón A, Collado A, González Navarro H, Hermenegildo C, Peiró C, Piqueras L, Sanz, MJ. Combined sub-optimal doses of Rosuvastatin and Bexarotene impairs angiotensin II-induced arterial mononuclear cell adhesion through inhibition of Nox5 signalling pathways and increased RXR/PPARα and RXR/PPARγ interactions. Antioxid Redox Signa. 10;22(11):901-20 (2015).

TABLE OF CONTENTS

LIST OF ABBREVIATIONS

AA – Arachidonic acid

AAA – Abdominal aortic aneurysm

ACE – Angiotensin converting enzyme

ADAM – Disintegrins and metalloproteinases

Akt – V-akt murine thymomaviral oncogene homolog kinase

Ang-II – Angiotensin-II

ApoE – Apolipoprotein E

AT – Angiotensin II receptor

BEX – Bexarotene

BrdU – 5-Bromo-2-DeoxyUridine

BSA – Bovine serum albumin

CAM – Cell adhesion molecule

CO – Carbon monoxide

COPD – Chronic obstructive pulmonary disease

CS – Cigarette smoke

CSE – Cigarette smoke extract

DAB – Diamino benzamide

DAF-2-FM diacetate – 4-amino-5-methylamino-2′,7′-difluorofluorescein diacetate

DAG – Diacylglycerol

DAPI – 4', 6-diamidino-2-phenylindole

DMSO – Dimethyl sulfoxide

Duox – Dual oxidase

D_v – Vessel diameter

EBM-2 – Endothelial cell basal medium-2

EDTA – Ethylenediamine tetraacetic acid

EGFR – Epidermal growth factor receptor

EGM-2 – Endothelial growth medium-2

ELISA – Enzyme-linked immunosorbent assay

eNOS – Endothelial nitric oxide synthase

ERK – Extracellular signal-regulated kinase

FEV1 – Forced expiratory volume in 1 second

FVC – Forced vital capacity

GFR – Growth Factor Reduced

GROα – Growth regulated oncogene-α

HUAEC – Human umbilical artery endothelial cell

HUVEC – Human umbilical vein endothelial cell

ICAM-1 – Intercellular adhesion molecule 1

IL – Interleukin

JAK – Janus kinases

JNK – Jun n-terminal kinase

LC-MS/MS – Liquid chromatography-electrospray ionization–tandem mass spectrometry

LTs – Leukotrienes

MAPK – Mitogen-activated protein kinase

MCP-1– Monocyte chemoattractant protein-1

MFI – Mean of fluorescence intensity

mTOR – Mammalian target of rapamycin

NAD(P)H – Nicotinamide adenine dinucleotide (phosphate)

NF-kB – Nuclear factor-*kB*

NO – Nitric Oxide

Nox – Nicotinamide adenine dinucleotide phosphate oxidase

p70S6k1 – 70 kDa ribosomal protein S6 kinase

PBS – Phosphate-buffered saline

PBS-T – PBS containing 0.1 % Tween 20

PCR – Polymerase chain reaction

PI3K – Phosphatidylinositol-3 kinase

PPAR – Peroxisome proliferator-activated receptor

qPCR – Quantitative polymerase chain reaction

RANTES – Regulated on activation normal T cell expressed and secreted chemokine

RBC – Red blood cells

RLU – Relative light units

ROCK – Rho-associated protein kinase

ROS – Reactive oxygen species

Rosu – Rosuvastatin

RT – Reverse transcription

RT-PCR – Reverse transcription polymerase chain reaction

RXR – Retinoid X receptor

SBP – Systolic blood pressure

SDS – Sodium dodecyl sulfate

SDS-PAGE – SDS-polyacrylamide gel electrophoresis

SEM – Standard error of the mean

siRNA – Small interfering RNA

SR-PSOX – Scavenger receptor for phosphatidylserine and oxidized low-density lipoprotein

TAE – Tris Acetate-EDTA

TC – Total cholesterol

TG – Triglycerides

TNFα – Tumor necrosis factor-α

VCAM-1 – Vascular cell adhesion molecule-1

VEGF – Vascular endothelial growth factor

VLA-4 – Very late antigen-4

Vmean – Mean of red blood cells velocity

VSMC – *V*ascular smooth muscle cells

XO – Xanthine oxidase

LISTA DE ABREVIATURAS

AA – Ácido araquidónico

Ang-I – Angiotensina-I

Ang-II – Angiotensina-II

ApoE – apolipoproteína E

AT – Receptores de angiotensina

COX – Ciclooxigenasa

DAG – Diacilglicerol

ECA – Enzima convertidora de la Angiotensina

EGF – Epidermal growth factor

EGFR – Receptor del factor de crecimiento epidérmico

EHT – Extracto acuoso de Humo de Tabaco

eNOS – Óxido nítrico sintasa endotelial

EPOC – Enfermedad Pulmonar Obstructiva Crónica.

ERO – Especies reactivas de oxigeno

ERO – Especies Reactivas del Oxígeno

ET – Endotelina

FT – Factor tisular

FXR – Receptor Farnesoide X

HUAEC – Células endoteliales de arteria de cordón umbilical humano

HUVEC – Células endoteliales de vena de cordón umbilical humano

ICAM-1 – Molécula de adhesión intercelular 1

IFN-γ – Interferón gamma

IGF – Factor de crecimiento insulinico tipo 1

Igs – Inmunoglobulinas

IL – Interleucina

IP_3 – Inositol trifosfato

JAK – Janus kinases

JNK – Quinasa Jun N -terminal

LFA- 1 – Lymphocyte function-associated antigen-1

LTs – leucotrienos

LXR – Receptor Hepático X

MAC – Moléculas de adhesión celular

MCP-1 – Monocyte chemoattractant/chemotactic protein-1

MMP – Metaloproteinasas

NF-kB – Factor nuclear kappa B

NO – Óxido nítrico

PAF – Factor activador de plaquetas

PDGF – Platelet-derived growth factor

PIP2 – Fosfatidil inositol difosfato

PLA_2 – Fosfolipasa A_2

PLC – Fosfolipasa C

PLD – Fosfolipasa D

PMN – Leucocitos polimorfonucleares

PPAR – Receptores activadores de la proliferación de peroxisomas

PSGL-1 – P-selectin glycoprotein ligand-1

RN – Receptor nuclear

SAPK – Proteína quinasa activada por estrés

SRA – Sistema renina-angiotensina

TGF – Transforming growth factor

TNFα – Factor de necrosis tumoral-α

VCAM-1 – vascular cell adhesion molecule-1

VLA-4 – Very late antigen-4

LIST OF FIGURES

LIST OF TABLES

INTRODUCCIÓN

1 INTRODUCCIÓN

1.1 INFLAMACIÓN Y ENFERMEDADES CARDIOVASCULARES

La inflamación (del latín *inflammatio*: encender, hacer fuego) es una respuesta inespecífica frente a las agresiones del medio, y está generada por los denominados "agentes inflamatorios". La respuesta inflamatoria ocurre en tejidos vascularizados y surge con el fin defensivo de aislar y destruir al agente dañino, así como reparar el tejido u órgano dañado. Se considera por tanto, un mecanismo de inmunidad innata, estereotipado, en contraste con la reacción inmune adaptativa, específica para cada tipo de agente infeccioso.

La respuesta inflamatoria se inicia, normalmente, con un daño tisular causado por el agresor: el organismo reconoce el daño y pone en marcha los mecanismos responsables de la localización y eliminación del agente extraño. Después se activan tanto mediadores solubles como componentes celulares de la inflamación que producen la amplificación de la respuesta inflamatoria. En condiciones normales, el agente agresor es destruido, se inhiben los mediadores inflamatorios, y se regenera el tejido dañado recuperando sus funciones fisiológicas. En algunas circunstancias, la inflamación puede que no cumpla adecuadamente su función de defensa o, que los mecanismos reguladores se alteren, dando lugar a una respuesta inflamatoria exagerada que agrava el daño tisular.

Según la persistencia del daño, la sintomatología clínica y la naturaleza de la reacción inflamatoria (relacionada ésta con la subclase de leucocito que predomina), se hace una distinción entre inflamación aguda e inflamación crónica:

- La inflamación aguda es más violenta; se caracteriza por acumulación de plasma en el tejido afectado, estimulación intravascular de plaquetas y presencia de neutrófilos (leucocitos polimorfonucleares, PMNs).
- La inflamación crónica supone un equilibrio entre los mecanismos de agresión y de defensa. Puede aparecer desde el comienzo de la enfermedad, o ser una secuela de la inflamación aguda cuando la respuesta inflamatoria es incapaz de eliminar al agente causal. Se distingue por el predominio de células

mononucleares (sobre todo macrófagos) y también linfocitos, células plasmáticas y otras.

1.1.1 Mediadores de la respuesta inflamatoria.

Los fenómenos básicos de la inflamación son regulados por los productos conocidos como mediadores de la inflamación, que son mediadores solubles o moleculares. Estos mediadores químicos, son de naturaleza diversa:

- *Plasmático*: el sistema del complemento, las cininas, el sistema de la coagulación y el fibrinolítico. Estos mediadores son los que desencadenan la reacción inflamatoria al reconocer toxinas y células dañadas y también contribuyen a amplificar la respuesta inflamatoria.
- *Celular (mediadores preformados y almacenandos en gránulos citoplásmicos o rápidamente sintetizados ante un estímulo inflamatorio):* los péptidos y las aminas (histamina y neuropéptidos), el óxido nítrico (NO), citocinas proinflamatorias como el factor de necrosis tumoral-α (TNFα), mediadores lipídicos como las prostaglandinas (PGs), los leucotrienos (LTs), el factor activador de plaquetas (PAF) o las quimiocinas, entre otros. Son, en parte, responsables de la amplificación de la respuesta inflamatoria.
- *Derivados de los microorganismos invasores*: péptidos formilados quimiotácticos y endotoxinas. Entre ellos encontramos a las moléculas vasoactivas, que actúan directamente en la vasculatura para aumentar la permeabilidad vascular, y los factores quimiotácticos, que promueven la extravasación de leucocitos desde el torrente sanguíneo hasta el foco inflamatorio.

Además, en el proceso inflamatorio participan diversos componentes o mediadores celulares como:

- *Leucocitos (neutrófilos, basófilos, eosinófilos, monocitos/macrófagos, linfocitos)*: estas células además de liberar mediadores inflamatorios, son capaces de adherirse al endotelio, de migrar a su través y, en general, de fagocitar y destruir a los agentes patógenos.
- *Plaquetas:* Aunque las plaquetas han sido tradicionalmente conocidas por su papel en la homeostasia, actualmente cada vez más estudios demuestran

claramente su papel en la inflamación. Como se representa en la figura 1, las plaquetas son capaces de reconocer, secuestrar y matar patógenos, de activar y reclutar leucocitos así como modular su comportamiento entre otras. Estas propiedades son en parte debidas al gran abanico de mediadores solubles y moléculas de superficie expresadas por las plaquetas (Jenne *et al.*, 2015).

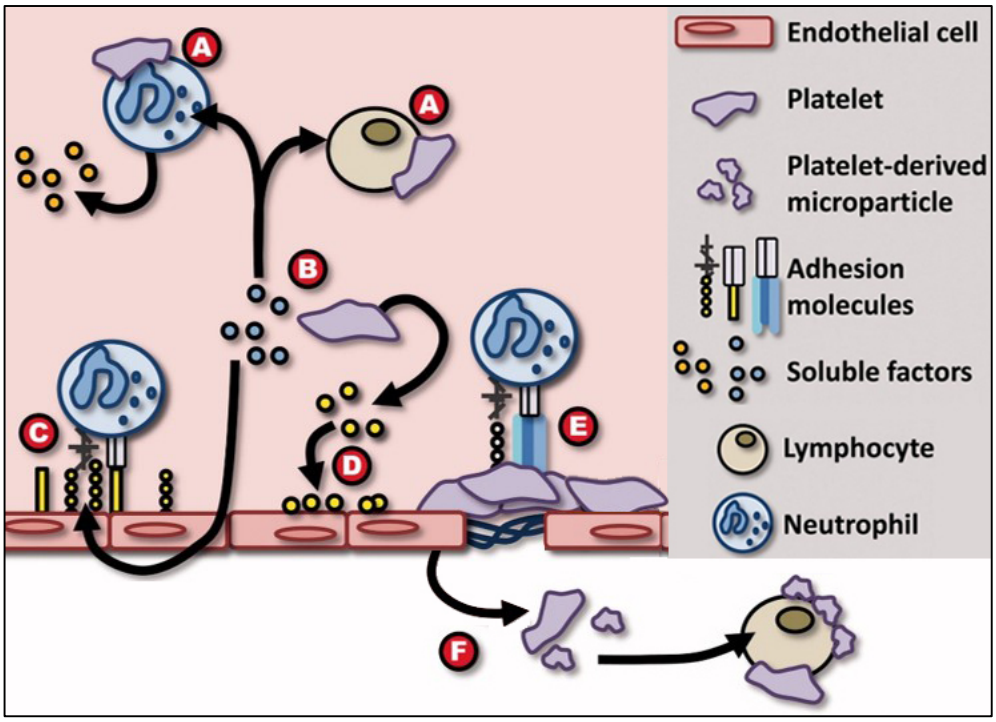

Figura 1: Las plaquetas tienen diversos papeles en la inflamación y respuesta inmune. (A) Las plaquetas se unen y activan leucocitos circulantes promoviendo funciones efectoras tales como la desgranulación. (B) Las plaquetas liberan mediadores solubles que activan a los leucocitos. (C) Dichos mediadores también activan al endotelio, lo que induce la expresión de moléculas de adhesión, lo que tiene como consecuencia una mayor adhesión de leucocitos. (D) las plaquetas liberan factores quimiotácticos que si son depositados en el endotelio promoviendo aún más el reclutamiento de leucocitos y su adhesión (E) Las plaquetas se adhieren al endotelio o a la matriz subendotelial, favoreciendo la adhesión de leucocitos en zonas de la vasculatura donde no se han expresado moléculas de adhesión por el endotelio. (F) Las plaquetas y las micropartículas de origen plaquetario, salen del torrente sanguíneo hacia los tejidos donde se unen y activan a los leucocitos, dirigiendo así la respuesta inflamatoria. Adaptado de:(Jenne *et al.*, 2015)

- *Células endoteliales*: sintetizan y liberan numerosos mediadores inflamatorios e interactúan con los leucocitos en la infiltración leucocitaria.

Una característica común a leucocitos, plaquetas y células endoteliales, además de su capacidad para liberar mediadores inflamatorios, es que presentan en su

superficie las llamadas moléculas de adhesión celular (MAC), que facilitan las interacciones entre estos tres tipos celulares (Celi *et al.*, 1997; Ley *et al.*, 2007).

1.1.2 Regulación de la infiltración leucocitaria.

En el proceso inflamatorio, y también en condiciones fisiológicas como parte de su función de vigilancia, los leucocitos deben abandonar el torrente circulatorio, mediante un proceso que se denomina infiltración leucocitaria. Los leucocitos deben atravesar la monocapa de células endoteliales que recubre la pared interna de los vasos sanguíneos, para pasar al espacio extravascular, donde realizarán sus funciones biológicas. Las MAC y los factores quimiotácticos son los principales mediadores en el proceso de infiltración leucocitaria, ya que, actuando directamente sobre los leucocitos, provocan la interacción de éstos con el endotelio vascular:

- *MAC*: son glicoproteínas que se expresan en la superficie de las células. Promueven la interacción entre los leucocitos y las células endoteliales o entre los leucocitos y la matriz extracelular.

- *Factores quimiotácticos*: son mediadores químicos solubles generados localmente en los sitios de daño tisular. Actúan como señales que atraen más leucocitos circulantes al foco inflamado y controlan la expresión de algunas MAC. Los factores quimiotácticos se pueden clasificar como:
  - Agentes quimiotácticos clásicos o inespecíficos, que atraen a todos los leucocitos en general: fragmentos C5a y C3a del complemento, moléculas lipídicas (LTB_4, PAF), péptidos bacterianos formilados (N-formil-metionil-leucil-fenilalanina o fMLP), etc.
  - Quimiocinas, que atraen determinados subtipos de leucocitos de forma selectiva: por ejemplo, la interleucina-8 (IL-8), la *monocyte chemoattractant/chemotactic protein*-1 (MCP-1), la eotaxina, etc.

Otros mediadores solubles que intervienen en la infiltración leucocitaria son las citocinas. Entre ellas destacan las citocinas proinflamatorias como el TNFα o la IL-1, que promueven la migración leucocitaria sin ser propiamente quimiotácticas, es decir, no actúan directamente sobre los leucocitos sino que hacen a las células endoteliales más adhesivas para éstos o inducen en diversos tipos celulares la liberación de otros mediadores (Celi *et al.*, 1997; Wagner *et al.*, 2000; Ley *et al.*, 2007).

1.1.3 Etapas de la infiltración leucocitaria

El proceso de infiltración leucocitaria, que abarca, pues, desde el contacto inicial de los leucocitos con el endotelio hasta que alcanzan el espacio extracelular, se ha simplificado en un modelo que predice tres etapas sucesivas y coordinadas: rodamiento, adhesión y migración[1]. Se define como una cascada puesto que la

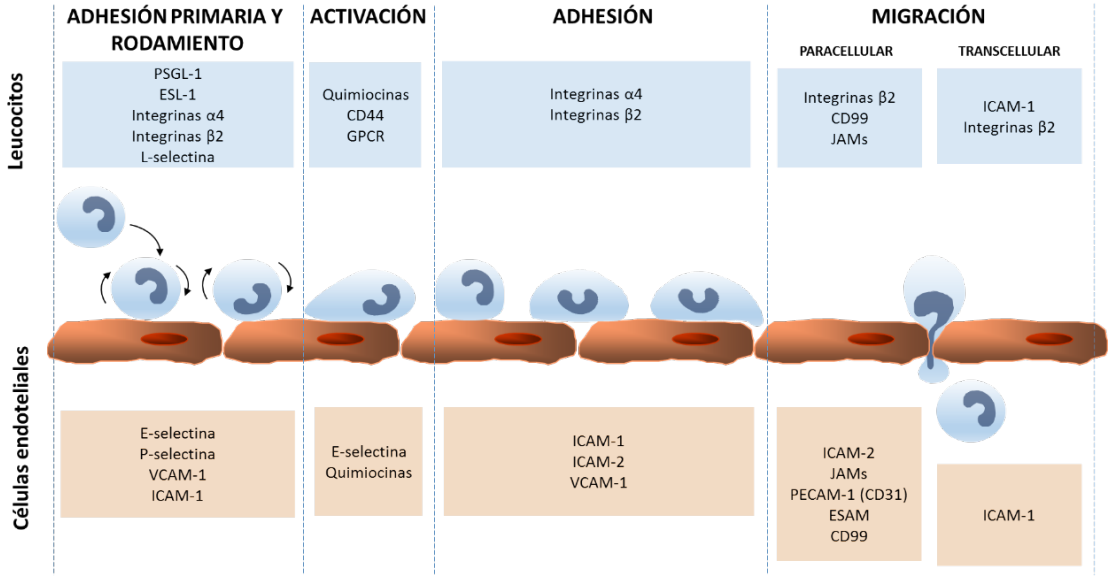

interrupción de la etapa inicial impide las siguientes (Springer, 1994; Ley *et al.*, 2007; Wagner *et al.*, 2008).

Figura 2: Etapas de la infiltración leucocitaria y principales moléculas implicadas. Adaptado de: (Ley *et al.*, 2007; Wagner *et al.*, 2008)

1.1.3.1 Adhesión primaria y rodamiento.

En primer lugar, las células endoteliales activadas aumentan su adherencia a los leucocitos ("los reconocen"). Este contacto inicial no es aleatorio, sino que constituye la adhesión primaria o laxa que enlentece el tránsito leucocitario y, aumenta la posibilidad de una interacción más estrecha de los leucocitos con el endotelio. Esta fase se denomina rodamiento leucocitario y es el paso limitante para las siguientes fases.

[1] Algunos autores consideran alguna de éstas como dos etapas y no como una sola, de modo que el proceso de infiltración leucocitaria puede extenderse a cuatro etapas: (1) interacción inicial leucocito-endotelio ("*tethering*"), (2) rodamiento de leucocitos sobre el endotelio ("*rolling*"), (3) activación leucocitaria y adhesión firme al endotelio y (4) migración transendotelial (Reinhardt and Kubes, 1998); e incluso a cinco etapas si la (3) se subdivide a su vez en otras dos.

El proceso se inicia con la liberación de mediadores generados por el tejido dañado (histamina, trombina, TNFα, IL-1, etc.) que producen una rápida activación de las células endoteliales. En consecuencia, (1) se producen sustancias quimiotácticas, y (2) aumenta la expresión de determinadas MAC; principalmente las selectinas, que determinan la interacción inicial leucocito-endotelio y el rodamiento leucocitario. Dicha interacción es reversible. Si no se desencadenan los mecanismos de adhesión firme, los leucocitos volverán al torrente circulatorio (Kubes *et al.*, 1994; Celi *et al.*, 1997; Ley *et al.*, 2007; Wagner *et al.*, 2008; McEver, 2010).

1.1.3.2 Activación y adhesión firme

Si el estímulo persiste, se produce la activación de los leucocitos en rodamiento, fenómeno aparentemente muy rápido que da lugar a la detención de los mismos de manera estable, produciéndose su adhesión firme al endotelio vascular.

Median en esta etapa:

- Las sustancias originadas en el foco infamatorio que, por la menor velocidad de los leucocitos en rodamiento, pueden interaccionar con ellos y activarlos: pueden ser exógenas (fMLP) o endógenas (C5a, PAF, LTB_4 y otros agentes quimiotácticos como las quimiocinas).
- MAC: integrinas de las membrana leucocitaria (como algunas β_2) cuya expresión aumenta como consecuencia de la activación, o sufren un cambio conformacional a estado activo (como integrinas α_4 o α_L) y sus ligandos, las inmunoglobulinas (Igs) (Springer, 1994; Sullivan *et al.*, 2004; Ley *et al.*, 2007).

1.1.3.3 Migración y quimiotaxis.

Finalmente, se inicia la migración a través del endotelio y la quimiotaxis, que es el movimiento unidireccional de los leucocitos a través del tejido hacia el foco de inflamación, atraídos por concentraciones crecientes de agentes quimiotácticos originados en el foco.

Este proceso lo regulan:

- MAC, tanto integrinas como Igs, como otras descritas recientemente (Ley *et al.*, 2007) que hacen posible la diapédesis.

- Los agentes quimiotácticos y determinadas quimiocinas, que forman un gradiente quimiotáctico que dirige la diapédesis y la migración a través del tejido (Luscinskas *et al.*, 1994; Ley *et al.*, 2007; Sallusto *et al.*, 2008).

1.1.4 Moléculas de adhesión celular

1.1.4.1 Consideraciones generales

La etapa central del proceso inflamatorio la constituye la interacción entre los leucocitos y el endotelio vascular, que da lugar a la extravasación de leucocitos desde el torrente circulatorio hasta el foco inflamado. Este fenómeno está regulado y coordinado con gran precisión, por la activación secuencial de proteínas de adhesión y sus correspondientes ligandos, presentes tanto en los leucocitos como en las células endoteliales (Springer, 1994; Konstantopoulos *et al.*, 1997; Krieg *et al.*, 2004; Sullivan *et al.*, 2004).

La función de las MAC, como moléculas reguladoras de la infiltración leucocitaria, es mediar la unión de los leucocitos a las células endoteliales, u otras células como las musculares, las plaquetas, etc., en condiciones fisiológicas o patológicas; así, las MAC están involucradas en la hemostasia, la inmunidad, la diferenciación, el crecimiento, la comunicación y la movilidad celular (Krieglstein *et al.*, 2001)

1.1.4.2 Características de las moléculas de adhesión

Las MAC son glicoproteínas de membrana que, de acuerdo a semejanzas estructurales y funcionales, se pueden agrupar, en cuatro grandes grupos: las selectinas, los ligandos de las selectinas de tipo mucina, las integrinas y las moléculas de adhesión de tipo Ig (Springer, 1994; Wang *et al.*, 2007). Cada uno de ellos participa de distinta forma en las tres etapas que se suceden en el proceso inflamatorio (rodamiento, adhesión y migración) y se coordinan perfectamente para asegurar la secuencia ordenada de interacciones celulares que supone proceso (Granger *et al.*, 2004).

Cumplen dos funciones principales:

- Se unen a ligandos específicos ubicados en otras células o en la matriz extracelular, facilitando las interacciones celulares y la migración de dichas células por los diferentes tejidos.
- Transducen señales reguladoras de la transcripción después de la interacción con sus ligandos (Ulbrich *et al.*, 2003).

Las interacciones que tienen lugar durante la inflamación son variadas: leucocito-leucocito, leucocito-endotelio, leucocito-plaqueta, plaqueta-endotelio, leucocito-músculo liso vascular, leucocito-matriz extracelular y leucocito-célula intersticial (Celi *et al.*, 1997; Wang *et al.*, 2007).

1.1.4.2.1 Familia de las selectinas

Las selectinas son glicoproteínas que se caracterizan por la presencia de un dominio de tipo lectina en la porción amino-terminal (N-terminal) y que pueden o no expresarse en la superficie celular (Bevilacqua *et al.*, 1993; Angiari, 2015). Hasta el momento se han identificado tres selectinas que se encuentran exclusivamente en células relacionadas con la fisiología vascular (leucocitos, plaquetas y endotelio); el prefijo hace referencia al tipo celular donde se encontraron inicialmente:

- *L-selectina*: se encuentra únicamente en los leucocitos, expresada como molécula de superficie, o bien actúa como molécula soluble (la activación leucocitaria conduce al corte de la L-selectina, generando una forma soluble de la molécula que es liberada al medio extracelular). La L-selectina se expresa de forma constitutiva en los leucocitos en reposo y es cortada de la membrana plasmática tras la activación de los mismos
- *E-selectina*: está en la superficie celular del endotelio. La E-selectina es inducida por distintos mediadores inflamatorios como citocinas, toxinas bacterianas, etc
- *P*-selectina: se almacena preformada en gránulos intracelulares específicos en las plaquetas (gránulos α) y también en las células endoteliales (cuerpos de Weibel-Palade); desde éstos puede movilizarse rápidamente a la superficie por diversos estímulos (Konstantopoulos *et al.*, 1997; McEver, 2010). La P-selectina se expresa constitutivamente pero queda almacenada para ser rápidamente translocada a la membrana plasmática por oxidantes, histamina,

trombina, etc., y además su expresión puede aumentar por algunas citocinas (Bevilacqua *et al.*, 1993; Springer, 1994; Yao *et al.*, 1996).

Los ligandos de las selectinas son carbohidratos (sialilados[2], fucosilados o sulfatados, a los que se unen a través del dominio lectina): la L-selectina de los leucocitos se une a mucinas expresadas en el endotelio y la E- y la P-selectina de endotelio o plaquetas se unen a otros ligandos presentes en los leucocitos (Foxall *et al.*, 1992(Foxall *et al.*, 1992; McEver *et al.*, 2010). Así, las selectinas median interacciones intercelulares temporales, siendo responsables de la adhesión primaria o laxa que permite el rodamiento de los leucocitos sobre el endotelio (Ley *et al.*, 2007). Los ligandos de las selectinas son:

-PSGL-1 para P y L- selectina

-Glycam 1, CD34 y MadCAM-1 para L- selectina

-ESL-1, PSGL-1, CD44 para E-selectina

1.1.4.2.2 Familia de las integrinas

Las integrinas son glicoproteínas de membrana heterodiméricas, constituidas por una subunidad o cadena α y una β que se unen entre sí mediante enlaces no covalentes. En humanos, hasta 2015, se han caracterizado 18 subunidades α y 8 subunidades β, lo que da lugar a más de 24 combinaciones heterodimericas (Teoh *et al.*, 2015); se pueden agrupar en varias subfamilias de acuerdo a sus cadenas β (cada subfamilia se caracteriza por una subunidad β común que se une a una entre varias subunidades α posibles): integrinas β_1 (CD29), integrinas β_2 (CD18), etc. De ellas destacamos:

Las integrinas β_2, cuya cadena común (CD18) se asocia a cuatro cadenas α diferentes:

- La CD11a/CD18 (Lymphocyte function-associated antigen-1 o LFA-1 o $\alpha_L\beta_2$), se expresa en todo tipo de leucocitos
- La CD11b/CD18 (Mac-1 o $\alpha_M\beta_2$), se expresa en granulocitos y monocitos
- La CD11c/CD18 (P150/95 o $\alpha_X\beta_2$) se expresa en granulocitos y monocitos
- La CD11d/CD18 o $\alpha_d\beta_2$, se expresa en células dendríticas y macrófagos.

[2] Las tres selectinas se caracterizan por reconocer carbohidratos de superficie que contienen una estructura del tipo del tetrasacárido sialil lewis^x (SLe^x) y su isómero sialil lewis^a (SLe^a) (Krieglstein and Granger, 2001).

Las integrinas que comparten la subunidad α4 (CD49d):

- La CD49d/β_7 o $\alpha_4\beta_7$.
- La CD49d/CD29 (*Very late antigen*-4 o VLA-4 o $\alpha_4\beta_1$),

Se expresan sobretodo en leucocitos (Krieglstein *et al.*, 2001). La mayoría de las integrinas se expresan constitutivamente pero además en muchos casos su expresión o su afinidad por su respectivo ligando puede incrementarse por distintos factores quimiotácticos u otros mediadores (Carlos *et al.*, 1994). Los ligandos de estas MAC son otras MAC presentes en el endotelio de tipo Ig, como *intercellular adhesion molecule* (ICAM)-1 e ICAM-2, *vascular cell adhesion molecule*-1 (VCAM-1), y también una gran variedad de proteínas de la matriz extracelular (fibronectina, laminina) o moléculas solubles (fibrinógeno, Factor de von Willebrand) (Granger *et al.*, 2004). Participan, en interacciones célula-célula y célula-matriz extracelular, mediando fundamentalmente la adhesión firme de los leucocitos a las células endoteliales activadas, la migración y la quimiotaxis de los leucocitos hacia los sitios de inflamación (Hynes, 1992; Wang *et al.*, 2007); interaccionan a nivel intracelular con proteínas del citoesqueleto (como la actina) para integrar la información del medio extracelular con la actividad de la célula, acción de la cual deriva su nombre.

1.1.4.2.3 Superfamilia de las inmunoglobulinas

Estas MAC son proteínas transmembrana que tienen uno o más dominios extracelulares homólogos a las Igs. Entre ellas se encuentran moléculas como ICAM-1, ICAM-2, VCAM-1, MAdCAM y *platelet endothelial cell adhesion molecule*-1 (PECAM-1). Se localizan sobre todo en el endotelio y algunas, además, en plaquetas, leucocitos y otras células (Granger *et al.*, 2004; Wang *et al.*, 2007). Algunas se expresan constitutivamente y otras requieren síntesis *de novo* inducida por múltiples estímulos como citocinas y toxinas bacterianas; adicionalmente, su expresión puede aumentar por algunos de esos estímulos (Springer, 1990; Wang *et al.*, 2007).

En general, son los ligandos endoteliales complementarios de otras MAC leucocitarias (sobre todo integrinas como, por ejemplo, LFA-1 y VLA-4), y también se unen a proteínas de la matriz extracelular o a moléculas solubles (Carlos *et al.*, 1994). Están involucradas, como las integrinas, en los mecanismos de adhesión

célula-célula y célula-matriz extracelular que determinan la firme adhesión y transmigración de los leucocitos (Springer, 1990; Wang *et al.*, 2007).

1.1.5 Quimiocinas

1.1.5.1 Generalidades

Las quimiocinas son proteínas pequeñas, de unos 70-130 aminoácidos (aa), glicosiladas o no y, en su mayoría, son secretadas. Sólo dos quimiocinas, CXCL16 y fractalquina (CX_3CL1), son proteínas de membrana (Baggiolini, 1998; Baggiolini, 2001; Moser *et al.*, 2004). A medida que se descubren nuevas moléculas, se ha hecho necesaria una nomenclatura sistemática para las quimiocinas y sus receptores. Consiste en el acrónimo relativo a la estructura (por ejemplo, "CXC") seguido o bien de "L", por ligando, en el caso de las quimiocinas, o bien de "R", en el caso de los receptores. Esta nomenclatura se ha adoptado de forma general para los receptores, si bien las quimiocinas suelen designarse por sus nombres tradicionales. CXCL16 se conoce sólo por su nombre sistemático (Baggiolini, 2001).

En general, presentan cuatro residuos cisteína (Baggiolini, 2001) en la porción N-terminal, a excepción de las linfotactinas-α y -β, que únicamente presentan dos (Kennedy *et al.*, 1995; Baggiolini, 2001); esta característica es la base para su clasificación. Las Cys están unidas entre sí por dos puentes disulfuro (Cys1-Cys3 y Cys2-Cys4), lo que confiere a las quimiocinas su característico plegamiento tridimensional. Así, aunque tienen una identidad relativamente pequeña en su secuencia de aa (Luster, 1998), su estructura tridimensional muestra una marcada homología (Baggiolini *et al.*, 1994; Schwarz *et al.*, 2002).

Los puentes disulfuro son esenciales para su reconocimiento por el receptor y su actividad biológica (Baggiolini, 2001).

1.1.5.2 Subfamilias estructurales de quimiocinas

De acuerdo con la posición relativa de las dos primeras Cys N-terminales, las quimiocinas se clasifican en cuatro subfamilias (Baggiolini, 1998; Luster, 1998). Las dos principales, y ampliamente caracterizadas, son las subfamilias de las quimiocinas CXC y las quimiocinas CC. Las quimiocinas C y CX3C constituyen las dos subfamilias "menores" (Moser *et al.*, 2004).

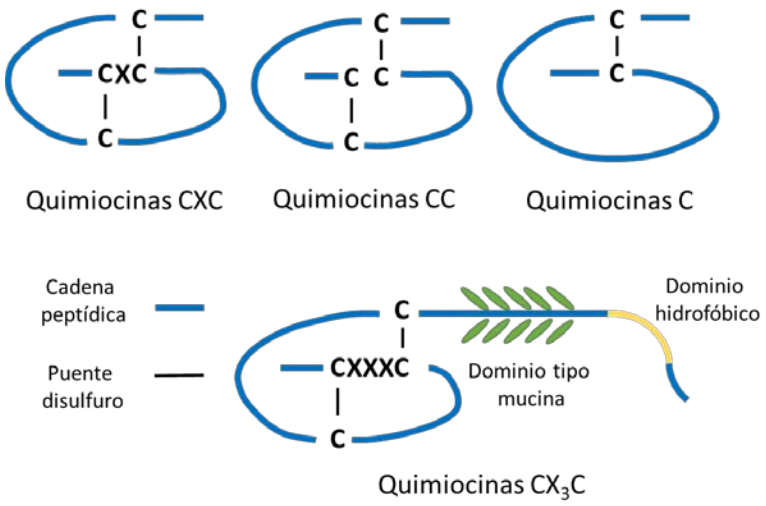

Figura 3: Esquema de la estructura de las diferentes subfamilias de quimiocinas. Adaptado de: (Rostene *et al.*, 2007).

1. *Subfamilia de las quimiocinas CXC (subfamilia α):*

Presentan las dos Cys separadas por un aminoácido variable. Su prototipo es la IL-8 o CXCL8.

Este grupo de las quimiocinas CXC puede, a su vez, subdividirse en otros dos, en base a la presencia o ausencia de una secuencia concreta de tres aa, ácido glutámico-leucina-arginina (motivo ELR), situados inmediatamente antes del primer residuo de Cys de la secuencia CXC. Este motivo determina, en parte, la unión específica de las quimiocinas que lo presentan a determinados receptores (Baggiolini, 1998); el elemento ELR tiene una gran correlación con la especificidad de las células diana (Gunn *et al.*, 1998).

2. *Subfamilia de las quimiocinas CC (subfamilia β):*

Tienen las dos Cys adyacentes, sin aminoácido intermedio.

Su prototipo es la MCP-1 o CCL2.

3. *Subfamilia de las quimiocinas C (subfamilia γ):*

Presentan una sola Cys N-terminal (faltan la primera y la tercera de las cuatro Cys).

Las linfotactinas-α y -β son los dos únicos miembros de la subfamilia.

4. Subfamilia de las quimiocinas CX3C (subfamilia δ):

Las dos primeras Cys N-terminales están separadas por tres aa.

La fractalquina o neurotactina o CX_3CL1 es el único representante de la subfamilia.

La fractalquina es una de las únicas dos quimiocinas, junto con CXCL16 que, además de comportarse como factor quimiotáctico, actúa como molécula de adhesión, ya que es una glicoproteína de tipo mucina anclada en la membrana (Bazan *et al.*, 1997). Y como es parte del objeto de estudio en esta Tesis se hará una descripción más detallada de ella.

CX_3CL1 puede encontrase en dos formas; como proteína transmembrana, que actúa como molécula de adhesión y como molécula soluble que posee una fuerte acción quimioatrayente para monocitos/macrófagos, células T y células NK (Bazan *et al.*, 1997; Combadiere *et al.*, 1998). Fractalquina ejerce su acción biológica mediante la unión específica a su receptor llamado CX_3C receptor 1 (CX_3CR1) (Imai *et al.*, 1997). Existen evidencias que sugieren que el eje CX_3CL1/CX_3CR1 puede estar involucrado en la fisiopatología de la aterosclerosis. Así, experimentos *in vivo* con modelos animales de aterosclerosis han demostrado que impidiendo la interacción CX_3CL1/CX_3CR1 se consigue un gran efecto protector (Combadiere *et al.*, 2003; Lesnik *et al.*, 2003; Teupser *et al.*, 2004). En humanos, una mutación en CX_3CR1, denominada CX_3CR1-M280, causa una adhesión y actividad quimiotáctica deficiente (McDermott *et al.*, 2001; Moatti *et al.*, 2001; McDermott *et al.*, 2003). Esta mutación de CX_3CR1 está ligada a un menor riesgo de padecer aterosclerosis, síndrome coronario agudo y disfunción endotelial en la arteria coronaria (McDermott *et al.*, 2001; Moatti *et al.*, 2001; McDermott *et al.*, 2003). Recientemente, el aumento en la expresión de CX_3CR1 ha sido detectado en monocitos circulantes de pacientes con enfermedad arterial coronaria (Apostolakis *et al.*, 2007).

Además, estudios recientes de nuestro laboratorio, han demostrado *in vivo* e *in vitro* que CX_3CL1 es una molécula clave en las diferentes propiedades de adhesión observadas entre endotelio arterial y venoso en respuesta al estímulo con Ang-II (Rius *et al.*, 2013c).

1.1.5.3 CXCL16

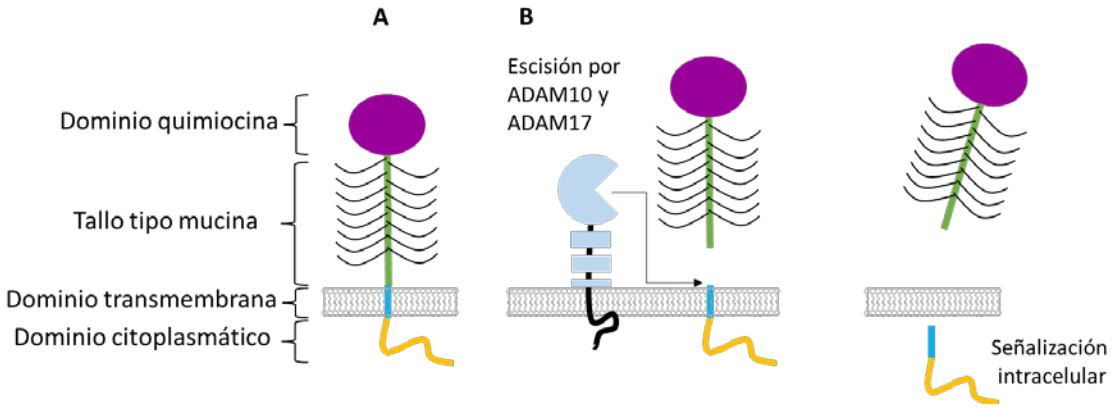

CXCL16 es una quimiocina perteneciente a la familia CXC que carece de la secuencia ELR y que estructuralmente es diferente de los demás miembros de la familia CXC.

Figura 4: Representación esquemática de la estructura y de la escisión proteolítica de CXCL16. (A) CXCL16 es expresada como una molécula con varios dominios. (B) La escisión enzimática, debido a la actividad de proteasas con dominio metaloproteasa y desintegrina (ADAM), cerca de la membrana celular produce la liberación del ectodominio compuesto por el tallo tipo mucina y el dominio quimiocina. Adaptada de: (Ludwig *et al.*, 2007)

Inicialmente, CXCL16 fue descrita como un receptor basurero para fosfatidilserina y lipoproteínas de baja densidad oxidadas (SR-PSOX) (Shimaoka et al., 2000). De forma independiente, CXCL16 fue descrita por otro grupo de investigación como un ligando para el receptor CXCR6 (BONZO, STRL33, TYMSTR) (Matloubian et al., 2000). Junto a Fractalquina (CX_3CL1), CXCL16 es una de las dos únicas quimiocinas conocidas que no se expresan como una proteína soluble sino como una quimiocina trasmembrana. Respecto a su estructura, la proteína humana de CXCL16 es una glicoproteina transmembrana de 30 kDa, formada por 254 aminoácidos, que forman 4 dominios diferentes: un dominio quimiocina, un dominio brazo tipo mucina, un dominio transmembrana y un dominio intracelular. (Figura 4A).

En humanos, el gen de CXCL16 se localiza en el cromosoma 17p13, separado del resto de quimiocinas conocidas (Matloubian et al., 2000). Tanto en humanos

como en ratón, CXCL16 tienen la particularidad de poseer seis cisteínas en el dominio quimiocina, propiedad que comparte en exclusiva con una subfamilia de quimiocinas CC (Matloubian et al., 2000; Shimaoka et al., 2000). CXCL16 es sintetizada como precursor intracelular que debe ser procesado y transportado a la superficie celular (Gough et al., 2004). La conversión de proteína trasmembrana a fracción soluble de CXCL16 (Figure 4B), resulta de la acción enzimática ejercida por dos proteasas con dominio metaloproteasa y desintegrina (ADAM), denominadas ADAM10 y ADAM17 (Schulte et al., 2007). ADAM10 media la escisión tanto constitutiva como inducible de CXCL16 (Abel et al., 2004; Gough et al., 2004; Hundhausen et al., 2007), mientras que ADAM17 parece estar involucrada solo en la escisión inducible de CXCL16 (Ludwig et al., 2005)

1.1.5.3.1 Expresión de CXCL16

CXCL16 es expresada por células endoteliales, epiteliales y de músculo liso, así como en macrófagos, células dendríticas, linfocitos T y B y plaquetas (Ludwig *et al.*, 2007; Izquierdo *et al.*, 2014). Diversos estudios han probado que citoquinas proinflamatorias como TNF-α, IL-1β, IFN-γ e IL-6 aumentan la expresión de CXCL16 en células vasculares (Hofnagel *et al.*, 2002; Abel *et al.*, 2004; Zeng *et al.*, 2012).

1.1.5.3.2 Funciones de CXCL16

Como se ha comentado anteriormente CXCL16 se puedes encontrar en forma soluble o unida a membrana. Por ello CXCL16 puede comportarse como:

- Factor quimiotáctico: La forma soluble de CXCL16 actúa como factor quimiotáctico para células que expresan el receptor CXCR6, como células T $CD4^+$ y $CD8^+$ T, células T natural killer invariantes (iNKT), células NK, células B y monocitos (Kim et al., 2002; Nakayama et al., 2003; Hofnagel et al., 2011), promoviendo así el reclutamiento leucocitario (Matloubian et al., 2000; Kim et al., 2001; Hara et al., 2006; van der Voort et al., 2010). Además, la fracción soluble de CXCL16 promueve proliferación celular, angiogénesis, y la trascripción de genes pro inflamatorios (Chandrasekar et al., 2004; Zhuge et al., 2005).

- Molécula de adhesión: La forma unida a membrana de CXCL16 promueve la adhesión firme de células que expresan el receptor CXCR6, causando la adhesión de monocitos, células T y NKT a las células endoteliales, así como la adhesión de células T y NKT a células dendríticas (Shimaoka et al., 2004; Hofnagel et al., 2011).

- Receptor basurero: En humanos, la forma unida a membrana de CXCL16 también media la internalización de bacterias y lipoproteínas oxidadas de baja densidad (oxLDL) en diferentes células inmunes. El aumento de expresión de CXCL16 inducido por IFN-γ produce un incremento en la internalización de oxLDL por los macrófagos y podría participar en la formación de células espumosas (Wuttge et al., 2004).

1.1.5.3.3 CXCL16 y enfermedades cardiovasculares.

El carácter dual de CXCL16, tiene la habilidad de atraer y promover la adhesión firme de linfocitos y monocitos, así como su presencia en células de la pared vascular, sugiere una potencial implicación de esta quimiocina en diversas enfermedades cardiovasculares (Izquierdo *et al.*, 2014). Además, la expresión de CXCL16 ha sido detectada en muestras procedentes de endarectomías carotideas humanas y en muestras de lesiones ateroscleróticas de ratones apoE$^{-/-}$ lo que apoya que CXCL16 tiene un papel en la aterosclerosis, inflamación vascular y angiogénesis (Wuttge et al., 2004).

Sin embargo el papel de esta quimiocina es controvertido, ya que experimentos llevados a cabo en modelos animales muestran que en ratones *CXCL16*$^{-/-}$*LDLr*$^{-/-}$ el desarrollo de aterosclerosis se ve acelerado, probablemente debido a la perdida de la función de receptor basurero de CXCL16 (Aslanian *et al.*, 2006). Por otra parte, otros estudios publicados observaron la relevancia de la expresión endotelial de CXCL16 en sitios propensos a la formación de la lesión y su papel en la formación de la placa aterosclerótica temprana (Hofnagel *et al.*, 2006). En este mismo sentido, estudios realizados *in vivo* mostraron que la ausencia del receptor CXCR6 en ratones *apoE*$^{-/-}$ produjo una disminución en la infiltración de la células T y macrófagos en la lesión, lo que se tradujo en una menor respuesta inflamatoria y por tanto, menor

lesión aterosclerótica (Galkina et al., 2007). Además, estudios utilizando un modelo de aterosclerosis acelerada en ratones *apoE*$^{-/-}$ inducida mediante la colocación de unas bandas alrededor de la arteria carótida, la sobreexpresión de CXCL16 promovió la evolución de las lesiones preexistentes a placas vulnerables, sin que ello afectara al tamaño de la placa (Yi *et al.*, 2011).

En humanos, niveles altos de CXCL16 soluble son considerados como un biomarcador de inflamación y aterosclerosis y se han detectado en pacientes con enfermedades arteriales crónicas, síndromes agudos coronarios y accidente cerebrovascular agudo (Izquierdo et al., 2014).

Estudios realizados recientemente, demostraron que CXCL16 se expresa en plaquetas y que, bajo ciertos estímulos, aumenta su expresión en la superficie de las mismas, así como su liberación al espacio extracelular (Seizer et al., 2011). Así mismo, la expresión de CXCL16 es mayor en plaquetas obtenidas de pacientes con procesos coronarios agudos frente a pacientes de procesos crónicos (Seizer et al., 2011). Además, estudios realizados tanto *in vivo* como *in vitro* demostraron que CXCL16 también es capaz de producir la activación de las plaquetas y su adhesión a otras células a través de la activación de CXCR6 que se expresa en la plaquetas (Borst et al., 2012).

Todos estos estudios sugieren que CXCL16 podría tener un papel importante en la inflamación vascular.

1.2 ATEROSCLEROSIS

1.2.1 Consideraciones generales.

La arteriosclerosis es una de las principales causas de morbilidad y mortalidad por enfermedades cardiovasculares en Europa, Estados Unidos y, de forma creciente, en Asia (Ross, 1993; Mozaffarian *et al.*, 2016) .

Anteriormente se consideraba que el proceso de aterogénesis consistía básicamente en una acumulación pasiva de lípidos en el interior de las paredes arteriales (Ross, 1993; Paoletti *et al.*, 2004; Libby, 2012) esto pudo deberse a que los altos niveles plasmáticos de colesterol, en particular los asociados a las lipoproteínas de baja densidad (LDL), constituyen uno de los principales factores de riesgo para el desarrollo

de la arteriosclerosis (Ross, 1993; Glass *et al.*, 2001). Sin embargo, los avances científicos más recientes atribuyen un papel central a la inflamación, la cual participa en todas las fases de la lesión arterosclerótica: en su inicio, en su progresión y en las complicaciones trombóticas de la enfermedad (Libby, 2002; Libby, 2012). Se acepta en general la hipótesis postulada por Rusell Ross en 1977, que considera que la aterosclerosis es el resultado de la respuesta a una disfunción endotelial (Ross, 1993). Se trata de un complejo proceso inflamatorio y proliferativo crónico de naturaleza multifactorial, en el que intervienen multitud de tipos celulares (Paoletti *et al.*, 2004; Hansson *et al.*, 2011; Hansson *et al.*, 2015).

Histológicamente, la arteriosclerosis se caracteriza por una lesión focal (la placa aterosclerótica) en arterias de mediano y gran calibre, constituida por un cúmulo de células, material extracelular y lípidos en el espacio comprendido entre el endotelio (íntima) y las células de la musculatura lisa vascular (media). Las células inflamatorias predominantes en las lesiones ateroscleróticas, son los macrófagos y linfocitos T, (Ross, 1993; Glass *et al.*, 2001) aunque estudios recientes otorgan cada vez más importancia al papel de neutrófilos, plaquetas y mastocitos (Swirski *et al.*, 2013).

1.2.2 Bases del proceso de aterogénesis.

1.2.2.1 Disfunción endotelial

Se han formulado diversas hipótesis en relación al origen de la arteriosclerosis. De acuerdo con la más aceptada, la "hipótesis de la respuesta al daño", la lesión aterosclerótica puede ser iniciada por diferentes agentes y destaca que el primer paso de la arteriosclerosis consiste en la disfunción o pérdida de la función protectora normal del endotelio (Ross, 1993). La disfunción endotelial se define como un estado proinflamatorio y protrombótico del endotelio que provoca la adhesión y subsiguiente migración leucocitaria a través del endotelio que da lugar a posteriores alteraciones vasomotoras (Landmesser *et al.*, 2004).

La disfunción endotelial está frecuentemente asociada a la exposición a factores de riesgo cardiovascular, como hipertensión, hipercolesterolemia, hiperhomocisteinemia, una elevación de proteínas glicosiladas en sangre (característica de pacientes diabéticos), la presencia de agentes químicos oxidantes en sangre

(frecuente en fumadores) o Infecciones crónicas por microorganismos como herpesvirus, *Chlamydia pneumoniae* y otros.

Las alteraciones en el flujo sanguíneo también parecen ser críticas en la determinación de los lugares arteriales propensos al desarrollo de la lesión aterosclerótica. Así, ésta se localiza preferentemente en regiones sometidas a fluctuaciones hemodinámicas (bifurcaciones, ramificaciones, curvaturas) como ocurre en las arterias carótidas y coronarias (Ross, 1993; Libby, 2002; Moore *et al.*, 2011; Libby, 2012).

1.2.2.2 Inicio y evolución de la lesión aterosclerótica

Los cambios más tempranos que tienen lugar en el endotelio (Fig. 5b), y que preceden a la formación de la placa aterosclerótica, suponen el comienzo de la acumulación de leucocitos mononucleares (monocitos, sobre todo, y linfocitos T) y de lípidos en el espacio subendotelial (Ross, 1993; Swirski *et al.*, 2013).

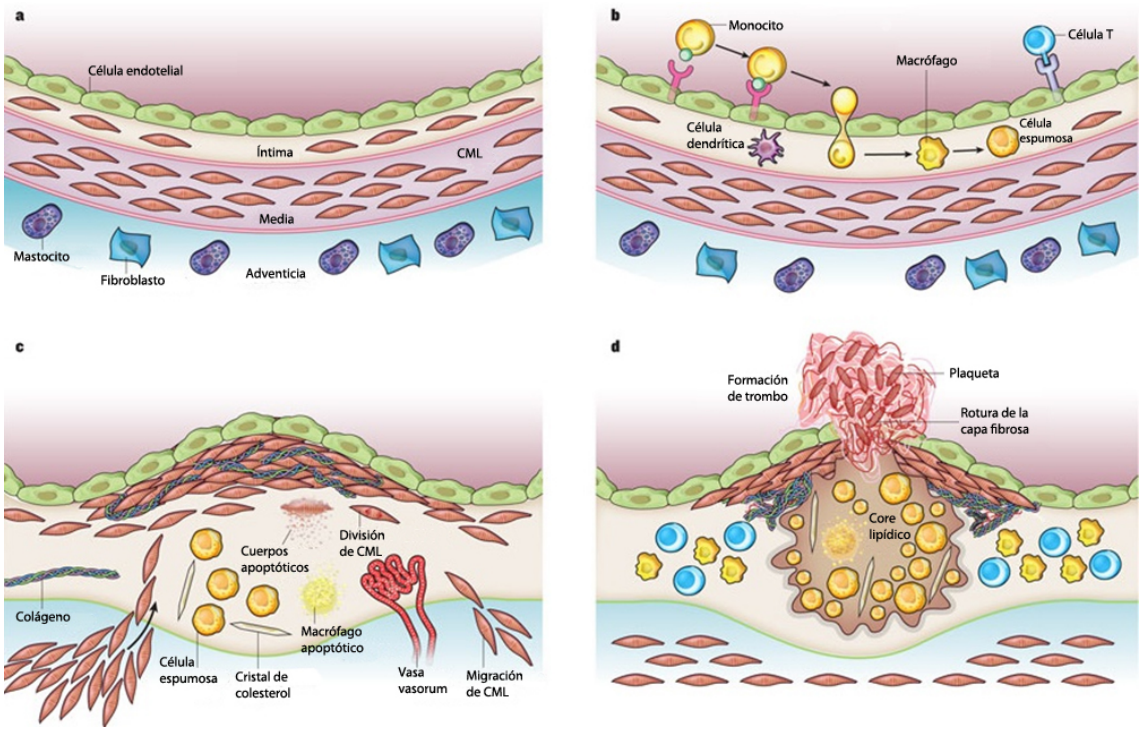

Figura 5: Proceso de formación de la lesión aterosclerótica. a) Estructura normal de una arteria. b) Los pasos iniciales de la aterosclerosis incluyen la adhesión de leucocitos circulantes a la monocapa endotelial activada, migración dirigida de los leucocitos unidos hacia la íntima, la maduración de los monocitos (leucocitos reclutados más numerosos) en macrófagos, y la captación de lípidos, produciendo células espumosas. c) La progresión de la lesión implica la migración de las células de músculo liso vascular (CMLV) de la media hacia la íntima, la proliferación de las CML residentes de la íntima y las CMLV derivados de la media, así como la síntesis aumentada de macromoléculas de la matriz extracelular tales como colágeno, elastina y proteoglicanos. Los macrófagos y las CMLV de la placa pueden

morir en lesiones avanzadas, algunos por apoptosis. Los lípidos derivados de células muertas y moribundas pueden acumularse en la región central de la placa, creando el núcleo necrótico. Las placas avanzadas también contienen cristales de colesterol y microvascularización. d) La trombosis, complicación final de la aterosclerosis. Es una fractura de la cubierta fibrosa de la placa, que permite a los componentes de coagulación de la sangre entrar en contacto con el interior de la placa, lo que provoca el trombo que se extiende en la luz del vaso, donde puede impedir el flujo de sangre. Adaptado de:(Libby *et al.*, 2011)

Los cambios que ocurren en el endotelio aterosclerótico son los siguientes:

a) Aumento de permeabilidad:

- El endotelio se hace más permeable a las LDL, excediéndose la capacidad del sistema de transporte inverso de colesterol que lo devuelve al torrente circulatorio. Este aumento de permeabilidad está mediado por sustancias como NO, prostaciclina, angiotensina-II (Ang-II) y endotelina (Mombouli *et al.*, 1999; Singh *et al.*, 2002; Tabas, 2007).

- Las LDL extravasadas son oxidadas en el espacio subendotelial por las células endoteliales, las células de la musculatura lisa y los macrófagos tisulares (Ross, 1993; Hansson *et al.*, 2011).

b) Adhesión y migración de leucocitos en el espacio subendotelial

- Las LDL oxidadas (LDLox), activan el endotelio para expresar MAC tipo E-selectina, P-selectina, ICAM-1 o VCAM-1, que atrapan a leucocitos mononucleares circulantes, especialmente monocitos, y actúan como receptores para las MAC como L-selectina, integrinas o PECAM-1, que están presentes ellos (Kume *et al.*, 1992; Klouche *et al.*, 1999; Hashimoto *et al.*, 2007).

- Las MAC actúan con diversas moléculas quimiotácticas, MCP-1 entre otras, generadas por las células endoteliales, las células de la musculatura lisa y los monocitos. Así, los leucocitos atraviesan el endotelio por diapédesis y colonizarán la íntima subendotelial. La infiltración de leucocitos se da especialmente en aquellas regiones arteriales de flujo sanguíneo turbulento, que muestran elevada expresión de las MAC endoteliales y leucocitarias (Libby *et al.*, 1995; Yoshizumi *et al.*, 2003).

- En el espacio subendotelial los monocitos se transforman en macrófagos que secretan más agentes quimiotácticos específicos, y atraen mayor número de monocitos circulantes (Ross, 1993; Libby, 2012; Swirski et al., 2013).

1.2.2.3 Formación de la estría grasa

La lesión aterosclerótica precoz o estría grasa es una lesión inflamatoria, que consiste en un cúmulo de macrófagos cargados de lípidos (células espumosas) y linfocitos T en la íntima, que se acompaña de proliferación de las células musculares lisas (Ross, 1993). Los macrófagos, captando las LDLox a través de sus receptores scavenger (receptores "basurero") (Glass *et al.*, 2001), se convierten en células espumosas por mediación de diversos factores como *granulocyte/macrophage colony stimulation factor* (GM-CSF), TNFα o IL-1 (Ross, 1993; Libby, 2012). Su formación incluye los siguentes pasos:

- *La inflamación supone un aumento de macrófagos y linfocitos T que se infiltran y se multiplican dentro de la lesión*. Lo que se traduce en la activación y proliferación de más leucocitos mononucleares, y la amplificación de la respuesta inflamatoria (Ross, 1993).

- *Adherencia y agregación plaquetaria*: El endotelio estimulado por las LDLox se vuelve procoagulante debido a:

  - Disminución de la secreción de NO y de prostaciclina, lo que provoca adherencia y agregación plaquetaria,

  - Síntesis de factor tisular (FT), responsable de la coagulación,

  - Inhibición de la síntesis del activador de plasminógeno tisular (tPA) y estimulación de la síntesis de del inhibidor del activador de plasminógeno-1 (PAI-1), lo que altera la fibrinólisis.

También contribuyen a este proceso: los linfocitos T activados, mediante la expresión de MAC como la L-selectina e integrinas, los monocitos/macrófagos y las células de la musculatura lisa, ya que también sintetizan FT (Ross, 1999; Libby, 2012).

1.2.2.4 Acumulación de células de la musculatura lisa en el espacio subendotelial

Las células endoteliales, los monocitos/macrófagos, las plaquetas y otras células como linfocitos T, células cebadas y las propias células de la musculatura lisa liberan diversas sustancias como citocinas y factores de crecimiento (*platelet-derived growth factor*- PDGF, *transforming growth factor*- TGF) que estimulan la proliferación y

migración de estas células de la musculatura lisa desde la media hacia el lumen arterial (Fig. 5c). La progresiva acumulación de las mismas contribuye la formación de la capa neoíntima. (Ross, 1993; Libby, 2012).

1.2.2.5 La lesión avanzada: placa fibrosa

La progresión de la estría grasa da lugar a la típica lesión neoíntima denominada placa fibrosa, que consta de una cubierta fibrosa que mantiene aislado un núcleo necrótico formado por lípidos, leucocitos, restos celulares y material extracelular. El engrosamiento de la pared arterial puede ser compensado por su dilatación gradual, pero llega un momento en que la compensación no es posible y la lesión se introduce en el lumen, lo que provoca un progresivo estrechamiento del vaso que puede dar lugar a síntomas isquémicos (Fig. 5d) (Ross, 1993; Glass *et al.*, 2001). Para que se desarrolle la lesión es necesario:

- *Infiltración leucocitaria sostenida*:

Prosigue la infiltración y proliferación de leucocitos en la íntima subendotelial, ampliándose los límites de la lesión. Las enzimas, citocinas y factores de crecimiento liberados por ellos pueden producir un daño mayor y necrosis (Ross, 1993; Libby, 2012).

- *Formación del núcleo necrótico*:

El núcleo necrótico es el resultado de:

- Necrosis celular y apoptosis de macrófagos, células endoteliales y de la musculatura lisa.

- Aumento de la actividad proteolítica: los macrófagos y las células de la musculatura lisa liberan enzimas especializadas como metaloproteinasas de la matriz (MMP) y otras que provocan la degradación de las fibras de colágeno que forman la matriz extracelular.

- Acumulación de lípidos (Ross, 1993; Glass *et al.*, 2001; Libby, 2012).

- *Formación de nuevos vasos sanguíneos (angiogénesis):*

En las arterias normales, la tensión parcial del oxígeno en la capa media está regulada por los niveles de oxígeno en la luz arterial y en la luz de los *vasa vasorum*. El

aumento de espesor en la pared arterial, debido al crecimiento de la placa de ateroma, provoca una hipoxia en la lesión que induce a un aumento en la expresión de moléculas angiogénicas que inducen la formación de nuevos vasos contribuyendo al crecimiento de la lesión. Esto es un factor de riesgo añadido, pues además de aumentar la inflamación, pueden romperse y provocar hemorragias. La evolución de la lesión aterosclerótica a partir de la capa fibrosa supone una gran vulnerabilidad a la rotura o ulceración, habitualmente en los sitios más finos, con la posible formación repentina de trombos, lo que causa la mayoría de las complicaciones agudas de la arteriosclerosis como el infarto de miocardio (Ross, 1993; Glass *et al.*, 2001; Libby, 2012).

1.2.3 Factores de riesgo

Como hemos citado anteriormente, los factores de riesgo para el desarrollo de la arteriosclerosis son diversos. Para el objetivo de la presente tesis doctoral nos vamos a centrar en la disfunción endotelial asociada a Angiotensina-II y humo de tabaco.

1.2.3.1 Angiotensina II

1.2.3.1.1 Consideraciones generales

La Ang-II, constituye el principal péptido efector del sistema renina-angiotensina (SRA). Desde hace tiempo se conoce su papel central en la regulación del tono vascular y la presión arterial y del equilibrio hidroelectrolítico y, más recientemente, se sabe de su capacidad de controlar el crecimiento celular; pero también hay cada vez más evidencias de que puede inducir respuesta inflamatoria en la pared vascular, respuesta que está implicada en la patogenia de muchas enfermedades como hipertensión, enfermedades cardiovasculares (infarto de miocardio y arteriosclerosis) y enfermedades renales. En particular, se sabe que la Ang-II promueve importantes alteraciones estructurales y funcionales a través de la activación de complejos efectos celulares, especialmente en las células endoteliales y las células de la musculatura lisa vascular (Piqueras *et al.*, 2000; Alvarez *et al.*, 2001; Brasier *et al.*, 2002; Volpe *et al.*, 2002; Alcazar *et al.*, 2003; Alvarez *et al.*, 2004; Watanabe *et al.*, 2005; Mateo *et al.*, 2006; Abu Nabah *et al.*, 2007; Mateo *et al.*, 2007b). Así, la Ang-II presenta una importante actividad moduladora del proceso aterogénico, induciendo la producción de especies reactivas del oxígeno (ERO), citocinas inflamatorias y quimiocinas y aumento de

expresión de distintas MAC (Piqueras *et al.*, 2000; Alvarez *et al.*, 2001; Brasier *et al.*, 2002; Alvarez *et al.*, 2004; Mateo *et al.*, 2006; Mateo *et al.*, 2007b; Rius *et al.*, 2013b).

1.2.3.1.2 Producción de la Ang-II

Tradicionalmente, el SRA ha sido descrito como un sistema endocrino en que la renina, enzima proteolítica producida y almacenada en el aparato yuxtaglomerular del riñón, actúa sobre el angiotensinógeno, una globulina α_2 circulante de origen hepático, y lo escinde en el enlace Leu-Val para formar la angiotensina-I (Ang-I), decapéptido inactivo. A su vez, la Ang-I es transformada por la acción de la enzima convertidora de la Ang-I (ECA), enzima muy ampliamente distribuida pero producida mayoritariamente en el endotelio pulmonar, que escinde los dos aminoácidos (His-Leu) del extremo C-terminal para formar la Ang-II.

La Ang-II, no es sólo una hormona endocrina que se produce y actúa en la circulación, sino que también se forma en muchos tejidos como cerebro, riñón, corazón y vasos sanguíneos, lo cual sugiere su función como hormona paracrina y autocrina (de Gasparo *et al.*, 2000). Además del componente sistémico, el SRA tiene otro componente tisular (local), por tanto, son capaces de producir Ang-II a nivel local (Berry *et al.*, 2001a; Berry *et al.*, 2001b; Volpe *et al.*, 2002). La ECA tisular está presente en órganos importantes como corazón, cerebro, vasos sanguíneos, corteza suprarrenal, riñón y útero (Berry *et al.*, 2001b). Los vasos sanguíneos son el lugar de mayor producción de Ang-II ; en ellos se han encontrado todos los componentes del SRA, excepto la renina, por lo que la producción local de Ang-II en el intersticio vascular parece depender de la renina circulante (Berry *et al.*, 2001b).

Alternativamente, la Ang-II se puede generar por otras rutas enzimáticas diferentes a la ECA (rutas “no-ECA”), a nivel de tejidos (Berry *et al.*, 2001b; Volpe *et al.*, 2002). Se genera directamente a partir de angiotensinógeno, gracias a la acción del tPA, la catepsina G y la tonina. A partir de la Ang-I, con la quimasa (muy importante en la generación local de Ang-II en corazón, riñón y vasos) y la catepsina G (Akasu *et al.*, 1998; Berry *et al.*, 2001b; Alcazar *et al.*, 2003; Li *et al.*, 2004). Estas rutas no-ECA son funcionalmente importantes a nivel vascular y se estima que la Ang-II formada por rutas no-ECA representa un 40% del total de la Ang-II humana, lo que sugiere que no se puede lograr la completa supresión del SRA únicamente a través de la inhibición de la ECA (Figura 6).

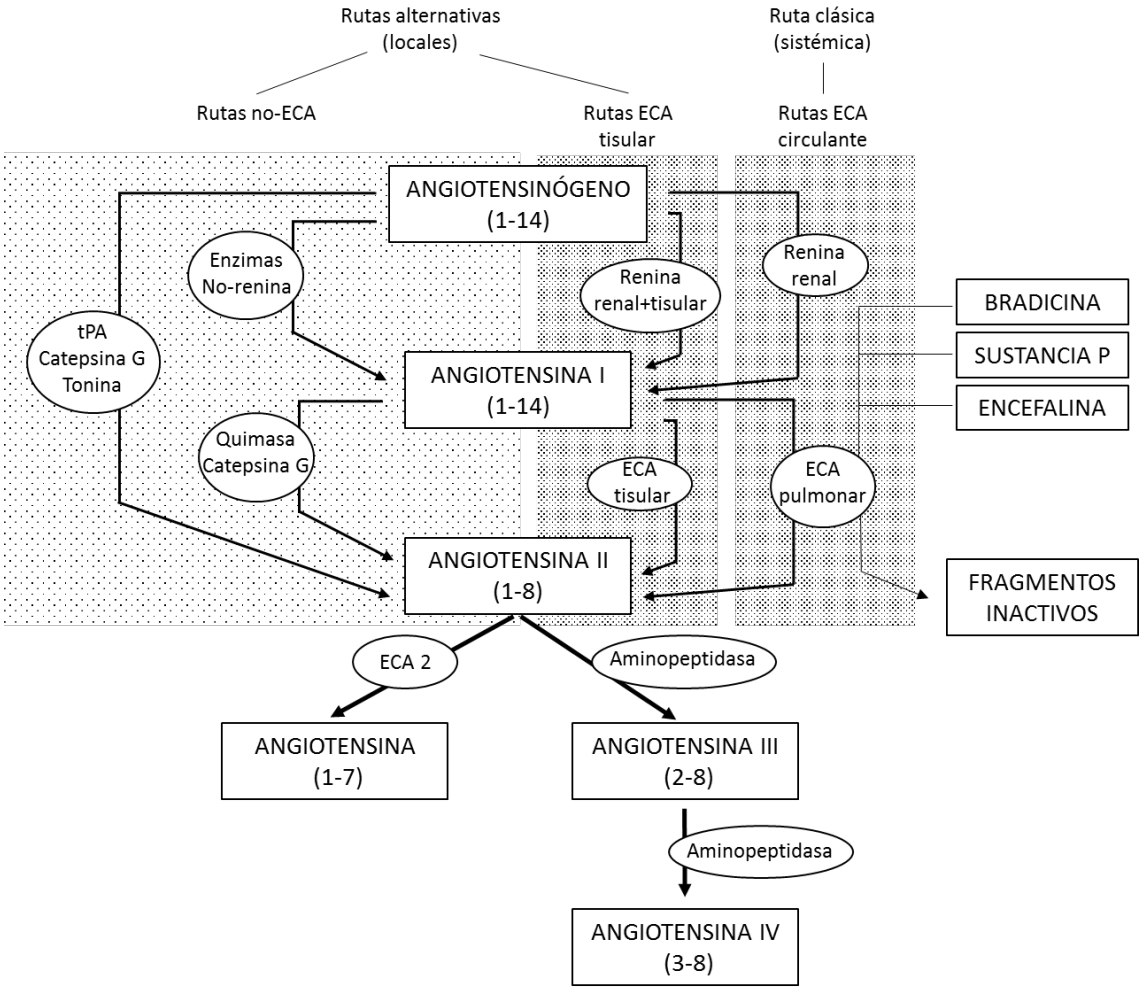

Figura 6: Metabolismo del angiotensinógeno para la generación de las hormonas peptídicas del sistema renina-angiotensina.

La respuesta inflamatoria vascular parece estar más relacionada con la Ang-II generada localmente que con la circulante, y muchos componentes enzimáticos tisulares implicados en la síntesis de Ang-II, están presentes en la placa aterosclerótica (Brasier *et al.*, 2002).

1.2.3.1.3 Caracterización de los receptores de Ang-II

La Ang-II media sus efectos al interaccionar con receptores específicos localizados en la membrana plasmática de sus células diana (de Gasparo *et al.*, 2000; Liu *et al.*, 2007). Los dos tipos principales, a los cuales se deben la mayoría de dichos efectos, son los receptores de tipo 1 (AT_1) y los receptores de tipo 2 (AT_2). Los AT_1 son los receptores a los que se atribuye la mayoría de las acciones clásicas y bien conocidas de esta hormona peptídica (vasoconstricción, liberación de aldosterona, sed, hipertrofia cardiaca, inflamación, etc.) (Unger *et al.*, 1996; Ardaillou, 1998; Piqueras *et al.*, 2000;

Berry *et al.*, 2001b; Alvarez *et al.*, 2004; Mateo *et al.*, 2006; Mateo *et al.*, 2007b). También se ha descrito la existencia de receptores diferentes a los anteriores como el AT_3, el AT_4 y otros, que no han sido completamente caracterizados; algunos de ellos son específicos para los metabolitos activos de Ang-II (Unger *et al.*, 1996; Ardaillou, 1998; Berry *et al.*, 2001b).

1.2.3.1.3.1 Caracterización de los receptores AT1

Los receptores AT_1 están distribuidos abundantemente y en numerosos tejidos adultos: sistema cardiovascular, riñones, glándulas suprarrenales, hígado, cerebro y pulmones (Warnholtz *et al.*, 1999; Kim *et al.*, 2000). Dentro del sistema cardiovascular, en los vasos, los receptores AT_1 se encuentran principalmente en las células de la musculatura lisa vascular, en las células endoteliales y en la adventicia. En el corazón, están presentes en los miocitos y en los fibroblastos (Berry *et al.*, 2001b; Brasier *et al.*, 2002). También se expresan en los leucocitos circulantes, principalmente en monocitos y PMNs (Shimada *et al.*, 1978; Ito *et al.*, 2001).

En roedores, el receptor AT_1 incluye dos subtipos funcionalmente diferentes: AT_{1A} y AT_{1B} (Ardaillou, 1998; Berry *et al.*, 2001b).

1.2.3.1.3.2 Caracterización de los receptores AT2

En el caso de los receptores AT_2, su expresión es muy marcada y amplia sólo en los tejidos fetales en desarrollo, ya que ésta decrece rápidamente tras el nacimiento (Henrion *et al.*, 2001). Así, en el adulto, los receptores AT_2 se expresan en niveles relativamente bajos y quedan restringidos a algunos territorios vasculares. También se han encontrado en corazón, útero, ovario, páncreas y, sobre todo, en médula adrenal y ciertos núcleos del cerebro (Ardaillou, 1998; Warnholtz *et al.*, 1999; Berry *et al.*, 2001a; Henrion *et al.*, 2001). La distribución del receptor AT_2 en el territorio vascular todavía no está bien caracterizada: no es homogénea sino que está sujeta a cambios según la edad, la especie, el tipo de vaso y determinadas condiciones como el embarazo o situaciones patológicas (hipertensión, entre otras) (Henrion *et al.*, 2001).

1.2.3.1.4 Efectos mediados por los receptores AT_1 y AT_2

Las acciones de la Ang-II se deben a su acción directa sobre sus receptores, a su acción indirecta a través de la liberación de otros factores, o bien, a su interacción con cascadas de señalización intracelular de otras sustancias (agentes vasoactivos, factores

de crecimiento y citocinas). Las respuestas finales son el resultado de la combinación de los efectos mediados por la interacción con sus receptores AT_1 y AT_2 (Berry *et al.*, 2001a). Estos efectos se recogen en la tabla 1.

AT_1	**AT_2**
Vasoconstricción	Vasodilatación
Proliferación celular	Inhibición del crecimiento celular
Hipertrofia celular	Apoptosis
Expansión de la matriz vascular	Síntesis de colágeno
Antinatriuresis	Natriuresis
Producción de ERO	Acciones antioxidantes
Liberación de ET	Producción de NO
Peroxidación lipídica	
Expresión de MAC	
Secreción de quimiocinas	
Secreción de aldosterona	
Secreción de vasopresina	
Sed	

Tabla 1: Principales efectos de la activación de los receptores AT_1 y AT_2. (ET: endotelina).

1.2.3.1.5 Ang-II y reclutamiento leucocitario

Cuando se produce inflamación o un daño vascular, estímulos proinflamatorios favorecen la adhesión de los leucocitos al lecho vascular. El primer estudio que relaciona Ang-II con la adhesión y activación leucocitaria se publicó en 1994 (Hahn, Jonas et al. 1994). Este estudio, describe tanto la expresión del receptor AT_1 de Ang-II en monocitos humanos, como el aumento de la adhesión de éstos a células endoteliales humanas estimuladas con Ang-II (Hahn *et al.*, 1994). Desde entonces, se han llevado acabo numerosos estudios que mediante enfoques directos e indirectos han evaluado los efectos y los mecanismos subyacentes de la activación de células endoteliales y leucocitos inducida por Ang-II. Hoy en día, no hay duda de la relevancia de esta hormona peptídica en el tráfico y la infiltración leucocitaria relacionada con diversos trastornos cardiovasculares.

1.2.3.1.5.1 Rodamiento leucocitario

La activación de las células endoteliales tiene como resultado la expresión en su superficie de selectinas (E- y P-selectina) que facilitan la adhesión inicial y el

rodamiento de leucocitos sobre el endotelio. La interacción de estas moléculas con receptores específicos expresados en la superficie de los leucocitos tales como el ligando para la glicoproteína P-selectina-1 (PSGL-1), ligando para la E-selectina-1 (ESL-1), CD44 y otros ligandos glicosilados están bien caracterizados (Ley *et al.*, 2007; Phillipson *et al.*, 2011).

Varios estudios han demostrado, mediante el bloqueo de estas moléculas usando anticuerpos anti-selectinas, la participación de las mismas en la adhesión y el rodamiento leucocitario inducido por Ang-II. En este contexto, un primer estudio de los mecanismos implicados en el reclutamiento de leucocitos por Ang-II *in vitro* mediante ensayos de adhesión reveló que en las células endoteliales coronarias de aorta, tras 4 h de incubación con Ang-II, se producía la adhesión de células HL-60 bajo condiciones de flujo (Grafe *et al.*, 1997). Estas respuestas fueron mediadas principalmente por un aumento en la expresión de E-selectina, ya que el bloqueo específico de esta CAM fue capaz de disminuir el aumento en el reclutamiento leucocitario inducido por Ang-II (Grafe *et al.*, 1997). Dado que las células endoteliales cultivadas *in vitro* son incapaces de expresar P-selectina tras varios pases (Kanwar *et al.*, 1995), era necesario investigar relevancia de las selectinas *in vivo*.

Estudios posteriores realizados en vénulas postcapilares de la microcirculación mesentérica de la rata, la acumulación de neutrófilos fue mediada principalmente por un efecto directo de Ang II sobre las células endoteliales, causando un rápido aumento en la expresión de P- selectina (menos de 15 min) a través de la interacción con su receptor AT_1 (Piqueras *et al.*, 2000). El bloqueo de esta CAM redujo las interacciones leucocito-endotelio inducidas por Ang -II dentro de la primera hora post- estimulación. En tiempos posteriores (4 h), tras una inyección intraperitoneal de Ang-II, la expresión P y E-selectina fue detectada en las vénulas postcapilares de la microcirculación mesentérica (Alvarez *et al.*, 2004). Mientras que la administración de un anticuerpo neutralizante contra P-selectina, consiguió reducir drásticamente las respuestas inducidas por Ang II, el bloqueo de E-selectina no resultó en ningún efecto significativo. Sin embargo, la administración combinada de ambos anticuerpos disminuyó todos los parámetros hasta niveles basales (Alvarez *et al.*, 2004).

En territorio arteriolar, la implicación de ambas selectinas en la adhesión de leucocitos al endotelio, también ha sido demostrada, ya que cuando P-, E- o ambas

selectinas eran bloqueadas, se observó un patrón de respuesta similar al observado en las vénulas post-capilares (Alvarez *et al.*, 2004). Sin embargo en las arteriolas, al contrario de lo observado en las vénulas post-capilares, era necesario la estimulación con Ang II durante varias horas para obtener un incremento significativo de las interacciones leucocito-endotelio. En este territorio vascular, no se observaron leucocitos en fase de rodamiento y fueron los monocitos las principales células que se adherían al endotelio arteriolar y no los neutrófilos como sucedía en el endotelio venular (Alvarez *et al.*, 2004). Por otra parte, la adhesión retardada observada en los leucocitos de las arteriolas, con respecto a la observada en las vénulas, podría indicar que en las arteriolas, la adhesión de leucocitos requiere la liberación adicional de otros mediadores proinflamatorios. De hecho, un estudio posterior reveló que, en las arterias, la expresión de TNF-α es necesaria para promover la adhesión selectiva de células mononucleares inducida por Ang-II (Mateo *et al.*, 2007b).

L-selectina, que también media del rodamiento de leucocitos, se expresa constitutivamente en la mayoría de los leucocitos y es liberada rápidamente después de la activación de leucocitos (Ley *et al.*, 2007; Phillipson *et al.*, 2011). Sin embargo, estudios demuestran que Ang-II no provocó ningún efecto directo sobre la expresión de L-selectina en los neutrófilos ni monocitos (Piqueras *et al.*, 2000) lo que sugiere que el reclutamiento inicial de leucocitos provocada por esta hormona peptídica se debe a su efecto sobre las células endoteliales y no sobre los leucocitos.

1.2.3.1.5.2 Activación leucocitaria

Durante el rodamiento, los leucocitos están expuestos a señales proinflamatorias liberadas por el endotelio activado, que causan a su vez la activación de las integrinas (pasan a un estado de alta avidez por sus receptores), siendo este paso importante para que se produzca la adhesión firme.

Por otro lado, la liberación de agentes quimiotácticos como las quimiocinas también provocan la activación leucocitaria. En este sentido, numerosos estudios han demostrado que Ang-II es capaz de aumentar la producción de varias quimiocina y citocinas proinflamatorias implicadas en la infiltración leucoctaria.

- *Quimiocinas*: la Ang-II aumenta la producción y liberación de las quimiocinas-CC MCP-1/CCL2, *macrophage inflammatory protein 1-α (*MIP-1α/CCL3), *regulated on activation, normal T cell expressed and secreted*

(RANTES/CCL5), MCP-3/CCL7 y eotaxina-3/CCL26, quimiotácticas principalmente para leucocitos mononucleares, y CXC como IL-8/CXCL8 e interferon-γ-induced protein 10 (IP-10/CXC10) principalmente quimiotácticas y activadoras de neutrófilos. Asimismo y más recientemente, nuestro grupo ha demostrado la implicación de la quimiocina CX_3C, CX_3CL1 o fractalquina, en la infiltración leucocitaria inducida por Ang-II. El receptor AT_1 es el principal receptor involucrado en ello, si bien la producción de RANTES/CCL5 parece ser también dependiente del AT_2. Así, la Ang-II participa igualmente en la activación, quimiotaxis y migración de las células inflamatorias hacia los tejidos (Wolf *et al.*, 1997; Nabah *et al.*, 2004; Mateo *et al.*, 2006; Abu Nabah *et al.*, 2007; Rius *et al.*, 2013b).

- *Citocinas*: algunas citocinas producidas en respuesta a la Ang-II son la IL-6, el TNFα y la IL-1 (Berry *et al.*, 2001b; Ruiz-Ortega *et al.*, 2001; Mateo *et al.*, 2006; Mateo *et al.*, 2007b). Esta producción parece mediada, al menos *in vitro*, por receptores AT_1; en el caso de la IL-1 también estarían implicados los AT_2 (Ruiz-Ortega *et al.*, 2001). La Ang-II favorece, la infiltración leucocitaria a través de la síntesis y liberación citocinas proinflamatorias que parecen las responsables de la liberación subsiguiente de quimiocinas; además, la IL-6 promueve la generación de angiotensinógeno en la pared vascular, por lo que incrementa la producción local de Ang-II y, por ello, la perpetuación de la inflamación vascular (Satou *et al.*, 2008).

Dos tipos de integrinas están afectadas por este proceso, las integrinas β_2 y las integrinas α_4. En estudios *in vivo* realizados por nuestro grupo de investigación, se observó que tanto a nivel venular como arteriolar, el bloqueo con un anticuerpo anti-integrina β_2, redujo la adhesión leucocitaria inducida por Ang-II (Alvarez *et al.*, 2004). Además, en estudios previos *in vitro* de nuestro grupo se demostró que el estímulo con Ang-II no era capaz de inducir un aumento directo en la expresión de integrinas β_2 en la superficie se los leucocitos (Piqueras *et al.*, 2000), por tanto dicho efecto puede deberse a que Ang-II promueve la activación del endotelio, la liberación de quimiocinas y por tanto la activación de las integrinas β_2 de los leucocitos que están interaccionando con el endotelio (Alvarez *et al.*, 2004)

Por otra parte, el bloqueo de las integrinas α4 solo produjo una disminución en la adhesión leucocitaria en el territorio venular y no en el arterial. (Alvarez *et al.*, 2004).

1.2.3.1.5.3 Adhesión

En la cascada de migración leucocitaria los leucocitos deben adherirse de manera firme al endotelio como paso previo a la migración.

Mediante técnicas inmunohistoquimicas, se ha observado que en el territorio vascular del mesenterio de la rata, la expresión de ICAM-1 se observa de forma constitutiva. Así mismo tras 4 horas de estímulo con Ang-II, tanto en vénulas como en arteriolas, la expresión de ICAM-1 y VCAM-1 se vio significativamente aumentada (Alvarez *et al.*, 2004). En el mismo estudio se realizaron ensayos *in vivo* observando que el pretratamiento con un anticuerpo anti-ICAM-1 no afectó a al aumento en la adhesión inducido por Ang-II en las arteriolas aunque produjo una disminución significativa de este parámetro en territorio venular. Lo que sugiere que en arterias, otros ligando para intergrinas β_2 como ICAM-2 o fibrinógeno podrían estar involucrados en este proceso (Alvarez *et al.*, 2004).

VCAM-1 es el principal ligando de las integrinas α4, el estímulo con Ang-II produce un aumento en su expresión en células endoteliales (Alvarez *et al.*, 2004) que esta mediado a través del receptor AT_1 (Pueyo *et al.*, 2000).

En un trabajo posterior llevado a cabo por nuestro grupo de investigación, se vio que Ang II, a través de la interacción con su receptor AT_1, induce aumento de expresión de fractalquina y acumulación selectiva de leucocitos mononucleares en el endotelio arterial, describiendo un comportamiento diferencial del endotelio arterial y venoso murino y humano en respuesta a este estímulo (Rius *et al.*, 2013c).

1.2.3.1.5.4 Migración

Esta ampliamente demostrada la capacidad de Ang-II de producir un aumento de la permeabilidad vascular favoreciendo así la migración de células a través del endotelio (Victorino *et al.*, 2002).

Por otra parte, estudios histológicos, han observado que tras 4 horas de exposición a Ang-II las células mononucleares se infiltraban en las arteriolas y migraban a través del endotelio (Alvarez *et al.*, 2004). La migración de leucocitos inducida por Ang-II se observó mediante microscopia intravital de forma clara en vénulas postcapilares tras 4 h de exposición al péptido. Este efecto estuvo, en parte mediado, por la interacción de las integrinas β2-ICAM-1, ya que la administración de anticuerpos contra estas moléculas

de adhesión redujo significativamente esta repuesta en los leucocitos. Además, los leucocitos que migraron a la cavidad peritoneal en repuesta a Ang-II presentaban un claro aumento en la expresión de esta integrina β_2 (Alvarez *et al.*, 2004)

1.2.3.1.6 Rutas de señalización intracelular de Ang-II

El receptor de Ang II está acoplado a proteínas G (Figura 7) y consta de tres subunidades Gαq/11, Gα12/13 y Gβγ (Hines et al., 2003). Su activación conduce a una cascada de señales intracelulares en la que participan la fosfolipasa C (PLC), la fosfolipasa A_2 (PLA_2), y la fosfolipasa D (PLD). La activación de la PLC produce inositol 1,4,5-trifosfato (IP_3) que conduce a aumentos de Ca^{2+} intracelular y diacilglicerol (DAG), capaz de activar la proteína quinasa C (PKC). Por otro lado, la activación de la PLA_2 causa la liberación de ácido araquidónico a partir de fosfatidilcolina. Por último, la activación de la PLD sobre el ácido fosfatídico conduce a la generación DAG, el cual, como ya se ha indicado, activa a la PKC (Touyz *et al.*, 2000).

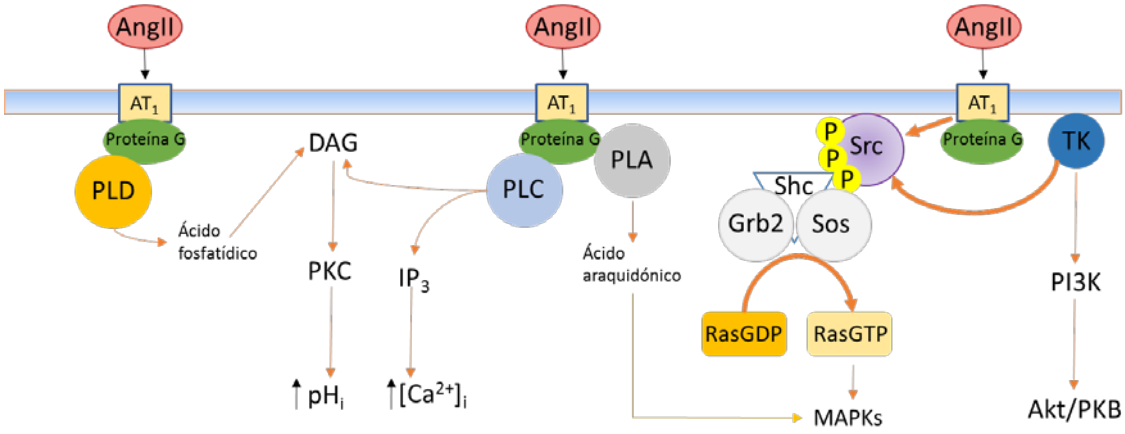

Figura 7: Rutas de activación celular de señalización intracelular de la Ang-II al unirse a su receptor AT1. PI3K fosfoinositol-3-quinasa, PKC proteina quinasa C, Akt/PKB, protein quinasa B, la via de activación RAS, está comprendida por una serie de tirosina cinasas: Src, Grb2, Sos, que participan en cadena en la fosforilacion de Ras, que finalmente activan la cascada de las MAPK.

Estos segundos mensajeros, a su vez, activan múltiples vías de señalización, por ejemplo, la vía de las proteínas quinasas activadas por mitógenos (MAPK), incluyendo quinasas reguladas por señales extracelulares 1 y 2 (ERK1/2), p38 MAPK, quinasa Jun N -terminal (JNK) y proteína quinasa activada por estrés (SAPK), tirosin quinasas, incluyendo $pp60^{c\text{-}src}$ quinasa (c- src), quinasa de adhesión focal (FAK), y Janus quinasas (JAK2 y Tyk2), receptores de tirosin quinasas incluyendo el receptor del factor de crecimiento epidérmico (EGFR), el factor de crecimiento derivado de plaquetas (PDGF) o

el factor de crecimiento insulínico tipo 1 (IGF) , y el factor nuclear-*k*B (NFKB). La activación de estos mediadores está relacionada con procesos de disfunción endotelial, inflamación, proliferación , angiogénesis, hipertrofia, fibrosis, y trombosis (Mehta *et al.*, 2007; Oro *et al.*, 2007; Aplin *et al.*, 2009; Rius *et al.*, 2013b; Montezano *et al.*, 2014; Domazet *et al.*, 2015).

Las vías de señalización intracelular mediadas por Ang-II más relevantes para la adecuada comprensión de esta Tesis Doctoral son:

1 Activación del complejo nicotinamida adenina dinucleótido fosfato oxidasa (NADPH oxidasa) y la generación de ERO.

Esta ampliamente documentado que Ang-II impide la función normal del endotelio descendiendo la biodisponibilidad del óxido nítrico ($NO^{\bullet}$) (Loot *et al.*, 2009; Nguyen Dinh Cat *et al.*, 2013). Estos efectos pueden estar mediados a través de la producción de anión superóxido que reacciona con el NO, lo que tiene como consecuencia la formación de peroxinitritos que son un potente oxidante. Por otra parte, la reacción entre el NO y O_2 disminuye la biodisponibilidad del NO y por tanto su capacidad de mantener la función normal del endotelio produciéndose por tanto disfunción endotelial (Loot *et al.*, 2009; Nguyen Dinh Cat *et al.*, 2013).

Además de su efecto sobre el NO, las ERO (principalmente H_2O_2) tienen efectos importantes en la modulación de varias vías de señalización redox-sensibles, presentes en las células endoteliales y que tienen efecto sobre la expresión de genes y proteínas indispensables para diversas funciones celulares. Como consecuencia se puede aumentar el crecimiento celular, la proliferación, la migración leucocitaria, la subsistencia o la reorganización del citoesqueleto. También pueden afectar a la forma celular, promover la expresión de MAC, la secreción de citocinas inflamatorias, etc. (Dworakowski *et al.*, 2008).

En resumen, el aumento vascular del nivel de ERO es el mecanismo principal a través del cual Ang-II está involucrada en procesos patológicos como la disfunción endotelial, la proliferación de células de músculo liso vascular y la aterosclerosis (Brasier *et al.*, 2002; Alcazar *et al.*, 2003).

Numerosas evidencias indican que Ang-II es capaz de activar la NADPH oxidasa (Nox) que es una importante fuente de especies reactivas del oxígeno (ERO) en las

células vasculares (Mehta *et al.*, 2007). Aunque, el mecanismo de activación de la NADPH oxidasa por Ang II es compleja y aún está poco estudiado, se sabe que las vías de NADPH están involucrados en procesos proinflamatorios y angiogénicos a través de la activación de numerosas moléculas de señalización incluyendo MAPK (JNK, p38 MAPK, ERK1/2 o ERK5), metaloproteinasas de la matriz, factores de transcripción (NFkB o AP1), STAT/JAK y canales iónicos (Garrido *et al.*, 2009; Majzunova *et al.*, 2013; Rius *et al.*, 2013b).

En el ser humano, hay cinco isoformas diferentes NADPH oxidasa llamados Nox1 hasta NOX5, y dos oxidasas relacionadas, DUOX1 y DUOX2, así como dos homólogos adicionales de las unidades citosólicas, NoxO1 y NoxA1 (Touyz *et al.*, 2011). Aunque todas las enzimas Nox son capaces de aumentar la concentración de ROS intracelulares, existen diferencias importantes en cuanto a su activación, composición de la subunidad, localización y expresión. A este respecto, Nox2, Nox4 y NOX5 son las isoformas más abundantes de NADPH oxidasa en las células endoteliales (Lassegue *et al.*, 2010) y son inducidas por Ang-II (Manea *et al.*, 2010; Montezano *et al.*, 2010; Douglas *et al.*, 2012; Rius *et al.*, 2013b), sólo NOX5 parece jugar un papel importante en la adhesividad endotelial arterial inducida por Ang-II, ya que Nox5 media tanto el aumento en la expresión de VCAM-1 y fractalquina/CX_3CL1 así como el consecuente aumento en la adhesión de células mononucleares (Montezano *et al.*, 2010; Rius *et al.*, 2013b).

A través de la activación de la NAD(P)H oxidasa, se genera anión superóxido ($O_2^{\bullet-}$), que es a su vez es transformado a peróxido de hidrógeno (H_2O_2), por la superóxido dismutasa. El H_2O_2 por la acción de la catalasa genera $O_2^{\bullet-}$ y agua. $O_2^{\bullet-}$y H_2O_2 pueden interactuar en presencia de hierro para generar radical hidroxilo ($OH^{\bullet}$), una molécula altamente reactiva. El $O_2^{\bullet-}$ además, se puede combinar con NO para formar peroxinitritos ($ONOO^-$), que también producen $^{\cdot}OH$ (Ray *et al.*, 2005).

2. Activación de la vía RhoA

La familia de las Rho GTPasas (guanina trifosfatasas) son reguladores del citoesqueleto y afectan a la migración celular, adhesión célula-célula, y adhesión célula-matriz. La activación de RhoA y su efector Rho-quinasa, está tomando cada vez más relevancia como mecanismo implicado en la vasoconstricción inducida por Ang II y en consecuencia está relacionado con la fisiopatología de las enfermedades vasculares (Loirand *et al.*, 2006). Además, se ha demostrado que RhoA puede ser activada

directamente por ERO (Aghajanian *et al.*, 2009). Otros estudios han observado que RhoA puede regular la activación de miembros de la familia de las MAPK, tales como la p38 MAPK (Marinissen *et al.*, 2004), siendo capaz esta ultima de modular la transcripción de varios genes a través de la activación del factor NF-kB (Wang *et al.*, 2006; Rius *et al.*, 2010); estando tanto p38 MAPK como NF-kB implicados en las respuestas inflamatorias y en el reclutamiento de células mononucleares inducido por Ang-II (Rius *et al.*, 2013c).

3. Activación de la vía PI3K/AkT/mTOR

La ruta de señalización homólogo al oncogén viral de timoma murino (AKT)/diana de rapamicina en células de mamífero (mTOR)/proteína ribosomal S6 de 70 kDa cinasa 1 (p70S6K1) tiene una elevada importancia en diversas funciones celulares tales como el ciclo celular, la supervivencia, la síntesis de proteínas y la angiogénesis (Grasso *et al.*, 2014).

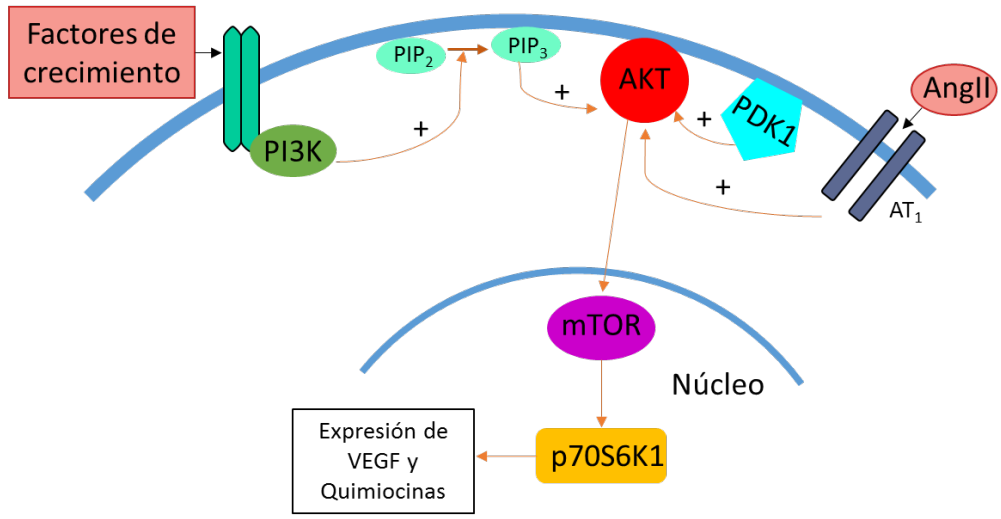

Figura 8: Esquema de la ruta PI3K/AKT/mTOR/p70S6K1

La estimulación de la ruta AKT/mTOR/p70S6K1 (Figura 8) se debe principalmente a la activación de la enzima fosfatidilinositol-3 cinasa (PI3K), concretamente la PI3K de clase I, por receptores con actividad tirosina cinasa en respuesta a factores de crecimiento como el factor de crecimiento epitelial (EGF), el factor de crecimiento derivado de plaquetas (PDGF) y el factor de crecimiento insulínico de tipo 1 (IGF-1). La activación de dicha via puede llevarse a cabo por la acción de diferentes quimiocinas, tales como KC/CXCL1, MCP-1/CCL2 o RANTES/CCL5 (Huang *et al.*, 2009; Mizutani *et al.*, 2009; Kuo *et al.*, 2012), a través

del reconocimiento de sus receptores GPCRs, superfamilia a la que también pertenecen los receptores AT1 y AT2 de Ang-II. Una vez activada, esta enzima genera fosfatdilinositol 3, 4, 5-trifosfato (PIP3) a partir de fosfatidilinositol 4, 5-bifosfato (PIP2). PIP3 interacciona entonces con los dominios homólogos de plecstrina (PH), presentes en diversas proteínas, siendo dos de ellas la proteína cinasa B AKT y el fosfoinosítido dependiente de cinasa 1 (PDK1). Tanto PIP3 como PDK1 participan en la activación de AKT. Una vez activada AKT, para lo cual debe tener lugar un mecanismo de fosforilación dual, ésta ejerce su función cinasa fosforilando la secuencia consenso RXRXXS/TB, donde X hace referencia a cualquier aminoácido y B a cualquier aminoácido hidrofóbico. Dicha secuencia se encuentra presente en diversas proteínas, siendo una de ellas mTOR, que regula procesos que incluyen la traducción de proteínas y la biogénesis de los ribosomas. Una vez activada, mTOR estimula diversos sustratos entre los que se encuentra la proteína efectora citosólica p70S6K1, que se activa por medio de diversos eventos de fosforilación y que junto a la proteína efectora nuclear p85S6K1 representan las dos isoformas de la proteína ribosomal S6 cinasa 1 (S6K1) (Grasso *et al.*, 2014).

En última instancia, la progresión de esta vía concluye en la expresión del factor de crecimiento del endotelio vascular (VEGF) y quimiocinas (Karnoub et al., 2008; Wang et al., 2014), por lo que algunos estudios han observado que la supresión de esta ruta inhibe la neovascularización patológica (Schnell *et al.*, 2008; Karar *et al.*, 2011; Pratheeshkumar *et al.*, 2012).

Estudios previos demuestran que la interacción de Ang-II/AT_1 a través de PI3K fosforila a AKT, y esta a su vez es capaz de activar la diana de la rapamicina en mamíferos (mTOR) (Taniyama *et al.*, 2004).

1.2.3.2 Humo de cigarro

Los estudios epidemiológicos demuestran que el hábito de fumar aumenta la incidencia de patología cardiovascular, incluso los fumadores pasivos también muestran mayor riesgo cardiovascular en comparación con los no fumadores (Bolinder *et al.*, 1994). Sin embargo, no se ha esclarecido cuales son los componentes de cigarro y los mecanismos responsables de esta asociación (Ambrose *et al.*, 2004).

1.2.3.2.1 Propiedades bioquímicas y físicas del humo de cigarro.

Convencionalmente los componentes del humo del cigarro se han separado en dos fases: la fase particulada y la fase gaseosa. La primera, se define como el material que es retenido cuando el humo del cigarro se hace pasar a través de un filtro de fibra de vidrio, que retiene aproximadamente el 99.9% del material particulado de tamaño >0.1 μm. La fase gaseosa, es el material que pasa a través del filtro.

La fase particulada contiene alrededor de 10^{17} radicales libres/g, y la fase gaseosa contiene $>10^{15}$ radicales libres/inhalación. Los radicales de la fase particulada tienen una larga vida media (horas a meses), mientras que los de la fase gaseosa tienen una vida media muy corta (segundos).

También el humo que es inhalado por los fumadores se divide en dos tipos: humo primario: que entra en la boca del fumador por la combustión directa del tabaco, y el humo alterno o secundario: que se emite por la combustión del extremo de cigarro. El humo primario contiene 8% de material particulado y 92% del componente gaseoso (Pryor et al., 1993). El humo del cigarro que está en el ambiente es una combinación del humo secundario (85%) y humo primario (15%). El humo secundario contiene relativamente mayor concentración de los componentes tóxicos gaseosos que el humo primario. De todos los constituyentes, la nicotina, presente en la fase particulada, es la sustancia adictiva.

1.2.3.2.2 Humo de cigarro, disfunción endotelial y aterosclerosis

El humo de cigarro predispone a diferentes patologías asociadas a la aterosclerosis, entre las cuales se puede mencionar, angina estable, patología coronaria aguda, muerte súbita, y accidentes cerebrovasculares (Stolle *et al.*, 2010). El humo del cigarro altera la expresión y actividad de la enzima NO sintasa, comprometiendo la reactividad vascular (Ferrer *et al.*, 2009). También el NO participa en la regulación de la adhesión leucocitaria, la activación plaquetaria, y la trombosis (Gkaliagkousi *et al.*, 2011).

La respuesta inflamatoria es un componente esencial para el inicio y evolución de la aterosclerosis. Se ha descrito que el humo de tabaco aumenta entre un 20 y un 25% el número de leucocitos en sangre periférica (Smith *et al.*, 2001), los niveles de marcadores inflamatorios (Tracy *et al.*, 1997) y de citocinas proinflamatorias (Kalra *et al.*, 1994; Shen *et al.*, 1996; Takahashi *et al.*, 2010). Los monocitos aislados de personas

fumadoras muestran mayor expresión de la integrina CD11b/CD18, que aumenta la adhesión de monocitos (Weber *et al.*, 1996).

Por otro lado, uno de los efectos del humo del cigarro es promover la aterosclerosis por el cambio del perfil lipídico del fumador, ya que éstos muestran niveles más elevados de LDL, colesterol y triglicéridos y disminución de HDL en comparación con los no fumadores (Craig *et al.*, 1989). El humo del cigarro también promueve la peroxídación lipídica y además las LDL oxidadas (LDLox), activan el endotelio para expresar MAC (Ambrose *et al.*, 2004).

El humo de cigarro tiene más de 4000 componentes conocidos, de los cuales sólo se han aislado unos pocos. El monóxido de carbono (CO), es uno de ellos, pero su efecto en la enfermedad atero-trombótica no ha sido bien evaluado. En un principio se le consideró el causante de las alteraciones cardiovasculares, pero existen datos que sugieren que el CO no participa en la aterosclerosis o la formación de trombos (Astrup *et al.*, 1979). Se sabe que los hidrocarbonos aromáticos policíclicos que se encuentran en la fracción particulada del humo de tabaco aceleran el proceso ateroscleróticó (Penn *et al.*, 1988).

La nicotina es el componente más estudiado, aunque es el que juega un papel importante en el incremento del gasto cardíaco, frecuencia cardíaca y presión arterial, su participación en los procesos atero-trombóticos genera controversia (Clouse *et al.*, 2000; Pellegrini *et al.*, 2001). En varios modelos, grandes dosis de nicotina favorecen la aparición de aterosclerosis. La mayoría de las evidencias sugieren que la nicotina, a concentraciones similares a las encontradas en los niveles sanguíneos de fumadores, tiene un efecto menor en el inicio y progresión de la aterosclerosis (Smith *et al.*, 2001; Sun *et al.*, 2001). De forma similar, el efecto de la nicotina en los factores de riesgo hemostáticos como plaquetas, fibrinógeno, t-PA, PAI-1, tiene un papel insignificante (Benowitz, 1997; Pellegrini *et al.*, 2001). Ya se mencionó que la nicotina es la sustancia adictiva del humo de cigarro, lo cual conduce a que el fumador mantenga el hábito y se exponga a los componentes dañinos.

Actualmente, el estrés oxidativo emerge con un papel relevante en la aterosclerosis. (Kojda *et al.*, 1999; Nedeljkovic *et al.*, 2003). En el humo de tabaco, los radicales libres provienen de: 1) de las fases particulada y gaseosa del humo del cigarro. 2) macrófagos circulantes y tisulares activados, 3) fuentes endógenas de ERO, como

eNOS desacopladas, xantina oxidasas (XO), NADPH ox y la cadena de transporte electrónico mitocondrial. La reacción entre radicales libre y NO, no sólo disminuye el NO disponible, sino que genera peroxinitritos, que aumentan el estrés oxidativo celular (Kojda *et al.*, 1999). Al aumentar el estrés oxidativo conjuntamente con la pérdida de efecto del NO el balance celular se desplaza hacia un ambiente proaterogénico y protrombótico (Ruberg *et al.*, 2002; Nedeljkovic *et al.*, 2003). Muchas de las alteraciones asociadas al humo de tabaco como la disfunción endotelial, efectos proinflamatorios en la pared arterial, efectos protrombóticos, aumento de la reactividad plaquetaria, disminución de la fibrinólisis y la peroxidación de lípidos se explican por el incremento del estrés oxidativo (Heitzer *et al.*, 2000; Guthikonda *et al.*, 2003; Kayyali *et al.*, 2003). Los agentes antioxidantes o aquellos que aumentan los niveles de NO mejoran o revierten los procesos proaterogénicos, proinflamatorios, y protrombóticos. Aunque el mecanismo responsable de las alteraciones cardiovasculares asociadas al humo de tabaco no se ha determinado, el estrés oxidativo parece que juega un papel crucial.

Nuestro grupo de investigación ha demostrado tanto *in vivo* como *in vitro*, que el humo de tabaco aumenta la adhesión de células mononucleares al endotelio arteriolar en un proceso dependiente de fractalquina/CX_3CL1(Rius *et al.*, 2013a). Mediante estudios realizados con leucocitos mononucleares de pacientes de EPOC se demostró que el bloqueo del eje CX_3CL1/CX_3CR1 reducía drásticamente la adhesión de dichas células al endotelio arterial estimulado con extracto de humo de tabaco (EHT) (Rius *et al.*, 2013a). Además, se observó que el EHT aumenta la expresión de CX_3CL1 y la adhesión de mononucleares al endotelio arterial a través un mecanismo de señalización celular redox-sensible que implicaba a Nox5 así como la subsiguiente activación de la p38 MAPK y del factor de transcripción NF-κB. En este mismo estudio, también se observó que el EHT, paralelamente a las vías redox, produjo un aumento de la expresión de CX_3CL1 y de la inflamación vascular mediante la síntesis y liberación de TNFα (Rius *et al.*, 2013a).

1.2.3.2.3 Enfermedad pulmonar obstructiva crónica

En el transcurso de los últimos años ha aumentado el interés por el estudio de diferentes aspectos de la enfermedad pulmonar obstructiva crónica (EPOC). Este avance se debe fundamentalmente al reconocimiento de la importancia de la EPOC como causa

de morbilidad, invalidez y mortalidad a nivel mundial. La Organización Mundial de la Salud estima que para el año 2020, la EPOC se ubicará en el tercer puesto de las causas más comunes de muerte y en el quinto lugar de las enfermedades discapacitantes (Lopez *et al.*, 1998). La SEPAR (Sociedad Española de Neumología y Cirugía Torácica), considera a la EPOC, un problema de salud por su repercusión social a consecuencia del aumento del tabaquismo, el envejecimiento de la población, la frecuencia de su agudización, y los elevados costes económicos que genera en los sistemas de salud (Izquierdo Alonso *et al.*, 2005).

1.2.3.2.3.1 Alteraciones morfológicas y funcionales de la EPOC.

La EPOC está considerada actualmente como una enfermedad multisistémica caracterizada por una inflamación sistémica y pulmonar (Sinden *et al.*, 2010; Malerba *et al.*, 2013; Choudhury *et al.*, 2014) que parece ser en última instancia responsable de varias comorbilidades de la EPOC (Sinden *et al.*, 2010; Decramer *et al.*, 2013; Choudhury *et al.*, 2014; Smith *et al.*, 2014). Entre ellas las más frecuentes son las enfermedades cardiovasculares (Sinden *et al.*, 2010; Decramer *et al.*, 2013; Choudhury *et al.*, 2014; Smith *et al.*, 2014). La enfermedad es una respuesta inflamatoria anormal de los pulmones, principalmente al humo del cigarro (también gases y partículas nocivas) que conduce a una disminución lenta, progresiva e irreversible de la ventilación pulmonar.

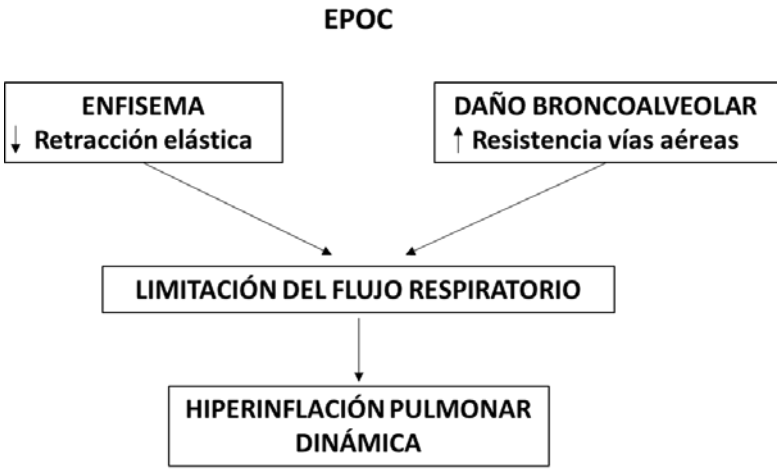

Figura 9: Alteraciones morfofuncionales responsables de la limitación del flujo espiratorio en pacientes con EPOC avanzada.

Las alteraciones morfológicas características de la EPOC avanzada son el daño bronquiolar y el enfisema, que se combinan en distintos grados produciendo limitación

crónica del flujo espiratorio. Esta limitación se debe principalmente a: 1) aumento de la resistencia de las vías aéreas pequeñas, secundaria a inflamación de la mucosa, la infiltración celular y fibrosis peribronquiolar y 2) por una disminución de la tracción que normalmente ejerce el tejido elástico pulmonar sobre las paredes de los bronquíolos, debido al enfisema y que es responsable de su colapso espiratorio precoz. La limitación del flujo espiratorio durante respiración tranquila conduce al atrapamiento aéreo o hiperinflación pulmonar dinámica (figura 9) (Manriquez *et al.*, 2004).

Añadido a los efectos pulmonares de la EPOC, la enfermedad afecta de forma significativa a otros órganos y sistemas. Estas alteraciones extrapulmonares asociadas a la patología se denominan efectos sistémicos de la EPOC. Las principales manifestaciones clínicas asociadas son la pérdida de peso, susceptibilidad a patologías cardiovasculares, alteraciones musculares y neurológicas severas. Los mecanismos involucrados en las manifestaciones sistémicas no se han esclarecido, pero se cree que son producto de alteraciones multifuncionales relacionadas a la inflamación, hipoxia tisular y estrés oxidativo, entre otras causas (Agusti, 2005).

1.2.3.2.3.2 Inflamación sistémica en EPOC

A nivel sistémico se puede detectar la misma reacción inflamatoria anómala al humo del cigarro que se observa en el pulmón. Desde el punto de vista clínico la malnutrición, la pérdida de peso y la disfunción de la musculatura esquelética, son las manifestaciones sistémicas más frecuentes de los pacientes EPOC, con una importante repercusión sobre la calidad de vida y pronóstico de los enfermos.

Durante la pasada década, las investigaciones en las manifestaciones sistémicas de la EPOC, han demostrado un aumento en los niveles de mediadores inflamatorios circulantes, como moléculas de fase aguda (proteína C reactiva, fibrinógeno) y citocinas (IL-6, IL-4 y TNFα) (Agusti, 2007; Foschino Barbaro *et al.*, 2007; Sin *et al.*, 2007; Barreiro *et al.*, 2008), los cuales no pueden ser amortiguados mediante aumento de la secreción de mediadores anti-inflamatorios como la IL-10.

Las células proinflamatorias son probablemente las encargadas de producir los efectos sistémicos. La probabilidad de que los monocitos circulantes liberen moléculas proinflamatorias, y contribuyan en la respuesta inflamatoria sistémica ha sido evaluada en pacientes EPOC estables. Los monocitos aislados de pacientes EPOC liberan significativamente más MMP-9, IL-6 y MCP-1. Además, existe activación de NFκB, lo

que sugiere que este factor de transcripción puede estar involucrado en la activación de monocitos circulantes de pacientes con EPOC (Aldonyte *et al.*, 2003). La activación de neutrófilos, conduce a la potenciación de la respuesta citotóxica y migratoria. Comparados con los controles, en los neutrófilos circulantes de pacientes EPOC, se observa un aumento en la expresión de CD11b/CD18, y son capaces de producir mayor cantidad de especies reactivas de oxígeno tanto en condiciones basales, como después de la estimulación *in vitro* (Noguera *et al.*, 2001).

La explicación más obvia de la inflamación sistémica, es que la patología se origine en el pulmón y de allí se extienda a otros órganos y sistemas. Sin embargo, no parece que los efectos extrapulmonares tengan su origen en la inflamación pulmonar, ya que los marcadores inflamatorios en el esputo y en el plasma no muestran una correlación directa (Vernooy *et al.*, 2002; Hurst *et al.*, 2006). En consecuencia, es poco probable que un exceso de mediadores inflamatorios desborde el compartimiento pulmonar, sino más bien, que el proceso inflamatorio se regule de diferente forma en los compartimientos pulmonar y sistémico (Michel *et al.*, 2001). A pesar de los numerosos estudios realizados con muestras pulmonares, en las que se detectó una disminución en el ratio de linfocitos T $CD4^+/CD8^+$ en pacientes EPOC, no hay suficientes estudios que revelen lo mismo en la circulación sistémica. Se ha descrito que el humo del cigarro por sí sólo puede desplazar el número de linfocitos $CD4^+$ y $CD8^+$, y que este efecto es reversible cuando se deja de fumar. Sin embargo, el hecho de que personas que han dejado el hábito de fumar presentan signos de inflamación sistémica, refuta la posibilidad de que los componentes del cigarrillo por sí mismos, constituyan el único factor responsable de la inflamación en los pacientes EPOC (Vernooy *et al.*, 2002). Varias vías independientes parecen estar involucradas en el proceso, como la hipoxia que es un problema recurrente en la EPOC. Ya que el mantenimiento de la homeostasis del oxígeno es vital para la supervivencia, los sistemas fisiológicos deben asegurar una óptima oxigenación de las células. El factor inducible por hipoxia-1 (HIF-1) juega un papel central para señalar la existencia de hipoxia a la maquinaria transcripcional del núcleo de todas las células. HIF-1 activa genes diana cuyos productos participan en la angiogénesis, el metabolismo energético, la eritropoyesis, la inflamación, la proliferación celular, el remodelado vascular y las respuestas vasomotoras (Calzada *et al.*, 2007; Perez-Amodio *et al.*, 2011).

Por otro lado, se sabe que el EHT aumenta los niveles de la citocina proinflamatoria TNFα (Mortaz *et al.*, 2009; Jeong *et al.*, 2010). En estudios previos se ha comprobado que existen niveles elevados de TNFα en el esputo y biopsias pulmonares de pacientes con EPOC (Keatings *et al.*, 1996; Mueller *et al.*, 1996; Gan *et al.*, 2004) y también se han encontrado incrementos de esta citocina en el suero de fumadores sanos (Petrescu *et al.*, 2010).

1.3 ANEURISMA AÓRTICO ABDOMINAL

El aneurisma aórtico abdominal (AAA) es la forma más común de aneurisma de aorta. Éste se define como el aumento del diámetro del tramo abdominal de la aorta en más de un 50 % con respecto al diámetro original del mismo en las tres láminas de la pared de la arteria: íntima, media y adventicia (Johnston et al., 1991; Michel et al., 2010). Se trata de una enfermedad vascular degenerativa potencialmente mortal clasificada como un tipo particular de aterotrombosis en el que tienen lugar la formación de núcleos necróticos en la túnica media, la presencia de trombos intraluminales y el desarrollo respuestas fibróticas, inflamatorias y angiogénicas en las túnicas media y adventicia (Michel, 2001; Sakalihasan *et al.*, 2005; Choke *et al.*, 2006b; Michel *et al.*, 2010). El AAA afecta de manera característica a varones a partir de la séptima década de la vida, siendo su prevalencia del 5 % en varones mayores de 50 años (Villar et al., 2013) y de hasta el 9 % en mayores de 65 (Daugherty et al., 2002). Dicha prevalencia aumenta paralelamente al incremento de la esperanza de vida y la disminución de la mortalidad por enfermedades cardiovasculares (Riambau et al., 2007). Además del sexo masculino y una edad superior a los 65 años, la hipertensión arterial, la hipercolesterolemia, la presencia de enfermedad aterosclerótica coronaria, periférica o cerebrovascular, una posible predisposición genética y el tabaquismo son factores de riesgo para el desarrollo de AAA, siendo el último de la enumeración el factor de riesgo principal (Michel et al., 2010; Villar et al., 2013). Hasta la fecha no se dispone de ninguna herramienta terapéutica efectiva que prevenga el desarrollo de esta patología. En cuanto al tratamiento de la misma, actualmente la cirugía reparadora, que conlleva un riesgo significativo de mortalidad y morbilidad, es la única opción (Brewster et al., 2003).

La mayor consecuencia clínica del AAA es su rotura, que se asocia con una mortalidad global cercana al 90 % (Noel et al., 2001). En cuanto a las mujeres, aunque el desarrollo de AAA es menos frecuente, la mortalidad relativa es mayor (Hultgren et al.,

2007). La rotura del AAA, cuyo riesgo aumenta exponencialmente con el tamaño del mismo (Vijaynagar et al., 2013), es un proceso en el que intervienen diversos factores bioquímicos, celulares, proteolíticos y biomecánicos. Concretamente, en los últimos años, el riesgo de rotura del AAA se ha relacionado con la formación de nuevos vasos sanguíneos o angiogenesis en el AAA y con la sobreexpresión de quimiocinas angiogénicas, tratándose ambos de procesos ya establecidos como característicos del propio desarrollo del AAA (Choke *et al.*, 2006a).

1.3.1 Angiogénesis

La angiogénesis se define como la formación de nuevos vasos sanguíneos a partir de las vénulas postcapilares preexistentes. Ésta tiene un papel central en diversos procesos tanto de desarrollo como patológicos, incluyendo la embriogénesis, el cáncer y la inflamación crónica (Chung *et al.*, 2011). El proceso de angiogénesis (Figura 10) se encuentra regulado por la expresión de factores proangiogénicos, o angiogénicos, y antiangiogénicos, o angiostáticos. Un balance correcto entre ambos tipos de factores conlleva el desarrollo del proceso de angiogénesis en condiciones fisiológicas relacionadas con el desarrollo normal mientras que un exceso de factores proangiogénicos da lugar al aumento de la angiogénesis implicada en procesos patológicos (Ferrara *et al.*, 2003; Tahergorabi *et al.*, 2012).

Los factores angiogénicos más importantes son el Factor de Crecimiento Endotelial Vascular (VEGF), los Factores de Crecimiento Transformante-alfa y -beta (TGF-α y TGF-β), las angiopoyetinas, el Factor de Crecimiento Epidermal (EGF) y el Factor de Crecimiento de Fibroblastos (FGF). Los factores angiostáticos más importantes son la angioestatina, la endoestatina y las tromboespondinas (TSPs) (Tahergorabi *et al.*, 2012).

Además de estos factores, las quimiocinas angiogénicas también parecen tener un papel crucial en el proceso de angiogénesis, tal y como se detalla en los siguientes apartados.

El proceso de angiogénesis puede verse acelerado por la presencia de una respuesta inflamatoria y el consiguiente influjo de macrófagos (Sunderkötter *et al.*, 1994). Esto, junto al hecho de que un aumento en la producción de proteasas resulta esencial para la migración de células endoteliales (Mignatti *et al.*, 1989), confiere a el proceso de angiogénesis una gran relevancia en el AAA. Dicha relevancia se debe a que

la expansión y rotura del AAA se caracterizan por la degradación de la matriz extracelular, el aumento en el recambio de proteínas, la reducción de la concentración de elastina y el aumento de la de colágeno, siendo todos ellos eventos asociados al incremento de la expresión de metaloproteasas y a la infiltración inflamatoria (Thompson *et al.*, 1996).

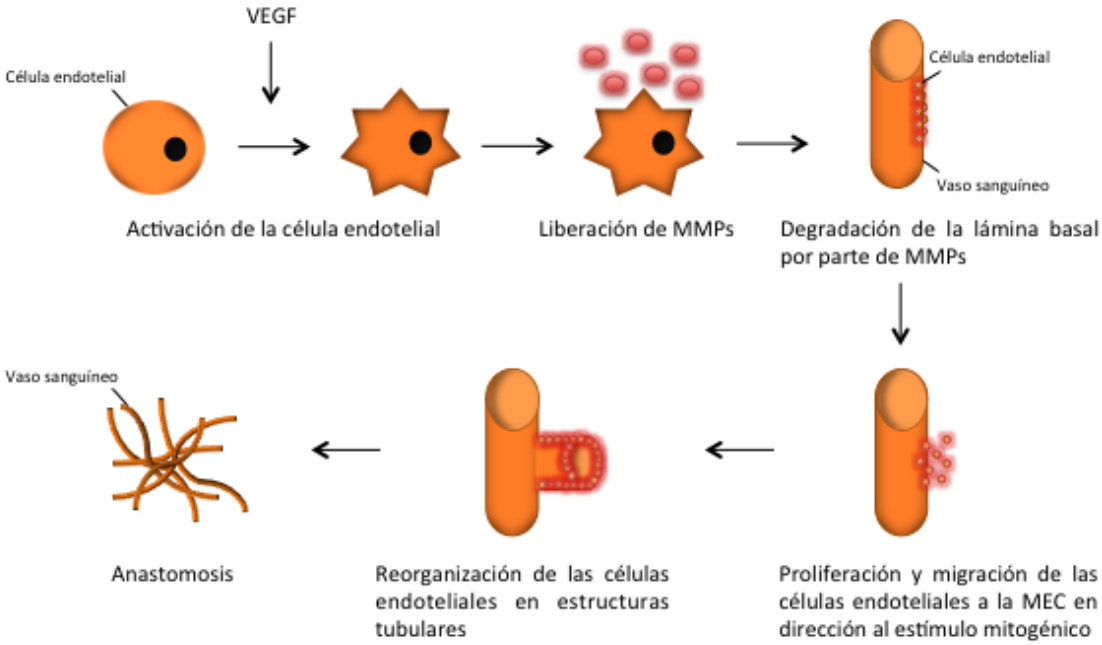

Figura 10: Proceso de angiogénesis. La angiogénesis es un proceso que consta de diversas etapas. Dicho proceso implica la activación de las células endoteliales que recubren las paredes de los vasos sanguíneos preexistentes en respuesta a un estímulo mitogénico como el Factor de Crecimiento Endotelial Vascular (VEGF). Ello conlleva la liberación de metaloproteasas de matriz (MMPs), por parte de las células, que degradan la matriz extracelular (MEC) del vaso. De este modo se facilita la proliferación de las células endoteliales de dicho vaso y la migración de las mismas en dirección al estímulo. El proceso concluye cuando, tras establecer interacciones entre ellas y con la MEC vía moléculas de adhesión celular, se produce su reestructuración en estructuras tubulares seguida de un proceso de anastomosis. Todo ello está mediado por factores proangiogénicos que incluyen, además de estímulos mitogénicos como el mencionado, quimiocinas angiogénicas Adaptado de: (Tahergorabi *et al.*, 2012; Vijaynagar *et al.*, 2013).

1.3.1.1 Quimiocinas y angiogénesis

Las quimiocinas CXC tienen propiedades duales en el proceso de angiogenesis ya que son, salvo alguna excepción, las quimiocinas CXC que presentan el motivo ELR, las que poseen propiedades pro-angiogénicas siendo, por el contrario, angiostáticas aquellas quimiocinas CXC que carecen de dicha secuencia. Las quimiocinas CXC que poseen ELR son la interleucina 8 (IL-8/CXCL8), el oncogén regulado por el crecimiento-alfa (GRO-α/CXCL1), denominado quimiocina derivada de queratinocitos

(KC/CXCL1) en ratón, el oncogén regulado por el crecimiento-beta (GRO-β/CXCL2), el oncogén regulado por el crecimiento-gamma (GRO-γ/CXCL3), el péptido activador 78 de neutrófilos derivado de células epiteliales (ENA-78/CXCL5), la proteína quimiotáctica de granulocitos-2 (GCP-2/CXCL6) y la proteína activadora de neutrófilos 2 (NAP-2/CXCL7). La mayoría son potentes quimioatrayentes y activadoras de los neutrófilos, y además, angiogénicas. Sin embargo, existen otras quimiocinas CXC que, a pesar de la presencia de la secuencia ELR, no poseen actividad quimiotáctica. Por su parte, aquellas que carecen del motivo ELR, activan específicamente linfocitos T y monocitos (Lee *et al.*, 2014).

En cuanto a la familia de las quimiocinas CC, tanto MCP-1/CCL2 como RANTES/CCL5 han demostrado tener propiedades inflamatorias y angiogénicas (Niu *et al.*, 2008; Suffee *et al.*, 2012a).

La intervención de las quimiocinas proangiogénicas en el proceso de angiogénesis puede tener lugar directa o indirectamente (Figura 11).

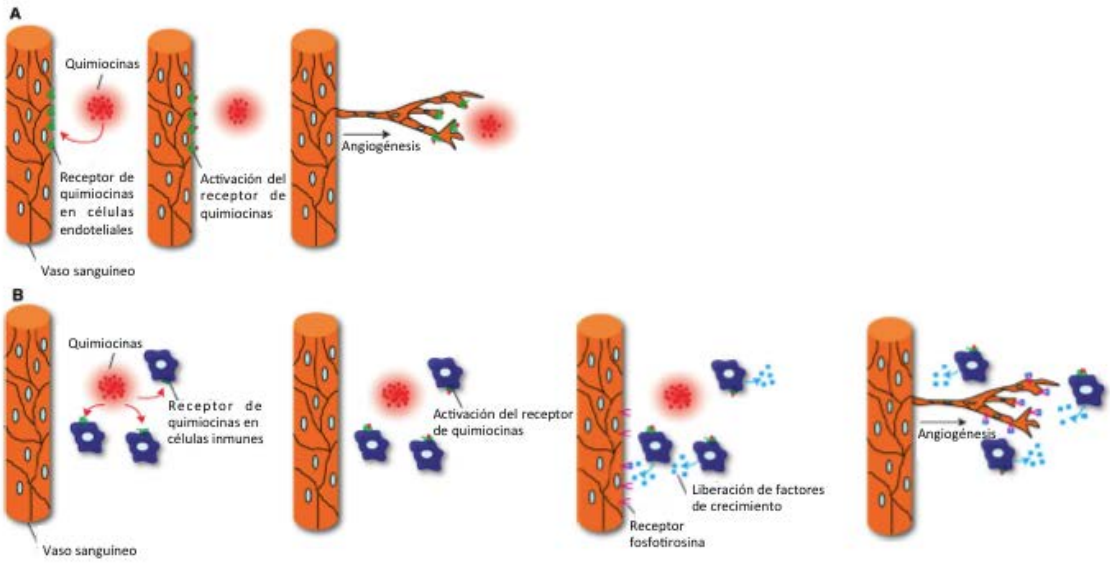

Figura 11: Efecto de las quimiocinas sobre las células endoteliales en el proceso angiogénico. Las quimiocinas pueden actuar directamente sobre las células endoteliales que expresan receptores de las mismas. Ello conlleva la migración de dichas células y el consiguiente proceso de angiogénesis (A). Por otro lado, las quimiocinas pueden inducir la angiogénesis de manera indirecta mediante la atracción de leucocitos que expresan receptores de quimiocinas, lo que conlleva la secreción de factores proangiogénicos tales como el Factor de Crecimiento Endotelial Vascular, por parte de las mismas, que activan a las células endoteliales iniciándose así el proceso de angiogénesis (B). Adaptado de: (Kiefer *et al.*, 2011).

1.3.2 AAA y sistema renina-angiotensina

Para que se produzca el proceso de la angiogenesis es necesario que se produzca la destrucción del vaso original para que se construya el nuevo vaso. El sistema renina-angiotensina (RAS) parece estar implicado en ambas fases del proceso (Willis *et al.,* 2011). Por ello, numerosos estudios avalan la hipótesis de que un desequilibrio del RAS podría estar implicado en la desarrollo y progresión del AAA (Daugherty *et al.,* 2006).

En modelos *in vivo* de AAA inducido por Ang-II en ratones knock-out (KO) para el gen de la apolipoproteína E ($apoE^{-/-}$) sometidos a una dieta grasa, la lesión por AAA se desarrolla notablemente transcurridos 28 días de administración de Ang-II (Daugherty et al., 2000) presentando características moleculares y celulares muy similares a las que caracterizan el AAA en humanos, tales como la secreción de la proteína quimiotáctica de monocitos-1 (MCP-1/CCL2), la infiltración de macrófagos, la secreción de MMPs, la disrupción de la lámina media, la rotura de la capa elástica y la neovascularización (Zhang *et al.*, 2009).

Estudios previos realizados usando el modelo de AAA inducido por Ang-II, demostraron que la administración de el antagonista del receptor AT_1 de la Ang-II, losartan, inhibe el desarrollo de la patología (Lu *et al.*, 2008).

En la misma línea un estudio de casos y controles realizado con pacientes observo que los pacientes en tratamiento con inhibidores de la enzima convertidora de angiotensina (ACE) presentaban menor probabilidad de ruptura de aneurisma (Hackam *et al.*, 2006)

1.4 MODULACIÓN FARMACOLÓGICA DEL RECLUTAMIENTO LEUCOCITARIO

1.4.1 Consideraciones generales

1.4.1.1 Receptores nucleares

Los receptores nucleares son factores transcripcionales que juegan un importante papel en la regulación de la expresión génica. Actualmente se conocen más de 50 proteínas pertenecientes a esta «superfamilia» génica y entre ellas existe una notable similitud estructural. Después de interactuar con sus ligandos

específicos, los receptores nucleares se unen a regiones específicas del genoma y modifican la transcripción de numerosos genes. De entre los receptores nucleares más conocidos destacan los PPAR (Receptores Activadores de la Proliferación de Peroxisomas). La familia PPAR consiste en tres isoformas, α, γ, y ß/δ, que comparten una estructura similar y sin embargo difieren en su afinidad a los distintos ligandos, así como en su expresión y actividad en los diferentes tejidos. Los receptores PPAR están involucrados en diversas funciones especialmente en aquellas relacionadas con la regulación del tono vascular, metabolismo energético e inflamación y por tanto representan una importante diana terapéutica para el tratamiento de enfermedades cardiovasculares (Oyekan, 2011).

Una vez activados por sus ligandos, los PPARs forman heterodímeros con otro receptor nuclear, el receptor del retinoide X (RXR), uniéndose posteriormente a los elementos de respuestas específicos en la región promotora de los genes diana, regulando así la función del gen.

Los ligandos de estos receptores PPARs, en particular aquellos que actúan sobre PPARα y PPARγ, interfieren negativamente con genes implicados en el proceso inflamatorio y angiogénico, actuando como factores de transcripción en células vasculares e inflamatorias (Moraes *et al.*, 2006; Bishop-Bailey, 2011).

1.4.1.1.1 PPARα

PPARα se expresa en células endoteliales, células de músculo liso vascular y monocitos/macrófagos (Chinetti *et al.*, 1998; Bishop-Bailey, 2000; Israelian-Konaraki *et al.*, 2005). Dentro de los ligandos que activan PPARα se incluyen diversos ácidos grasos insaturados como el ácido linoleico y acido araquidónico, eicosanoides como la prostaciclina y el leucotieno B_4 así como ligandos sintéticos como los fibratos (Moraes *et al.*, 2006).

En células endoteliales, los ligandos de PPARα interfieren en mecanismos implicados en el reclutamiento leucocitario y la adhesión celular, ejerciendo así un efecto protector frente a la inflamación vascular. Diversos estudios evidencian que ligandos sintéticos de los receptores PPARα, como los fibratos, reducen la expresión vascular de VCAM-1 mediada por quimiocinas, limitando así la adhesión de células inflamatorias al endotelio activado. (Chinetti *et al.*, 1998; Marx *et al.*, 1999).

Además, PPARα es capaz de modular la producción de NO. Los agonistas de los receptores PPARα aumentan la expresión de eNOS y la liberación de NO (Goya *et al.*, 2004).

En las células de músculo liso vascular, la activación de PPARα regula el proceso inflamatorio inhibiendo la producción de IL-1 inducida por IL-6 y prostaglandinas, así como reduciendo la expresión de COX-2 (Chinetti *et al.*, 1998; Staels *et al.*, 1998).

Los agonistas de PPARα han demostrados además, propiedades antiangiogénicas a través de la inhibición de la expresión de factores proangiogénicos como VEGF (Pozzi *et al.*, 2007; Panigrahy *et al.*, 2008)

1.4.1.1.2 PPARγ

PPARγ se expresa en células endoteliales, células de músculo liso vascular y macrófagos (Vidal-Puig *et al.*, 1997; Bishop-Bailey, 2000; Law *et al.*, 2000). Entre sus ligandos se incluyen ácidos grasos como el ácido araquidónico y el ácido docosahexaenoico, prostaglandinas como la prostaglandina A1, prostaglandina A2 y prostaglandina D2, así como ligandos sintéticos de la familia de las glitazonas (pioglitazona), fármacos aprobados para el tratamiento de la diabetes mellitus tipo 2 por sus efectos hipoglucemiantes (Moraes *et al.*, 2006)

Los ligandos de PPARγ inhiben la proliferación y migración de células vasculares (Delerive *et al.*, 1999; Hennuyer *et al.*, 1999). En las células endoteliales, los agonistas de PPARγ disminuyen la expresión de TNFα, IL-6 e IL-1 β, así como atenuar la expresión de VCAM-1 e ICAM-1 inducida por TNFα (Bruemmer *et al.*, 2005). De forma similar a los agonistas PPARα, los activadores de los receptores PPARγ son capaces de aumentar la producción de NO en el endotelio vascular (Calnek *et al.*, 2003).

En las células de músculo liso vascular, los agonistas PPARγ inhiben la proliferación y migración celular, la liberación de metaloproteasas, la liberación de especies reactivas del oxígeno y la expresión del receptor AT_1 de Ang-II (Hsueh *et al.*, 2001; Diep *et al.*, 2002; Bruemmer *et al.*, 2005).

Respecto a su actividad antiangiogénica, la activación de PPARγ inhibe la respuesta proangiogénica inducida por VEGF mediante la supresión de su receptor VEGFR2 (Xin *et al.*, 1999; Bishop-Bailey, 2011).

1.4.1.1.3 PPAR β/δ

PPARβ/δ se expresa prácticamente en todos los tipos celulares (Kliewer *et al.*, 1994). Entre sus agonistas se encuentran ácidos grasos, prostaciclinas y diversos compuestos sintéticos como L-165,041, GW501516, compuesto F, L-783,483 y GW742 (Berger *et al.*, 1999; Duval *et al.*, 2002; Carlson *et al.*, 2003).

Más recientemente, se ha demostrado el papel de PPARβ/δ en la regulación de la inflamación. Estudios llevados a cabo por nuestro grupo de investigación han demostrado que la activación de PPARβ/δ mediante el compuesto GW501516 inhibe las interacciones neutrófilo-endotelio inducidas por TNFα en condiciones de dinámicas de flujo laminar *in vitro* (Piqueras *et al.*, 2009). Además, en dicho estudio mediante el empleo de la microscopía intravital se demostró que GW501516 disminuía las interacciones leucocito-endotelio inducidas por TNFα en la microcirculación cremastérica del ratón (Piqueras *et al.*, 2009).

Al contrario que PPARα y PPARγ, PPARβ/δ ha demostrado actividad proangiogénica (Piqueras *et al.*, 2007; Bishop-Bailey, 2011). Así, el tratamiento de células endoteliales con el ligando selectivo de PPARβ/δ, el compuesto GW501516, estimula la proliferación, migración y morfogénesis de HUVEC (Piqueras *et al.*, 2007). Estos efectos estuvieron acompañados de una mayor expresión del receptor VEGFR1 y un aumento en la liberación de VEGF en células endoteliales (Piqueras *et al.*, 2007)

1.4.2 Estatinas

Las estatinas son inhibidores de la 3-hidroxi-metil-glutaril-CoA reductasa (HMG-CoA reductasa), la enzima que cataliza la reacción limitante de la ruta del mevalonato, que da lugar a la síntesis de colesterol. Son fármacos que poseen la capacidad de bloquear la síntesis de colesterol (Alberts, 1988). Además, poseen la capacidad de reducir la mortalidad cardiovascular y los accidentes cerebrovasculares, efectos que son independientes de la reducción lipídica. De hecho cuando la rosuvastatina es administrada a personas sanas sin hiperlipidemia pero con niveles

elevados de proteína C reactiva, la incidencia de eventos cardiovasculares, se vio reducida. (Ridker et al., 2008). Estas propiedades de las estatinas, llamadas pleiotrópicas, incluyen la inhibición de la inflamación, la modulación de la función endotelial, propiedades antioxidantes, antiangiogénicas o antitrombóticas. (Wang *et al.*, 2010; Babelova *et al.*, 2013; Patterson *et al.*, 2013; Mihos *et al.*, 2014), que pueden jugar un papel importante en la protección cardiovascular mediada por las estatinas. En la misma línea, hay evidencias que indican que las estatinas favorecen la correcta función de las células endoteliales (Mira et al., 2009)

Mediante la inhibición de la síntesis del L-mevalonato, las estatinas también impiden también la síntesis de otras moléculas importantes, como son el farmesil-pirofosfato (FPP) y geranil-geranil-pirofosfato (GGPP). Estas moléculas juegan un papel importante en la modificación postraduccional (prenilación) de una gran variedad de proteínas entre las que se encuentran las pequeñas proteínas de unión a GTP Ras y Rho (Takemoto *et al.*, 2001). Como consecuencia de la inhibición de la isoprenilación de Ras y Rho mediada por las estatinas, se impide la conversión de estas proteínas al estado unido a GTP (forma activa). Dado que los miembros de estas familias están implicados en funciones celulares como la motilidad, proliferación y secreción es probable que la inhibición de estas proteínas medie algunos de los efectos pleiotrópicos de las estatinas (Babelova *et al.*, 2013).

1.4.2.1 Estatinas, inflamación y reclutamiento leucocitario

La primera etapa del reclutamiento leucocitario es la disfunción endotelial, la cual se caracteriza por una disminución de la síntesis, liberación y actividad del óxido nítrico (NO) derivado del endotelio. Estudios *in vitro* e *in vivo* han demostrados que las estatinas son capaces de aumentar la biodisponibilidad del NO (Laufs *et al.*, 1998; Rikitake *et al.*, 2001; Stalker *et al.*, 2001).

Las estatinas también han demostrados su eficacia inhibiendo el proceso inflamatorio. Estudios *in vitro e in vivo* han observado que las estatinas disminuyen la secreción de citoquinas proinflamatorias como IL-6 y quimiocinas como IL-8/CXCL8 o MCP-1/CCL2, así como moléculas de adhesión del subtipo CD11 y masconcretamente de CD11a/CD18 o $\alpha_L\beta_2$ o lymphocyte function-associated antigen 1 (LFA-1) en leucocitos (Weber *et al.*, 1997; Weitz-Schmidt *et al.*, 2001) y P-selectina e ICAM-1 en el endotelio (Stalker *et al.*, 2001; Mira *et al.*, 2009). En esta

misma línea, se ha observado que las estatinas impiden la migración leucocitaria a los lugares de inflamación (Stalker et al., 2001). Además, estudios realizados en humanos han demostrado dichas propiedades antiinflamatorias de las estatinas (Rezaie-Majd *et al.*, 2002).

Por otro lado, numerosas evidencias científicas sugieren la interconexión entre las estatinas y los Receptores Activadores de la Proliferación Peroxisomal (PPARs) (Desjardins *et al.*, 2008; Plutzky, 2011; Balakumar *et al.*, 2012).

1.4.2.2 Estatinas, angiogénesis y AAA

Además de las propiedades antiinflamatorias e inmunomoduladoras citadas en el apartado anterior, es importante resaltar que algunos estudios recientes, indican que las estatinas son efectivas reduciendo la progresión y formación del AAA (Kertai et al., 2004). Numerosos ensayos clínicos evidencian la relación entre el tratamiento con estatinas y la disminución en el crecimiento del AAA (Schouten et al., 2006; Karrowni et al., 2011). Por otra parte, diversos estudios clínicos sugieren que las propiedades antiangiogénicas de las estatinas podrían ser debidas a la disminución que estas causan en los niveles de VEGF (Cimato et al., 2014) y en su capacidad de aumentar el número de células endoteliales progenitoras circulantes (Tousoulis et al., 2011). Estudios experimentales realizados *in vivo* han demostrado que el tratamiento con simvastatina disminuye la formación de AAA inducida Ang-II en ratones apoE $^{-/-}$ (Zhang et al., 2009).

1.4.2.3 Efectos adversos

Aunque las estatinas son fármacos generalmente bien tolerados, miopatías y alteraciones renales agudas son efectos adversos frecuentemente relacionados con el uso de estos fármacos, en particular de simvastatina y rosuvastatina (Fox et al., 2007; Golomb et al., 2008; Dormuth et al., 2013). Debido a que estos efectos adversos están relacionados con la dosis (Fox et al., 2007; Golomb et al., 2008; Dormuth et al., 2013), sería interesante identificar otros fármacos, que en combinación con las estatinas, provean de los beneficios cardiovasculares disminuyendo al mínimo las posibles reacciones adversas.

1.4.3 Receptores del Retinoide X

Existen tres tipos de RXR: RXRα, RXRβ y RXRγ. RXRα actúa como mediador de los efectos biológicos de diversas hormonas, vitaminas y fármacos. Para ello, al unirse su ligando específico, RXRα se activa y homodimeriza o heterodimeriza con otros receptores nucleares tales como los PPAR (Figura 12), participando en el reclutamiento de otros factores de transcripción y modulando así la transcripción de determinados genes diana (Szanto *et al.*, 2004). Tal y como hemos comentado anteriormente, RXRα puede formar heterodímeros con el Receptor Farnesoide X (FXR), LXRs o PPARs (Moraes *et al.*, 2006; Sanz *et al.*, 2012). Por ello, RXRα se encuentra implicado en numerosas cascadas de transducción de señales asociadas a la regulación de la glucosa y el metabolismo lipídico (Streb *et al.*, 2003).

El Bexaroteno es un fármaco que presenta una alta afinidad por RXRα sin afectar a genes dependientes del receptor del ácido retinoico (RAR) siendo por ello menos tóxico que los retinoides de origen natural o los retinoides selectivos del RAR (Farol et al., 2004). Actualmente es frecuentemente utilizado en el tratamiento del linfoma cutáneo de células T (Farol et al., 2004). Además, se están realizando ensayos para evaluar su efectividad en otras enfermedades metabólicas (Lalloyer et al., 2006), el Parkinson (McFarland et al., 2013) y el Alzheimer (Cramer et al., 2012).

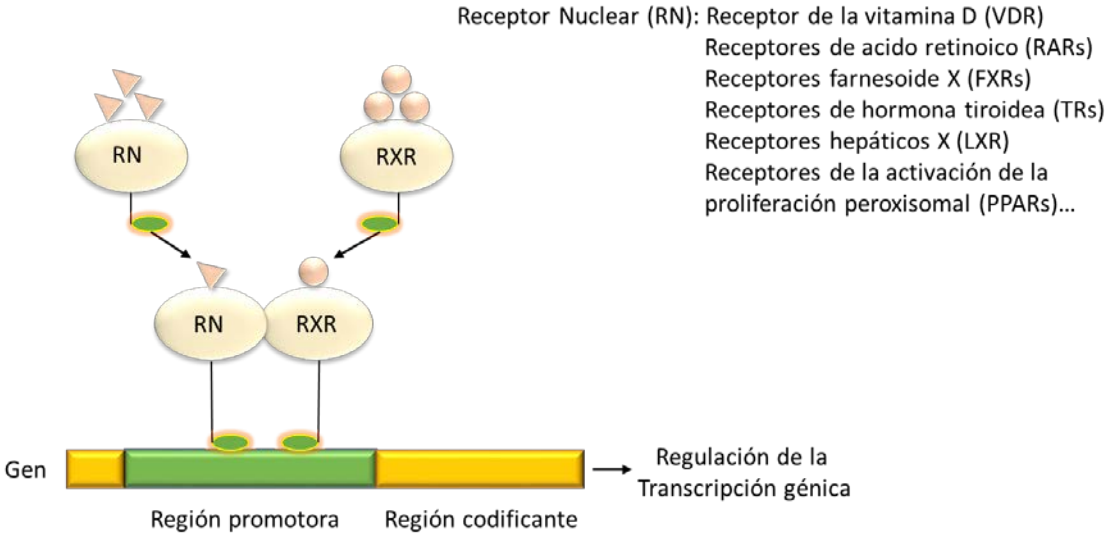

Figura 12: Mecanismo de acción de los receptores nucleares heterodiméricos. Tras activarse en respuesta al reconocimiento de sus ligandos, el Receptor del Retinoide X (RXR) dimeriza consigo mismo o con otros receptores nucleares (RN) como los Receptores

Activadores de la Proliferación Peroxisomal (PPAR), con el Receptor Hepático X (LXR), con el Receptor Farnesoide X (FXR), etc. Figura basada en *Cortes et al, 2005*(Cortes *et al.*, 2005).

1.4.3.1 Bexaroteno, inflamación y reclutamiento leucocitario

Diversos estudios *in vivo* como *in vitro* han demostrado que algunos ligandos del receptor RXR, entre ellos bexaroteno, reducen la inflamación en diferentes etapas del proceso inflamatorio (Szanto et al., 2004). Además, algunos estudios han observado que bexaroteno es capaz de reducir la progresión de la lesión aterosclerótica en ratones apoE$^{-/-}$ (Claudel et al., 2001; Lalloyer et al., 2006), así como de reducir el estrés oxidativo inducido por concentraciones elevadas de glucosa en células endoteliales humanas (Chai et al., 2008).

Estudios más recientes llevados a cabo por nuestro grupo, han observado que la activación de RXRα inhibe las interacciones leucocito-endotelio mediadas por TNFα, bajo condiciones dinámicas de flujo laminar en HUVEC, así como las interacciones *in vivo* en la circulación cremastérica de ratón. Dichos efectos anti inflamatorios se correlacionaron con una menor expresión de moléculas de adhesión y la inhibición de la secreción de quimiocinas como GROα o MCP-1 por parte del endotelio. Además, se observó que dichos efectos estaban mediados a través de la activación y heterodimerización con PPARγ (Sanz et al., 2012)

1.4.3.2 Bexaroteno y angiogénesis

Diversos estudios tanto *in vivo* como *in vitro* han descrito que bexaroteno es un importante modulador de la angiogénesis. En este sentido, mediante el empleo de un modelo animal de inducción de angiogénesis estimulado por VEGF, se observó que bexaroteno era capaz de revertir la formación de nuevos vasos en un 70% (Yen *et al.*, 2006). En dicho estudio, análisis *in vitro*, pusieron de manifiesto la capacidad de bexaroteno de disminuir la motilidad y la invasividad de las células tumorales en estudio. Además, el análisis del medio condicionado por células tumorales A549 y MDA-MB-231 reveló un descenso en la secreción de factores proangiogénicos (VEGF, bFGF, EGF) y metaloproteasas por las células tratadas con bexaroteno. Además, comprobaron que los efectos antiangiogénicos del bexaroteno estaban mediados a través de la heterodimerización RXR-PPARγ (Yen *et al.*, 2006)

Además, estudios preliminares han demostrado que la administración oral de bexar

oteno inhibe de manera dosis dependiente el crecimiento de xenoinjertos de células tumorales humanas de pulmón en ratones inmunodeficientes (*nude mice*). En el mismo estudio, se observó que bexaroteno inhibía la angiogénesis (expresión de CD31) en dichos tumores y la liberación de VEGF en células epiteliales A549 a través de la inhibición de la vía ERK1/2 y JNK (Fu *et al.*, 2007).

Por otro lado, un estudio llevado a cabo por los mismos autores ha demostrado que la activación de RXR por bexaroteno inhibe la proliferación, la migración, la invasividad y la formación de estructuras tubulares inducidas por VEGF en HUVEC (Fu et al., 2011). Dichas respuestas de bexaroteno estuvieron acompañadas por una disminución en la liberación de las metaloproteasas MMP-2 y MMP-9, así como por una reducción de la activación de las vía de señalización intracelular Smad2/3 y la expresión del factor de transcripción Runx2 (Fu et al., 2011).

1.4.3.3 Bexaroteno y efectos adversos

Sin embargo, el tratamiento en humanos con bexaroteno va acompañado de efectos adversos inevitables y relacionados con la dosis administrada, generalmente hipertrigliceridemia, hipercolesterolemia y en menor medida hipotiroidismo (de Vries-van der Weij *et al.*, 2009; Vakeva *et al.*, 2012). A pesar de ello, rosuvastatina reduce los niveles de triglicéridos (Florentin *et al.*, 2013) y en Reino Unido, las guías clínicas para la prescripción segura de Bexaroteno, ya recomiendan su administración conjunta con una estatina a fin de evitar los problemas dislipémicos asociados al tratamiento. Estos efectos parecen ser debidos a que la rosuvastatina no es metabolizada por la isoenzima citocromo P450 3A4 (CYP3A4) y su transformación metabólica por las isoenzimas citocromo P450 2C9 (CYP2C9) y citocromo P450 2C19 (CYP2C19) es mínima (Soran *et al.*, 2008).

OBJECTIVES

2 OBJECTIVES

Increased levels of circulating mediators, including Ang-II and cytokines, have been detected in cardiovascular and cardiometabolic diseases such as hypertension, obesity and diabetes, and can exert deleterious effects on endothelial function (Granger *et al.*, 2004; Marinou *et al.*, 2010). These agents initiate an inflammatory signaling cascade associated with ROS generation, increased cell-surface expression of cell adhesion molecules (CAMs) and enhanced leukocyte adhesiveness to endothelial cells (Libby, 2002; Granger *et al.*, 2004). These responses are associated with endothelial dysfunction, and a pro-thrombotic and pro-inflammatory state of the endothelium (Landmesser *et al.*, 2004) that contributes to the early stages of atherogenesis (Libby, 2002; Landmesser *et al.*, 2004; Galkina *et al.*, 2009).

Ang-II is the main effector peptide of the rennin-angiotensin system and is implicated in atherogenesis (Dzau, 2001).We demonstrated that 4 h exposure to Ang-II *in vivo* caused arteriolar leukocyte adhesion in the mesenteric microcirculation of the rat (Alvarez *et al.*, 2004). Notably, mononuclear leukocyte recruitment by Ang-II was found to be mediated largely by tumor necrosis factor-α (TNFα) and the subsequent increased endothelial expression of fractalkine (CX_3CL1)(Mateo *et al.*, 2007; Rius *et al.*, 2013b). Consequently, pharmacological modulation of inflammatory cell infiltration of the subendothelial space may impede the atherogenic process associated with different cardiovascular risk factors related to the rennin-angiotensin system.

Statins are a group of 3-hydroxy-3-methylglutaryl coenzyme A reductase inhibitors which were primarily used because of their lipid-lowering properties due to their capacity to block cholesterol biosynthesis (Alberts, 1988). Thereafter, their ability to reduce cardiovascular mortality and stroke was found to go beyond their lipid-lowering attributes. Indeed, when rosuvastatin was administered to healthy subjects without hyperlipidemia but with elevated high-sensitivity C-reactive protein levels, the incidence of major cardiovascular events was reduced (Ridker *et al.*, 2008). These so-called pleiotropic effects of statins include modulation of inflammatory reactions and anti-oxidant properties, which may additionally play important roles in statin-mediated cardiovascular protection (Mira *et al.*, 2009). Accordingly, there is evidence indicating that statins favorably influence endothelial

cell function (Mira *et al.*, 2009) and impair leukocyte trafficking at sites of inflammation (Stalker *et al.*, 2001). Furthermore, a growing body of experimental data suggests a potential interplay between statins and peroxisome proliferator-activated receptors (PPARs) (Desjardins *et al.*, 2008; Balakumar *et al.*, 2012), and activation of PPARs can down-regulate the expression of CAMs, proinflammatory genes and leukocyte-endothelial cell interactions (Moraes *et al.*, 2006). Though statins in general are well tolerated, myopathy and acute renal events have been a significant concern with the use of high potency statin drugs, in particular simvastatin and rosuvastatin (Rosu) (Golomb *et al.*, 2008; Hoffman *et al.*, 2012; Dormuth *et al.*, 2013). Since these adverse effects are frequently dose-related (Golomb *et al.*, 2008; Hoffman *et al.*, 2012; Dormuth *et al.*, 2013), there remains an overt need to identify agents that, when combined with statins, can provide the greatest benefit on cardiovascular disease with the least added risk.

Bexarotene (Bex) is a retinoid X receptor (RXR)-selective agonist currently used in the treatment of cutaneous T-cell lymphoma. We have previously shown that Bex can inhibit mononuclear leukocyte attachment to stimulated arterial endothelial cells through down-regulation of redox-sensitive pathways and *via* RXR/PPARγ interaction (Farol *et al.*, 2004; Sanz *et al.*, 2012). Indeed, it is well established that PPARs form permissive RXR heterodimers which synergistically respond to agonists of RXR and the partner receptor (Plutzky, 2011). Unfortunately, Bex treatment is associated with unavoidable and dose-limiting side-effects, in particular hypertriglyceridemia, hypercholesterolemia and to a lesser extent hypothyroidism (de Vries-van der Weij *et al.*, 2009; Vakeva *et al.*, 2012). However, Rosuvastatin (Rosu) administration can reduce triglyceride levels (Florentin *et al.*, 2013) and the U.K. consensus statement on safe clinical prescribing of Bex recommend the use of this statin to prevent the dyslipidemic effects associated with administration of the RXR agonist (Scarisbrick *et al.*, 2013). In an attempt to identify more effective strategies to treat and prevent atherosclerosis, coronary heart disease, and co-morbid metabolic disorders characterized by endothelial dysfunction, we have established the following objective:

1- To evaluate the effect of combined treatment with different concentrations of Rosuvastatin and Bexarotene on the vascular inflammation caused by Ang-II and to investigate the underlying mechanisms involved.

Abdominal aortic aneurysm (AAA) is a degenerative disease of the aorta, that mainly affects elderly population over the age of 65 (Golledge *et al.*, 2006). AAA can be detected in human by non invasive imaging techniques, however nowadays there are not pharmacological treatments to prevent the progresion of this disease (Golledge *et al.*, 2006).

In recent years, new microvessel formation or angiogenesis in aortic aneurysmal disease has been related with the risk of rupture and complications (Choke *et al.*, 2006). Ang-II has been implicated in both angiogenesis and pathological vascular growth (Willis *et al.*, 2011). Indeed, an imbalance of the renin-angiotensin system has been associated with the pathogenesis of AAA (Daugherty *et al.*, 2006) and, Ang-II-induced AAA formation in apolipoprotein E deficient mice ($apoE^{-/-}$) shares many characteristic features of the human disease, including chemokine generation, macrophage infiltration and neovascularization (Zhang *et al.*, 2009). Given the high mortality rate associated with AAA, in humans, it is important to find new pharmacological approaches to halt its progression.

In this regard, emerging evidence indicates that a single anti-angiogenic drug may not be sufficient to combat the wide array of angiogenic factors produced during AAA and the pathways involved in the angiogenic process. Thus, we have established the following objective:

2- To examine the combined effect of different concentrations Rosuvastatin and Bexarotene on the Ang-II induced AAA and angiogenesis and to investigate the underlying mechanisms involved.

Ang-II is implicated in atherogenesis beyond its hemodynamic effects (Dzau, 2001). We demonstrated that 4 h exposure to Ang-II *in vivo* causes arteriolar leukocyte adhesion in the rat mesenteric microcirculation (Alvarez *et al.*, 2004). Interestingly, while mononuclear cells were found to be the primary cells attached to the arteriolar endothelium, the leukocytes interacting with the venular endothelium were predominantly neutrophils. Despite these findings, the same CAMs were expressed in both the arteriolar and venular endothelia in response to Ang-II (Alvarez *et al.*, 2004),

suggesting that other mechanisms were responsible for the differential cellular distribution within the microcirculation.

In addition to CAMs, chemoattractant molecules, such as chemotactic cytokines or chemokines, have the potential to recruit and activate specific subsets of immune cells and are involved in the regulation of leukocyte trafficking (Zernecke *et al.*; Baggiolini, 2001).

Chemokines comprise a large family of low-molecular-weight cytokines, CXCL16 is a transmembrane chemokine expressed on endothelial, epithelial and smooth muscle cells, as well as on macrophages, dendritic cells, B and T cells and platelets (Ludwig et al., 2007; Izquierdo et al., 2014). CXCL16 was identified in human carotid endarterectomy samples and in lesions of apoE$^{-/-}$ mice fed a Western diet, which implies a role in atherogenesis (Wuttge et al., 2004). CXCL16, is expressed in two distinct forms: membrane-bound CXCL16 promotes the firm adhesion of cells expressing its cognate receptor, CXCR6. Proteolytic cleavage of membrane-bound CXCL16 results in the release of soluble CXCL16, which acts as a chemoattractant for CXCR6^{+} cells (Ludwig et al., 2007). The ability of CXCL16 to both attract and arrest blood monocytes and lymphocytes, as well as its presence in vascular wall cells, makes it an attractive candidate for involvement in atherosclerotic lesion formation. Interestingly, while CXCL16$^{-/-}$LDLr$^{-/-}$ mice had accelerated atherosclerosis likely because of the lack of CXCL16 function as an scavenger receptor (Aslanian et al., 2006), recent published observations have shown the relevance of endothelial CXCL16 expression at sites prone to lesion formation and its role in early atherosclerotic plaque formation (Hofnagel et al., 2011). Similarly, the absence of CXCR6 in apoE$^{-/-}$ mice resulted in reduced T cell number and macrophage infiltration within the lesion, diminishing atherosclerosis (Galkina et al., 2007). Therefore, we hypothesized that CXCL16 may be implicated in the Ang-II–induced proatherogenic effects and established the following objective:

3- To investigate the potential role of CXCR6/CXCL16 axis in Ang-II-induced vascular inflammation and the underlying mechanisms involved.

Chronic obstructive pulmonary disease (COPD) is a complex respiratory disorder characterized by a progressive and largely irreversible decrement in lung

function associated with an abnormal chronic inflammatory response of the lungs to noxious particles and gases, mostly from cigarette smoke (CS). COPD is now considered a multisystem disease characterized by pulmonary and systemic inflammation (Sinden *et al.*, 2010; Malerba *et al.*, 2013; Choudhury *et al.*, 2014), and the latter is believed to be responsible for many COPD comorbidities (Sinden *et al.*, 2010; Decramer *et al.*, 2013; Choudhury *et al.*, 2014; Smith *et al.*, 2014). Among them, cardiovascular disease is one of the most relevant (Sinden *et al.*, 2010; Decramer *et al.*, 2013; Choudhury *et al.*, 2014; Smith *et al.*, 2014). Indeed, epidemiological studies have demonstrated that smoking is a significant risk factor for heart disease including aneurysm formation and rupture, and stroke through atherosclerosis development (Forsdahl *et al.*, 2009). As previously outlined, one of the earliest stages of atherogenesis is endothelial dysfunction, which in smokers has been widely described (Messner *et al.*, 2014).

The mechanisms by which CS promotes a proinflammatory, prothrombotic and proatherogenic environment in the vessel wall are not fully understood. Because platelets can mediate the endothelial adhesion of circulating leukocytes and they express CXCL16 and CXCR6 on their surface (Seizer *et al.*, 2011; Borst *et al.*, 2012), we have established the following objective:

4- To investigate the potential contribution of CXCR6/CXCL16 axis on platelet-leukocyte arrest in COPD dysfunctional arterial endothelium and to dilucidate the underlying mechanism involved.

MATERIAL AND METHODS

3 MATERIAL AND METHODS

3.1 HUMAN *IN VITRO* CELL CULTURE STUDIES

All investigation with human samples carried out in the present study conforms to the principles outlined in the Declaration of Helsinki and was approved by the institutional ethics committee at the University Clinic Hospital of Valencia, Spain. Written informed consent was obtained from all volunteers.

3.1.1 Isolation of human endothelial cells

Human umbilical artery endothelial cells (HUAECs) and human umbilical vein endothelial cells (HUVECs) were isolated from human umbilical cords obtained from Gynaecology and Obstetrician Unit from University Clinic Hospital of Valencia, Spain. Written informed consent was obtained from all volunteers.

Cells were isolated by collagenase treatment (Jaffe et al., 1973) and maintained in human endothelial cell basal medium-2 (EBM-2, Lonza Iberica, Spain) supplemented with endothelial growth medium-2 (EGM-2, Lonza Iberica, Spain) and 10% fetal calf serum (FCS). Prior to every experiment, cells were incubated for 16 h in medium containing 1% FCS and then returned to 10% FCS-supplemented medium at the commencement of all experimental protocols.

3.1.2 Cigarette smoke extract (CSE) preparation

In order to obtain cigarette smoke extract, 3R4F research grade cigarettes were used. The composition of 3R4F research grade cigarettes was as follows: total particulate matter, 10.9 mg/cigarette; tar, 9.5 mg/cigarette; and nicotine, 0.726 mg/cigarette. 10% CSE was prepared by bubbling smoke from one cigarette 3R4F into 10 ml of EGM-2 culture media without fetal bovine serum (FBS) at a rate of 1 cigarette/2 min. The pH of the CSE was adjusted to 7.4 and sterile filtered through a 0.22 μm filter. CSE preparation was standardized by measuring the absorbance (optical density= 0.86 ±0.05) at a wavelength of 320 nm. The pattern of absorbance (spectrogram) observed at λ320 showed very little variation between different preparations of CSE. CSE was freshly prepared for each experiment and diluted with culture media supplemented with 0.1% FBS immediately before use. Control medium was prepared by bubbling air through 10 ml of culture media without FBS, the pH was adjusted to 7.4, and the medium was sterile filtered as described above.

In previous studies, a range of concentrations of CSE were tested (0.1-3%) (Rius *et al.*, 2013a). Based on these studies a final concentration of 1% was used in all experiments in the fourth study.

3.1.3 Leukocyte-HUAEC interactions under flow conditions

Flow chamber technique was used to visualize cell adhesion under dynamic flow conditions.

HUAEC and HUVEC were seeded on a 35 mm diameter fibronectin pre-coated plates. Once confluent and after the corresponding treatment, the plates were placed in a parallel flow chamber (Dynamic flow assay in a parallel plate flow chamber, Glyco Tech flow, USA).

As shown in figure 13, parallel flow chamber system, consist of a base plate with an entrance and exit port through which cells and media are perfused, coupled into the 35 mm diameter culture plates on which the cellular monolayer is placed, a gasket that controls the chamber diameter, and a vacuum outlet so that a pump can be held in place. Thus, a flow channel is created over the endothelial monolayer, and the infusion rate condition is set up by the suction pump emulating the human conditions of blood flow over the endothelium.

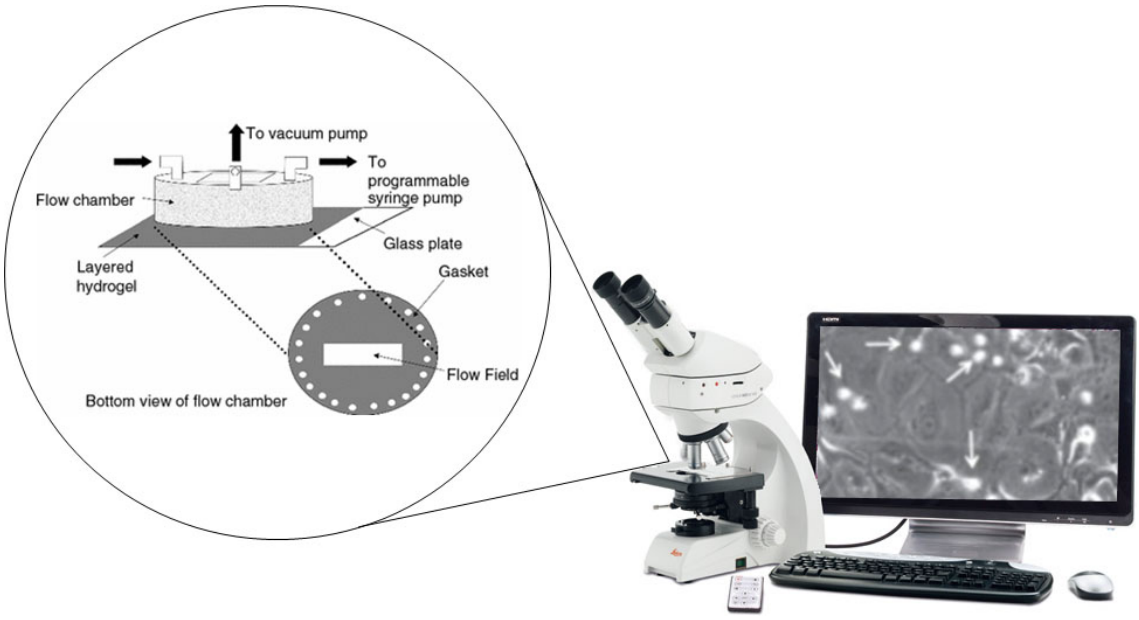

Figure 13: Parallel flow chamber system.

The Glycotech flow chamber was assembled and placed onto an inverted microscope stage, and freshly-isolated human mononuclear cells (1 x 10^6/ml) or whole blood were then perfused across the endothelial monolayers (HUAECs or

transfected HUAECs). In all experiments, leukocyte interactions were determined after 5 min at 0.5 dyn/cm^2. Cells interacting on the surface of the endothelium were visualized and recorded (x20 objective, x10 eyepiece) using phase contrast microscopy (Axio Observer A1, Carl Zeiss microscope, Germany).

3.1.3.1 Flow chamber experimental protocols

Before starting each assay, HBSS solution (Lonza Iberica, Spain) without calcium and magnesium, tempered to 37°C, was perfused in order to adjust the flow at 0.156 ml/min (corresponding to a shear stress of 0,5 dyn /cm^2). Then, a solution of human whole blood or the suspension of isolated human blood cells in HBSS (with Ca^{+2} and Mg^{+2}) was perfused for 5 min. At least 5 fields were recorded for 10 s each, for further analysis. Those leukocytes that established a stable contact with the endothelial monolayer for at least 10 s were considered as attached. Adherent cells were counted while the perfusion medium remained in continuous infusion.

3.1.3.2 Experimental protocols

To measure the leukocyte-HUAEC and leukocyte-HUVEC interactions, HUVECs and HUAECs at passage 1 were grown until confluence. Cell were washed with warm PBS, and incubated in EBM-2 medium, with 1% FBS. After 24 h the different treatments were applied.

3.1.3.2.1 First study

HUAECs were stimulated with Ang-II (1 μM, Calbiochem, Germany) for 4 h. Rosu (10- 30 nM, Axxora, BioVision, CA), Bex (0.3-1 μM, Axxora, BioVision, CA), or combinations of both, were added to plates 20 h prior to Ang-II.

In another set of experiments, cells were incubated with the ROCK inhibitor Y27632 (10 μM, Sigma-Aldrich, MO) 1 h before Ang-II stimulation (1 μM, 4 h).

Some cells was transfected using a RhoA-specific siRNA or control-siRNA, and at 48 hours post-transfection, cells were stimulated with Ang-II (1 μM) for 4 h. Then, leukocyte-HUAEC interactions under flow conditions were evaluated.

Finally, cells were transfected with control siRNA, RXRα-specific siRNA, PPARα-specific siRNA or PPARγ-specific siRNA and stimulated with Ang-II (1 μM; 4 h) at 48 h post-transfection. In some experiments, cells were pretreated with

Rosu (10 nM) plus Bex (0.3 μM) 20 h prior to Ang-II challenge. Then, leukocyte-HUAEC interactions under flow conditions were evaluated

Human mononuclear cells were obtained from buffy coats of healthy donors by Ficoll-Hypaque density gradient centrifugation (Mateo et al., 2007a).

3.1.3.2.2 Third study

In order to elucidate the involvement of CXCL16 in the leukocyte adhesion induced by Ang-II, HUAECs were stimulated with Ang-II 1 μM for 24 h and 10 min before the experiment were incubated with the following treatments:

- MOPC-21 antibody (2 μg/ml, Sigma-Aldrich, MO), used as control.
- Polyclonal antibody neutralizing CXCL16 function (2 μg/ml, R&D Systems, MN).

3.1.3.2.3 Fourth study

In order to elucidate the involvement of CXCL16 in the leukocyte adhesion induced by CSE 1%, HUAECs were stimulated with CSE 1% for 24 h and 10 min before the experiment were incubated with the following treatments:

- MOPC-21 antibody (2 μg/ml, Sigma-Aldrich, MO), used as control.
- Polyclonal antibody neutralizing CXCL16 function (2 μg/ml, R&D Systems, MN).

3.1.4 RT-PCR

3.1.4.1 RNA extraction

After treatments, RNA from cells were extracted using TRIzol Reagent (Invitrogen, Thermo Fisher Scientific, MA) following the manufacturer's instructions. TRIzol was used as an isolating agent, which allows to maintain the integrity of the RNA during the homogenization process, while lysing the cells and cell components (Chomczynski *et al.*, 1987). Growth media was removed from culture dish and TRIzol® Reagent was added to the cells in the culture dish. The cells were directly lysed in the culture dish by pipetting the cells up and down several times. Then, 200 μl of chloroform was added and the samples were vortexed for 15 s. Thereafter, they were centrifuged for 15 minutes at 15,000 g and 4° C. After centrifugation, the mixture was separated into three distinct phases: the red bottom

part was the organic phase containing proteins, the purple interface contained the genomic DNA and the aqueous phase contained the RNA. The RNA phase was carefully transferred to a new cold eppendorf tube. 500 µl of isopropanol was added and gently mixed. Samples were incubated for 5-10 minutes to allow RNA precipitation and then centrifuged at 12,000 g at 4°C for 10 minutes. The supernatant was removed and washed with 1 ml ethanol 70%, the samples were vortexed again and centrifuged (7500 g at 4°C for 5 minutes). Finally, the ethanol was removed and the pellet was resuspended in 20 µl of nuclease-free water (Thermo Fisher Scientific, MA)

After RNA purification, the concentration was determined by spectrophotometry using the NanoDrop spectrophotometer (ND-100 v3.7.1, Thermo Fisher Scientific, MA). The concentration was given in ng/µl and detected in 260/280 absorbance ratio.

3.1.4.2 Retrotranscription (RT).

After RNA extraction and concentration measurement, the reverse transcription (RT) of 500 ng of RNA from each sample into cDNA was carried out by the action of the reverse transcriptase enzyme in a Mastercycler Gradient thermocycler (Eppendorf, Germany). The enzyme used was MultiScribeTM Reverse Transcriptase (Applied Biosystems, Thermo Fisher Scientific, MA, 50U/µl). The RT was performed with the kit High-Capacity cDNA Reverse Transcription (Applied Biosystems, Thermo Fisher Scientific, MA) following the supplier's instructions.

The mix used was prepared on ice with the reagents shown in Table 2.

Reagent	Volume/Reaction (µl)
10x RT Buffer	2
25x dNTP Mix (100 mM)	0.8
10x RT Random Primers	2
MultiScribe™ Reverse Transcriptase	1
RNase Inhibitor	1
Nuclease-free water	4.2

RNA sample	500 ng

Table 2: Master mix components.

For each reaction, 10 µl of Master Mix and 10 µl of the previously diluted sample (500 ng) with nuclease-free water were used. Thereafter, the samples were placed in the thermocycler and the experimental conditions shown in Table 3 were followed.

Step	Temperature [ºC]	Time [min]
Step 1	25	10
Step 2	37	120
Step 3	85	5
Step 4	4	∞

Table 3: RT program.

Once the programme was finished, the cDNA obtained was kept at -20°C until use.

3.1.4.3 Quantitative polymerase chain reaction (qPCR).

The determination of AT_1 receptor and CXCL16 mRNA expression levels was performed by quantitative PCR (qPCR) using the Luminaris Color HiGreen High ROX qPCR Master Mix kit following manunfacturer´s recommendations (Thermo Fisher Scientific, MA).

A mix with the primers of each gene and an endogenous control (Table 4), was prepared.

Reagent	Volume [µl]
High Green buffer	10
Forward Primer (20 µM)	0.3
Reverse Primer (20 µM)	0.3
cDNA	4
Nuclease-free water	7

Table 4. Reagent used for qPCR

The sequences of the primers used to amplify each gen were designed using Primer Express program and are shown in Table 5.

Gen	Primer	Sequence [5'-3']
Human AT_1 receptor	Forward	ACGTGTCTCAGCATTGATCGAT
	Reverse	TCGAAGGCGGGACTTCATT
Human CXCL16	Forward	ACCACAGTCCATGCCATCAC
	Reverse	TCCACCACCCTGTTGCTGTA
Human GAPDH	Forward	ACCACAGTCCATGCCATCAC
	Reverse	TCCACCACCCTGTTGCTGTA

Table 5: Sequences of the primers used for qPCR assay

The reactions were performed in a 96-well plate (MicroAmp ™, Fast Optical 96-well Reaction Plate with Barcode, Applied Biosystems, Thermo Fisher Scientific, MA) using the 7900 Fast Thermal Cycler thermal cycler System. The results were analyzed using the software provided by the manufacturer (Applied Biosystems, Thermo Fisher Scientific, MA). The PCR cycling program was perform as shown in table 6.

Step	Temperature, ºC	Time	Number of cycles
UDG pre-treatment	50	2 min	1
Initial denaturation	95	10 min	1
Denaturation	95	15 s	40
Annealing / Extension	60	60 s	

Table 6: PCR cycling protocol

Analysis of the relative gene expression data was performed by duplicates using the $2^{-\Delta\Delta Ct}$ method. mRNA levels were normalized to the expression of human GAPDH used as endogenous control and relativized to the vehicle treated group.

3.1.5 Flow cytometry studies

3.1.5.1 Determination of ICAM-1 and VCAM-1 expression in HUAEC

Cells were detached with StemPro Accutase reagent cell dissociation reagent (Gibco, Thermo Fisher Scientific, MA), washed and incubated at 2 x 10^6 cells/ml with a 1/100 dilution of primary antibodies against human VCAM-1 (dilution 1:50 in PBS-BSA 0.3 %, Clone 1.G11B1, AbD Serotec, UK) or ICAM-1 (dilution 1:50 in PBS-BSA 0.3 %, Clone 6.5B5, AbD Serotec, UK) in PBS with 0.2% BSA and 0.05% NaN_3 for 1 h on ice. Detection of primary antibodies was performed using the appropriate Alexa Fluor 488-secondary antibody (30 min, dilution 1/250 in 0.2% PBS-BSA). After 2 washes, cells were fixed 2% paraformaldehyde (15 min) then washed and resuspended in PBS. The fluorescence signal of the labelled cells was then analyzed by flow cytometry (FACSVerse Flow Cytometer, BD Biosciences, CA). The expression of ICAM-1 and VCAM-1 was expressed as the mean of fluorescence intensity (MFI).

3.1.5.2 Determination of CX_3CL1 expression in HUAECs

In order to evaluate the expression of CX_3CL1, confluent endothelial cells were submitted to different treatments. Then cells were detached with StemPro Accutase reagent cell dissociation reagent (Gibco, Thermo Fisher Scientific, MA) and nonspecific binding sites were blocked with 3% PBS-BSA, 10 min, cells were washed with PBS and a PE-labeled mAb against human fractalkine was added (dilution 1:25 in PBS-BSA 0.5 %, Clone 51637, R&D Systems, MN). After 1 h incubation cells were fixed in 2% paraformaldehyde. Cells were centrifuged, washed with PBS, resuspended in PBS and analyzed by flow cytometry (FACSVerse, BD Biosciences, CA). The expression of CX_3CL1, was expressed as the mean of fluorescence intensity (MFI).

3.1.5.3 Determination of CXCL16 expression in HUAECs

To evaluate the expression of CXCL16, confluent endothelial cells were submitted to different treatments. Then, cells were detached with StemPro Accutase reagent cell dissociation reagent (Gibco, Thermo Fisher Scientific, MA),and nonspecific binding sites were blocked with 3% PBS-BSA, 10 min and cells were

washed with PBS. For this purpose, APC-labeled mAb against human CXCL16 was added (dilution 1:25 in PBS-BSA 0.5%, Clone 256213, R&D Systems, MN), after 1 h incubation the cells were fixed in paraformaldehyde 2%. Cells were centrifuged, washed with PBS, resuspended in PBS and analyzed by flow cytometry (FACSVerse, BD Biosciences, CA).

3.1.5.4 Experimental protocols

3.1.5.4.1 First study

Confluent endothelial cells were stimulated with Ang-II (1 μM) for 4 h (ICAM-1 and VCAM-1 expression) or 24 h (CX_3CL1 expression). In some experiments, cells were pretreated with Rosu (10 nM), Bex (0.3 μM) or a combination of Rosu (10 nM) plus Bex (0.3 μM) 20 h prior to Ang-II stimulation. The fluorescence signal of the labeled cells was then analyzed by flow cytometry (FACSVerse Flow Cytometer, BD Biosciences, CA). The expression of ICAM-1, VCAM-1 and CX_3CL1, was expressed as the mean of fluorescence intensity (MFI).

3.1.5.4.2 Third study

In a first set of *in vitro* experiments, HUAEC were grown to confluence and stimulated with 1 μM Ang-II (with or without an Ang-II AT_1 receptor antagonist, EXP3174, 100 μM) or INF-γ (20 ng/ml) for 24 h. CXCL16 protein expression was detected by flow cytometry.

To evaluate the potential involvement of NADPH and xanthine oxidase (XO) on Ang-II-induced responses, cells were incubated for 1 h with a NADPH oxidase inhibitor (apocynin, 30 μM, Sigma-Aldrich, MO) or with a XO inhibitor (allopurinol, 100 μM, Sigma-Aldrich, MO) and then stimulated with Ang-II for 24 h. The doses of these compounds were used as previously described (Beltran et al., 2009; Rius et al., 2013a). Since, the NADPH oxidase isoforms Nox2, Nox4, and Nox5 are all expressed in endothelial cells, (BelAiba et al., 2007; Pendyala et al., 2009) in subsequent experiments, HUAECs were transfected with either control or Nox2, Nox4, Nox5-specific siRNA. Forty eight hours post-transfection, HUAECs were stimulated with Ang-II and CXCL16 expression was evaluated.

To investigate the possible contribution of RhoA to Ang-II-induced CXCL16 expression, cells were treated with a RhoA inhibitor (C3 transferase, 2 μg/ml,

Cytoskeleton Inc., CO) 4 h before Ang-II stimulation and CXCL16 expression was measured 24 h later by flow cytometry

In another set of experiments, HUAEC were transfected for 48 h with control or RhoA-specific siRNA prior to Ang-II stimulation and Ang-II-induced responses were similarly determined.

Finally, to further elucidate the signaling pathways involved in Ang-II-induced responses, endothelial cells were pretreated with inhibitors of ERK1/2 (PD098059, 20 μM, Sigma-Aldrich, MO), p38MAPK (SB202190, 20 μM, Sigma-Aldrich, MO) and NFκB (MOL294, 2.5 μM, donated by Dr. Kahn, Department of Pathobiology, University Washington, Seattle, WA) 1 h prior to Ang-II stimulation. These concentrations have been employed in previous studies to inhibit ERK1/2, p38MAPK, or NFκB activation (Goebeler et al., 1999; Henderson et al., 2002; Rius et al., 2013a; Rius et al., 2013b). CXCL16 expression was determined by flow cytometry 24 h after stimulation with Ang-II.

3.1.5.4.3 Fourth study

In a first set of *in vitro* experiments, HUAEC were grown to confluence and stimulated with 1% CSE or INF-γ (20 ng/ml) for 24 h. CXCL16 protein expression was detected by flow cytometry.

To evaluate the potential involvement of NADPH and XO on CSE-induced responses, cells were incubated for 1 h with a NADPH oxidase inhibitor (apocynin, 30 μM, Sigma-Aldrich, MO) or with a XO inhibitor (allopurinol, 100 μM, Sigma-Aldrich, MO) and then stimulated with 1% CSE for 24 h. HUAEC were transfected with either control or Nox2, Nox4, Nox5-specific siRNA. Forty eight hours post-transfection, HUAEC were stimulated with 1 % CSE and CXCL16 expression was evaluated.

To investigate the possible contribution of RhoA to CSE-induced CXCL16 expression, HUAEC were transfected for 48 h with control or RhoA-specific siRNA prior to CSE stimulation and CSE-induced responses were measured 24 h later by flow cytometry.

In another set of experiments, cells were treated with a RhoA inhibitor (C3 transferase, 2 μg/ml, Cytoskeleton Inc., CO) 4 h before CSE stimulation and CXCL16 expression was similarly determined.

To elucidate the signaling pathways involved in CS-induced responses, endothelial cells were pretreated with inhibitors of ERK1/2 (PD098059, 20 μM, Sigma-Aldrich, MO), p38MAPK (SB202190, 20 μM, Sigma-Aldrich, MO) and NFκB (MOL294, 2.5 μM, donated by Dr. Kahn, Department of Pathobiology, University Washington, Seattle, WA) 1 h prior to CSE stimulation. CXCL16 expression was determined by flow cytometry 24 h after stimulation with 1% CSE.

3.1.6 Immunofluorescence studies

3.1.6.1 Determination of ICAM-1 and VCAM-1 expression in HUAEC

Cells were fixed with 4% paraformaldehyde and blocked in a PBS solution containing 1% BSA. Next, they were incubated overnight with a primary mouse antibodies against VCAM-1 (dilution 1:100 in PBS-BSA 0.3 %, Clone 1.G11B1, AbD Serotec, UK) or ICAM-1 (dilution 1:100 in PBS-BSA 0.3 %, Clone 6.5B5, AbD Serotec, UK), followed by a 45 min incubation at room temperature with an Alexa Fluor 488-conjugated goat anti-mouse secondary mAb (1/1000 dilution). Cell nuclei were counterstained with 4'-6-diamidino-2-phenylindole (DAPI, Invitrogen, Thermo Fisher Scientific, MA). Images were captured with a fluorescence microscope (Axio Observer A1, Carl Zeiss, Germany) equipped with a 40x objective lens and a 10x eyepiece.

3.1.6.2 Determination of CX_3CL1 expression in HUAEC

Cells were fixed with 4% paraformaldehyde and blocked in a PBS solution containing 1% BSA. For fractalkine detection, samples were incubated at 4°C overnight with a primary mouse mAb against human CX_3CL1 (dilution 1:200 in PBS-BSA 0.1 %, Clone 81513, R&D Systems, MN), followed by incubation with a secondary antibody FITC-conjugated rabbit anti-mouse monoclonal antibody (1/1000 dilution) at room temperature for 45 min. Cell nuclei were stained with 4'-6-diamidino-2-phenylindole (DAPI, Invitrogen, Thermo Fisher Scientific, MA). Images

were captured with an immunofluorescence microscope (Axio Observer A1, Carl Zeiss microscope, Germany) equipped with a 40x objective lens and a 10x eyepiece.

3.1.6.3 Determination of CXCL16 expression in HUAEC

In order to evaluate CXCL16 expression a similar protocol as above was used. The cells were fixed with 4% paraformaldehyde and blocked in a PBS solution containing 1% BSA. Then, cells were incubated at 4°C overnight with a primary goat policlonal antibody against human CXCL16 (dilution 1:200 in PBS-BSA 0.1 %, R&D Systems, MN), followed by incubation with a secondary antibody FITC-conjugated rabbit anti-goat monoclonal antibody (1/1000 dilution) at room temperature for 45 min. Cell nuclei were counterstained with 4'-6-diamidino-2-phenylindole (DAPI, Invitrogen, Thermo Fisher Scientific, MA). Images were captured with a fluorescence microscope (Axio Observer A1, Carl Zeiss, Germany) equipped with a 40x objective lens and a 10x eyepiece.

3.1.6.4 Experimental protocols

3.1.6.4.1 First study

Confluent endothelial cells were grown on glass coverslips and stimulated with Ang-II (1 μM) for 4 h (ICAM-1 and VCAM-1 expression) or 24 h (CX_3CL1 expression). In some experiments, cells were pretreated with Rosu (10 nM), Bex (0.3 μM) or a combination of Rosu (10 nM) plus Bex (0.3 μM) 20 h prior to Ang-II stimulation.

3.1.6.4.2 Third study

For CXCL16 detection, confluent endothelial cells were grown on glass coverslips and stimulated with 1 μM Ang-II (with or without an Ang-II AT_1 receptor antagonist, EXP3174, 100 μM) for 24 h.

3.1.6.4.3 Fourth study

For CXCL16 detection, confluent endothelial cells were grown on glass coverslips and stimulated with 1% CSE or INF-γ (20 ng/ml) for 24 h.

3.1.7 Detection of soluble mediators by ELISA

After coating the plates overnight with the primary antibody, non-specific binding sites were blocked with 3% BSA for 1 h. Supernatants and standards were added to PBS/0.5% BSA/0.05% NaN_3 for 2 h. Biotinylated detector antibodies were added for 2 h, followed by neutravidin horseradish peroxidase (Perbio Science, UK) for 1 h. All plate washes were carried out in four cycles in freshly-prepared PBS/0.2% Tween 20. Enhanced K-Blue TMB substrate (Thermo Fisher Scientific Inc., MA) was added for 30 min and the enzyme reaction was stopped by the addition of 0.19 M sulphuric acid. Absorbance was read at 450 nm and the data were processed by GraphPad Prism software. Results are expressed as pM chemokine in the supernatant. Antibody pairs were purchased from R&D Systems, MN.

3.1.7.1 Experimental protocols

3.1.7.1.1 First study

Confluent endothelial cells were stimulated with Ang-II (1 μM) for 4 h. In some experiments, cells were pretreated with Rosu (10 nM), Bex (0.3 μM) or a combination of Rosu (10 nM) plus Bex (0.3 μM) 20 h prior to Ang-II stimulation. Human chemokines GROα (CXCL1), IL-8 (CXCL8), MCP-1 (CCL2) and RANTES (CCL5) were measured in HUAEC culture supernatants by ELISA.

3.1.7.1.2 Second study

Confluent HUVEC were stimulated with Ang-II (1 μM) for 24 h and some cells were preincubated with EXP3174 (1 h, 100 μM). In some experiments, cells were pretreated with Rosu (3 μM), Bex (0.3 μM) or a combination of Rosu (3 μM) plus Bex (0.3 μM) 20 h prior to Ang-II stimulation. Human chemokines GROα (CXCL1), MCP-1 (CCL2) and RANTES (CCL5), and VEGF were measured in culture supernatants by ELISA.

In another set of experiments, HUVEC were incubated for 1 h with the PI3K inhibitor (10 μM) and then stimulated with Ang-II (24 h).The human chemokines GROα (CXCL1), MCP-1 (CCL2) and RANTES (CCL5), and VEGF were measured in cell culture supernatants by ELISA.

3.1.8 Gene knockdown by small interfering RNA (siRNA)

Confluent HUAEC and HUVEC cultures were transfected with either control or specific siRNA using Lipofectamine RNAiMAX reagent (Invitrogen, Thermo Fisher Scientific, MA).

To achieve the maximal transfection activity and lowest cytotoxicity, an optimization of the concentration of Lipofectamine RNAiMAX was performed. Cells were seed in a 6 well plate until 60% of confluency. The day before the experiment cell media was replace by antibiotic free medium. The efficiency of transfection was determined by western blot following the protocol described in *3.1.9.* After data analysis, the optimal transfection conditions were selected and are shown in table 7.

Name	**Supplier**	**Si RNA Concentration (nM)**	**Lipofectamine(µl)**
RhoA	Thermo Fisher Scientific Inc. (MA).	80	3.5
Nox2	Dharmacon (CO).	80	3.5
Nox4	Dharmacon (CO).	80	2.5
Nox5	Dharmacon (CO).	80	2.5
RXRα	Dharmacon (CO).	100	3
PPARα	Dharmacon (CO).	100	3
PPARβ/δ	Dharmacon (CO).	100	3
PPARγ	Dharmacon (CO).	100	3

Table 7: Concentration values for each siRNA and volume of Lipofectamine for each transfection assay.

3.1.8.1 Experimental protocols

3.1.8.1.1 First study

Confluent HUAEC cultures were transfected with either control or RhoA, Nox2, Nox4, Nox5, RXRα, PPARα, PPARβ/δ and PPARγ-specific siRNA using Lipofectamine RNAiMAX reagent (Invitrogen, Thermo Fisher Scientific, MA).

Some cells was transfected using a control or RhoA-specific siRNA, and at 48 hours post-transfection, cells were stimulated with Ang-II (1 μM) for 4 h. Then, leukocyte-HUAEC interactions under flow conditions were evaluated (see *3.1.3).*

In a different experimental setting, cells were transfected with control or RhoA–specific siRNA. At 48 h post transfection, HUAEC were stimulated with Ang-II (1 μM) for 4 h and Nox5 expression was quantified by immunoblot (see *3.1.9.)*

In additional experiments, control or siRNA Nox5-transfected HUAEC were stimulated with Ang-II (1 μM for 1 h) and quantification of RhoA-GTP activity was determined as detailed in *3.1.12.*

In another set of experiments, cells were transfected with control, RXRα, PPARα or PPARγ-specific siRNA and stimulated with Ang-II (1 μM; 4 h) at 48 h post-transfection. In some experiments, cells were pretreated with Rosu (10 nM) plus Bex (0.3 μM) 20 h prior to Ang-II challenge. Then, leukocyte-HUAEC interactions under flow conditions were evaluated as described in *3.1.3.*

Additionally, cells were transfected with control, RXRα, PPARα or PPARγ-specific siRNA and stimulated with Ang-II (1 μM; 1 h) at 47 h post-transfection. In some experiments, cells were pretreated with Rosu (10 nM) plus Bex (0.3 μM) 20 h prior to Ang-II challenge. Quantification of RhoA-GTP activity was determined as described in *3.1.12.*

In other experiments, Control or siRNA Nox5-transfected HUAEC were stimulated with Ang-II (1 μM for 4 h) and quantification of intracellular NO content was determined as described in *3.1.13.*

Finally, cells were transfected with control, RXRα, PPARα or PPARγ-specific siRNA and stimulated with Ang-II (1 μM; 4 h) at 44 h post-transfection, cells were pretreated with Rosu (10 nM) plus Bex (0.3 μM) 20 h prior to Ang-II challenge and quantification of NO bioavailability was determined (see *3.1.13)*

3.1.8.1.2 Second study

HUVEC were transfected with control, RXRα, PPARα, PPARβ/δ or PPARγ-specific siRNA. 48 h post-transfection the cells were pretreated with Bex (0.3 μM)

and/or Rosu (3 µM) for 24 h. Then the cells were stimulated with Ang-II (1 µM, 24 h). The number of tube-like structures was determined as described in *3.1.14.*

3.1.8.1.3 Third study

Confluent HUAEC cultures were transfected with control, Nox2, Nox4, Nox5 or RhoA-specific siRNA. At 48 h post-transfection, cells were stimulated with Ang-II (1 µM, 24 h). CXCL16 expression was determined by flow cytometry (see *3.1.5).*

3.1.8.1.4 Fourth study

Confluent HUAEC cultures were transfected with control, Nox2, Nox4, Nox5 or RhoA-specific siRNA using Lipofectamine RNAiMAX reagent (Invitrogen, Thermo Fisher Scientific, MA). At 48 h post-transfection, cells were stimulated with 1% CSE for 24 h. CXCL16 expression was determined by flow cytometry as described in *3.1.5.*

3.1.9 Study of the protein expression by western blot.

3.1.9.1 Preparation of protein samples

To obtain the protein samples, cells were subjected to the different treatments, washed once with ice-cold PBS and detached with trypsin, collected and transferred to eppendorf tubes before centrifugation (1,200 rpm, 10 min, 4°C). Subsequently TNG buffer (50 mM Tris-HCl (pH 8), 150 mM NaCl, 1% Nonidet P-40), with protease inhibitors (1 mM PMSF, 40 µg/ml aprotinin, and 40 µg/ml leupeptin) and phosphatase (1 mM sodium ortovanadate and 1 mM NaF) were added to every sample. Immediately, cells were exposed to 3 freeze-thaw-mix cycles. Afterwards, they were centrifuged (13,000 g, 4ºC, 30 min) to eliminate cell debris. Protein concentration was determined in the supernatant using the Bradford assay, 10 µl protein samples were incubated with 190 µl Bradford solution (Bradford Reagent, Bio-Rad, Germany; 1:5 dilution in water) for 5 min. Thereafter, absorbance was measured at 592 nm (Tecan infinite® M200 Absorbance reader, TECAN, Germany). A standard curve was made with BSA (Thermo Fisher Scientific, MA).

Sample protein concentrations were then normalized with ice-cold sterile water. Laemmli sample buffer (3x, (Laemmli, 1970) was added and samples were heated at 95°C for 5 min. Samples were kept at -20°C until western blot analysis.

3.1.9.2 SDS-PAGE and Immunoblotting

Proteins were separated by discontinuous SDS-polyacrylamide gel electrophoresis (SDS-PAGE) according to Laemmli *et al* (Laemmli, 1970). Equal amounts of protein were loaded on discontinuous polyacrylamide gels. The concentration acrylamide was adjusted for an optimal separation of the proteins depending on their molecular weights. Electrophoresis was carried out in the running buffer (25 mM Tris, 200 mM glycine, 0,1% SDS, pH=8.3) at 100 V for 60 min for protein separation. The molecular weight of proteins was determined by comparison with a prestained protein ladder (Spectra multicolour broad range protein ladder, Thermo Fisher Scientific, MA). After protein separation, proteins were transferred to a polyvinylidene difluoride membrane (Immun-Blot PVDF, Bio-Rad, Germany), by immunoblotting.

3.1.9.3 Protein detection

Prior to immunodetection, unspecific protein binding sites were blocked by incubating the membrane in 3 % protease free BSA-PBS (Sigma-Aldrich, MO) for 30 min at room temperature. Subsequently, the membrane was incubated with the respective primary antibody (table 8) at 4°C overnight. After four washing steps with PBS containing 0.1 % Tween 20 (PBS-T), the membrane was incubated with the secondary antibody for 2 h at room temperature, followed by four additional washing steps with PBS-T. To visualize the proteins, membranes were incubated with an anti-rabbit IgG conjugated to horseradish peroxidase (1:2000 dilution, Cell Signaling Technology, MA) or anti-mouse IgG conjugated to horseradish peroxidase (1:2000 dilution, Cell Signaling Technology, MA). For detection, luminol (5-Amino-2,3-dihydro-1,4-phthalazinedione) was used as a substrate. The membrane was incubated with Amersham ECL reagent (GE Healthcare, UK) for 1 min in the dark. Signals were detected using a luminescent reader (Fujifilm image Reader LAS1000, Fuji, Japan) and analyzed with ImageJ software (NIH, Windows free version).

To verify that the same amount of each protein was loaded, an internal loading control was used. Thus, once the membranes were developed, the primary and secondary antibodies were removed from nitrocellulose with a specific commercial solution (Blot Stripping Restore Western Buffer, Thermo Fisher Scientific, MA), blocked and incubated with a rabbit monoclonal antibody against human β-actin

(1:1000 dilution, Sigma-Aldrich, MO), for 1 h at 37ºC. After washing four times with washing buffer, the membrane was incubated with an anti-rabbit secondary antibody (1:2000 dilution, Cell Signaling Technology, MA) for 1 h at room temperature. After incubation, the membrane was washed and developed following a procedure similar as the above described.

All protein detection measured was normalized to β-actin control.

Name	Supplier	Dilution
Mouse polyclonal antibody against human RhoA	Abcam, UK	1/250
Mouse polyclonal antibody against human Nox2	Abcam, UK	1/250
Rabbit polyclonal antibody against human Nox4	Abcam, UK	1/500
Rabbit polyclonal antibody against human Nox5	Sigma-Aldrich, MO	1/500
Rabbit polyclonal antibody against human RXRα	Santa Cruz Biotechnology, CA	1/500
Mouse polyclonal antibody against human PPARα	Santa Cruz Biotechnology, CA	1/500
Rabbit polyclonal antibody against human PPARβ/δ	Abcam, UK	1/500
Rabbit polyclonal antibody against human PPARγ	Santa Cruz Biotechnology, CA	1/500
Rabbit polyclonal antibody against human PPARα	Abcam, UK	1/500
Rabbit polyclonal antibody against human AKT	Cell Signaling Technology, MA	1/500
Rabbit polyclonal antibody against human mTOR	Cell Signaling Technology, MA	1/500
Rabbit polyclonal antibody against human p70S6K1	Cell Signaling Technology, MA	1/500
Rabbit polyclonal antibody against human phospho-AKT (Ser473)	Cell Signaling Technology, MA	1/500
Rabbit polyclonal antibody against human phospho-mTOR (Ser2448)	Cell Signaling Technology, MA	1/500

Rabbit polyclonal antibody against human phospho-p70S6K1 (Thr421/Ser424)	Cell Signaling Technology, MA	1/500
Rabbit polyclonal antibody against mouse AKT	Cell Signaling Technology, MA	1/500
Rabbit polyclonal antibody against mouse mTOR	Cell Signaling Technology, MA	1/500
Rabbit polyclonal antibody against mouse p70S6K1	Cell Signaling Technology, MA	1/500
Rabbit polyclonal antibody against mouse phospho-AKT (Ser473)	Cell Signaling Technology, MA	1/500
Rabbit polyclonal antibody against mouse phospho-mTOR (Ser2448)	Cell Signaling Technology, MA	1/500
Rabbit polyclonal antibody against mouse phospho-p70S6K1 (Thr421/Ser424)	Cell Signaling Technology, MA	1/500

Table 8: Protein detection antibodies used for western blot analysis.

3.1.10 Immunoprecipitation

Immunoprecipitation was used to detect PPARα-RXRα and PPARγ-RXRα heterodimerization. Cell extracts were obtained as indicated in *3.1.9.1*. Cell lysate containing 200 μg of protein was incubated with 5 μg of the rabbit polyclonal antibody against human PPARα or PPARγ (Table 123), with rotation at 4°C overnight. Next, 50 μl of anti-Rabbit IgG Beads (Affymetrix, eBioscience, UK) were added to the cell lysates and again subjected to rotation at 4°C for 1 h. The samples were then centrifuged at 3,000 rpm for 1 min at 4°C and supernatant discarded. Samples were washed four times in 1ml of TNG buffer, centrifugated at 3,000 rpm at 4°C for 1 min and the supernatant was discarded each time. 100 μl of Laemmli sample buffer was added to the samples, heated to 90°C for 5 min, centrifuged at 13,000 rpm for 1 min and redisolved in SDS-PAGE. Immunoblotting was performed using an antibody against RXRα as indicated in *3.1.9.*

3.1.11 NADPH oxidase activity assay

In the first study, the activity of NADPH oxidase was measured in HUAEC homogenates by lucigenin-derived chemiluminiscence. Endothelial cells were pretreated for 20 h with Rosu (10 nM), Bexa (0.3 μM) or a combination of Rosu (10 nM) plus Bexa (0.3 μM) prior to Ang-II stimulation (1 μM, 1 h) since superoxide

release induced by Ang-II is detected after 1 h challenge (Estelles *et al.*, 2005). In some experiments, cells were pretreated with the antioxidant apocynin (30 μM, 1 h) or with a RhoA inhibitor (C3 transferase, 2 μg/ml, 4 h) before Ang-II stimulation (1 μM, 1 h).

After treatments, HUAEC were washed with ice-cold PBS, scraped and centrifuged at 13,000 rpm for 1 min at 4°C. The cell pellet was homogenized in lysis buffer (pH 7.0) containing 50 mM KH_2PO_4, 1 mM EGTA and 150 mM sucrose at 4°C, and protein content was determined. Cell homogenates (50 μl) were placed in duplicates in a 96-well plate containing reaction mixture (100 μl) of lysis buffer and lucigenin (5 μM). The plates were incubated in a temperature controlled BMG LABTECH Omega plate reader (37ºC) for 15 min and the basal activity of the NADPH oxidase was measured. Next, the reaction substrate NADPH (100 μM, 25 μl) was added to each well by injectors in the plate reader to initiate the reaction. The luminescence was measured every 10 s for 5 min in an Optocomp luminometer (MGM Instruments, CT). The enzymatic activity was expressed as relative light units (RLU)/μg of protein/min.

3.1.12 RhoA activation assay

In the first study, RhoA activity levels were determined using a commercial Rho A G-LISA™ assay kit (absorbance-based), following the manufacturer's instructions (Cytoskeleton Inc., CO).

HUAEC were grown to 70% confluence in six-well plates. Then, some cells were untransfected or transfected with a control siRNA or specific siRNA against Nox5, RXRα, PPARα or PPARγ using Lipofectamine RNAiMAX as described in *3.1.8.* Twenty-four hours after transfection, cells were pretreated for 20 h with with Rosu (10 nM), Bexa (0.3 μM) or a combination of Rosu (10 nM) plus Bexa (0.3 μM) prior to Ang-II stimulation (1 μM, 1 h) since Ang-II-induced RhoA activation peaks within the first hour of challenge (Shatanawi *et al.*, 2011). In additional assays, untransfected HUAEC were pretreated with the antioxidant apocynin (30 μM, 1 h) and subsequently stimulated with Ang-II (1 μM, 1 h).

3.1.13 Measurement of NO Production by HUAEC

In the first study, intracellular NO was monitored with 4-amino-5-methylamino-2′,7′-difluorofluorescein diacetate (DAF-2-FM diacetate, Invitrogen, Thermo Fisher Scientific, MA).), a fluorescence indicator of NO that emits fluorescence in response to a reaction with NO, as previously described (Peiro *et al.*, 2013). To measure intracellular NO, HUAEC were seeded on 24-wells plates. At 80% confluence, HUAEC were pretreated for 20 h with Rosu (10 nM), Bexa (0.3 μM) or a combination of Rosu (10 nM) plus Bexa (0.3 μM) and then stimulated with Ang-II (1 μM, 4 h). In another set of experiments, cells were pretreated with the antioxidant apocynin (30 μM, 1 h) or with a RhoA inhibitor (C3 transferase, 2 μg/ml, 4 h) before Ang-II stimulation (1 μM, 4 h). Finally, cells were transfected with a control siRNA or specific siRNAs against Nox5, RXRα, PPARα or PPARγ as described in *3.1.8.* Twenty-four hours after transfection, HUAEC were pretreated for 20 h with or without Rosu (10 nM) plus Bexa (0.3 μM) and then stimulated with Ang-II (1 μM, 4 h).

After completion of the treatments, cells were loaded with 2.5 μM (DAF-2-FM diacetate) in EBM-2 supplemented with EGM-2 and 10% FCS for 30 min. After loading, cells were rinsed with PBS. To quantify the DAF-related fluorescence, cells were observed under an inverted fluorescence Nikon Eclipse Ti-S microscope. Fluorescence from five different fields per well was measured (excitation wavelength: 488 nm; emission wavelength: 515 nm). Fluorescence signals were quantified using NIS-Elements 3.2 software (Nikon Izasa S.A, Spain).

3.1.14 Morphogenesis or tube formation assay *in vitro*

For the second study, 100 μl of pre-cooled BD Matrigel™ Matrix Growth Factor Reduced (GFR) (BD Biosciences, CA) was added to a 96 well plate on ice. For polymerization of the Matrigel™ Matrix, the plates were incubated at 37°C for 30 min. 12,000 HUVECs/well were seeded onto the Matrigel™.

For the different assays, HUVEC were incubated for 24 h with vehicle or Ang-II (1 μM). Some plates were pretreated with Bex (0.3-10 μM) and/or Rosu (1-10 μM) for 24 h prior to Ang-II stimulation. The AT_1 Ang-II receptor antagonist EXP3174 (100 μM) kindly donated by Merck Sharp & Dohme (Spain) was added 1

h before Ang-II challenge. In additional assays, some cells were preincubated with antagonists against different chemokine receptors. HUVEC were incubated with the CXCR2 antagonist (SB225002, 100 nM, Tocris Bioscience, UK), the CCR2 antagonist (BMSCCR2 22, 10 μM, Tocris Bioscience, UK) or the CCR5 antagonist (DAPTA, 10 nM, Tocris Bioscience, UK) with or without the dual CCR1/CCR3 antagonist (UCB35625, 100 nM, Tocris Bioscience, UK) 1 h prior to Ang-II stimulation. Additionally, some cells were treated with the VEGF receptor1/2 antagonist (Cyclo-VEGFI, 10 μM, Calbiochem, Germany) 1 h prior to Ang-II (1 μM, 24 h) challenge. The concentrations of these compounds employed have been described previously (White *et al.*, 1998; Sabroe *et al.*, 2000; Polianova *et al.*, 2005; Piqueras *et al.*, 2007).

Phase contrast micrographs (Axio Observer A1, Carl Zeiss microscope, Germany) and the mean number of tubes in 5 low-power (×100) random fields were recorded.

3.1.15 Proliferation assay

Proliferation assay was performed by Bromodeoxy Uridine (5-Bromo-2-DeoxyUridine, BrdU) incorporation. BrdU is a synthetic pyrimidine analogue of thymidine, which is selectively incorporated into cell DNA at the S phase of the cell cycle. HUVECs were seeded on glass coverslips incubated during 24 h with BrdU (50 μM, Invitrogen, Thermo Fisher Scientific, MA). Next, cells were washed with warm PBS and incubated in the presence of the AT_1 Ang-II receptor antagonist EXP3174 (100 μM) 1 h prior to Ang-II simulation (1 μM, 24 h). Some cells were pretreated with Bex (0.3 μM) with or without Rosu (3 μM) for 24 h before Ang-II stimulation.

After Ang-II stimulation cell medium was flush out and BrdU-positive cells were detected by immunofluorescence with an anti-BrdU Alexa Fluor-488 antibody (Invitrogen, Thermo Fisher Scientific, MA). Total cell count was performed by 4', 6-diamidino-2-phenylindole (DAPI, Thermo Fisher Scientific, MA) nuclear staining. Each experiment was done in triplicate. Proliferation rate was determined as percentage of BrdU positive cells relative to total cell count.

3.1.16 Wound-healing for migration assay

Wound healing migration assay was performed as described previously (Bruneau *et al.*, 2013). HUVEC were grown up to 100% confluence. Cell monolayers were pretreated as described above and wounded by scraping them with a micropipette tip and incubating them with 1 μM of Ang-II. After an additional 24 h, cell migration into the wound was assessed by microscopy using with a phase-contrast microscope (Axio Observer A1, Carl Zeiss microscope, Germany). The degree of wound closure was measured as the percentage of the area covered by migrating cells in the initial wound using ImageJ software. Experiments were done in triplicate each and analysis was made using Image J software (Windows free version).

3.2 STUDIES IN COPD PATIENTS AND AGE-MATCHED CONTROLS

3.2.1 Patient selection

A total of 36 subjects (21 COPD patients and 15 control age-matched subjects without COPD) were included in this study. COPD patients and control subjects were recruited by the Pneumonology Unit of University Clinic Hospital of Valencia, Valencia, Spain. All patients had COPD confirmed by medical history, clinical and functional examinations according to criteria established by the American Thoracic Society (Standards of diagnosis and care of patients with chronic obstructive pulmonary disease) Am J Respir Crit Care Med 1995;152 (Suppl):77-120): smoking history of 10 pack/year, the post-bronchodilator ratio of low forced expiratory volume in 1 second (FEV1) and forced vital capacity (FVC), FEV1/FVC ratio was <0.70 and the post-bronchodilator FEV1 was <80%. One pack-year was defined as smoking 20 cigarettes per day for one year. Individuals in the control group were volunteers seen at the respiratory function laboratory for routine preoperative assessment. They had no history of pulmonary disease or respiratory symptoms and had a normal spirometry. Written informed consent was obtained from all volunteers. Spirometry was performed on a Master Scope (Jaeger, Germany), after inhalation of 0.4 mg of salbutamol. A minimum of three airflow and volume tracings were obtained and the highest value for FEV1 and FVC as percent predicted normal were

used for calculations. Most of the patients included in this study presented moderate COPD according to the GOLD classification (Global Initiative for Chronic Obstructive Lung Disease. Global strategy for the diagnosis, management, and prevention of COPD. [January 2015]; Available from: http://www.goldcopd.org). Accordingly, 57% were GOLD2 (moderate) and 43% were GOLD3 (severe). Clinical features of patients and age matched controls are shown in Table 9.

	Control non-smoker volunteers	**COPD Subjects**
Numbers per group (n)	15	21
Smoking (Pack-year)	None	48,1±6,75
Age	65,13 ± 2,23	65,76±1,75
FEV1 (% Predicted)	103,24 ± 4,55	47,9±2,88**
FEV1/FVC (%)	79,88 ± 1,67	50,02±1,91**
Gender (M)	100%	100%

Table 9: Patient demographics of the subjects studied (data expressed as mean ± SEM). Definition of abbreviations: Pack-year (nº cigarettes per day per smoking years / 20). FEV1 % Predicted, forced expiratory volume in 1 s (%); FVC, forced vital capacity. **p<0.01 versus control group.

3.2.2 Flow cytometry

3.2.2.1 Measurement of platelets activation

To assess the grade of platelet activation, PAC-1^+ platelets (detects activated integrin $\alpha_{IIb}\beta_3$) and the expression of P-selectin (CD62P) were measured in platelets from COPD patients and control-matched individuals by flow cytometry. Duplicate samples (25 µl) of citrated blood, diluted 1/10 in glucose buffer (1 mg/ml glucose in PBS/0.35 % BSA), were incubated in the dark for 30 min with a CF-conjugated monoclonal antibody against human CD41 (5 µl, Immunostep Spain) and a FITC-conjugated monoclonal antibody against human PAC-1 (2.5 µl, BD Biosciences, CA) or with an APC-conjugated monoclonal antibody against human P-selectin (5 µl, Immunostep, Spain). Samples were run in a flow cytometer (FACSVerse flow cytometer, BD Biosciences, CA). $CD41^+$ (platelets) populations were selected according to the gating strategy illustrated in Figure I and expressed as the mean of fluorescence intensity (MFI).

3.2.2.2 Determination of CXCR6 and CXCL16 expression

To determine the expression of CXCR6 and CXCL16 on platelets and CXCR6 on circulating neutrophils, monocytes and lymphocytes from COPD patients and control-matched individuals, duplicate samples (100 µl) of heparinized whole blood were incubated in the dark for 30 min with saturated amounts of PE-conjugated monoclonal antibodies against human CXCR6 (10 µl, clone 56811, R&D Systems, MN) or CXCL16 (10 µl, Clone 256213, R&D Systems, MN). In some experiments, blood samples were incubated with EDTA (10 mM, for 15 min at 37ºC) to promote platelet dissociation as described (Postea et al., 2012). RBCs were lysed and leukocytes were fixed using a commercial lysis buffer. Samples were run in a flow cytometer. The expression of CXCR6 (PE fluorescence) was measured on $CD41^+$ (platelets), $CD16^+CD14^-$ (neutrophils), $CD14^+$ (monocytes) and $CD3^+$ (lymphocytes) populations according to the gating strategy illustrated in Figure 14.

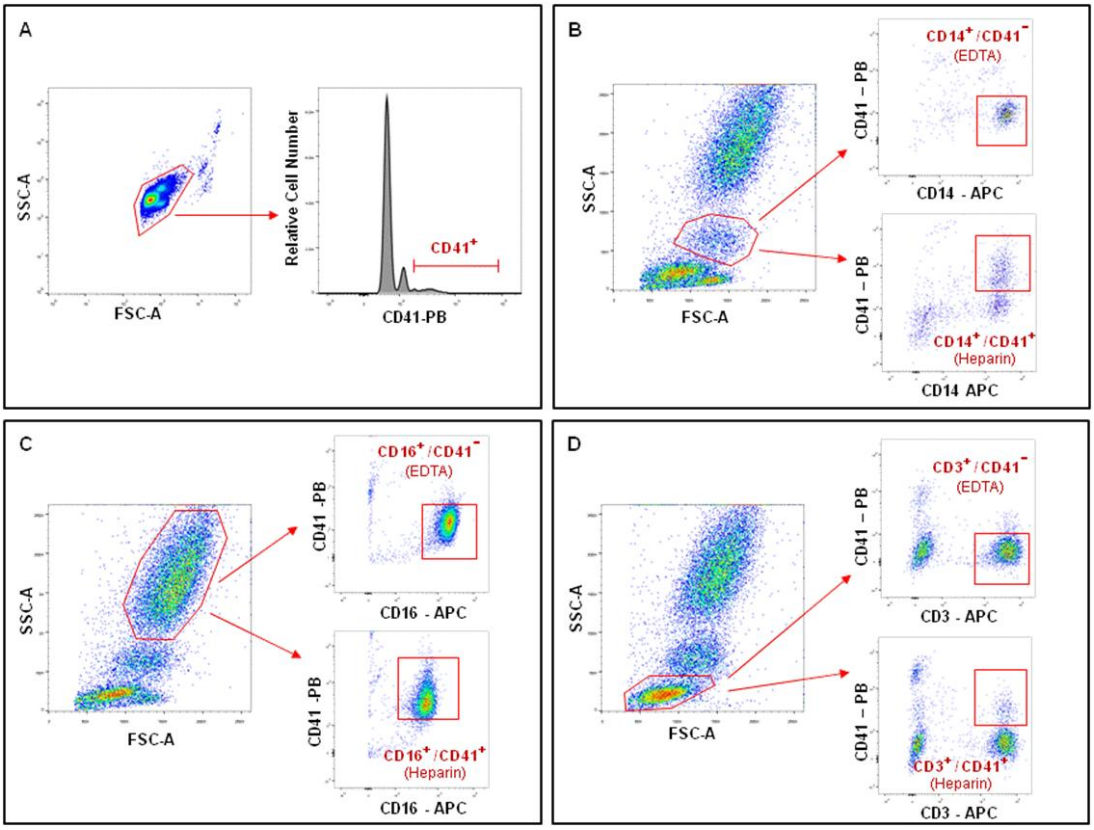

Figure 14: Flow-cytometry detection and morphologic gating of human monocytes, lymphocytes, neutrophils and platelets in whole blood. (A) Platelets were gated according to the side scatter in the logarithmic scale and defined as $CD41^+$ population. (B) Neutrophil-platelet complexes were selected as $CD16^+$ $CD14^-$ $CD41^+$ population from heparinized whole blood, and platelet-free neutrophils were gated as $CD16^+CD14^-CD41^-$ from blood incubated with EDTA (C) Monocyte-platelet complexes were selected as $CD14^+CD41^+$ population from heparinized whole blood, and platelet-free monocytes were gated as

$CD14^{+}CD41^{-}$ from blood incubated with EDTA.(D) Lymphocyte-platelet complexes were selected as $CD3^{+}$ $CD41^{+}$ population from heparinized whole blood, and platelet-free lymphocytes were gated as $CD3^{+}CD41^{-}$ from blood incubated with EDTA.

3.2.2.3 Flow chamber assay

In order to study the leucocyte-HUAEC interactions, a dynamic flow chamber assay was performed using whole blood from both groups under investigation. Diluted whole blood (1/10 in HBSS) of COPD patients and control-matched subjects was perfused across unstimulated or 1% CSE-stimulated endothelial monolayers as described in part *3.1.3* and leukocyte-endothelial cell interactions were determined. Some plates were incubated with a polyclonal neutralizing antibody against human CXCL16 (2 μg/ml, R&D Systems, MN) or with an isotype matched control antibody (MOPC-21, 2 μg/ml, Sigma-Aldrich, MO) 10 min before blood perfusion. In order to evaluate the contribution of the platelets in the adhesion process, some experiments were carried out in parallel with heparinized blood incubated or not with EDTA (10 mM, for 15 min, 37ºC).

3.2.2.4 Determination of CXCL16 in plasma

To determine CXCL16 plasma levels, heparinized human whole blood (10 U heparin/ml) from COPD patients and healthy control-matched volunteers was collected. Before centrifugation to obtain plasma, further heparin was added to the blood sample (100 U/ml). This procedure was used to help to dissociate chemokines from blood cells. Plasma samples were stored at −80°C. Human CXCL16 was measured in plasma by ELISA. Results are expressed as pM chemokine in the supernatant.

3.3 ANIMAL STUDIES

The animal protocol conforms to the Guide for the Care and Use of Laboratory Animals published by the US National Institutes of Health (NIH publication No. 85-23, revised 1996) and was approved by the Ethics Review Board of the School of Medicine, University of Valencia. Mice (22–30g, Charles River) were bred and maintained under specific pathogen-free conditions. For the entire experimental period, the mice were fed with an autoclaved diet with free access to water.

3.3.1 Study of leukocyte-endothelial cell interaction *in vivo* by intravital microscopy

3.3.1.1 Animal preparation

Mice were anesthetized by i.p. injection with a mixture of xylazine hydrochloride (10 mg/kg) and ketamine hydrochloride (200 mg/kg). The mouse cremasteric preparation used in this study was similar to that described previously (Piqueras *et al.*, 2009). The cremaster muscle was dissected from the tissues and exteriorized on an optical clear viewing pedestal. The muscle was cut longitudinally with a cautery and held flat against the pedestal by attaching silk sutures to the corners of the tissue. The muscle was then perfused continuously with warmed bicarbonate-buffered saline (pH 7.4) at a rate of 1 ml/min. The cremasteric microcirculation was observed using an intravital microscope (Nikon Optiphot-2, SMZ1, Netherlands) equipped with a 50x objective lens (Nikon SLDW, Netherlands) and a 10x eyepiece. A video camera (Sony SSC-C350P, Germany) mounted on the microscope projected the image onto a colour monitor and the images were CCD recorded for playback analysis. Cremasteric arterioles (20-40 μm in diameter) were selected for the study and the diameter was measured online using a video caliper (Microcirculation Research Institute, Texas A&M University, College Station, TX). Centerline blood cell velocity was also measured online using an optical Doppler velocimeter (Microcirculation Research Institute). Vessel blood flow was calculated from the product of mean RBC velocity (Vmean = centerline blood cell velocity/1.6) and cross-sectional area, assuming cylindrical geometry. Wall shear rate (γ) was calculated based on the Newtonian definition: $\gamma = 8 \times (V_{mean}/D_v)\ s^{-1}$, in which D_v is vessel diameter (House *et al.*, 1987).

The number of adherent of leukocytes was determined offline during playback of the recorder images. A leukocyte was defined as adherent to arteriolar endothelium when it was stationary for at least 30 s. Leukocyte adhesion was expressed as the number of leukocytes per 100 μm length of vessel. In each animal, leukocyte responses were measured in three to five randomly selected arterioles. At the end of the experiments, animals were humanely euthanized by anesthetic overdose.

3.3.1.2 Experimental protocols

3.3.1.2.1 First study

In the first study, Ang-II was administered to randomly selected groups of C57Bl6 (Charles River, Spain) mice *via* subcutaneous osmotic minipumps (Alzet 2004 osmotic minipumps, Charles River, Spain) set to deliver saline or Ang-II (500 ng/kg/min) for 14 days. This dose was selected based on its mild effects on blood pressure and clear leukocyte infiltration as previously described (Scalia *et al.*, 2011). A second group of mice were infused with Ang-II and administered by gavage with Bexarotene (10 mg/kg/day); a third group was infused with Ang-II and Rosuvastatin (1.25 mg/kg/day delivered by osmotic minipumps), and a final Ang-II infused group was treated with a combination of both drugs. The experimental groups were:

1- Vehicle
2- Ang-II (500 ng/kg/min)
3- Ang-II (500 ng/kg/min) + Rosu (1.25 mg/kg/day)
4- Ang-II (500 ng/kg/min) + Bex (10 mg/kg/day)
5- Ang-II (500 ng/kg/min) + Rosu (1.25 mg/kg/day) + Bex (10 mg/kg/day)

3.3.1.2.1.1 Whole mount immunohistochemistry study of the mice cremasteric circulation

Once intravital microscopy determinations were performed, mice were sacrificed and the cremaster muscle was isolated and fixed in 4% paraformaldehyde for 10 minutes. The protocol followed was similar to that previously described (Massena *et al.*, 2010); briefly, whole-mounted muscles were incubated for 2 h in 0.2% Triton X-100, 1% BSA and 0.5% horse serum in PBS.

Then, they were washed twice with PBS buffer and incubated overnight at 4°C with a primary antibody rabbit anti-mouse CX_3CL1 (dilution 1:100, Affymetrix, eBioscience, UK) or eFluor 450-conjugated rat monoclonal against mouse CD31 (PECAM-1) (dilution 1:100, clone 390, Affymetrix, eBioscience, UK). Samples were subsequently washed with PBS and incubated for 1.5 h at room temperature with Alexa Fluor 488-conjugated goat anti-rabbit secondary antibody (dilution 1:500, Invitrogen, Thermo Fisher Scientific, MA). All antibodies were diluted in 0.1% PBS/BSA. The muscles were then mounted with Slowfade Gold Reagent

(Invitrogen, Thermo Fisher Scientific, MA). Images were acquired with a fluorescence microscope (Axio Observer A1, Carl Zeiss, Germany) equipped with a 40x objective lens and a 10x eyepiece.

3.3.1.2.1.2 Immunohistochemistry study of the mice cremasteric circulation

After completion of the intravital microscopy measurements, the cremaster muscle was isolated and fixed in 4% paraformaldehyde, dehydrated using a graded acetone series at 4°C, and embedded in paraffin wax for assessment of ICAM-1, VCAM-1 and E-selectin expression as previously described (Sanz *et al.*, 2012). Tissue sections (5 μm) were incubated against mouse ICAM-1 (dilution 1:50, clone 3E2, BD Biosciences, CA), VCAM-1 (dilution 1:50, clone 429, BD Biosciences, CA) and E-selectin (dilution 1:50, clone 390, R&D Systems, MN) overnight at 4°C and then for a further 60 min at 37°C with a biotinylated anti-rabbit secondary antibody (1:500 dilution, Santa Cruz Biotechnology CA), streptavidin-HRP (LABVISION Corporation, CA), and diaminobenzidine substrate. Slides were counterstained with hematoxylin (Sigma-Aldrich, MO). Positive staining was defined as an arteriole displaying a brown reaction product.

3.3.1.2.1.3 Determination of CD11b integrin expression by flow cytometry

Heparinized whole blood samples were stained for 30 min with saturated amounts of PE-conjugated anti-CD115 mAb (1:10 dilution, clone T38-320, BD Biosciences, CA), VH-450-conjugated anti-Ly6g mAb (1:10 dilution, clone 1A8, BD Biosciences, CA) and APC-conjugated anti-CD11b mAb (1:10 dilution, clone M1/70, BD Biosciences, CA). Red blood cells were lysed using a commercial lysing solution (BD Biosciences, CA) and samples were run in a flow cytometer (FACSVerse Flow Cytometer, BD Biosciences, CA). The expression of CD11b (CFS fluorescence) in monocytes and neutrophils was measured according to the expression of CD115 and Ly6g; respectively and expressed as the mean of fluorescence intensity (MFI).

3.3.1.2.1.4 Plasma chemokine detection

KC (CXCL1), MCP-1 (CCL2) and RANTES (CCL5) in mice plasma samples were measured using commercial enzyme-linked immunoassay (ELISA) kits following manufacture's instruction . The OD values were recorded on a microplate reader at 450 nm. The concentrations of cytokines in samples were calculated from a standard curve generated using recombinant chemokines. The mouse KC (CXCL1) and MCP-1 (CCL2) ELISA kit were for R&D Systems, MN. The mouse RANTES (CCL5) ELISA kit was for RayBiotech, GA.

3.3.1.2.1.5 Measurement of glucose and lipid profile

Circulating glucose and lipid levels in plasma of mice fasted overnight were measured using enzymatic procedures (WAKO chemicls USA, inc., VA) and the Ascensia Elite glucometer (Bayer HealthCare, Germany).

3.3.1.2.1.6 Measurement of blood pressure

Systolic blood pressure was measured in conscious mice using a non-invasive tail cuff system with a photoelectric sensor (Niprem 645, Cibertec S.A., Spain) using a Niprem 1.8 software (Cibertec S.A., Spain). During the procedure animals were placed in the restrainer tube of a chamber that was kept at 36°C (LE5002 Pressure Meter, PANLAB, Spain) as previously described (Zhang et al., 2009). Mice were acclimated to the instrument for 5 continuous days before baseline measurements and then daily for the remainder 14 days. Blood pressure measurements were determined every day. Each data are the average of 10 values recorded for each animal and used for analysis.

In an additional group of experiments, Ang-II 1000 ng/kg/min was administered via subcutaneous osmotic minipumps for 14 days. A second group of mice were infused with Ang-II and administered by gavage with Bex (10 mg/kg/day); a third group was infused with Ang-II and Rosu (1.25 mg/kg/day delivered by osmotic minipumps), and a final Ang-II infused group was treated with a combination of both drugs.

3.3.1.2.2 Third study

Male mice of C57BL/6J background carrying targeted knock in of GFP to disrupt the CXCR6 gene (Charles River, Spain) were used. Male $CXCR6^{gfp/+}$ mice

were used as heterozygote controls ($CXCR6^{-/+}$) and homozygote $CXCR6^{gfp/gfp}$ animals that do not express functional CXCR6 receptor as CXCR6 deficient mice ($CXCR6^{-/-}$). Ang-II was administered to randomly selected groups of $CXCR6^{+/-}$ or $CXCR6^{-/-}$ mice via subcutaneous osmotic minipumps set to deliver saline or Ang-II (500 ng/kg/min) for 14 days. The experimental groups were:

1- $CXCR6^{+/-}$ vehicle
2- $CXCR6^{+/-}$ Ang-II (500 ng/kg/min)
3- $CXCR6^{-/-}$ vehicle
4- $CXCR6^{-/-}$ Ang-II (500 ng/kg/min)

3.3.1.2.2.1 Determination of CD11b integrin and CD69 expression by flow cytometry

Heparinized whole blood samples were stained for 30 min with saturated amounts of PE-conjugated anti-CD115 mAb (1:10 dilution, clone T38-320, BD Biosciences, CA) and APC-conjugated anti-CD11b mAb (1:10 dilution, clone M1/70, BD Biosciences, CA), to study monocyte activation or PE-conjugated anti-CD3 mAb (1:10 dilution, clone 145-2C11, BD Biosciences, CA) and APC-conjugated anti-CD69 mAb (1:10 dilution, clone H1.2F3, BD Biosciences, CA), to study T cells activation. Red blood cells were lysed using a commercial lysing solution (BD Biosciences, CA) and samples were run in a flow cytometer (FACSVerse Flow Cytometer, BD Biosciences, CA). The expression of CD11b (CFS fluorescence) in monocytes and neutrophils was measured according to the expression of CD115 and Ly6g; respectively and expressed as the mean of fluorescence intensity (MFI). The expression of CD69 (CFS fluorescence) was measured in T cells according to the expression of CD3 and expressed as the mean of fluorescence intensity (MFI).

3.3.1.2.2.2 Whole mount immunohistochemistry of the mice cremasteric circulation

Immunofluorescence studies were carried out following a similar protocol to that previously described in *3.3.1.2.1.1*. For this experiment, muscles were incubated overnight at 4°C with a primary rabbit anti-mouse CXCL16 mAb (1:200 dilution, Immunostep, Spain) or eFluor 450-conjugated rat monoclonal against mouse CD31 (PECAM-1) (dilution 1:100, clone 390, Affymetrix, eBioscience, UK). Samples were

then washed with PBS and incubated for 1.5 h at room temperature with Alexa Fluor 488-conjugated donkey anti-rabbit secondary antibody (1/500 dilution).

3.3.1.2.3 Fourth study

In the fourth study, $CXCR6^{+/-}$ and $CXCR6^{-/-}$ male mice were used again. Some of them were exposed to cigarette smoke (CS). Mice were placed in a plexiglass chamber (volume of 20 l) covered by a disposable filter. The smoke produced by cigarette burning was introduced at a rate of 25 ml/min into the chamber with the continuous airflow generated by a mechanical ventilator, with no influence on the chamber temperature (<0.1°C variation). The animals received smoke from 5 research grade cigarettes (3R4F) per exposure, 2 exposures a day during 3 days. Experiments were carried out 16 h after the last exposure. The experimental groups were:

1- $CXCR6^{+/-}$ unexposed
2- $CXCR6^{+/-}$ exposed to CS
3- $CXCR6^{-/-}$ unexposed
4- $CXCR6^{-/-}$ exposed to CS

3.3.1.2.3.1 Determination of CD11b integrin expression by flow cytometry

Determination of CD11b-integrin expression was carried out following the same protocol to that previously described in *3.3.1.2.2.3*.

The expression of CD11b (APC fluorescence) in monocytes was measured in $CD115^{+}$ cells and the percentage of monocytes expressing the integrin was determined.

3.3.1.2.3.2 RT-PCR

The lung and cremaster of mice were frozen at -20°C immediately after animal sacrifice for subsequent RNA extraction. For tissue homogenization an Ultra-Turrax (IKA®-Werke GmbH & Co, Germany) were used. Reverse transcription was performed on 500 ng of total RNA with TaqMan reverse transcription reagents kit (Applied Biosystem, Thermo Fisher Scientific, MA). cDNA was amplified using standard protocols employing the primers showed in table 10, in a 7900HT Fast Real-Time PCR System (Applied Biosystem, Thermo Fisher Scientific, MA) using Universal Master Mix (Applied Biosystems, Thermo Fisher Scientific, MA). Relative quantification of

the different transcripts was determined with the $2^{-\Delta\Delta Ct}$ method using GAPDH as endogenous control and normalized to control group.

Gen	Primer	Sequence [5'-3']
***Mouse* CXCL16**	Forward	GCTTTGGACCCTTGT CTCTTGC
	Reverse	GTGCTGAGTGCTCTGACTATGTGC
Mouse GAPDH	Forward	TGACCACAGTCCATGCCATC
	Reverse	GACGGACACATTGGGGGTAG

Table 10: Sequences of the primers used for qPCR assay.

3.3.1.2.3.3 Whole mount immunohistochemistry of the mice cremasteric circulation

Immunofluorescence studies were carried out following the same protocol to that previously described in *3.2.1.2.2.2*.

3.3.1.2.3.4 Immunohistochemistry study in murine lung

In some animals, lungs were removed, fixed with 4% paraformaldehyde and embedded in paraffin. Sections (4μm) were obtained and stained with hematoxylin/eosin. Leukocytes were counted in 10 different fields and averaged. Images were acquired with a microscope (Axio Observer A1, Carl Zeiss, Germany) equipped with a 40x objective lens and a 10x eyepiece.

3.3.2 Atherosclerosis model in apoE$^{-/-}$ mice

3.3.2.1 Experimental protocol

To evaluate the diet-induced atherosclerosis lesion in the aortic root, apoE$^{-/-}$ (C57BL/6J) female mice were obtained from Charles River laboratories and kept on a low-fat standard diet (2.8% fat, Panlab, Spain). At 8 weeks of age, mice were fed with a high fat atherogenic diet (10.8% total fat, 0.75% cholesterol, Ssniff, Germany) for 8 weeks (atherogenic diet group).

3.3.2.1.1 First study

In a first study, some mice fed with atherogenic diet received Bex (10 mg/kg/day by oral gavage), Rosu (1.25 mg/kg/day delivered with the osmotic

minipumps) or the combination of both drugs. The control mouse group was maintained on a low-fat standard diet for 8 weeks. The experimental groups were:

1- Control diet
2- Atherogenic diet
3- Atherogenic diet + Rosu (1.25 mg/kg/day)
4- Atherogenic diet + Bex (10 mg/kg/day)
5- Atherogenic diet + Rosu (1.25 mg/kg/day) + Bex (10 mg/kg/day)

3.3.2.1.1.1 Evaluation of diet-induced atherosclerosis

After treatments, hearts containing the aortic root were removed from mice, washed with PBS, fixed with 4% paraformaldehyde/PBS overnight and paraffin-embedded for sectioning and analysis, as described (Rius *et al.*, 2013c).

Atherosclerosis was evaluated in at least 3-5 aortic root cross-sections stained with hematoxylin/eosin (Gonzalez-Navarro et al., 2010). Lesion size was quantified as the intima-to-media ratio in cross-sections of paraffin-embedded aortic root. For macrophage quantification in lesions, a rat anti-Mac-3 mAb (1:200 dilution, clone M3/84, Santa Cruz Biotechnology, CA) was used. After peroxidase inactivation (H2O2, 0.3%) and blockade with horse serum, samples were incubated overnight (4ºC) with the primary antibody. Detection was performed with a biotin-conjugated goat anti-rat secondary antibody (1:300 dilution, Santa Cruz Biotechnology, CA) followed by HRP-streptavidin (LABVISION Corporation, CA) and DAB substrate (AbD Serotec, UK) incubation. Slides were counterstained with hematoxylin (Sigma-Aldrich, MO). and mounted with EUKITT (Deltalab, Spain). For T-cell detection within the lesion, aortic root cross-sections were blocked as above and incubated overnight with a rabbit polyclonal anti-CD3 antibody (1:75 dilution, Santa Cruz Biotechnology, CA) followed by an incubation for 1 h at room temperature with an Alexa Fluor 488-conjugated goat anti-rabbit secondary antibody (1:200 dilution, Invitrogen, Thermo Fisher Scientific, MA) and mounted with Slow-Fade Gold antifade reagent. Preparations were analyzed by fluorescent microscopy with an inverted fluorescent microscope (Axio Observer A1, Carl Zeiss, Germany).

3.3.2.1.1.2 Measurement of glucose and lipid profile

Circulating glucose and lipid levels in plasma of mice fasted overnight were measured using enzymatic procedures (WAKO chemicals inc., VA) and the Ascensia Elite glucometer (Bayer HealthCare, Germany).

3.3.3 Abdominal Aortic Aneurysm in apoE$^{-/-}$ mice

3.3.3.1 Animal surgery

To induce AAA, Alzet osmotic minipumps (Model 2004) were implanted into 8-week-old apoE$^{-/-}$C57BL/6 or C57BL/6 wild type mice (Charles River, Spain) in order to administer saline or Ang-II subcutaneously at a dose of 500 ng/kg/min for 28 days, during which mice were fed a Western-type diet (0.15% cholesterol with 42% fat calories, Ssniff, Germany).

3.3.3.2 Experimental protocol

3.3.3.2.1 Second study

In the second study, apoE$^{-/-}$ and C57BL/6 mice were infused for 28 days with Ang-II and subjected to a western-type diet (WD). Additionally, some groups of Ang-II-infused mice received Bex (10 mg/kg/day by oral gavage), Rosu (10 mg/kg/day delivered with the osmotic minipumps) or the combination of both drugs. The dose of Bexa administered has previously been found not to inhibit acute TNFα-induced responses *in vivo* (Sanz *et al.*, 2012), whereas Rosu was administered at doses that did not inhibit *in vivo* vascular inflammation or AAA formation albeit orally given in the drinking water (Wang *et al.*, 2011). Since the subcutaneous administration of the statin using an osmotic minipump allows 100% drug bioavailability and its oral administration results in 34.5% bioavailability in mice (Peng *et al.*, 2009) we chose this route to ensure a full dosage effect. The experimental groups for this study were:

1- C57BL/6 wild type vehicle + WD
2- C57BL/6 wild type + WD + Ang-II (500 ng/kg/min)
3- C57BL/6 wild type + WD + Ang-II (500 ng/kg/min) + Rosu (10 mg/kg/day)

4- C57BL/6 wild type + WD + Ang-II (500 ng/kg/min) + Bexa (10 mg/kg/day)
5- C57BL/6 wild type + WD + Ang-II (500 ng/kg/min) + Rosu (10 mg/kg/day) + Bex (10 mg/kg/day)
6- ApoE$^{-/-}$ C57BL/6 vehicle + WD
7- ApoE$^{-/-}$ C57BL/6 Ang-II (500 ng/kg/min)
8- ApoE$^{-/-}$ C57BL/6 + WD + Ang-II (500 ng/kg/min) + Rosu (10 mg/kg/day)
9- ApoE$^{-/-}$ C57BL/6 + WD + Ang-II (500 ng/kg/min) + Bex (10 mg/kg/day)
10- ApoE$^{-/-}$ C57BL/6 + WD + Ang-II (500 ng/kg/min) + Rosu (10 mg/kg/day) + Bex (10 mg/kg/day)

3.3.3.2.1.1 Immunohistochemistry analysis

Aortas from apoE$^{-/-}$ mice were fixed with 4% paraformaldehyde, embedded in paraffin and cut into 5 μm cross sections. After peroxidase inactivation (H_2O_2 0.3%) and blockade with horse serum, samples were incubated overnight (4ºC) with the primary antibody.

For macrophage quantification, a rat anti mouse-Mac-3 monoclonal antibody was used, following the same protocol to that previously described in 3.3.2.1.1.1.

In addition, CD31 (PECAM-1) staining was performed with a rabbit anti-mouse-CD31 polyclonal antibody (1:100 dilution, Abcam, UK). Detection was carried out with a biotin-conjugated goat anti-rabbit secondary antibody (1:300 dilution, Santa Cruz Biotechnology CA) followed by HRP-Streptavidin (LABVISION Corporation, CA) and DAB substrate incubation. Mac-3 staining in each section was determined and normalized to the total aorta area. Microvessel formation was determined by counting CD31^{+} microvessels per high power field using a phase contrast microscope (Axio Observer A1, Carl Zeiss, Germany).

3.3.3.2.1.2 Measurement of blood pressure and lipid profile in mice

Systolic blood pressure was measured in conscious apoE$^{-/-}$ and C57BL6 mice using a non-invasive tail cuff system (LE5002 Pressure Meter, PANLAB, Spain). Plasma lipid levels were measured in mice fasted overnight. Total Cholesterol (TC), Triglycerides (TG), High-density lipoprotein cholesterol (HDL-C), Non-HDL-

Cholesterol were determined using enzymatic procedures (WAKO chemicals inc., VA).

3.3.3.2.1.3 Determination of Rosuvastatin plasma levels.

Alzet osmotic minipumps (Model 2004) were implanted into apoE$^{-/-}$ mice for subcutaneous deliver of Rosuvastatin at a dose of 10 mg/kg/day for 5 days (n=6). Another group of apoE$^{-/-}$ mice (n=6) received Rosuvastatin at the same dose by oral gavage for the same period of time. At the end of the experimental protocol, blood samples were collected into heparin containing tubes.

Analysis of Rosuvastatin plasma levels were determined by liquid chromatography-electrospray ionization–tandem mass spectrometry (LC-MS/MS) method (Trivedi *et al.*, 2012). Chromatographic separation (5 µl injection) was performed in an Acquity TQD mass spectrometer (Waters, Milford, MA, USA) using an AcquityUPLC BEH column 18 (2.1×50 mm, 1.7 µm particle size). The mass spectrometer was equipped with a Z-spray electrospray ionization source. A gradient of (A) Milli-Q purified water with 0.2 % formic acid and (B) 95% methanol/ 5% water (0.2% formic acid) was used. The flow rate was 0.4 ml/min. The conditions were: capillary: 3.5 KV, skimmer: 5 V, RF Lens: 0.2 V, source temperature: 120 ºC, desolvation temperature: 350ºC. MS1 parameters were LM resolution, 13; HM resolution, 13; ion energy, 1. MS2 parameters were LM resolution, 13; HM resolution, 13; ion energy, 1; multiplier 650 V. Mass spectrometric analysis was performed by monitoring ion transitions at m/z 482.2→258.2, with collision energy of 30 V. Spectra were acquired in positive and negative ionization multiple reaction monitoring (MRM) mode with interchannel delay of 0.05 s.

3.3.3.2.1.4 Determination of chemokines, VEGF and RXR in the aortic aneurysm

The aortic arch of mice were frozen at -20°C immediately after animal sacrifice for subsequent RNA extraction. PCR was performed following the same protocol to that previously described in 3.3.1.2.3.2.

mRNA levels were normalized to the expression cyclophilin used as endogenous control and relativized to the vehicle treated group.

The sequences of the primers used to amplify each of the genes are showed in table 11.

Gen	Primer	Sequence [5'-3']
Mouse CXCL1/GROα	Forward	GAAGCTCCCTTGGTTCAGAAAA
	Reverse	GCAGTCTGTCTTCTTTCTCCGTTAC
Mouse CCL2/MCP-1	Forward	GCCCAGCACCAGCACCAG
	Reverse	GGCATCACAGTCCGAGTC
Mouse CCL5/RANTES	Forward	CTCGGTCCTGGGAAAATGG
	Reverse	TGCTGATTTCTTGGGTTTGCT
Mouse VEGF	Forward	TCTCACCGGAAAGACCGATT
	Reverse	CTGTCAACGGTGACGATGATG
Mouse RXRα	Forward	ATGGCCCGTGTGGATCTTT
	Reverse	GGATGGTGATGCATCTTTTGG
***Mouse* cyclophilin**	Forward	TGGAGAGCACCAAGACAGACA
	Reverse	TGCCGGAGTCGACAATGAT
***Mouse* CXCL16**	Forward	AGCTTGCTCACTCGGATTCC
	Reverse	TCCGACAAAACCGAAAGAAAA
Mouse CCL2/MCP-1	Forward	GCCCAGCACCAGCACCAG
	Reverse	GGCATCACAGTCCGAGTC
Mouse VEGF	Forward	TCTCACCGGAAAGACCGATT
	Reverse	CTGTCAACGGTGACGATGATG
***Mouse* CXCR6**	Forward	GGCCTATGCAGGCACCTATG
	Reverse	GCCTCGAAGAGTTTTGCACAT
***Mouse* Cyclophilin**	Forward	TGGAGAGCACCAAGACAGACA
	Reverse	TGCCGGAGTCGACAATGAT

Table 11: Sequences of the primers used for qPCR assay.

3.3.3.2.1.5 Mouse aortic ring assay

Aortic ring assays were performed as previously described (Piqueras *et al.*, 2007). C57BL/6 mice (8- to 12-week-old) were humanely euthanized by cervical dislocation and aortas were harvested and cut into 0.5 mm-thick segments. After overnight serum starvation, each ring was mounted in 100 µl of growth factor-depleted matrigel (BD Biosciences, CA). Each well was overlaid with 150 µl of DMEM plus 2.5% fetal calf serum supplemented with vehicle or 1 µM Ang-II. Some aortic rings were co-incubated with Bexarotene (0.3 µM) with or without

Rosuvastatin (3 μM). Other rings were treated with the AT_1 Ang-II receptor antagonist (EXP3174, 100 μM). Rings were incubated for up to 8 days at 37°C in 5% CO_2 with renewal of the medium and treatment every other day. Angiogenesis was quantified by counting the number of microvessel sprouts that grew from each ring after 8 days. Each experiment was performed in triplicate. After washing with PBS, rings were imaged using a phase contrast microscope (Axio Observer A1, Carl Zeiss, Germany).

3.3.3.2.1.6 Murine matrigel plug assay

The Matrigel plug assay was performed in 8 week old C57BL/6 mice as previously described (Piqueras *et al.*, 2007). The Matrigel plug assay was performed in 8 week old C57BL/6 mice in six experimental groups: growth factor depleted matrigel (0.4 ml/plug) containing vehicle (0.01% DMSO, n=5), 1 μM Ang-II (n=5), 1 μM Ang-II + EXP3174 (100 μM, n=5), 1 μM Ang-II + Bex (0.3 μM, n=5), 1 μM Ang-II + Rosu (3 μM, n=5) or 1 μM Ang-II + Bex (0.3 μM) + Rosu (3 μM, n=5). The Matrigel preparations (500 μl) were injected subcutaneously in the mid-ventral abdominal region of anesthetized C57BL/6 mice. Mice were anaesthetized by injecting (ip) ketamine (100 mg/kg) plus xylazine (10 mg·/kg) and constantly monitored by veterinarian surveillance of reflex absence. Animals were euthanized in a CO_2 chamber after day 10 of implantation. The plugs were removed, weighed and homogenized in 1 ml deionized H_2O on ice and cleared by centrifugation at 10,000 rpm for 6 min at 4°C. The supernatant was collected and used in triplicate to measure hemoglobin content using Drabkin's solution (Sigma-Aldrich, MO).

3.3.3.2.2 Third study

Using the AAA model, some groups of Ang-II-infused mice were also treated with an Ang-II AT_1 receptor antagonist (Losartan, 10 or 30 mg/kg/day) delivered with the osmotic minipumps. The experimental groups were:

1- $ApoE^{-/-}$ C57BL/6 vehicle + WD
2- $ApoE^{-/-}$ C57BL/6 + WD + Ang-II (500 ng/kg/min)
3- $ApoE^{-/-}$ C57BL/6 + WD + Ang-II (500 ng/kg/min) + Losartan (10 mg/kg/day)

4- ApoE$^{-/-}$ C57BL/6 + WD + Ang-II (500 ng/kg/min) + Losartan (30 mg/kg/day)

3.3.3.2.2.1 Immunohistochemistry studies in mouse aorta

For macrophages and CD31 quantification, the experiments were performed as explained in *3.3.3.2.1.1*.

For T cell quantification, the experiments were performed as explained in *3.3.2.1.1.1*.

In addition, CXCR6^{+} cells infiltration was measured. Aortic root cross-sections were blocked as above and incubated overnight with a rabbit anti mouse CXCR6 polyclonal antibody (1:100 dilution, Santa Cruz Biotechnology, CA) followed by an incubation for 1 h at room temperature with an Alexa Fluor 488-conjugated goat anti-rabbit secondary antibody (1:200 dilution, Invitrogen, Thermo Fisher Scientific, MA). Preparations were mounted with Slow-Fade Gold antifade reagent and analyzed by fluorescent microscopy with an inverted fluorescent microscope (Axio Observer A1, Carl Zeiss, Germany).

3.3.3.2.2.2 Analysis of CXCL16, CXCR6, MCP-1 and VEGF expression in AAA

PCR was performed following the same protocol to that previously described in 3.3.3.2.1.4. The sequences of the primers used to amplify each of the genes are showed in table 11.

3.4 MOUSE *IN VITRO* CELL CULTURE STUDIES

Confluent murine aortic endothelial cells (Innoprot, Derio, Spain) were stimulated with Ang-II (1 μM) for 4 h. In some experiments, cells were pretreated with Rosu (10 nM), Bex (0.3 μM) or a combination of Rosu (10 nM) plus Bex (0.3 μM) 20 h prior to Ang-II stimulation. Nox2, Nox4, dual oxidase 1 and 2 (Duox1 and Duox2) mRNA expression was detected.

PCR was performed following the same protocol to that previously described in 3.1.4. mRNA levels were normalized to the expression cyclophilin used as endogenous control and relativized to the vehicle treated group.

The sequences of the primers used to amplify each of the genes are showed in Table 12.

Gen	Primer	Sequence [5'-3']
***Mouse* Nox2**	Forward Reverse	TCAAGACCATTGCAAGTGAACAC TCAGGGCCACACAGGAAAA
Mouse Nox4	Forward Reverse	AGCATCTGCATCTGTCCTGAAC ACTGTCCGGCACATAGGTAAAAG
Mouse Duox1	Forward Reverse	AGCTCTCCGGGTCTGCAA CACATCTTCAGCCCTTTGTAGCTT
Mouse Duox2	Forward Reverse	GATCAGCATCAGACAGGGTTAGG TCTTCACGACGCGCTTTCT
Mouse Cyclophilin	Forward Reverse	TGGAGAGCACCAAGACAGACA TGCCGGAGTCGACAATGAT

Table 12: Sequences of the primers used for qPCR assay.

3.5 STATISTICAL ANALYSIS

Differences between multiple groups were analyzed with one way ANOVA with Bonferroni's procedure for *post hoc* analysis and differences between two groups was determined by paired or unpaired Student's t test, as appropriate. Fisher exact test was used to determine the differences between groups in AAA incidence.

RESULTS

4 RESULTS

4.1 RESULTS OF THE STUDY: COMBINED SUB-OPTIMAL DOSES OF ROSUVASTATIN AND BEXAROTENE IMPAIRS ANGIOTENSIN II-INDUCED ARTERIAL MONONUCLEAR CELL ADHESION THROUGH INHIBITION OF Nox5 SIGNALING PATHWAYS AND INCREASED RXR/PPARα AND RXR/PPARɣ INTERACTIONS

4.1.1 A combination of Rosuvastatin (Rosu) and Bexarotene (Bex) at suboptimal concentrations reduces Ang-II-induced HUAEC mononuclear cell adhesion

Initially, we evaluated the effect of Ang-II challenge on mononuclear leukocyte-endothelial cell interactions *in vitro* using the dynamic flow chamber assay. Thus, freshly-isolated human mononuclear cells were perfused across human umbilical artery endothelial cell (HUAEC) monolayers stimulated or not with Ang-II (1 μM) for 4 h. Ang-II caused a significant increase in mononuclear leukocyte adhesion to arterial endothelial cells (Figure 15). To assess the effect of Rosu on Ang-II-induced mononuclear cell recruitment, HUAECs were pretreated with the statin at two different concentrations (10 and 30 nM), 20 h prior to Ang-II stimulation. Whilst 10 nM Rosu had no impact on Ang-II-induced mononuclear cell recruitment, preincubation with 30 nM Rosu significantly reduced Ang-II-induced mononuclear leukocyte adhesion (Figure 15A). A similar approach was followed to test the effect of Bex preincubation on Ang-II-induced responses, based on previous observations (Sanz *et al.*, 2012). As anticipated, 1 μM but not 0.3 μM Bex significantly inhibited mononuclear cell adhesion to Ang-II stimulated HUAECs (Figure 15B). To evaluate the potential synergism of both drugs, different combinations of Rosu and Bex were assessed. All the combinations tested significantly impaired Ang-II-induced mononuclear cell attachment to the arterial endothelium (Figure 15C). Unexpectedly, the combination of Rosu at 10 nM and Bex at 0.3 μM, which displayed no significant effect when either treatment was tested alone, reduced adhesion by 51% (Figure 15C). Consequently, in all subsequent

in vitro experiments, this combination of Rosu and Bex (designated Rosu+Bex) was employed to explore the underlying mechanisms involved in this response.

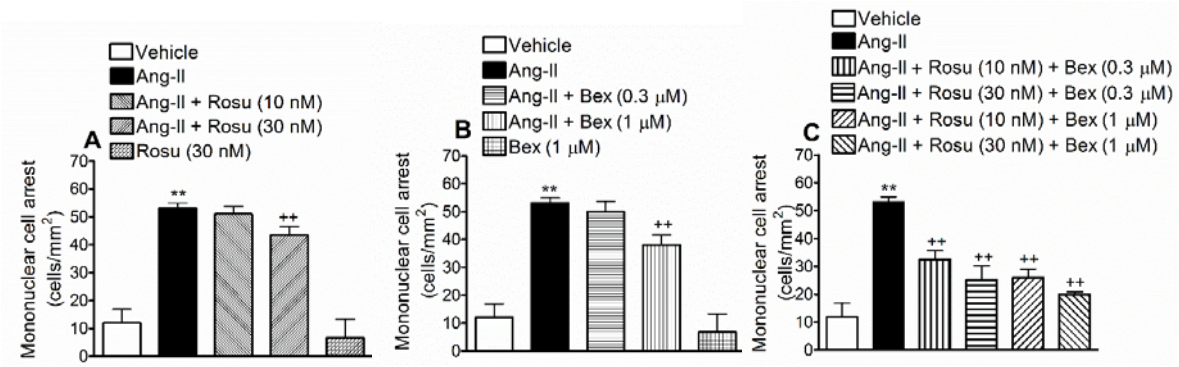

Figure 15: Combination of Rosuvastatin (Rosu) and Bexarotene (Bex) at suboptimal concentrations reduces Ang-II-induced HUAEC mononuclear cell adhesion under physiological flow. HUAECs were stimulated with Ang-II (1 μM) for 4 h. In some experiments, cells were pretreated with Rosu (10-30 nM) (A), Bex (0.3-1 μM) (B) or combinations of both (C), 20 h before Ang-II stimulation. Freshly isolated human mononuclear cells (10^6 cells/ml) were perfused across the endothelial monolayers for 5 min at 0.5 dyn/cm^2, and leukocyte adhesion quantified. Results are the mean ± SEM of n=5 independent experiments; **p<0.01 relative to the vehicle group, $^{++}$p<0.01 relative to the Ang-II stimulated cells.

Additionally, since there is evidence to support that Ang-II can decrease AT_1 receptor expression, albeit in vascular smooth muscle cells (VSMC) (Nickenig *et al.*, 1996), we evaluated this possibility. As illustrated in figure 16, we found that neither Ang-II stimulation for 4 h nor the pretreatment of the endothelial cells with the drugs, in combination or alone, affected AT_1 receptor expression.

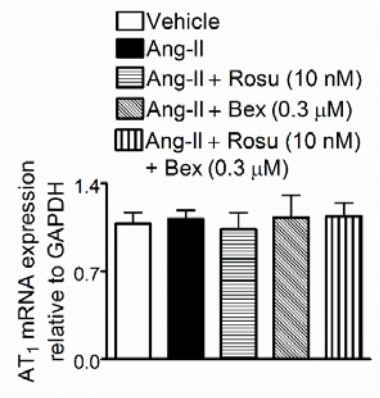

Figure 16: Effect of Rosu+Bex on endothelial Ang-II AT_1 receptor mRNA expression. Cells were treated with Rosu (10 nM), Bex (0.3 μM) or a combination of Rosu (10 nM) plus Bex (0.3 μM) for 20 h and then stimulated with Ang-II (1 μM, 4 h). mRNA expression was determined by the $2^{-\Delta\Delta Ct}$ method. Results are the mean ± SEM of the $2^{-\Delta\Delta Ct}$ values of n= 5 independent experiments.

4.1.2 Decreased expression of ICAM-1 and VCAM-1 are involved in the reduced Ang-II-induced HUAEC-mononuclear cell adhesion caused by suboptimal concentrations of Rosu+Bex

To investigate whether the inhibitory effects exerted by Rosu+Bex on Ang-II-induced mononuclear leukocyte adhesion were mediated through modulation of endothelial CAM expression, intercellular adhesion molecule-1 (ICAM-1) and vascular cell adhesion molecule-1 (VCAM-1) protein expression were determined by flow cytometry and immunocytochemistry. Stimulation with Ang-II resulted in a significant up-regulation of ICAM-1 and VCAM-1 expression when compared with unstimulated control HUAECs, as measured both by flow cytometry and immunofluorscence (Figure 17A and B). Pretreatment of cells with Rosu or Bex did not modify the increased endothelial CAM expression induced by the peptide (Figure 17A and B). In contrast, preincubation of HUAEC with Rosu+Bex resulted in a significant decrease in Ang-II-induced ICAM-1 and VCAM-1 expression, by 42 and 66%, respectively (Figure 17A and B).

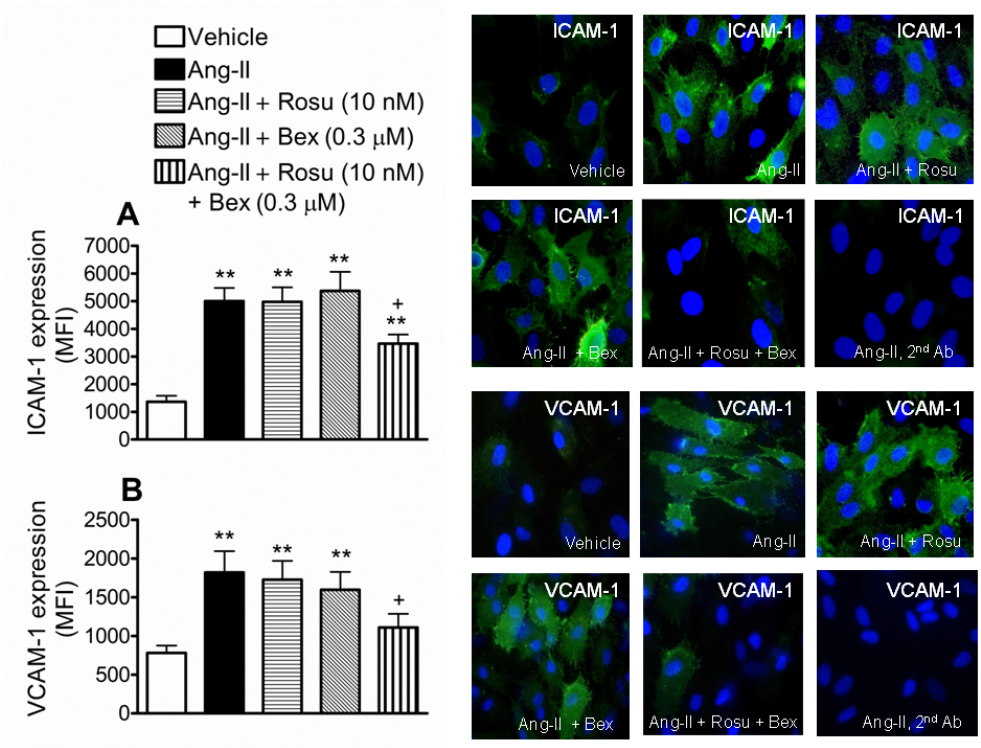

Figure 17: Effect of Rosu+Bex on endothelial cell adhesion molecule expression. Cells were treated with Rosu (10 nM), Bex (0.3 μM) or a combination of Rosu (10 nM) plus Bex (0.3 μM) for 20 h and then stimulated with Ang-II (1 μM, 4 h). ICAM-1 (A) and VCAM-1 (B) protein expression was determined by flow cytometry and immunofluorescence. Right panels show representative images of endothelial cells. Nuclei were counterstained with

DAPI (blue) and green fluorescence shows ICAM-1 (top) or VCAM-1 (bottom). Results are expressed as mean fluorescence intensity (MFI) and presented as mean ± SEM of n=5-9 independent experiments; **$p<0.01$ relative to the vehicle group, $^{+}p<0.05$ relative to the Ang-II stimulated cells.

4.1.3 Inhibition of Ang-II-induced HUAEC chemokine synthesis by combination of Rosu+Bex at suboptimal concentrations

Since Ang-II stimulation of endothelial cells can induce the production and release of different CXC and CC chemokines, in addition to the expression of the membrane-bound chemokine fractalkine (Nabah *et al.*, 2004; Mateo *et al.*, 2006; Rius *et al.*, 2013b), we next evaluated the effect of Rosu+Bex on Ang-II-induced chemokine synthesis in human arterial endothelial cells. Significant increases in the levels of growth regulated oncogene-α (GROα or CXCL1), interleukin-8 (IL-8 or CXCL8), monocyte chemotactic protein-1 (MCP-1 or CCL2) and regulated on activation, normal T cell expressed and secreted (RANTES or CCL5) were detected in the supernatant of HUAEC subjected to Ang-II stimulation for 4 h, as measured by ELISA (Figure 18A-D). This increase was not inhibited when HUAECs were preincubated with either of the drugs alone, but was markedly diminished by pretreatment of cells with the combination of Rosu+Bex (Figure 18A-D). Similarly, when HUAECs were stimulated with 1 μM Ang-II for 24 h, a significant increase in the expression of fractalkine was observed, both by flow cytometry and immunofluorescence (Figure 18E and F). Again, preincubation of cells with Rosu+Bex caused a significant down-regulation of the cell-membrane chemokine expression (Figure 18E and F).

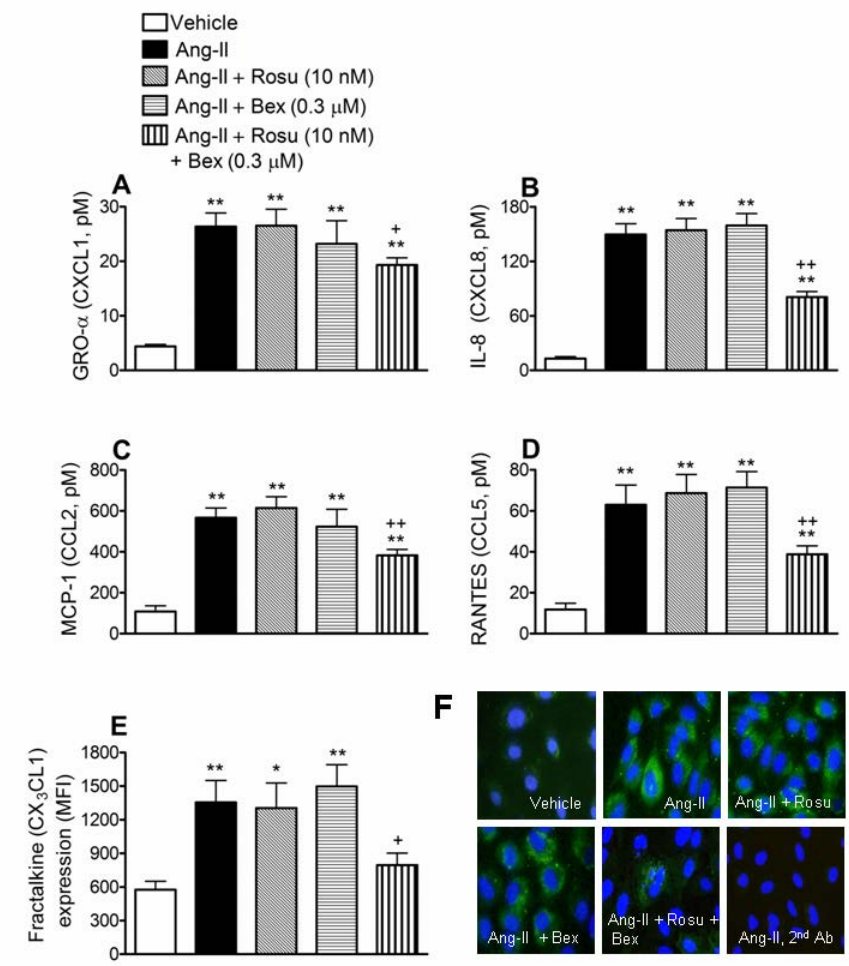

Figure 18: Suboptimal concentrations of Rosu+Bex decreases Ang-II-induced chemokine production in HUAEC. Cells were treated with Rosu (10 nM), Bex (0.3 μM) or a combination of Rosu (10 nM) plus Bex (0.3 μM) for 20 h and then stimulated with Ang-II (1 μM) for 4 h. GROα (A), IL-8 (B), MCP-1(C) and RANTES (D) release was determined by ELISA in the cell-free supernatant. Results are expressed as pM concentration and presented as mean ± SEM of n=7-9 independent experiments; **p<0.01 relative to the vehicle group, $^{+}$p<0.05 or $^{++}$p<0.01 relative to the Ang-II stimulated cells. In a second set of experiments, HUAECs were treated with Rosu (10 nM), Bex (0.3 μM) or a combination of Rosu (10 nM) plus Bex (0.3 μM) for 20 h and then stimulated with Ang-II (1 μM) for 24 h. CX_3CL1 expression in HUAEC was determined by flow cytometry (E) and visualized by immunofluorescence (green). Nuclei were counterstained with DAPI; images are representatives of n=5-7 independent experiments per group (F). Results are the mean ± SEM of n=5-7 independent experiments; **p<0.01 relative to the vehicle group, $^{+}$p<0.05 relative to the Ang-II stimulated cells.

4.1.4 Combination of Rosu+Bex at suboptimal concentrations inhibits Ang-II-induced HUAEC RhoA activation and subsequent mononuclear cell recruitment

It is well recognized that small GTP-binding proteins (G-proteins), such as Ras, Rho and Rac, are activated by Ang-II through interaction with its AT_1 receptor (Higuchi *et al.*, 2007). To characterize the signaling mechanisms by which Rosu+Bex modulate arterial mononuclear cell adhesion stimulated by Ang-II, we first established their effect on Ang-II-induced RhoA activation. As illustrated in Figure 19A, Ang-II stimulation of HUAEC for 1 h caused a significant increase in RhoA activation. Whereas pretreatment of cells with Rosu or Bex 20 h prior to Ang-II stimulation failed to modify RhoA activation, preincubation with the combination Rosu+Bex caused a significant inhibition of this response (Figure 19A). To evaluate the impact of RhoA activation on Ang-II-induced mononuclear cell recruitment, we silenced RhoA expression in endothelial cells with small interfering RNA (siRNA). Forty–eight hours after transfection with RhoA–specific siRNA, HUAEC exhibited a >69% reduction in RhoA protein compared with control siRNA-treated cells (Figures 19B). Ang-II stimulation (1 μM, 4 h) produced a significant increase in mononuclear cell arrest in control siRNA cells, which was abrogated in RhoA-silenced HUAECs (Figure 19C).

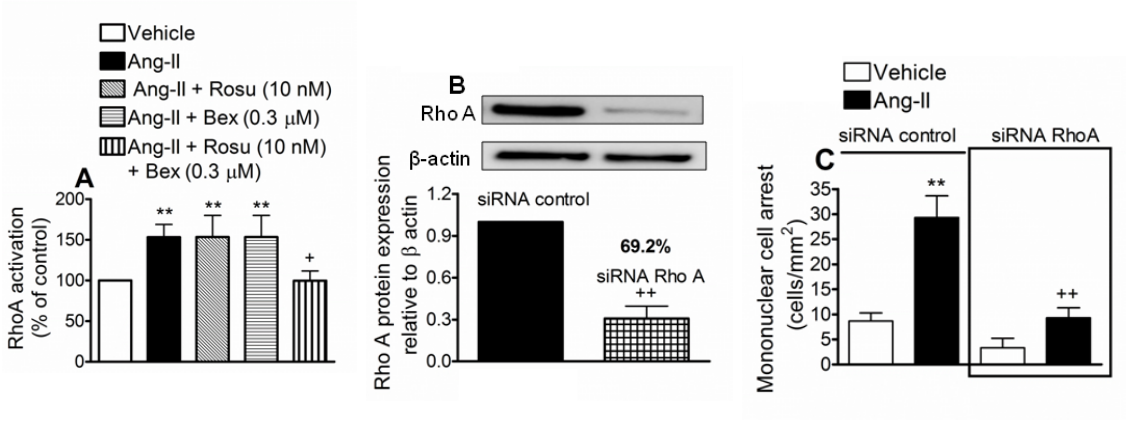

Figure 19: Inhibitory effects of Rosu+Bex at suboptimal concentrations on Ang-II-induced HUAEC RhoA activation. HUAEC were stimulated with Ang-II (1 μM) for 1 h. In some experiments, cells were treated with Rosu (10 nM), Bex (0.3 μM) or a combination of Rosu (10 nM) plus Bex (0.3 μM) for 20 h before Ang-II stimulation. Quantification of RhoA-GTP activity was determined using a colorimetric G-Lisa kit activation RhoA assay (A). Results are the mean ± SEM of n=6-9 independent experiments and presented as percentage of control; **p<0.01 relative to the vehicle group, $^{+}$p<0.05 relative to the Ang-II

stimulated cells. A second group of cells was transfected using a RhoA-specific siRNA or control-siRNA, and at 48 hours post-transfection protein expression was determined by immunoblot (B). Control or RhoA-specific siRNA-transfected cells were stimulated with Ang-II (1 μM) for 4 h. Then, freshly isolated human mononuclear cells were perfused over the endothelial monolayers for 5 min at 0.5 dyn/cm^2 and leukocyte adhesion was quantified (C). Results are the mean ± SEM of n=5-6 independent experiments; **p<0.01 relative to the vehicle group, $^{++}$p<0.01 relative to values in Ang-II group in control siRNA transfected cells.

Furthermore, inhibition of the RhoA downstream target, Rho-associated protein kinase (ROCK), resulted in a significant impairment in Ang-II-induced arterial mononuclear leukocyte adhesion (figure 20).

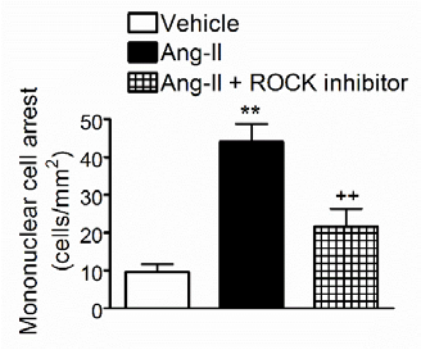

Figure 20: ROCK inhibition impairs Ang-II-induced mononuclear cell arrest. Endothelial cells were pretreated with the ROCK inhibitor Y27632 (10 μM) 1 h before Ang-II stimulation (1 μM, 4 h). Then, freshly isolated human mononuclear cells were perfused over the endothelial monolayers for 5 min at 0.5 dyn/cm2 and leukocyte adhesion was quantified. Results are the mean ± SEM of at least 5 independent experiments; **p<0.01 relative to the vehicle group, $^{++}$p<0.01 relative to the Ang-II stimulated cells.

4.1.5 Combination of Rosu+Bex at suboptimal concentrations inhibits Ang-II-induced Nox5 expression in HUAECs

The production of ROS and subsequent activation of redox-sensitive signaling pathways mediate many of the inflammatory responses induced by Ang II (Laursen *et al.*, 1997; Lassegue *et al.*, 2010). Accordingly, endothelial Ang-II stimulation activated NADPH oxidase in HUAECs (Figure 21A). Notably, this activation was diminished by cell pretreatment with Rosu+Bex, but not when either drug was used separately (Figure 21A). Ang-II caused increased endothelial expression of Nox2, Nox4 and Nox5 (Rius *et al.*, 2013c), and Figure 21B-D. Interestingly, whilst the expression of these Nox isoforms induced by Ang-II were unaffected by Rosu or Bex

pretreatment of the cells, Nox2 and Nox5 but not Nox4 expression was markedly reduced by preincubation with Rosu+Bex (Figure 21B-D).

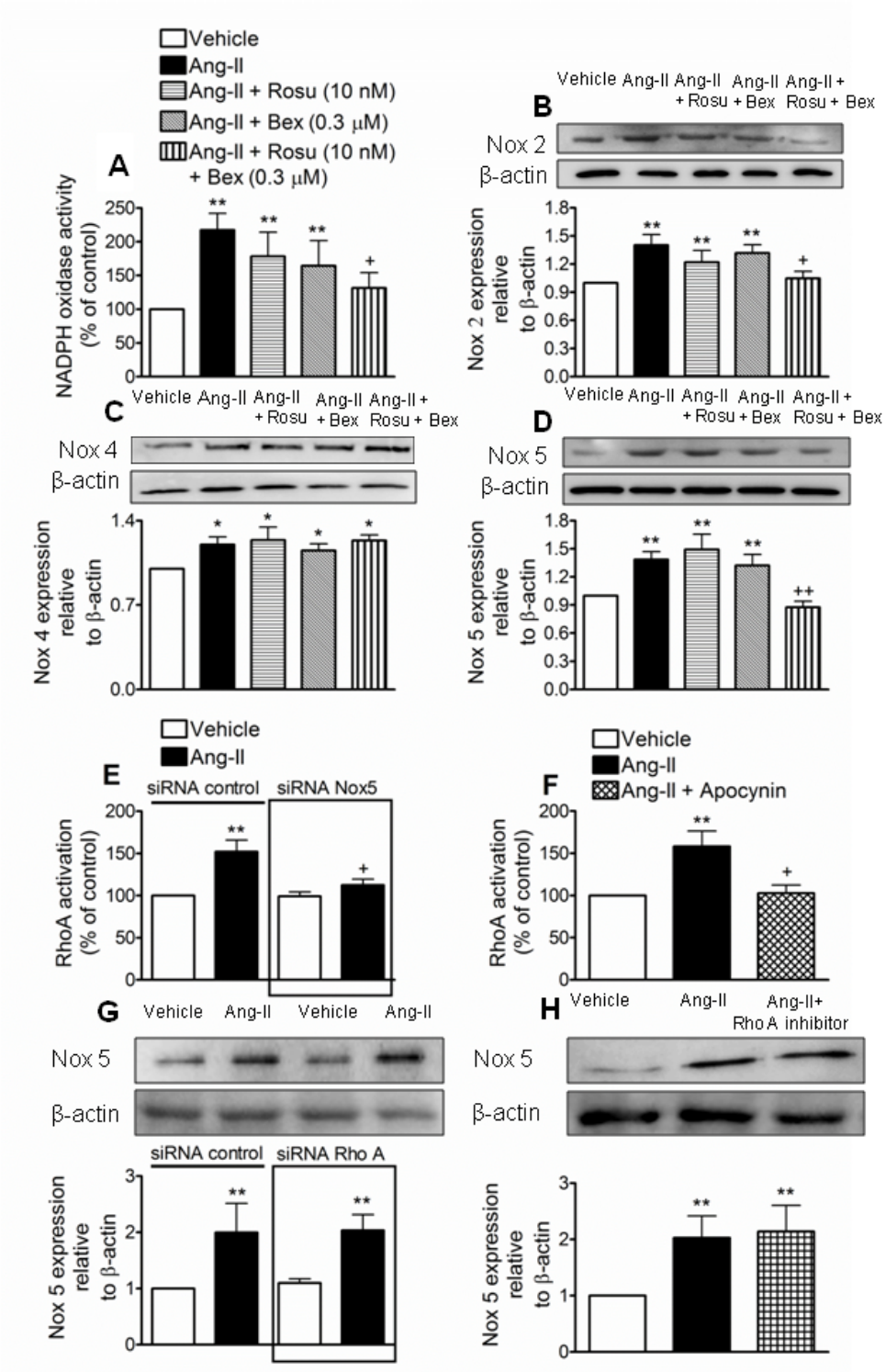

Figure 21: Suboptimal concentrations of Rosu+Bex decrease Ang-II-induced endothelial Nox5 expression. Endothelial cells were incubated with Rosu (10 nM), Bex (0.3 μM) or a combination of Rosu (10 nM) plus Bex (0.3 μM) for 20 h and then stimulated with Ang-II (1 μM, 1 h) and the generation of superoxide anions by NADPH oxidase was determined by lucigenin-derived chemiluminiscence (A). Results (mean ± SEM of 4-7

independent experiments performed in duplicate) are presented as percentage of control; **p<0.01 relative to the vehicle group, $^{+}$p<0.05 relative to the Ang-II stimulated cells. HUAEC were treated with Rosu (10 nM), Bex (0.3 μM) or a combination of Rosu (10 nM) plus Bex (0.3 μM) for 20 h and then stimulated with Ang-II (1 μM, 24 h). Nox2 (B), Nox4 (C) and Nox5 (D) expression was determined by immunoblotting. Results (mean ± SEM of 5-7 independent experiments) are expressed as fold increase of Nox:β-actin. Representative blots are shown; *p<0.05 or **p<0.01 relative to the vehicle group, $^{+}$p<0.05 or $^{++}$p<0.01 relative to the Ang-II stimulated cells. In additional experiments, control or siRNA Nox5-transfected HUAEC were stimulated with Ang-II (1 μM for 1 h) and quantification of RhoA-GTP activity was determined as before (E). Results are the mean ± SEM of n=7-8 independent experiments and are presented as percentage of control siRNA transfected cells, **p<0.01 relative to the respective vehicle group, $^{+}$p<0.05 relative to the respective Ang-II stimulated cells. In other plates, HUAEC were pretreated with the NADPH inhibitor apocynin (30 μM) 1 h before Ang-II stimulation and quantification of RhoA activity was determined (F). Results are the mean ± SEM of n=5 independent experiments and presented as percentage of control; *p<0.05 relative to the vehicle treated group, $^{+}$p<0.05 relative to the Ang-II stimulated cells. In a different experimental setting, cells were transfected with control or RhoA–specific siRNA. At 48 h post transfection, HUAEC were stimulated with Ang-II (1 μM) for 4 h and Nox5 expression was quantified by immunoblot (G). Results (mean ± SEM of at least 5 independent experiments) are expressed as fold increase of Nox5:β-actin of control siRNA transfected cells. A representative blot is shown above; **p<0.01 relative to the vehicle treated group. Untransfected cells were pretreated with a RhoA inhibitor (C3 transferase, 2 μg/ml for 4 h) prior to Ang-II stimulation and Nox5 expression determined by immunoblot (H). Results (mean ± SEM of at least 5 independent experiments) are expressed as fold increase of Nox5:β-actin. A representative blot is shown above; **p<0.01 relative to the vehicle treated group.

Since mononuclear cell arrest was found to be largely mediated *via* endothelial Nox5 expression (Rius *et al.*, 2013c) and ROS generation can activate RhoA (Nguyen Dinh Cat *et al.*, 2013), we next questioned whether the absence of endothelial Nox5 or antioxidant pretreatment resulted in a failure to activate this GTP-binding protein. To do this, we used both siRNA targeting Nox5 and also the antioxidant apocynin. Nox5 protein expression was significantly reduced (62%) after 48 h incubation with a specific siRNA (Figure 22).

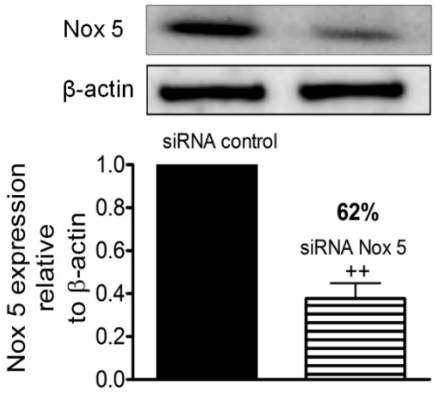

Figure 22: Transfection of HUAEC with Nox5 specific siRNA. Gene silencing was performed in HUAECs using either control- or Nox5-specific siRNA. After 48 h, protein expression of Nox5 was determined by immunoblot to assess silencing efficiency. Results (mean ± SEM of n= 5 independent experiments) are expressed relative to β-actin. A representative blot is shown. $^{++}p<0.01$ relative to values in control siRNA transfected cells.

Further, knockdown of Nox5 or apocynin pretreatment resulted in the blockade of Ang-II-induced RhoA activation (Figure 21E and F). Conversely, in RhoA-silenced HUAECs, or in HUAECs pretreated with a RhoA inhibitor (cell permeable C3 transferase), the increased expression of Nox5 protein triggered by Ang-II remained unchanged (Figure 21G and H).

Moreover, while Ang-II-induced endothelial ROS generation was neutralized by preincubation with apocynin, it was unaffected by pretreatment of the cells with the RhoA inhibitor (Figure 23).

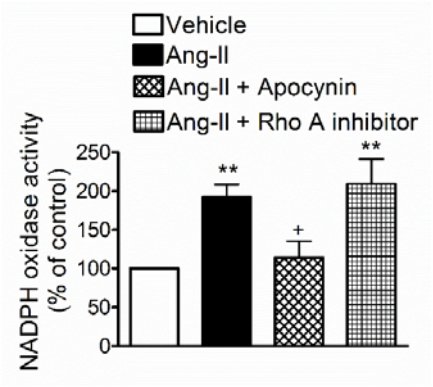

Figure 23: Apocynin but not RhoA inhibition blocks Ang-II-induced NADPH activation. Endothelial cells were pretreated with the antioxidant apocynin (30 μM for 1 h) or with a RhoA inhibitor (C3 transferase, 2 μg/ml for 4 h) before Ang-II stimulation (1 μM, 1 h). Generation of superoxide anions by NADPH oxidase was determined by lucigenin-derived chemiluminiscence. Results (mean ± SEM of at least 5 independent experiments performed in duplicate) are presented as percentage of control; $^{**}p<0.01$ relative to the vehicle group, $^{+}p<0.05$ relative to the Ang-II stimulated cells.

4.1.6 Suboptimal concentrations of Rosu+Bex provokes increased expression of endothelial RXRα, PPARα and PPARγ

Given that statins and Bex can activate PPARs and RXRα nuclear receptors respectively (Desjardins *et al.*, 2008; Balakumar *et al.*, 2012; Sanz *et al.*, 2012), we investigated whether the combination of Rosu+Bex exerted its inhibitory activity through changes in the endothelial expression of RXRα, PPARα, PPARβ/δ or PPARγ. Immunoblot analysis showed that Ang-II-stimulated HUAECs, preincubated or not with Ros or Bex alone, expressed comparable levels of RXRα and PPAR nuclear receptors to vehicle controls (Figure 24A-D). Importantly, when cells were treated with Rosu+Bex for 20 h followed by stimulation with Ang-II for 4 h, RXRα, PPARα and PPARγ were significantly up-regulated while PPARβ/δ expression was unchanged (Figures 24A-D).

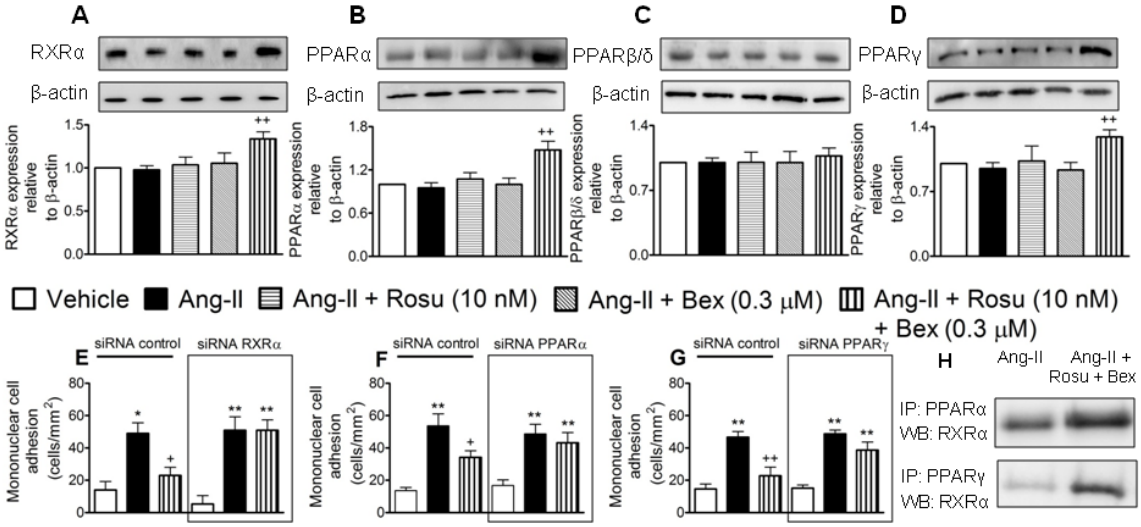

Figure 24: Suboptimal concentrations of Rosu+Bex increases RXRα, PPARα and PPARγ but not PPARβ/δ expression in HUAEC stimulated with Ang-II. RXRα, PPARα or PPARγ knockdown abolished the inhibitory effect of Rosu+Bex on Ang-II-induced mononuclear leukocyte-endothelial cell interactions. HUAEC were incubated with Ang-II (1 μM) for 4 h. In some experiments, cells were pretreated with Rosu (10 nM), Bex (0.3 μM) or a combination of Rosu (10 nM) plus Bex (0.3 μM) for 20 h before Ang-II stimulation. RXRα (A), PPARα (B), PPARγ (C) and PPARβ/δ (D) expression was determined by immunoblot. Results (mean ± SEM of n=5-7 independent experiments) are expressed as fold increase relative to β-actin. Representative gels are shown. $^{++}p<0.01$ relative to the Ang-II treated group. Cells were transfected with control siRNA, RXRα-specific siRNA (E), PPARα-specific siRNA (F) or PPARγ-specific siRNA (G) and stimulated with Ang-II (1 μM; 4 h) at 48 h post-transfection. In some experiments, cells were pretreated with Rosu (10 nM) plus Bex (0.3 μM) 20 h prior to Ang-II challenge. Freshly isolated human mononuclear cells (10^6 cells/ml) were perfused over the endothelial

monolayers for 5 min at 0.5 dyn/cm^2, and leukocyte adhesion quantified. Results are the mean ± SEM of n= 4-5 independent experiments. *p<0.05 or **p<0.01 relative to the respective vehicle group, $^{+}$p<0.05 or $^{++}$p<0.01 relative to the respective Ang-II stimulated cells. RXRα/PPARα and RXRα/PPARγ interactions (H) were assessed by immunoprecipitation of PPARα or PPARγ and subsequent immunoblotting for RXRα. Blots are representative of 4 independent experiments.

To understand how increased expression of RXRα, PPARα or PPARγ might contribute to the reduction of Ang-II-induced leukocyte-endothelial cell interactions elicited by pre-exposure of HUAEC to Rosu+Bex, we evaluated leukocyte adhesion to HUAECs individually silenced for expression of RXRα, PPARα and PPARγ. Knockdown of RXRα, PPARα and PPARγ resulted in a 57-66% decrease in receptor expression relative to control-siRNA cells (Figure 25).

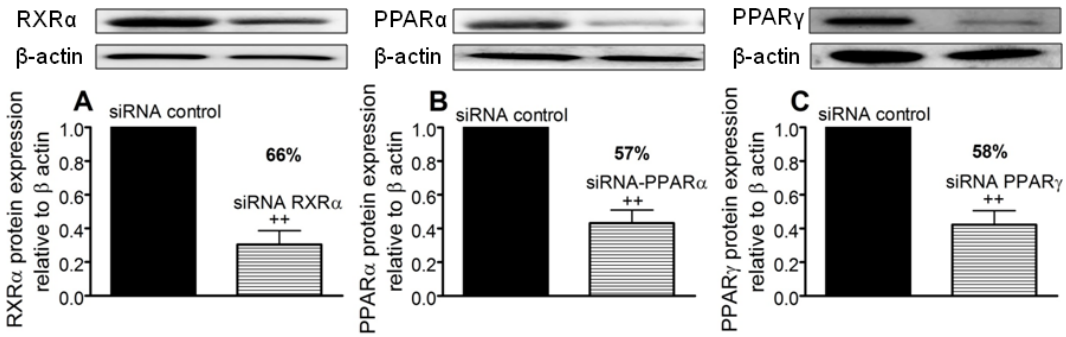

Figure 25: Transfection of HUAEC with RXRα, PPARα, or PPARγ specific siRNAs. Gene silencing was performed in HUAECs using either control siRNA or specific siRNA to RXRα, PPARα or PPARγ. After 48 h, protein expression of RXRα (A), PPARα (B), or PPARγ (C) was determined by immunoblot to assess silencing efficiency. Results (mean ± SEM of n= 4-5 independent experiments) are expressed relative to β-actin. Representative blots are shown. $^{++}$p<0.01 relative to values in the respective control siRNA group.

Notably, silencing of RXRα, PPARα or PPARγ abolished the suppressive effects of Rosu+Bex on leukocyte adhesion to HUAEC stimulated with Ang-II (Figure 24E-G). Furthermore, when HUAEC were immunoprecipitated with an anti-PPARα or an anti-PPARγ antibody, followed by immunoblotting with an anti-RXRα antibody, enhanced dimerization of RXRα with PPARα or PPARγ was detected with Rosu+Bex, relative to Ang-II-only stimulated cells (Figure 24H), although the interaction seemed to be more pronounced with PPARγ.

4.1.7 Reduction of RXRα, PPARα or PPARγ expression blunted the inhibition of Ang-II-induced HUAEC RhoA activation and Nox5 expression by Rosu+Bex at suboptimal concentrations

To gain further insight into the inhibitory mechanisms involved in the Ang-II-induced mononuclear cell arrest by Rosu+Bex, HUAEC were transfected with siRNAs against RXRα, PPARα or PPARγ. Interestingly, the inhibitory effect of Rosu+Bex on RhoA activation or Nox5 down-regulation in cells stimulated with Ang-II was abolished in cells silenced for these nuclear receptors (Figure 26).

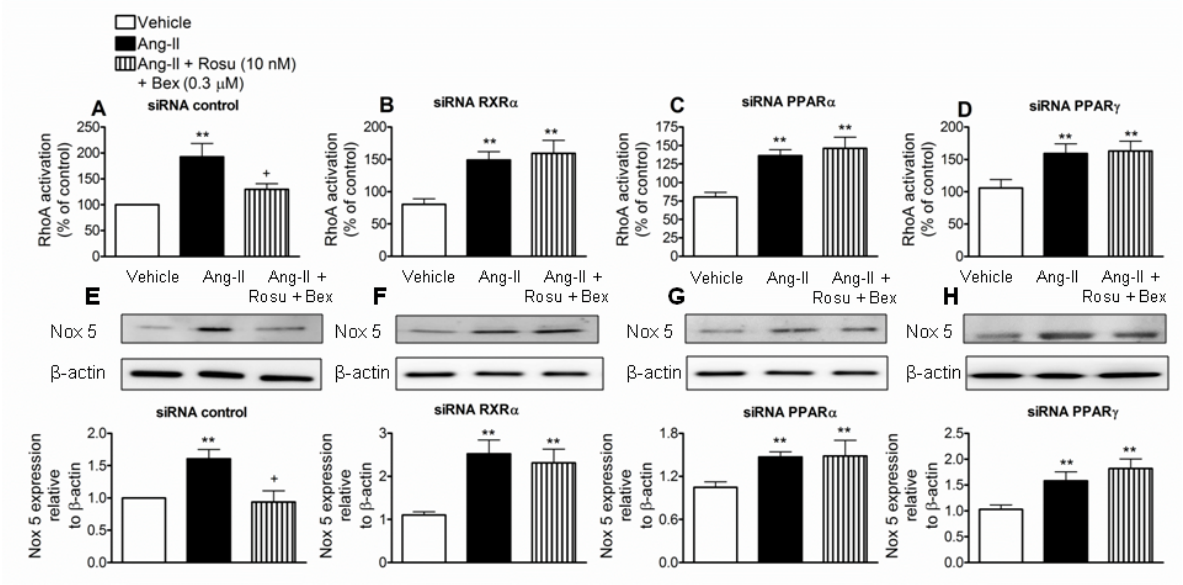

Figure 26: Silencing of endothelial RXRα, PPARα or PPARγ blunted the inhibition of Ang-II-induced HUAEC RhoA activation and Nox5 expression by the combination of Rosu+Bex at suboptimal concentrations. Cells were transfected with control siRNA (A), RXRα-specific siRNA (B), PPARα-specific siRNA (C) or PPARγ-specific siRNA (D) and stimulated with Ang-II (1 μM; 1 h) at 47 h post-transfection. In some experiments, cells were pretreated with Rosu (10 nM) plus Bex (0.3 μM) 20 h prior to Ang-II challenge. Quantification of RhoA-GTP activity was determined using a colorimetric G-Lisa RhoA activation assay. Results are the mean ± SEM of n=5-7 independent experiments and presented as percentage of control siRNA transfected cells; **p<0.01 relative to the respective vehicle group, +p<0.05 relative to the respective Ang-II stimulated cells. Following a similar protocol but after stimulation with 1 μM Ang-II for 24 h at 24 h post-transfection, Nox5 expression (E-H) was determined by immunoblotting. Results (mean ± SEM of 5-6 independent experiments) are expressed as fold increase of Nox5:β-actin of control siRNA transfected cells. Representative blots are shown; **p<0.01 relative to the respective vehicle group, +p<0.05 relative to the respective Ang-II stimulated cells.

4.1.8 Combination of Rosu+Bex at suboptimal concentrations restored the inhibition in nitric oxide (NO) bioavailability induced by Ang-II in HUAECs s

It is well known that Ang-II impairs endothelial function by decreasing nitric oxide (NO) bioavailability (Loot *et al.*, 2009; Nguyen Dinh Cat *et al.*, 2013). These effects can be mediated through superoxide anion generation and reaction with NO, resulting in its quenching to form peroxynitrite, and endothelial NO synthase (eNOS) inhibition and uncoupling (Loot *et al.*, 2009; Nguyen Dinh Cat *et al.*, 2013). Therefore, we evaluated the effect of Rosu+Bex on the Ang-II-induced decrease in NO bioavailability in HUAEC. Ang-II stimulation of the cells reduced NO levels in HUAECs (Figure 27A). Notably, this reduction was reversed by cell pretreatment with Rosu+Bex, but not when either drug was used separately (Figure 27A). Pretreatment of the cells with the antioxidant apocynin or a RhoA inhibitor (cell permeable C3 transferase) reversed the reduction in NO availability induced by Ang-II (Figure 27B). Similarly, silencing of Nox5 prevented the decrease in NO bioavailability provoked by Ang-II (Figure 27C). More importantly, in the absence of RXRα, PPARα or PPARγ, Rosu+Bex was unable to fully restore endothelial NO levels (Figure 27D-G).

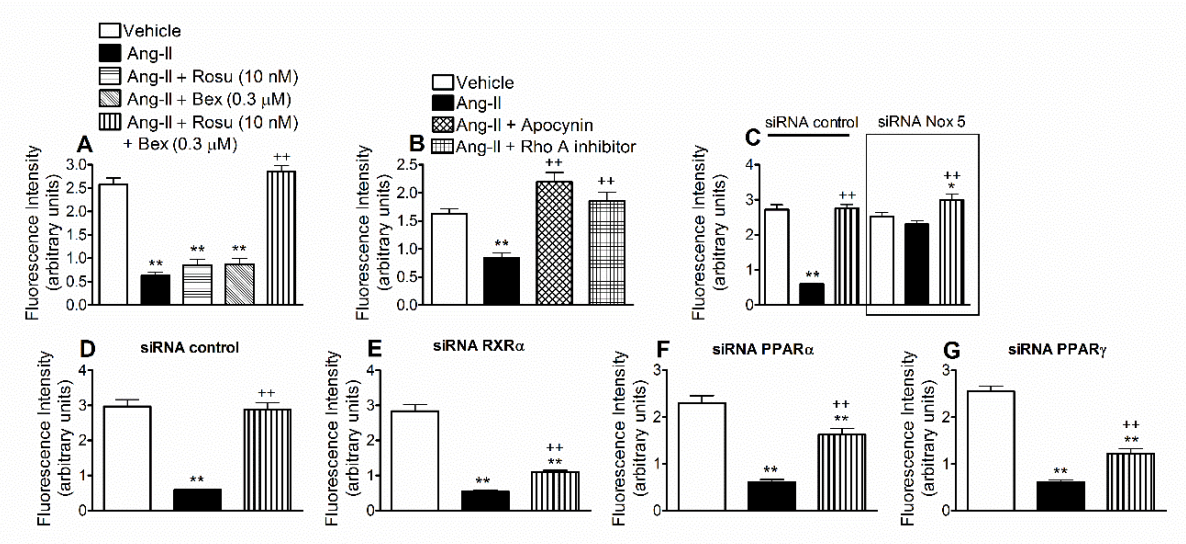

Figure 27: Combination of Rosu+Bex at suboptimal concentrations reversed the inhibition in nitric oxide (NO) bioavailability induced by Ang-II in HUAECs. Endothelial cells were incubated with Rosu (10 nM), Bex (0.3 μM) or a combination of Rosu (10 nM) plus Bex (0.3 μM) for 20 h and then stimulated with Ang-II (1 μM, 4 h), and intracellular NO was monitored with (DAF-2-FM diacetate) (A). Results (mean ± SEM of at

least 5 independent experiments performed in triplicate); **p<0.01 relative to the vehicle group, $^{++}$p<0.01 relative to the Ang-II treated group. In additional experiments, endothelial cells were pretreated with the antioxidant apocynin (30 μM for 1 h) or with a RhoA inhibitor (C3 transferase, 2 μg/ml for 4 h) before Ang-II stimulation (1 μM, 1 h). Intracellular NO was monitored with (DAF-2-FM diacetate) (B). Results (mean ± SEM of at least 5 independent experiments performed in triplicate); **p<0.01 relative to the vehicle group, $^{++}$p<0.01 relative to the Ang-II treated group. Control or siRNA Nox5-transfected HUAEC were stimulated with Ang-II (1 μM for 4 h) and quantification of intracellular NO content was determined as before (C). Results are the mean ± SEM of n=5 independent experiments performed in triplicate, *p<0.05 or **p<0.01 relative to the respective vehicle group, $^{++}$p<0.01 relative to the respective Ang-II stimulated cells. In other experiments, cells were transfected with control siRNA (D), RXRα-specific siRNA (E), PPARα-specific siRNA (F) or PPARγ-specific siRNA (G) and stimulated with Ang-II (1 μM; 4 h) at 44 h post-transfection. In some experiments, cells were pretreated with Rosu (10 nM) plus Bex (0.3 μM) 20 h prior to Ang-II challenge and quantification of NO bioavailability was determined. Results are the mean ± SEM of n=5 independent experiments performed in triplicate, **p<0.01 relative to the respective vehicle group, $^{++}$p<0.01 relative to the respective Ang-II stimulated cells.

4.1.9 Suboptimal doses of Rosu+Bex impairs Ang-II-induced leukocyte-arteriolar adhesion in vivo

To connect our *in vitro* observations with what happens *in vivo*, we utilized a chronic model of Ang-II infusion. Animals were implanted with osmotic mini-pumps constantly releasing either Ang-II (500 ng/kg/min) (Scalia *et al.*, 2011) or vehicle, for 14 days. Consistent with the *in vitro* analysis, animals chronically infused with Ang-II showed a significant enhancement in arteriolar leukocyte adhesion compared with vehicle-infused mice (Figure 28A). Co-infusion of Rosu at 1.25 mg/kg/day, or oral administration of Bex at 10 mg/kg/day, did not change arteriolar leukocyte adhesion caused by Ang-II systemic infusion (Figure 28A). However, when the animals were co-infused with Ang-II plus the statin, and Bex was co-administered daily, leukocyte adhesion was significantly reduced by 65% (Figure 28A). Moreover, Ang-II-induced expression of CD11b in circulating monocytes was also reduced by Rosu+Bex administration, whereas neutrophil CD11b expression was not affected by any treatment (Figure 28B and C). Additionally, immunohistochemistry analysis of cremasteric arterioles showed that the Ang-II-induced increase in ICAM-1, VCAM-1, E-selectin and fractalkine expression was blunted by co-treatment with Rosu+Bex in mice (Figure 28D). As expected, a significant reduction in circulating levels of chemokines, including CXCL1 and MCP-1, and a tendency for reduction in

RANTES, were also observed in animals treated with Rosu+Bex and chronically subjected to Ang-II (Figures 28E-G).

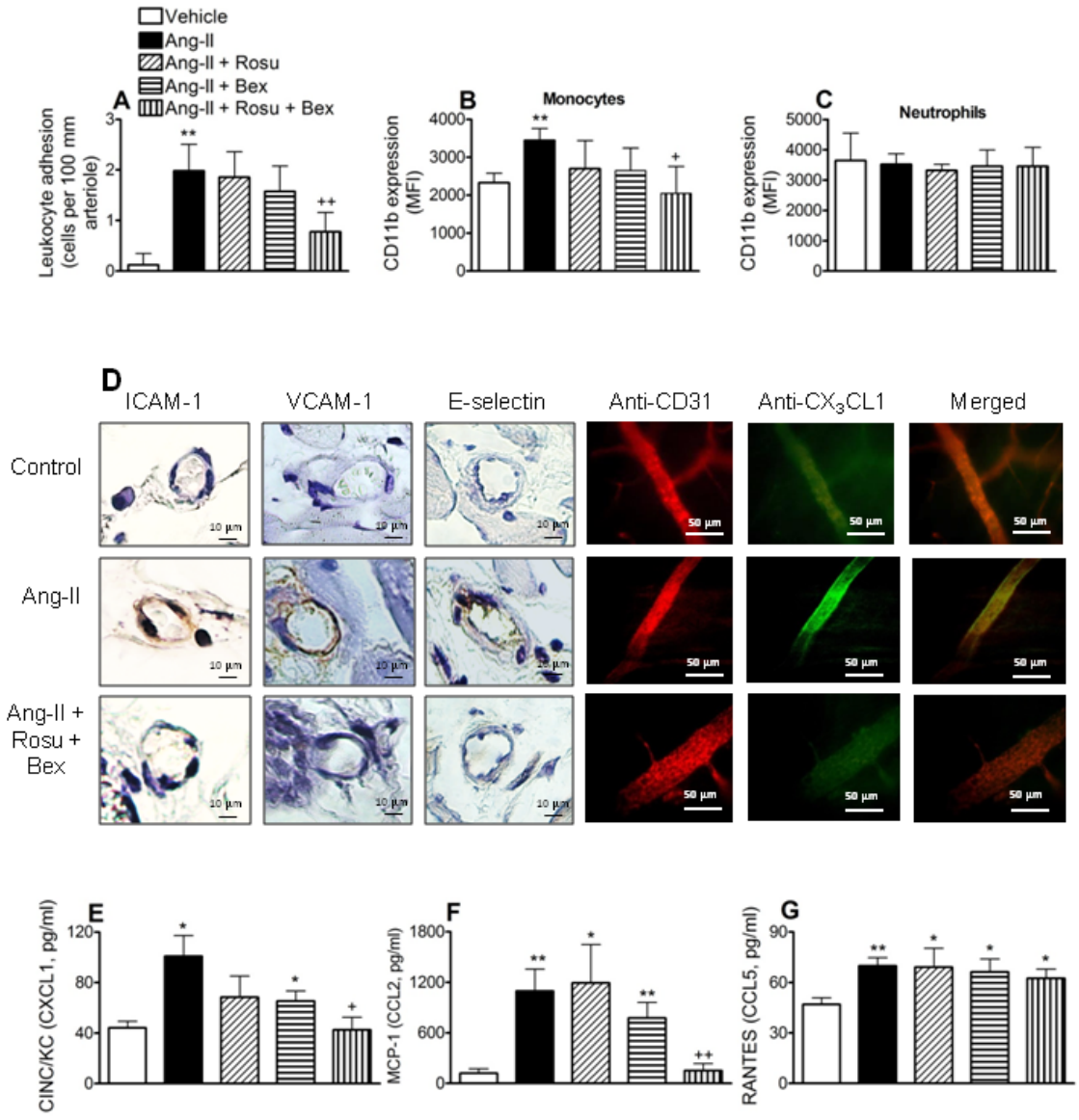

Figure 28: *In vivo* effects of suboptimal doses of Rosu+Bex. Ang-II (500 ng/kg/min) or saline was delivered to mice using osmotic minipumps for 14 days. A group of Ang-II-infused mice was administered with Bex at 10 mg/kg/day by gavage or with Rosu at 1.25 mg/kg/day delivered through the osmotic minipump. An additional group of Ang-II chronically-stimulated animals was treated with a combination of both compounds. Leukocyte adhesion to arterial endothelium was evaluated in the cremasteric microcirculation (A). CD11b expression in heparinized whole blood was determined by flow cytometry on circulating monocytes and neutrophils (B-C). ICAM-1, VCAM-1, E-selectin and CX_3CL1 expression were determined by immunohistochemistry in the cremasteric arterioles. CD31 staining was used to distinguish vessels (D). Circulating levels of CINC/KC (E), MCP-1(F) and RANTES (G) were measured by ELISA in plasma samples. Results are the mean±SEM of n=5-6 independent experiments. *$p<0.05$ or **$p<0.01$ relative to vehicle-infused mice; $^{+}p<0.05$ or $^{++}p<0.05$ relative to the Ang-II-infused animals.

In this experimental setting, glucose levels and lipid profile were unaffected by the different treatments (Table 13).

	Vehicle	**Ang-II**	**Ang-II + Rosu**	**Ang-II + Bex**	**Ang-II + Rosu + Bex**
Systolic Blood Pressure (mm Hg)	122.0±6.4	124.3±6.2	119.6±5.8	124.4±6.2	123.2±6.4
Blood glucose (mg/dl)	94.8±6.1	97.8±8.5	92.4±4.9	96.4±4.2	99.3±6.6
Total cholesterol (mg/dl)	120.9±8.2	131.1±10.7	116.6±4.1	124.4±4.1	117.8±10.1
Triglycerides (mg/dl)	83.5±7.3	85.1±7.8	78.9±9.9	80.5±7.2	82.5±9.7

Table 13: Effect of suboptimal doses of Rosu+Bex on blood glucose and lipid profile on vehicle or Ang-II-infused animals. Ang-II (500 ng/kg/min) or saline was delivered to mice using osmotic minipumps for 14 days. A group of Ang-II-infused mice was administered with Bex at 10 mg/kg/day by gavage or with Rosu at 1.25 mg/kg/day delivered through the osmotic minipump. An additional group of Ang-II chronically-stimulated animals was treated with a combination of both compounds. Blood glucose and circulating levels of total cholesterol and triglycerides were evaluated at day 14. Results are the mean±SEM of n=5 independent experiments.

In regard to blood pressure, Ang-II infusion at this dose caused a small but significant increase in this parameter at day 14 which was more marked when the peptide was infused at 1000 ng/kg/min (Table 14). However, none of the treatments applied affected the increase in blood pressure induced by Ang-II (Table 14).

	BP (mm Hg) Day 0	BP (mm Hg) Day 14
Vehicle	102.3±7.6	97.8±1.5
Ang-II 500 ng/kg/min	100.4±2.8	113.6±5.5*
Ang-II 500 ng/kg/min + Rosu	97.6±5.8	108.7±4.3*
Ang-II 500 ng/kg/min + Bex	97.5±3.6	112.6±6.2*
Ang-II 500 ng/kg/min + Rosu + Bex	101.3±3.9	112.4±5.8*
Ang-II 1000 ng/kg/min	97.4±6.2	119.1±4.6**
Ang-II 1000 ng/kg/min + Rosu	97.6±5.2	117.5±5.2**
Ang-II 1000 ng/kg/min + Bex	101.4±3.9	116.6±4.6**
Ang-II 1000 ng/kg/min + Rosu + Bex	101.6±4.2	119.4±4.5**

Table 14: Effect of suboptimal doses of Rosu+Bex on blood pressure. Ang-II (500 ng/kg/min or 1000 ng/kg/min) or saline was delivered to mice using osmotic minipumps for 14 days. Two groups of Ang-II-infused mice were administered with Bex at 10 mg/kg/day by gavage and another two groups with Rosu at 1.25 mg/kg/day delivered through the osmotic minipump. Two additional groups of Ang-II chronically-stimulated animals were treated with a combination of both compounds. Blood pressure was evaluated at day 0 and 14. Results are the mean±SEM of n=5 independent experiments. *$p<0.05$ or **$p<0.01$ relative to vehicle-infused mice at day 14.

In an additional group of experiments using murine aortic endothelial cells, increased Nox2 and Nox4, but not dual oxidase 1 and 2 (Duox1 and Duox2), mRNA expression was detected in Ang-II-stimulated cells (Figure 29). Interestingly, whereas Nox2 expression was impaired by cell pretreatment with Rosu+Bex, Nox4 expression was unaffected by the combination treatment (Figure 29). In accord with the results from human cells, neither drug affected Ang-II-induced Nox2 or Nox4 expression when evaluated separately (Figure 29).

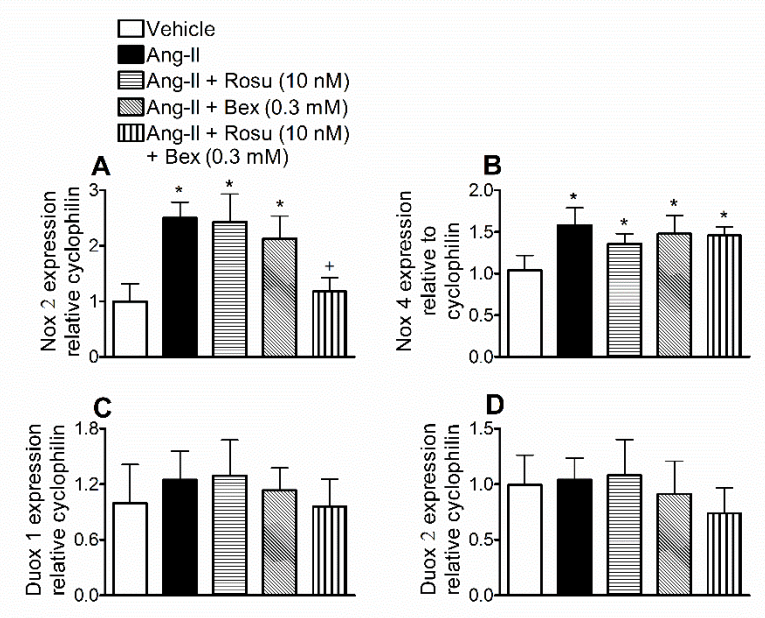

Figure 29: Suboptimal concentrations of Rosu+Bex decrease Ang-II-induced murine endothelial Nox2 expression. Aortic murine endothelial cells were incubated with Rosu (10 nM), Bex (0.3 μM) or a combination of Rosu (10 nM) plus Bex (0.3 μM) for 20 h and then stimulated with Ang-II (1 μM, 4 h). Nox2 (A), Nox4 (B), Duox 1 (C) and Duox 2 (D) mRNA expression was determined by RT-PCR. Results (mean ± SEM of 4 independent experiments) are expressed as fold increase of Nox/Duox:cyclophilin. *p<0.05relative to the vehicle group, $^{+}$p<0.05 relative to the Ang-II stimulated cells.

4.1.10 Suboptimal doses of Rosu+Bex reduces atherosclerosis development and cell composition in apoE$^{-/-}$ mice on atherogenic diet.

To explore the potential relevance of these findings for atherosclerosis, 8-week-old apoE$^{-/-}$ mice were fed with a high fat atherogenic diet for 8 weeks. As expected, animals subjected to atherogenic diet presented increased lesion formation and infiltration of macrophages and T cells within the lesion (Figure 30). Co-infusion

of Rosu at 1.25 mg/kg/day, or oral administration of Bex at 10 mg/kg/day, had no effect on these parameters (Figure 30). Notably, chronic treatment with the statin plus Bex substantially decreased lesion formation and the associated mononuclear cell infiltration (Figure 30).

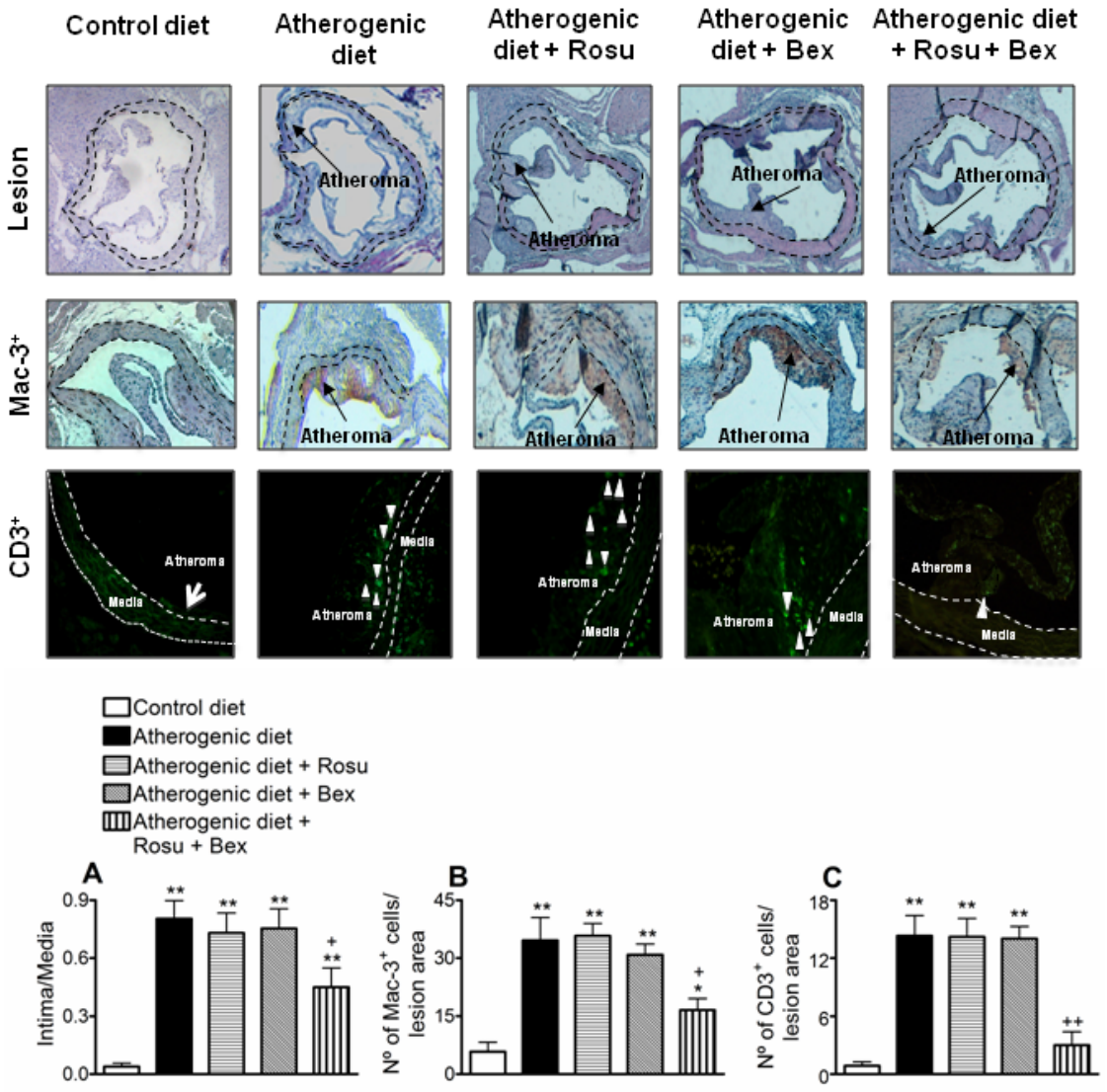

Figure 30: Suboptimal doses of Rosu+Bex reduced atherosclerosis development and cell composition in apoE$^{-/-}$ mice on atherogenic diet. Mice were sacrificed at 16 weeks of age after 8 weeks on a low fat standard diet (control diet), high fat atherogenic diet (atherogenic diet) or high fat atherogenic diet treated with Rosu (1.25 mg/kg/day delivered by osmotic minipumps), Bex (10 mg/kg/day) by gavage, or with a combination of both drugs. Atheroma lesion was determined in 3-5 histological sections per mice (A). The discontinuous lines delineate the limits of the media. Macrophage (Mac-3$^+$, B) and T-cell (CD3$^+$, C) infiltration were also evaluated. Representative images of aortic root cross-sections, Mac-3$^+$ stained area (brown staining) and CD3$^+$ cells (white arrowheads) for the control or atherogenic diet-fed mice treated or not with the drugs are shown. Black arrows point to Mac-3$^+$ areas within the lesion. Results are the mean ± SEM of n=5-7 animals per

group. *p<0.05 or **p<0.01 relative to values animals subjected to a control diet; $^{+}$p<0.05 or $^{++}$p<0.01 relative to values in untreated animal subjected to an atherogenic diet.

Neither glucose level nor the lipid profile in atherogenic animals were significantly affected by the different treatments applied (Table 15).

	ApoE$^{-/-}$ mice + control diet	**ApoE$^{-/-}$ mice + atherogenic diet**	**ApoE$^{-/-}$ mice + atherogenic diet + Rosu**	**ApoE$^{-/-}$ mice + atherogenic diet + Bex**	**ApoE$^{-/-}$ mice+ atherogenic diet + Rosu + Bex**
Blood glucose (mg/dl)	86.9±6.6	92.3±8.4	84.0±6.4	87.6±5.2	86.6±6.0
Total cholesterol (mg/dl)	168.7±7.6	320.3±22.8*	275.5±20.6*	306.1±40.8*	291.1±23.5*
Triglycerides (mg/dl)	70.4±5.6	113.3±19.2*	111.1±14.6*	130.8±8.5*	125.5±13.0*

Table 15: Suboptimal doses of Rosu+Bex have no effect on blood glucose levels and lipid profile in apoE$^{-/-}$ mice subjected to an atherogenic diet. Mice were sacrificed at 16 weeks of age after 8 weeks on a low fat standard diet (control diet), high fat atherogenic diet (atherogenic diet) or high fat atherogenic diet treated with Rosu (1.25 mg/kg/day delivered by osmotic minipumps), Bex (10 mg/kg/day) by gavage, or with a combination of both drugs. Circulating levels of glucose, total cholesterol and triglycerides were evaluated. Results are the mean ± SEM of n=5 animals per group. *p<0.05 relative to values in animals subjected to a control diet.

4.2 RESULTS OF THE STUDY: COMBINED TREATMENT WITH BEXAROTENE AND ROSUVASTATIN REDUCES ANGIOTENSIN-II-INDUCED ABDOMINAL AORTIC ANEURYSM IN apoE$^{-/-}$ MICE AND ANGIOGENESIS

4.2.1 Simultaneous administration of bexarotene and rosuvastatin decreases Ang-II-induced AAA formation, monocyte infiltration, chemokine expression and neovascularization in the aneurysmal tissue.

To evaluate the possible effect bexarotene or/and rosuvastatin on aneurysm formation, apoE$^{-/-}$ and C57BL/6 mice were infused for 28 days with Ang-II and subjected to a western-type diet. As shown in Figure 31, continuous infusion of apoE$^{-/-}$ mice with Ang-II induced AAA development. In contrast, no abdominal aortic aneurysms were observed in C57BL/6 mice infused with the peptide (Figure 31A) as previously described (Manning *et al.*, 2002). The infusion of Ang-II resulted in AAA incidence of 80% in apoE$^{-/-}$ mice. However, combined therapy with bexarotene (10 mg/kg/day) plus rosuvastatin (10 mg/kg/day) reduced AAA incidence to a 25% (Figure 31B). Similarly, while no changes in aortic diameter were detected in C57BL/6 wild type mice infused with Ang-II, a significant increase in suprarenal aortic diameter was found in apoE$^{-/-}$ mice chronically stimulated with Ang-II (0.84±0.01 mm *vs* 1.82±0.16 mm, $p<0.05$) which in the latter was significantly reduced by the combined treatment with bexarotene and rosuvastatin (1.10±0.06 mm, $p<0.05$) (Figure 31C).

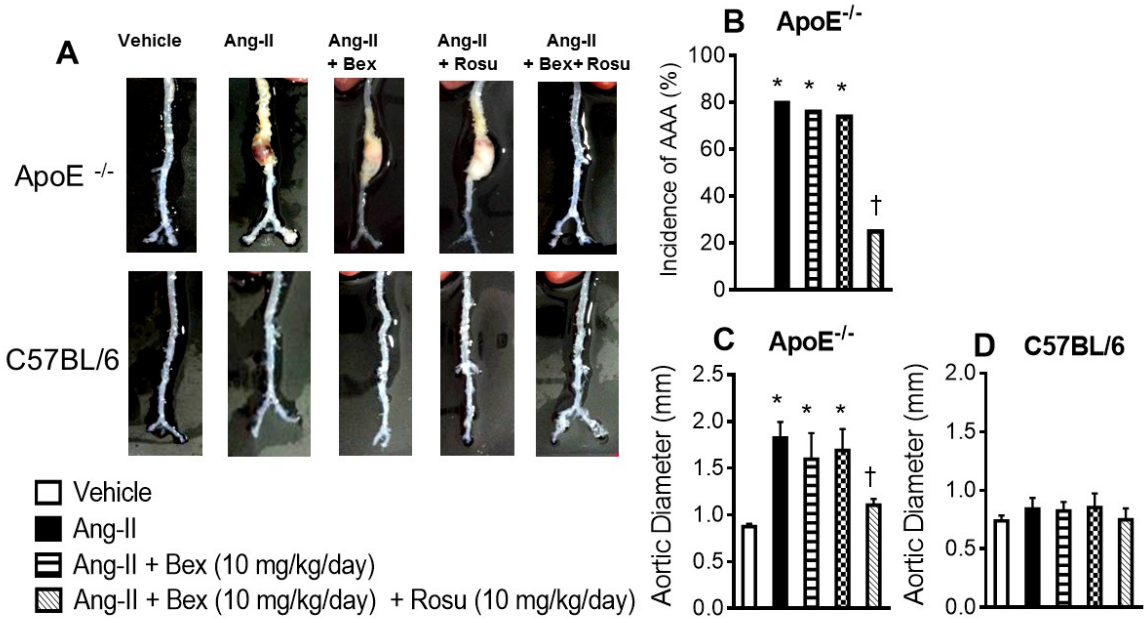

Figure 31: Effects of Bexarotene (Bex, 10 mg/kg/day) in combination with rosuvastatin (Rosu, 10 mg/kg/day) on Ang-II-induced AAA formation in apoE$^{-/-}$ and C57BL/6 mice. (A) Representative aortas from apoE$^{-/-}$ and C57BL/6 mice. The gross appearances of the aorta were photographed digitally and the maximal external diameter of the suprarenal aorta was measured. A definition of increased in outer diameter of >50 % indicated the development of aortic aneurysm. (B) Incidence of AAA in apoE$^{-/-}$ mice. Results are expressed in percentage. *p<0.05 vs. vehicle-infused mice; †p<0.05 vs. Ang-II-infused animals. (C) Aortic diameter (mm) in apoE$^{-/-}$ and in (D) C57BL/6 mice. Results are the mean±SEM (n=6-10 animals/group). *p<0.05 vs. vehicle-infused mice; †p<0.05 vs. Ang-II-infused animals.

Additionally, abundant infiltration of Mac-3^{+} macrofages was detected in the media and adventitia of the aortic aneurysms from untreated Ang-II-infused mice (Figure 32). This inflammatory infiltrate was only significantly impaired in those mice subjected to the combined treatment (Figure 32A and B, p=0.033).

While CD31^{+} microvessels were almost undectatble in the cross sections of the aortas from control mice, a large number of capillary vessels were observed in untreated Ang-II-stimulated aortas. Interestingly, mice treated simultaneously with bexarotene and rosuvastatin showed a marked decrease in capillary formation (Figure 32A and C, p=0.030). Moreover, the increased mRNA expression of proangiogenic chemokines (CXCL1, CCL2 and CCL5) and VEGF in the aortas from untreated Ang-II-infused mice was markedly reduced by the combination therapy (Figure 2D-G, p<0.05). Inasmuch, no changes in RXRα receptor mRNA expression were found in the AAA induced by Ang-II compared with vehicle infused controls

(Figure 32H, p>0.05). Moreover, RXRα expression was unaffected by the administration of bexarotene, rosuvastatin or both drugs (Figure 32I, p>0.05).

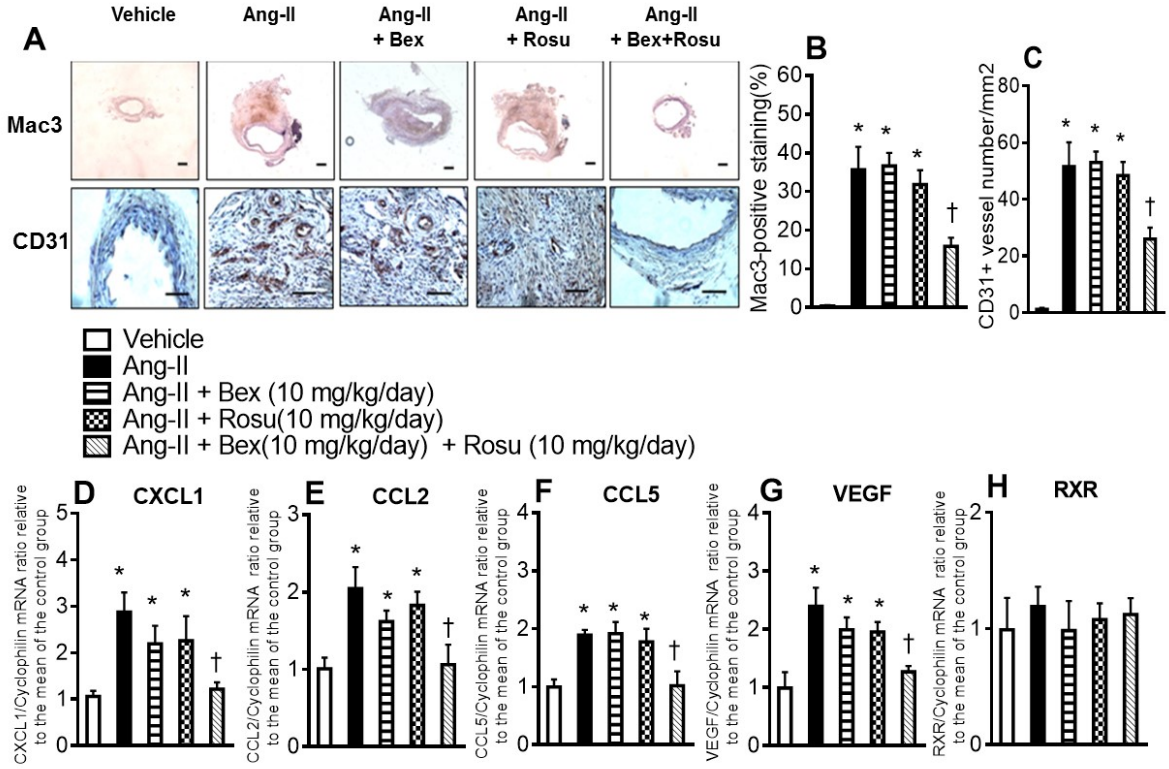

Figure 32: Bexarotene (Bex, 10 mg/kg/day) in combination with rosuvastatin (Rosu, 10 mg/kg/day) reduced macrophage infiltration, neovascularization and inflammation in the Ang-II-induced AAA mouse model. (A). Representative photomicrographs of macrophage staining and $CD31^+$ microvessels in aortic cross sections. Bar graphs represent (B) area of Mac-3 positive staining (Scale bar=200 μm) and (C) $CD31^+$ microvessels per mm^2 in AAA (Scale bar, 50 μm). Results are the mean±SEM (n=6 animals/group) *p<0.05 vs. vehicle-infused mice; †p<0.05 vs. Ang-II-infused animals. In the AAA, gene expression of (D) CXCL1, (E) CCL2 (F) CCL5, (G) VEGF and (H) RXR was analyzed by real-time RT-PCR Results are the mean±SEM of the ratio between each gene and *cyclophilin* gene expression and are referred to mean of the vehicle treated group set at 1.0 (n=6 animals/group). *p<0.05 vs. vehicle-infused mice; †p<0.05 vs. Ang-II-infused animals.

We would like to point out that subctutaneous administration of 10 mg/kg/day rosuvastatin for 5 days resulted in 108.8±2.0 $ng.ml^{-1}$ circulating levels of the statin determined by liquid chromatography-electrospray ionization–tandem mass spectrometry (LC-MS/MS) method. On the other hand, systolic blood pressure was significantly increased in those animals subjected to chronic Ang-II infusion regardless the strain investigated (Table 16). In $apoE^{-/-}$ but not in C57BL/6 mice, significant increases in total plasma and non HDL cholesterol were found in those individuals chronically infused with Ang-II and fed with a western diet. In contrast,

triglyclerides and HDL cholesterol concentrations were not affected (Table 16). Finally chronic administration of bexarotene or/and rosuvasatin did not provoke any changes on the systolic blood pressure and lipid profile of apoE$^{-/-}$ mice chronically stimulated with Ang-II and subjected to a western diet for 28 days (Table 16).

		SBP (mmHg)	TC (mg.dl^{-1})	Triglycerides (mg.dl^{-1})	HDL-C (mg.dl^{-1})	non-HDL-C (mg.dl^{-1})
apoE $^{-/-}$	Control	136,1±22,2	340,3±24,2	96,2±2,5	35,6±4,5	303,6±17,9
	Ang-II	219,2±23,4*	522,2±23,4*	76,8±18,9	34,7±5,2	487,5±56,1*
	Ang-II+ Bex	189,1±13,6*	526,3±11,1*	89,5±5,6	28,5±7,7	497,7±43,5*
	Ang-II+ Rosu	212,5±11,9*	511,2±32,8*	92,8±18,2	29,1±4,1	481,9±82,2*
	Ang-II+ Bex + Rosu	182,8±14,8*	516,5±52,7*	99,2±2,2	36,2±1,3	480,5±17,1*
C57BL/6	Control	118,3±18,3	154,8±10,2	53,8±4,2	70,2±12,4	83,0±17,4
	Ang-II	198,2±24,6*	177,9±7,2	54,2±6,3	90,4±15,9	87,4±11,9
	Ang-II+ Bex	183,8±14,8*	162,2±2,3	56,2±3,9	70,5±19,4	81,8±20,2
	Ang-II+ Rosu	192,3±12,3*	163,4±9,5	60,9±3,3	74,3±10,3	96,6±6,8
	Ang-II+ Bex + Rosu	187,1±23,2*	177,3±7,3	57,8±4,3	90,6±3,2	87,6±8,06

Table 16: Effect of Bexarotene and Rosuvastatin on systolic blood pressure and lipid profile in apoE$^{-/-}$ and C57BL6 mice. Treatment with bexarotene and/or rosuvastatin did not alter systolic blood pressure (SBP) or total plasma cholesterol (TC), triglycerides, HDL-cholesterol (HDL-C) or non HDL cholesterol (non-HDL-C) levels in Ang-II-infused apoE$^{-/-}$ or C57BL/6 mice subjected to a western diet for 28 days. Results are the mean ± SEM (n= 6-8 animals/group).*$p<0.05$ vs. respective control mice.

4.2.2 Bexarotene plus rosuvastatin attenuates AKT/mTOR/p70S6K1 phosphorylation in Ang-II-induced AAA.

Since previous studies have observed that the AKT/mTOR/p70S6K1 pathway can also be involved in AAA formation (Lawrence *et al.*, 2004), we next determined the effect of combined bexarotene and rosuvastatin administration on AKT/mTOR/p70S6K1 activation in homogenates of aneurysmal tissue. Western blot analysis of the aorta revealed increases in AKT (Figure 33A), mTOR (Figure 33B) and p70S6K1 (Figure 33C) phosphorylation in apoE$^{-/-}$ mice subjected to Ang-II infusion. Interestingly, the combination therapy attenuated Ang-II induced AKT, mTOR and p70S6K1 activation (Figure 33, $p<0.05$).

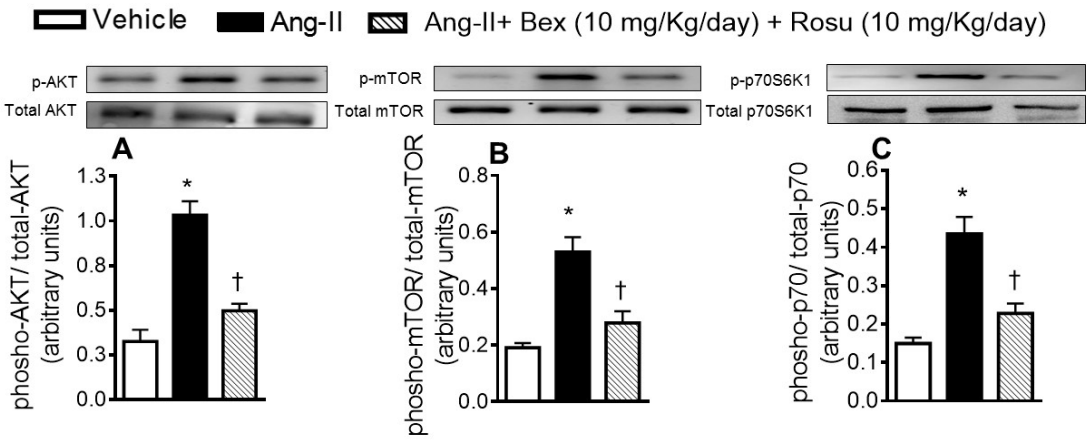

Figure 33: The combined administration of bexarotene (Bex, 10 mg/kg/day) and rosuvastatin (Rosu, 10 mg/kg/day) decreased Ang-II-induced phosphorylation of AKT, mTOR and p70S6K1 in the aorta tissue of apoE$^{-/-}$ mice. Bar graphs show protein expression ratios of (A) phospho AKT/total AKT, (B) phospho mTOR/total mTOR and (C) phospho p70S6K1/total p70S6K1 determined by western blotting of the aneurysm wall tissue. Results are the mean±SEM (n=6 animals/group). Representative western blot gels are also shown. *$p<0.05$ vs. vehicle-infused mice; †$p<0.05$ vs. Ang-II-infused animals.

4.2.3 A combination of bexarotene and rosuvastatin at suboptimal concentrations reduces endothelial tube formation, proliferation and migration induced by Ang-II

To further evaluate the effect of the combined bexarotene and rosuvastatin treatment on angiogenesis, HUVEC were stimulated with 1 μM Ang-II for 24 h. Bexarotene (0.3-10 μM) and rosuvastatin (1-10 μM) inhibited in a concentration-

dependent manner the tube-like structures induced by the peptide hormone (Figure 34A and B). Interestingly, while suboptimal concentrations of bexarotene (0.3 μM) or rosuvastatin (3 μM) were unable to inhibit Ang-II-induced tube formation, significant reductions in this parameter were achieved when the two compounds were administered together (Figure 34C and D, $p<0.001$). As expected, pretreatment of the cells with 100 μM EXP3174, an AT_1 Ang-II receptor antagonist, inhibited Ang-II induced tubulogenesis (Figure 34C).

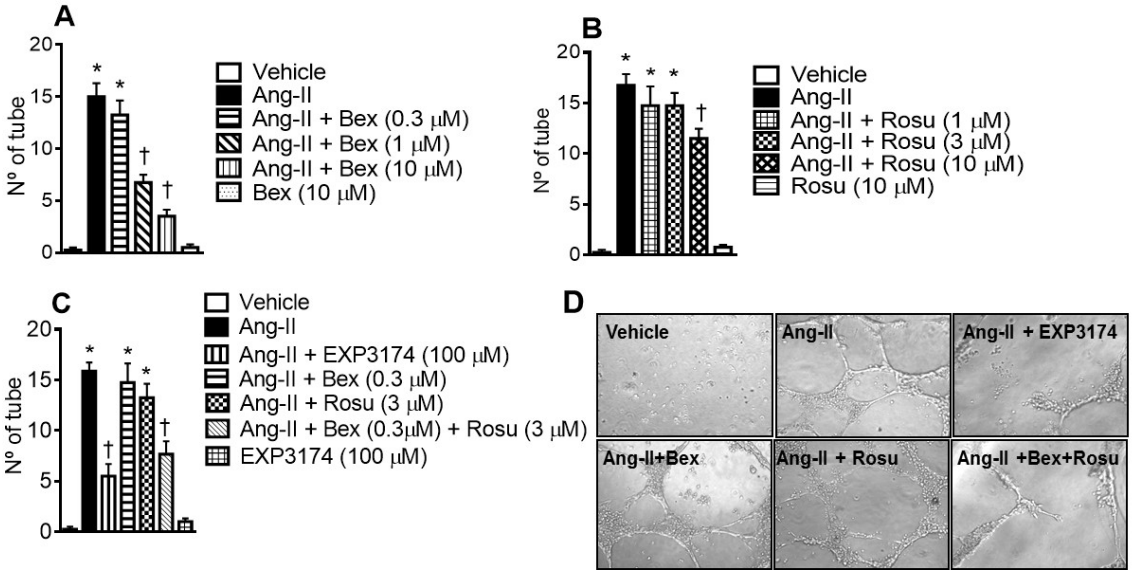

Figure 34: The combination of bexarotene and rosuvastatin at suboptimal concentrations decreased Ang-II-induced tube formation. Endothelial differentiation assay was performed on Matrigel. HUVEC were incubated with vehicle (0.01 % DMSO), bexarotene (Bex, 0.3-10 μM) (A) or rosuvastatin (Rosu, 1-10 μM) (B) 24 h before Ang-II stimulation (1 μM, 24 h). In other experiments, HUVEC were pretreated with EXP3174 (100 μM, 1 h) or with bexarotene (0.3 μM), rosuvastatin (3 μM) or both for 24 h and then stimulated with Ang-II (24 h) (C). Results are the mean±SEM of the number of tube-like structures in 5 low-magnification (×100) fields (n=6 independent experiments). *$p<0.01$ vs vehicle; †$p<0.05$ vs Ang-II. (D) Representative images of the endothelial differentiation assays.

Proliferation and migration of endothelial cells are essential steps in angiogenesis (Piqueras *et al.*, 2007), and we have found that pretreatment of these cells with bexarotene (0.3 μM) plus rosuvastatin (3 μM), but not with either agent alone, decreased Ang-II-induced HUVEC proliferation by 52% (Figure 35A, $p=0.001$). Similarly, a significant reduction in the migratory potential of Ang-II-stimulated HUVEC was observed when bexarotene and rosuvastatin were both present (25% inhibition, Figure 35B and C, $p=0.023$).

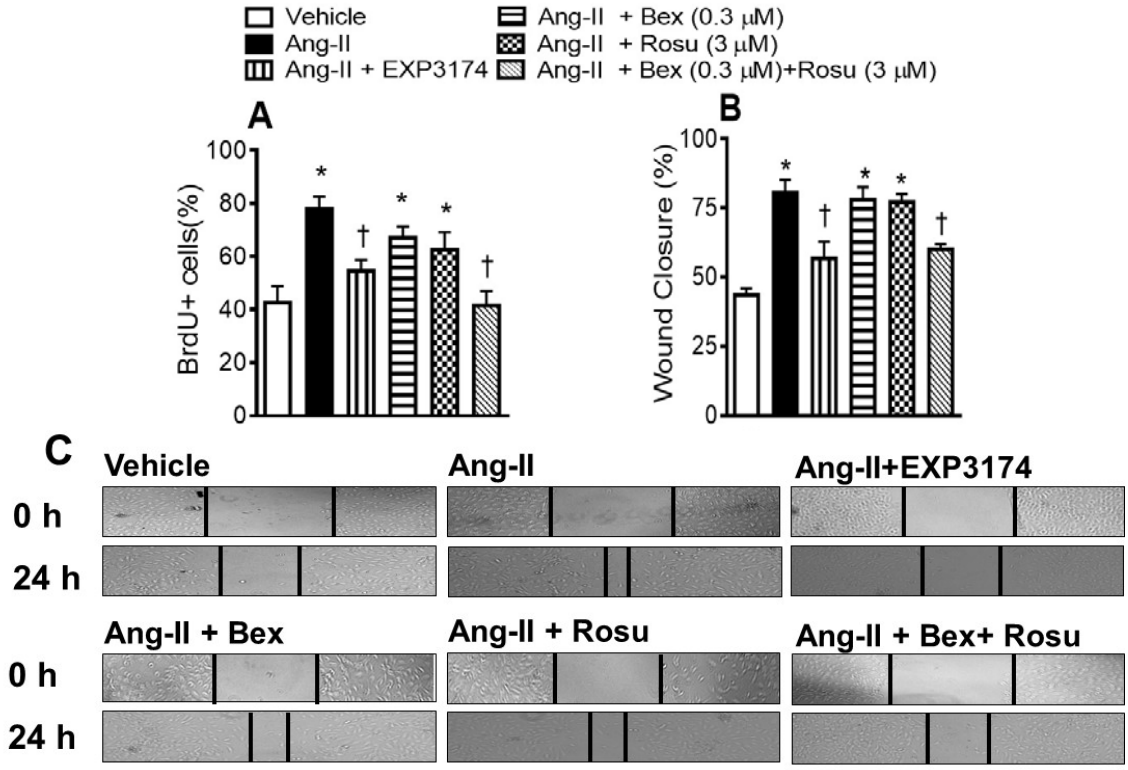

Figure 35: The combination of bexarotene (Bex, 0.3 μM) and rosuvastatin (Rosu, 3 μM) at suboptimal concentrations decreased Ang-II-induced endothelial cell proliferation and migration. (A) Percentage of proliferating endothelial cells were analysed by BrdU incorporation. *p<0.05 vs. vehicle; †p<0.05 vs. Ang-II. Results are the mean±SEM (n=5) (B) Bar graph represents percentage of wound closure with the different treatments. The degree of wound closure was measured as the percentage of the area covered by migrating cells in the initial wound. Results are the mean±SEM (n=5). (C) Representative photomicrographs of wounds (t=0 and t=24 h); black lines highlight the linear scratch/wound.

4.2.4 Bexarotene in combination with rosuvastatin at suboptimal concentrations inhibits endothelial cell sprouting and matrigel vascularization in mice.

In order to confirm the sinergistic antiangiogenic activity exerted by combined bexarotene/rosuvastatin treatment, we next tested the activity of both drugs in the *ex vivo* murine aortic ring assay and in the *in vivo* model of matrigel assay. In the *ex vivo* murine aortic ring assay, 8-day stimulation with Ang-II (1 μM) resulted in increased endothelial cell sprouting versus vehicle-exposed aortic segments, an effect mediated via Ang-II/AT_1 receptor interaction (Figure 36A). In agreement with our previous observations, incubation with both drugs markedly reduced Ang-II-induced

angiogenesis (Ang-II: 14.7±1.1; Ang-II+bexarotene+rosuvastatin: 7.25±1.1 microvessel per ring, Figure 6A, p<0.001).

On the other hand, in the *in vivo* matrigel assay, Ang-II-induced increases in hemoglobin content was blunted by EXP3174 (Figure 36B). Interestingly, the combined treatment with both drugs prompted a significant decrease in the matrigel plug hemoglobin content compared with that in plugs containing only Ang-II (Figure 36B, p<0.001).

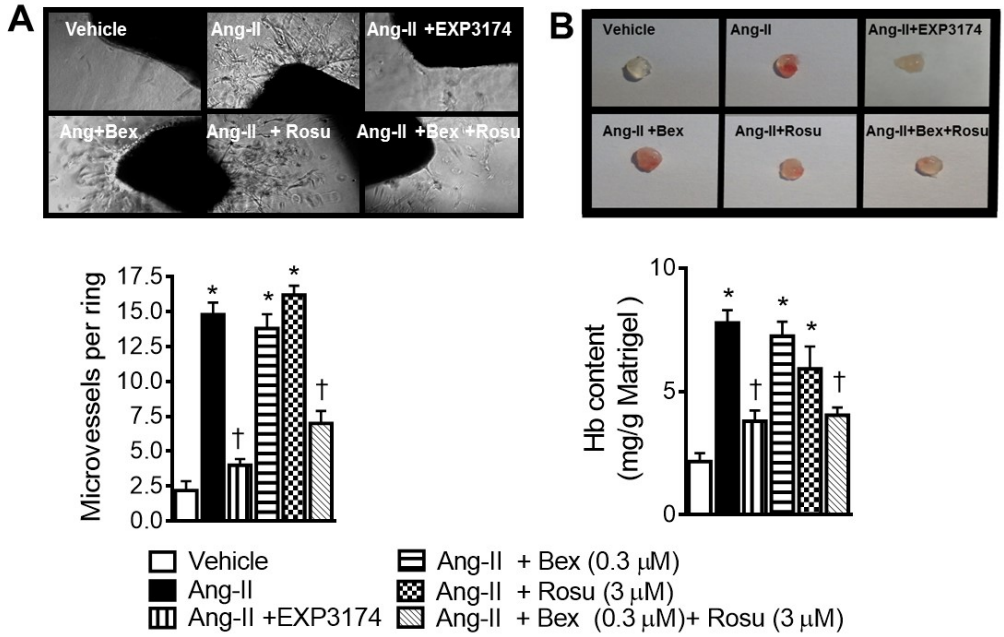

Figure 36: The combination of suboptimal concentrations of bexarotene (Bex, 0.3 μM) and rosuvastatin (Rosu, 3 μM) decreased endothelial cell out-growth in the ex vivo murine aortic ring assay and reduced vascularization in the *in vivo* Matrigel plug assay. (A) Figure shows quantitative analysis of microvessel sprouting after 8 days with treatment with EXP3174 (100 μM) or with bexarotene (0.3 μM), rosuvastatin (3 μM) or both and stimulated with Ang-II (1 μM). The number of microvessels per aortic ring was counted and analyzing three rings per treatment group for each mouse. Results are the mean±SEM (n=5 animals per group). *p<0.01 vs vehicle; †p<0.05 vs Ang-II (B) Figure shows hemoglobin (Hb) content in the matrigel plugs. Results are the mean±SEM (n=5). *p<0.01 vs vehicle plugs; †p<0.05 vs Ang-II plugs.

4.2.5 Inhibition of Ang-II-induced endothelial angiogenic chemokines and VEGF production by a combination of bexarotene plus rosuvastatin at suboptimal concentrations.

Significant increases in CXCL1, CCL2 and CCL5 levels were detected in the supernantants of Ang-II-stimulated HUVEC through AT_1 receptor interaction (Figure 37A-C). Notably, the combination of bexarotene (0.3 μM) with rosuvastatin (3 μM) synergistically reduced the Ang-II-induced increase in CXCL1, CCL2, and CCL5 levels by 64, 43 and 41%, respectively (Figure 37A-C, $p<0.05$). To determine the potential contribution of these chemokines to the angiogenic activity of Ang-II, different chemokine receptors were selectively blocked. As shown in Figure 37D, the CXCR2 antagonist that blocks most of the action of the *glutamic acid-leucine-arginine* or ELR^+-CXC chemokines, only partially reduced the tube formation caused by Ang-II (21% inhibition, $p=0.033$). Interestingly, CCR2 blockade decreased Ang-II-induced capillary-like structure formation by 45% (Figure 37E, $p=0.042$). Similarly, tubulogenesis owing to Ang-II was markedly diminished when CCR1, CCR3 and CCR5 receptors were simultaneously blocked (51% inhibition, Figure 37E, $p=0.020$).

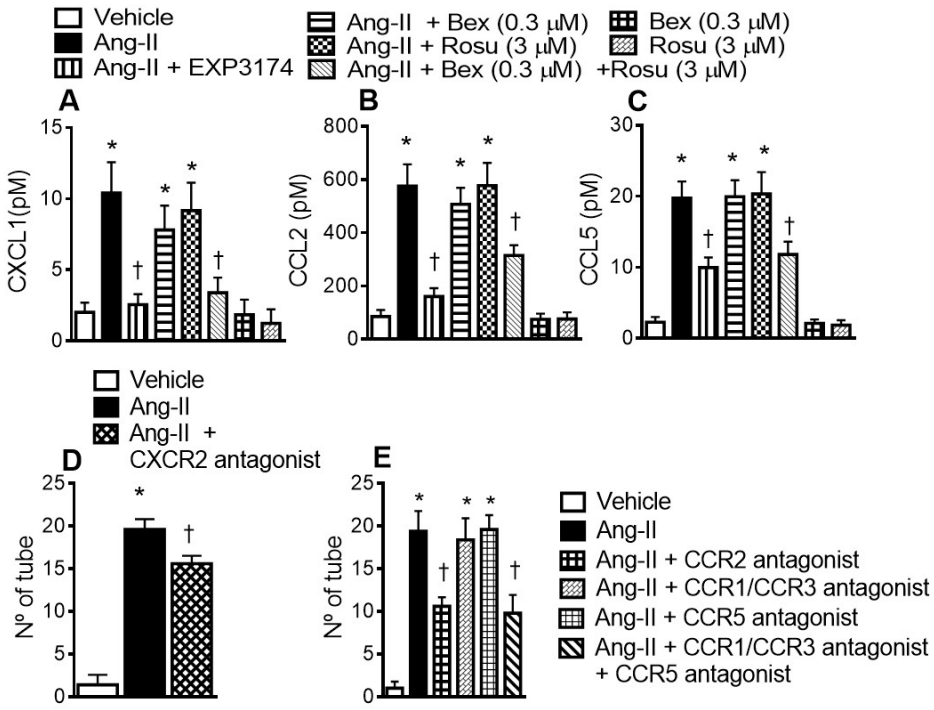

Figure 37: Inhibition of (A) CXCL1, (B) CCL2 and (C) CCL5 synthesis in Ang-II-stimulated HUVEC by pretreatment with a combination of suboptimal concentrations of bexarotene (Bex, 0.3 μM) and rosuvastatin (Rosu, 3 μM). Results are the mean±SEM (n=5-6). In other experiments, (D) HUVEC were seeded on matrigel and pretreated with a CXCR2 antagonist (SB225002, 100 nM) (E) a CCR2 antagonist (BMSCCR2 22, 10 μM), the dual CCR1/CCR3 antagonist (UCB35625, 100 nM) and/or the CCR5 antagonist (DAPTA, 10 nM) 1 h before Ang-II stimulation (24 h). Results are the mean±SEM (n=5). *p<0.05 vs. vehicle; †p<0.01 vs. Ang-II

Ang-II can also cause the generation and release of the angiogenic factor VEGF from endothelial cells (Willis *et al.*, 2011). First, we found that 1 h preincubation with EXP3174 (100 μM) reduced the VEGF release evoked by Ang-II (Figure 38A, p<0.001). Second, bexarotene plus rosuvastatin diminished Ang-II-induced VEGF release by 40% (Figures 38A, p<0.001). Finally, preincubation with a VEGFR1/2 antagonist drastrically decreased Ang-II-induced tubulogenesis (Figure 38B, p<0.001).

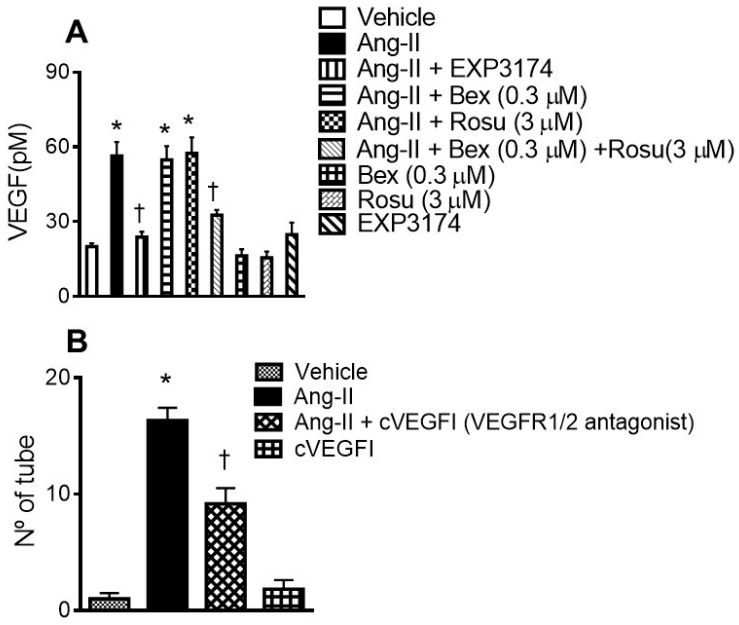

Figure 38: Bexarotene plus rosuvastatin at suboptimal concentrations inhibited VEGF release from Ang-II-stimulated HUVEC. Cells were incubated for 1 h with EXP3174 (100 μM) or 24 h with bexarotene (Bex, 0.3 μM), rosuvastatin (Rosu, 3 μM) or both drugs and then stimulated with Ang-II (24 h). VEGF (pM in cell supernatants) was measured by ELISA (A). Results are the mean ± SEM (n=5-6 independent experiments). *p<0.05 vs. vehicle (0.01% DMSO); †p<0.05 vs. Ang-II. In other experiments, cells were pretreated with a VEGF1/2 antagonist (10 μM) 1 h before Ang-II stimulation (B). Results are the mean±SEM of the number of tube-like structures in 5 low-magnification (×100) fields (n=5 independent experiments). *p<0.05 vs. vehicle, †p<0.05 vs. Ang-II.

4.2.6 RXRα and its heterodimer partners PPARα and PPARγ are involved in the anti-angiogenic activity exerted by the combination of suboptimal concentrations of bexarotene plus rosuvastatin.

To achieve further insights into the underlying mechanism, we first investigated the potential involvement of the RXRα receptor. Forty-eight-hour post-transfection with a RXRα-specific siRNA, HUVEC showed a >75% reduction in RXRα protein levels compared with control siRNA-transfected cells (Figure 39A, p<0.001).

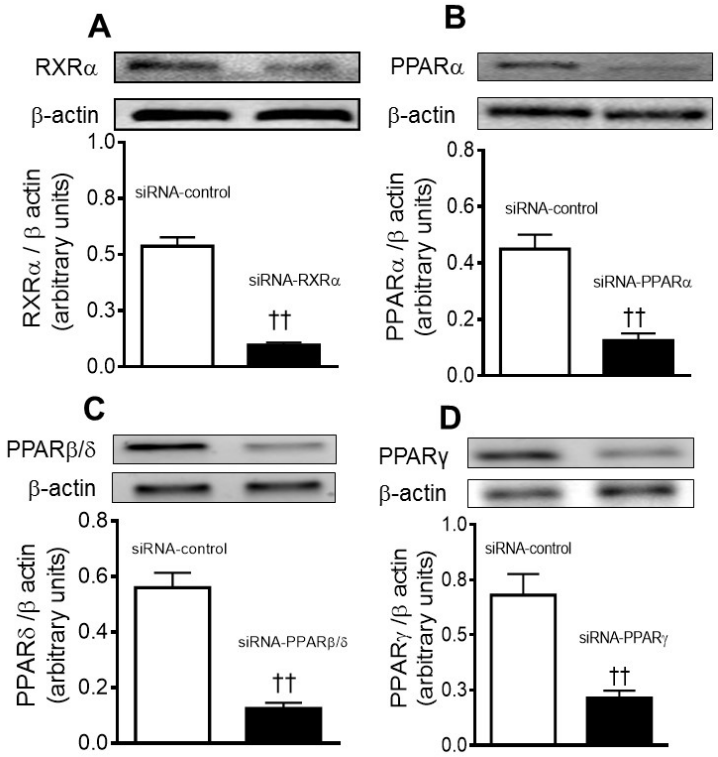

Figure 39: Gene silencing was performed using either control or RXRα, PPARα, PPARβ/δ or PPARγ-specific siRNA. After 48 h post-transfection protein expression was determined by western blot. Protein quantification was performed by densitometry. Bar graphs represent protein expression ratios of (A) RXRα/β-actin, (B) PPARα/β-actin and (C) PPARδ/β-actin (D) PPARγ/β-actin. Results are the mean±SEM (n=5 independent experiments). Representative gels are also shown. ††$p<0.05$ vs. values in the respective siRNA control group.

Of importance, RXRα-specific siRNA abolished the suppressive effects of bexarotene plus rosuvastatin on the tubulogenesis induced by Ang-II (Figure 40A and E, $p<0.050$).

RXRα can dimerize with other nuclear hormone receptors that are also potent regulators of angiogenesis, such as PPARs (Xin *et al.*, 1999; Varet *et al.*, 2003; Piqueras *et al.*, 2007). Therefore, we sought to explore the potential involvement of PPARs in the responses promoted by the drug combination. Again, a siRNA approach was employed (Figure 39). While the inhibitory effects of the bexarotene/rosuvastatin combination on Ang-II–induced capillary formation were reversed in PPARα and PPARγ siRNA-transfected cells (Figure 40B, D, $p<0.05$), PPARβ/δ knockdown did not affect these responses (Figure 40C). Additionally, immunoprecipitation assays revealed that RXRα/PPARα and RXRα/PPARγ

interactions were enhanced when endothelial cells were pretreated with the drug combination (Figure 40F).

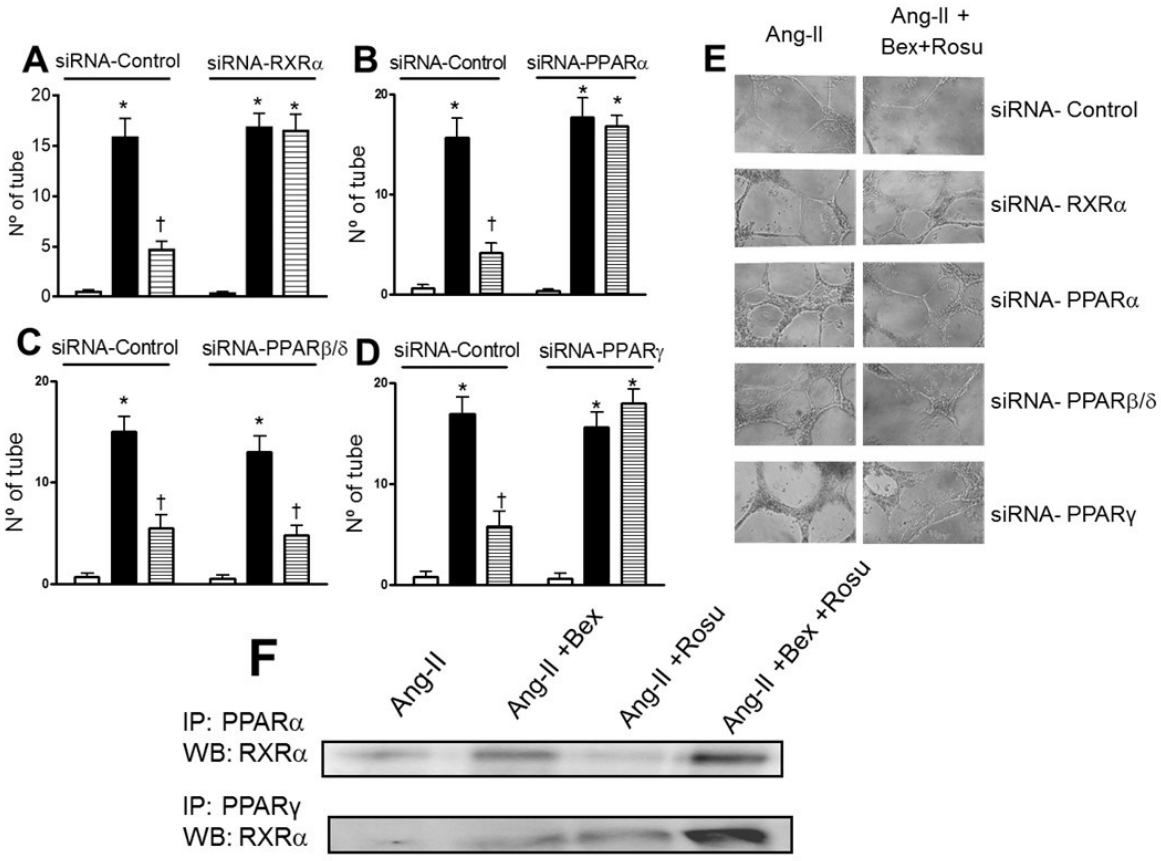

Figure 40: Knockdown of RXRα, PPARγ or PPARα but not PPARβ by small interference RNA abrogated the inhibitory effect of bexarotene plus rosuvastatin in combination on Ang-II-induced endothelial cell tube formation. HUVECs were transfected with control (A), RXRα (B), PPARα, (C), PPARβ/δ or (D) PPARγ specific-siRNA. 48 h post-transfection the cells were pretreated with bexarotene (Bex, 0.3 μM) and/or rosuvastatin (Rosu, 3 μM) for 24 h. Then the cells were stimulated with Ang-II (1 μM, 24 h). The number of tube-like structures was determined in 5 low-magnification (×100) fields was quantified. Results are the mean±SEM of n=5-6 independent experiments. *p<0.05 relative to the vehicle group.†p<0.05 relative to the Ang-II-stimulated cells. (E) Panel shows representative photomicrographs of the endothelial differentiation assay. (F) RXRα/PPARγ or RXRα/PPARα interaction was assessed by immunoprecipitation of PPARα or PPARγ and subsequent Western blotting for RXRα. Blots are representative of n=6 independent experiments.

4.2.7 Bexarotene in combination with rosuvastatin at suboptimal concentrations inhibits the activation of Akt/mTOR/P70S6K1 signaling pathway induced by Ang-II.

Since PI3K/AKT/mTOR pathway seems to play a role on Ang-II induced AAA formation; we next examined its potential involvement in the angiogenic response provoked by Ang-II in HUVEC. The 15-min challenge with 1 μM Ang-II triggered a marked phosphorylation of AKT, mTOR and p70S6K1 through interaction with its AT_1 receptor (Figure 41). Preincubation of the cells with bexarotene (0.3 μM) plus rosuvastatin (3 μM) decreased Ang-II-induced phosphorylation of the different members of this signaling pathway (Figure 41A-C, $p<0.05$). Moreover, this effect was reproduced when the cells were preincubated with LY294002 (10 μM), a selective PI3K inhibitor (Fig. 41D-F).

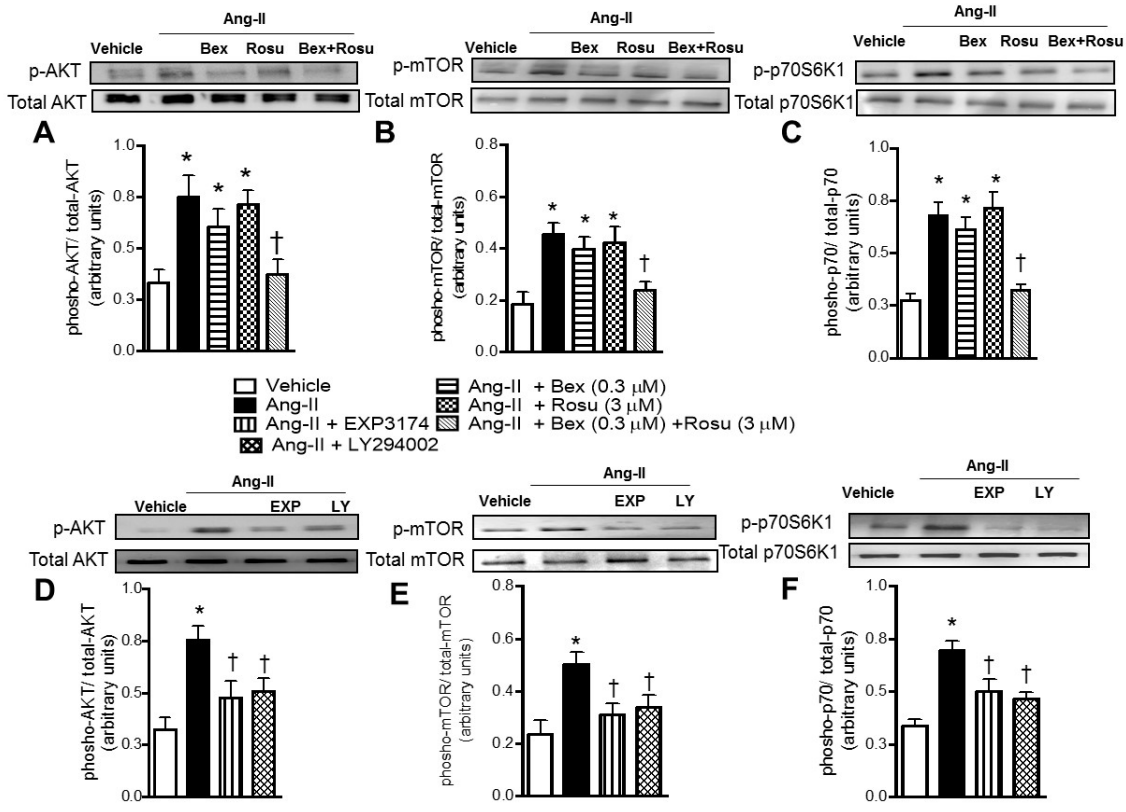

Figure 41: Phosphorylation of AKT, mTOR and p70S6K induced by Ang-II was reduced by pretreatment of the cells with the combination of suboptimal concentrations of bexarotene and rosuvastatin. Cells were pretreated with bexarotene (Bex, 0.3 μM) and/or rosuvastatin (Rosu, 3 μM) for 24 h. After treatments, HUVEC were stimulated with Ang-II (1 μM, 15 min). Bar graphs represent protein expression ratios of (A) phospho AKT/total AKT, (B) phospho mTOR/total mTOR and (C) phospho p70S6K1/total

p70S6K1 determined by western blotting. Results are the mean±SEM of n=5 independent experiments. *p<0.05 vs. vehicle; †p<0.05 vs. Ang-II. In another set of experiments, some plates were pretreated with EXP3174 (100 μM) or a PI3K inhibitor (LY294002, 10 μM) 1 h before Ang-II stimulation and protein expression ratios of (D) phospho AKT/total AKT, (E) phospho mTOR/total mTOR and (F) phospho p70S6K1/total p70S6K1 was determined. Results are the mean±SEM of n=5 independent experiments. Representative gels are also shown. *p<0.05 vs. vehicle; †p<0.05 vs. Ang-II.

Furthermore, the inhibition of PI3K decreased the production of proangiogenic chemokines (CXCL1, CCL2 and CCL5) or VEGF and the tubulogenesis exerted by Ang-II (Figures 42A-E, p<0.05).

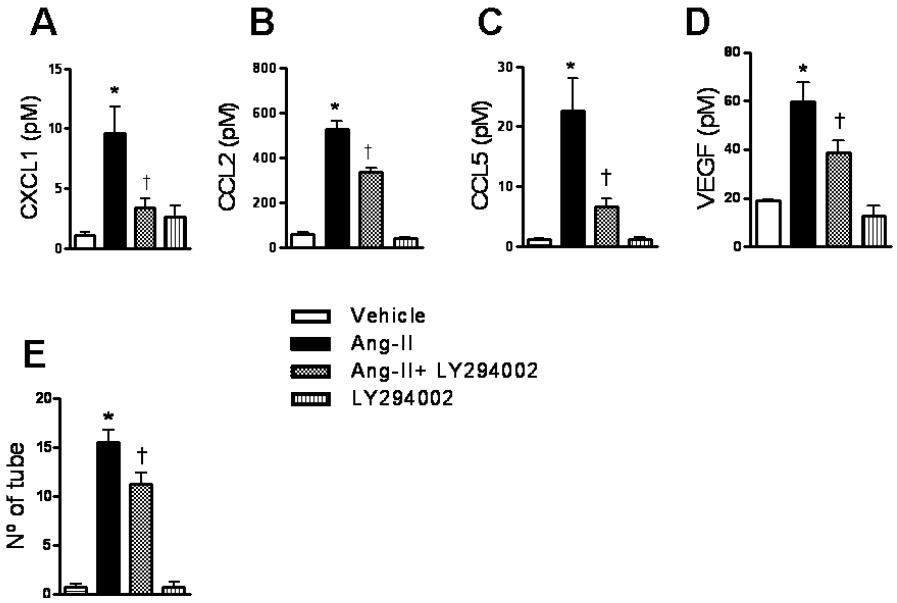

Figure 42: Inhibition of PI3K decreases Ang-II-induced chemokine and VEGF production and tube formation. Cells were incubated for 1 h with the PI3K inhibitor (10 μM) and then stimulated with Ang-II (24 h). (A) CXCL1, (B) CCL2, (C) CCL5 and (D) VEGF production (pM in cell supernatants) was determined by ELISA. Results are the mean±SEM (n=5-6 independent experiments). †p<0.05 vs. Ang-II. (E) After treatments, the number of tube-like structures in 5 low-magnification (×100) fields were quantified. Results are the mean±SEM of the number of tube-like structures in 5 low-magnification (×100) fields (n=5 independent experiments). *p<0.05 vs. vehicle, †p<0.05 vs. Ang-II.

4.3 RESULTS OF THE STUDY: CXCL16/CXCR6 AXIS IS INVOLVED IN ANGIOTENSIN-II-INDUCED ENDOTHELIAL DYSFUNCTION.

4.3.1 Arteriolar leukocyte adhesion is reduced in CXCR6$^{-/-}$ mice

To examine leukocyte-endothelial cell interactions induced by Ang-II in the cremasteric microcirculation, intravital microscopy was used. CXCR6$^{-/+}$ or CXCR6$^{-/-}$ mice were infused with saline or Ang-II 500 ng/kg/min for 14 days. Stimulation with Ang-II induced a significant increase in arteriolar leukocyte adhesion in CXCR6$^{-/+}$ mice, whereas CXCR6$^{-/-}$ mice showed a 59,5% inhibition in this parameter (Figure 43A). Moreover, Ang-II increased CD11b expression in circulating monocytes and CD69 expression in lymphocytes, whereas neutrophil CD11b expression was not affected. Up-regulation of CD11b and CD69 induced by Ang-II was also significantly reduced in CXCR6$^{-/-}$ mice (Figure 43B, C and D). Immunofluorescence analysis of the cremasteric microvasculature (Figure 43E) revealed that stimulation with Ang-II resulted in a substantial increase in endothelial CXCL16 expression within the cremasteric arterioles in wild type mice.

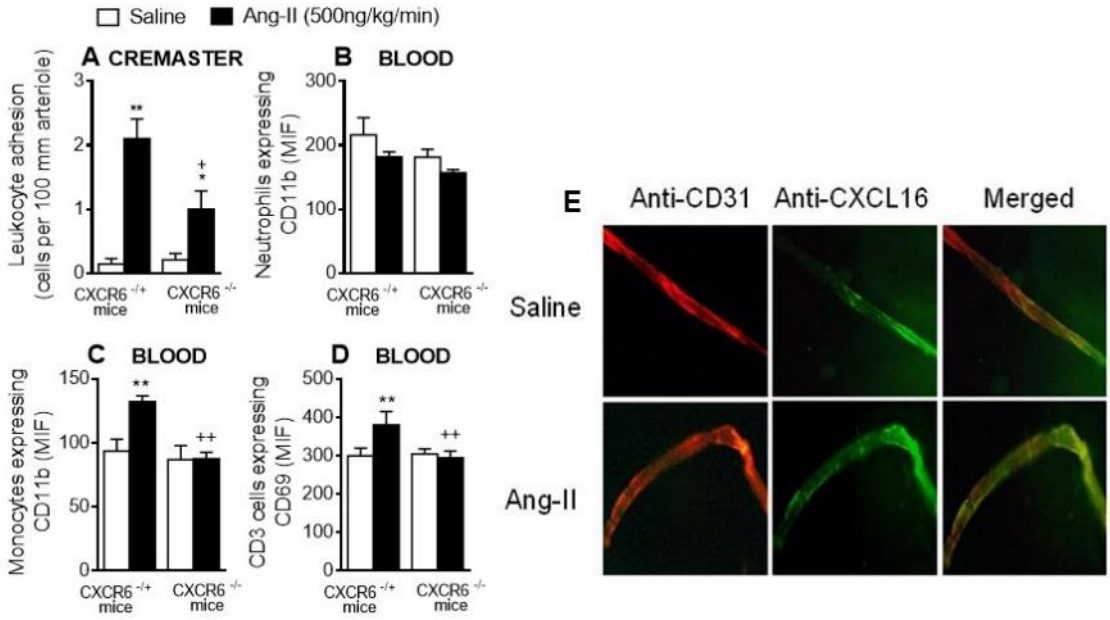

Figure 43: Effect of Ang-II stimulation in CXCR6 expressing and CXCR6 knockout mice. Heterozygous (CXCR6$^{-/+}$) and homozygous (CXCR6$^{-/-}$) mice were infused or not with Ang-II 500 ng/kg/min for 15 days. (A) Leukocyte–arteriolar endothelium interactions were measured by intravital microscopy. (B and *C*) CD11b expression was determined by flow cytometry of circulating neutrophils and monocytes in heparinized whole blood. (D) CD69 expression was determined by flow cytometry of circulating CD3^{+} cells in heparinized whole

blood. Results are expressed as mean ± SEM (n=4–6 animals per group). * $p<0.05$ or **$p<0.01$ relative to vehicle -infused mice; $^{+}p<0.05$ or $^{++}p<0.01$ relative to $CXCR6^{-/+}$ mice. (*E*) Cremaster muscle was fixed for CXCL16 and endothelium (CD31) staining. CXCL16 expression is shown in green (stained with an Alexa Fluor 488-conjugated donkey anti-rabbit secondary antibody) and vessel endothelium (red) was stained with a PE-conjugated anti-mouse CD31 monoclonal antibody. Overlapping expression of CXCL16 and CD31 is shown in yellow. Results are representative of 5–6 animals per group.

4.3.2 Chronic administration of losartan dose-dependently decreased Ang-II-induced AAA formation, monocyte and lymphocyte infiltration, chemokine expression and neovascularization in the aneurysmal tissue.

To evaluate the possible effect of Ang-II AT_1 antagonist, losartan, on aneurysm formation, $apoE^{-/-}$ mice were infused for 28 days with Ang-II and subjected to a high fat diet. As shown in Figure 44, continuous infusion of $apoE^{-/-}$ mice with Ang-II induced AAA development. The infusion of Ang-II resulted in AAA incidence of 70% in $apoE^{-/-}$ mice. However, chronic treatment with losartan (30 mg/kg/day) reduced AAA incidence in a 76% (Figure 44B). In contrast, no changes were observed when losartan was administered at the dose of 10 mg/kg/day (Figures 44A and B). Similarly, a significant increase in suprarenal aortic diameter was found in $apoE^{-/-}$ mice chronically stimulated with Ang-II (0.93±0.03 mm vs 2.04±0.19 mm, $p<0.01$) which in the later was significantly reduced by the treatment with losartan (30 mg/kg/day) (1.44±0.24 mm, $p<0.05$) compared to the untreated group (Figure 44C)

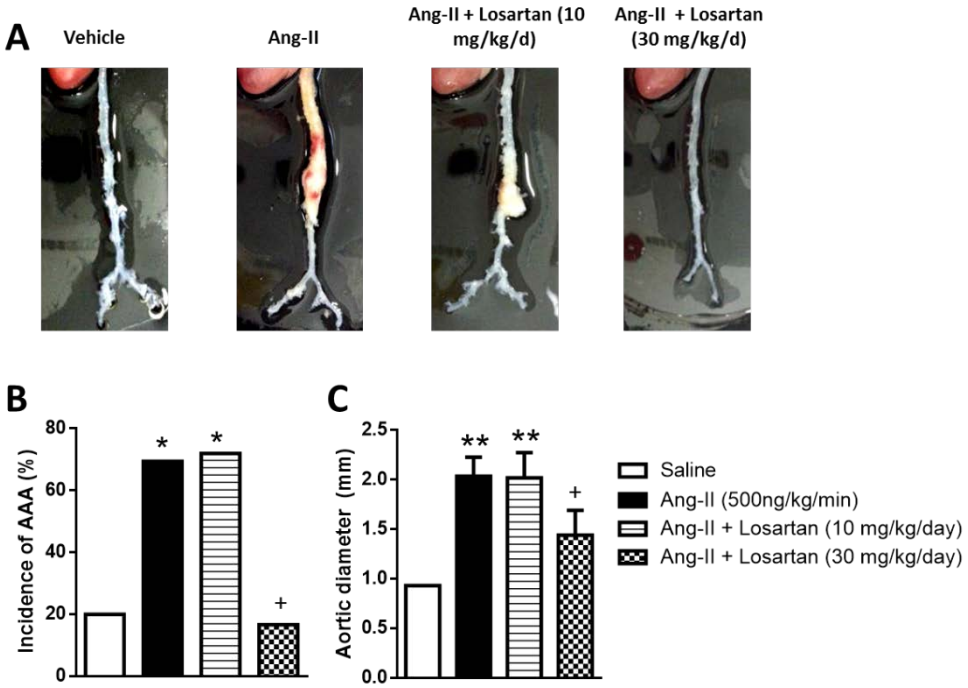

Figure 44: Effect of chronic administration of losartan on Ang-II-induced AAA formation in apoE$^{-/-}$ mice. (A) Representative aortas from apoE$^{-/-}$ mice. The gross appearances of the aorta were photographed digitally and the maximal external diameter of the suprarenal aorta was measured. A definition of increased in outer diameter of >50 % indicated the development of aortic aneurysm. (B) Incidence of AAA in apoE$^{-/-}$ mice. Results are expressed in percentage. *p<0.05 vs. vehicle-infused mice; +p<0.05 vs. Ang-II-infused animals. (C) Aortic diameter (mm) in apoE$^{-/-}$ mice. Results are the mean±SEM (n=6-10 animals/group). **p<0.01 vs. vehicle-infused mice; +p<0.05 vs. Ang-II-infused animals.

Ang-II infusion promoted macrophage and lymphocyte content in aneurysms tissues. Chronic treatment with losartan at 10 mg/kg/day had no effect on these parameters (Figure 45A-C). However, losartan at the dose of 30 mg/kg/day substantially decreased macrophage and lymphocyte content by 95 % and 90,2% respectively (Figure 45A-C).

As illustrated in Figure 45A and D, an increased number of capillary vessels were observed in Ang-II-stimulated aortas. Interestingly, mice treated with losartan at the dose of 30 mg/kg/day showed a marked decrease in capillary formation (Figure 45A and D, p<0.05) compared to vehicle treated mice.

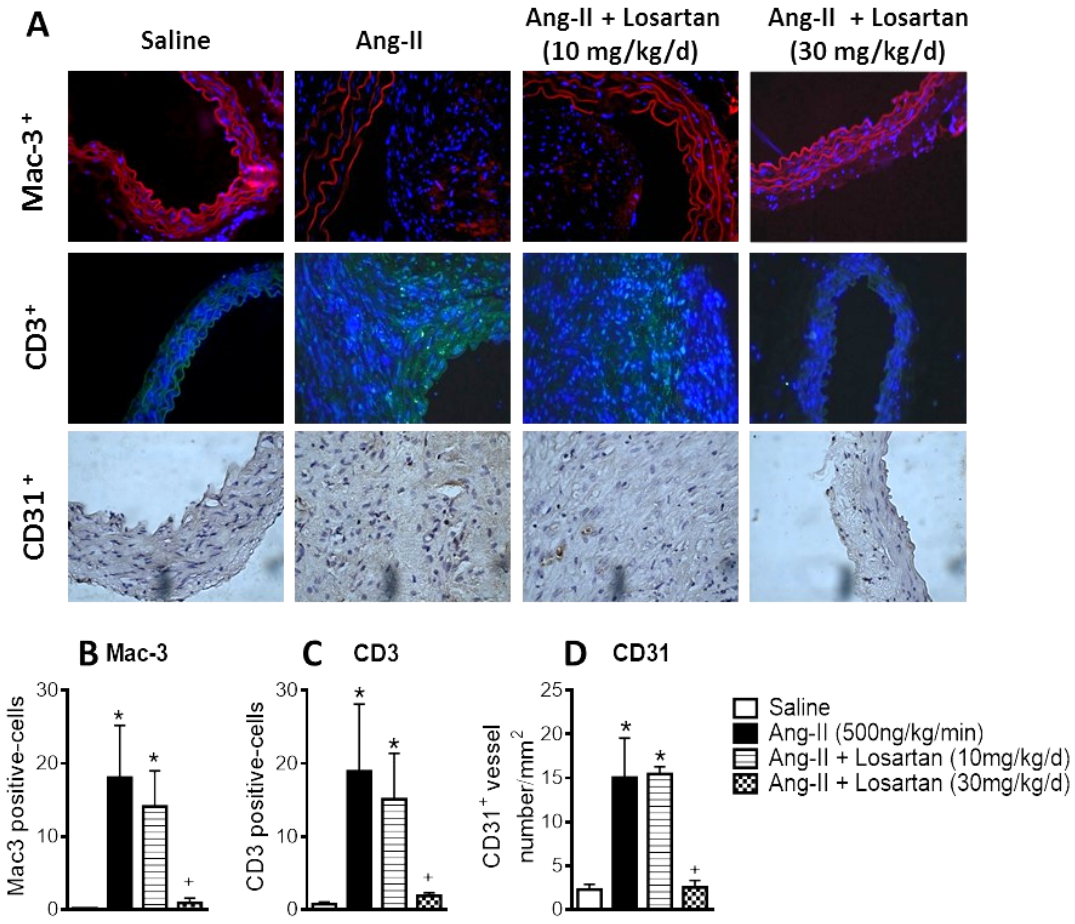

Figure 45: Losartan (30 mg/kg/day) reduces macrophage and lymphocyte content as well as neovascularization, in the Ang-II-induced AAA mouse model. (A) Representative photomicrographs of macrophage, lymphocyte and $CD31^+$ microvessel staining in aortic cross sections. Bar graphs represent percentage of (B) Mac-3^+ cells (C) $CD3^+$ cells and (D) number of $CD31^+$ microvessels per mm^2 in aneurysm aortic sections. Results are expressed as the mean±SEM (n=4-6 animals/group). *p<0.05 vs. vehicle-infused mice; +p<0.05 vs. Ang-II-infused animals.

Additionally, immunohistochemistry analysis of the aortic tissue showed that chronic administration of Ang-II 500 ng/kg/min plus a high fat diet for 28 days induced a significant increase in the number of cell expressing CXCR6 which was reduced by the treatment with losartan (30 mg/kg/day) by 85% compared to the non-treated group (Figure 46A and B). This result was further confirmed by RT-PCR (Figure 46C).

Moreover, increased mRNA expression of the chemokines CXCL16 and CCL2 (MCP-1) and the growth factor VEGF was observed in the aortas from Ang-II-

infused mice. Notably, therapy with losartan 30 mg/kg/day significantly decreased these parameters (Figure 46D-F, p<0.05).

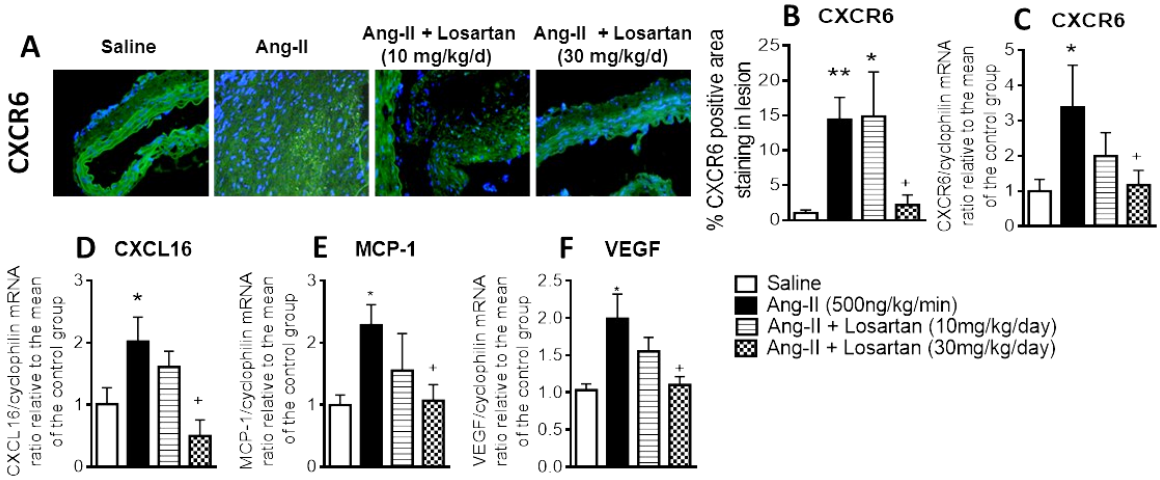

Figure 46: Losartan at the dose of 30 mg/kg/day reduced CXCR6 expression and inflammation in the Ang-II-induced AAA mouse model. (A) Representative photomicrographs of CXCR6 staining in aortic cross sections. Bar graphs represent (B) area of CXCR6 positive staining in AAA. Results are expressed as the mean±SEM (n=4-6 animals/group) *p<0.05 and **p<0.01 vs. vehicle-infused mice; $^{+}$p<0.05 vs. Ang-II-infused animals. In the AAA, mRNA expression of (C) CXCR6, (D) CXCL16 (E) MCP-1 and (F) VEGF was analyzed by real-time RT-PCR. Results are expressed as the mean±SEM of the ratio between each gene and cyclophilin gene expression and are referred to mean of the vehicle treated group set at 1.0 (n=4-6 animals/group). *p<0.05 vs. vehicle-infused mice; $^{+}$p<0.05 vs. Ang-II-infused animals.

4.3.3 Ang-II induces functional CXCL16 expression in HUAEC

To extend these findings to human cells, we next investigated the effect of Ang-II on CXCL16 expression in human arterial endothelial cells. RT-PCR analysis revealed that endothelial cells stimulated for 1 h with Ang-II (1 μM) or IFNγ (20 ng/mL) did not modify CXCL16 expression levels in HUAEC (Figure 47A). In contrast, stimulation for 4 h with either Ang-II or IFNγ resulted in a clear upregulation of CXCL16 mRNA expression (Figure 47B). These responses were corroborated by flow cytometry and immunofluorescence analysis, since incubation with Ang-II (1 μM) for 24 h induced a substantial upregulation of CXCL16 at the protein level (Figure 47C and D). This effect was mediated through interaction of Ang-II with its AT_1 receptor, since pretreatment of the endothelial cells with 100 μM EXP3174, an Ang-II AT_1 receptor antagonist, inhibited these responses (Figure 47).

To define the potential contribution of CXCL16 to mononuclear leukocyte-endothelium interactions induced by Ang-II, we performed an *in vitro* assay using the dynamic model of the flow chamber. Mononuclear leukocyte adhesion to Ang-II–stimulated HUAEC was markedly increased (Figure 47E). Notably, neutralization of CXCL16 activity in arterial endothelial cells resulted in a significant reduction in Ang-II–induced mononuclear cell adhesion to HUAEC (50%). These findings suggest that CXCL16 upregulation seems to play a clear role in the arterial mononuclear cell recruitment that arises in response to Ang-II.

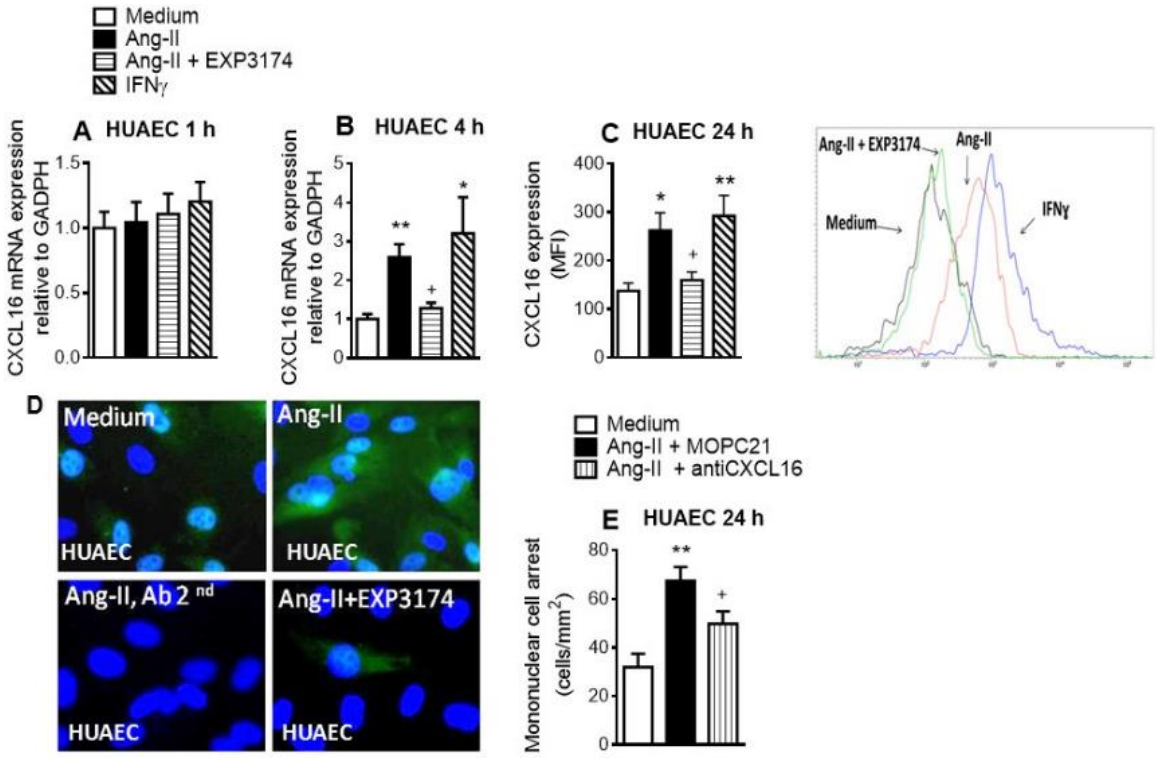

Figure 47: Expression and function of CXCL16 in Ang-II-stimulated HUAEC and the effect of a CXCL16 neutralizing antibody on mononuclear leukocyte adhesion. HUAEC were stimulated with Ang-II or IFN γ (20 ng/ ml) for 1, 4 or 24 h. Relative quantification of mRNA levels for CXCL16 and GAPDH after (A) 1 h and (B) 4 h (n=5–7 independent experiments). Columns show fold increase in CXCL16 mRNA expression relative to control GAPDH. Values are expressed as mean ± SEM of the $2^{-\Delta\Delta Ct}$ values. (C) Protein expression was determined by flow cytometry. Results are the mean±SEM of n=7 independent experiments. MFI indicates mean fluorescence intensity. Representative histograms are also shown. (D) CXCL16 was visualized in HUAEC by immunofluorescence (green). Nuclei were counterstained with 4'6-diamidino-2-phenylindole (DAPI) (n=5 independent experiments). (E) Endothelial cells were stimulated with Ang-II for 24 h. Some cells were incubated with a CXCL16 neutralizing antibody (2 μg/ml) or with an irrelevant isotype-matched monoclonal antibody (MOPC21, 2 μg/ml). Subsequently, human mononuclear cells (1×10^6 cells/ml) were perfused over the monolayers for 5 min at 0.5 dyn/cm2 and leukocyte accumulation quantified (n=7 independent experiments). Values are expressed as the mean ±

SEM. *p<0.05 or **p<0.01 relative to values in the medium group; $^{+}$p<0.05 relative to Ang-II group.

4.3.4 Nox5 but not Nox2 or Nox4, are involved in Ang-II–induced CXCL16 expression and mononuclear cell arrest in HUAEC

The production of ROS and activation of redox-sensitive signaling pathways mediate many of the inflammatory responses of Ang-II (Laursen *et al.*, 1997; Lassegue *et al.*, 2010). Because potential sources of superoxide anion in the vasculature include the activation of NADPH oxidases (Nox) and xantine oxidase (XO) (Kvietys *et al.*, 2012), we next aimed to assess whether these enzymeswere involved in Ang-II–induced responses. Preincubation of endothelial cells for 1 h with an unspecific NADPH inhibitor (apocynin) decreased Ang-II–induced CXCL16 protein expression by 45.8% (Figure 48A). In contrast, pretreatment of endothelial cells with the XO inhibitor allopurinol did not exert any activity on this parameter (Figure 48A).

Nox2, Nox4, and Nox5 are the most abundant Nox isoforms in endothelial cells (Lassegue et al., 2010). Therefore, to determine which Nox isoforms are involved in Ang-II–induced responses, we used a siRNA approach. Interestingly, while Nox4 silencing had no impact on Ang-II induced CXCL16 expression in HUAEC (Figure 48C), a tendency for reduced CXCL16 expression was observed in Nox2-silenced cells (Figure 48B), and silencing of Nox5 resulted in an 90.36% reduction of CXCL16 expression in HUAEC (Figure 48D)

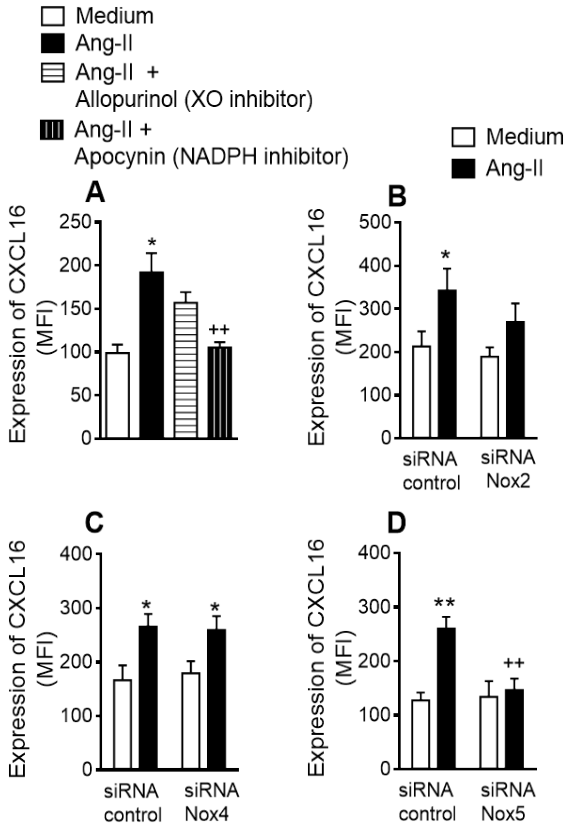

Figure 48: Ang-II–induced CXCL16 expression (A) are inhibited by apocynin but not by allopurinol. Nox5 but not Nox2 or Nox4 small interfering RNA (siRNA) inhibits Ang-II–induced CXCL16 expression in HUAEC (B–D). HUAEC were stimulated with 1 μM Ang-II for 24 h. Some cells were pretreated with apocynine (30 μM) or allopurinol (100 μM) 1 h before Ang-II stimulation. Results are the mean±SEM of n=7 independent experiments. *p<0.05 relative to values in the medium group; $^{++}$p<0.01 relative to values in the Ang-II–stimulated group. In endothelial cells transfected with Nox2, Nox4 or Nox5 siRNA or control siRNA, results are the mean±SEM of n=6 independent experiments. *p<0.05 or **p<0.01 relative to values in the medium group; $^{++}$p<0.01 relative to values in Ang-II group in control siRNA–transfected cells. XO indicates xantine oxidase. MFI indicates mean fluorescence intensity.

4.3.5 RhoA, p38 MAPK and NF-κB are involved in Ang-II–Induced CXCL16 expression.

Signalling through AT_1 receptor interaction results in the induction of a variety of redox-sensitive pathways, including RhoA, extracellular signal-regulated kinases (ERK)1/2 and p38 mitogen-activated protein kinase (MAPK) (Das *et al.*, 2004; Mehta *et al.*, 2007; Montezano *et al.*, 2010; Rius *et al.*, 2013b). The activation of these different components of the MAPK family is associated with that of nuclear factor (NF)-κB (Guo *et al.*, 2006; Rius *et al.*, 2010). In addition, NF-κB pathways

have been implicated in CXCL16 expression (Xia *et al.*, 2013). Thus, we examined the potential involvement of these signaling pathways in Ang- II–induced CXCL16 expression. The increased expression of CXCL16 protein triggered by Ang-II was blunted in cells pretreated with a RhoA inhibitor (cell permeable C3 transferase) or in RhoA-silenced HUAECs (Figure 49A and B).

Additionally, preincubation of arterial endothelial cells with a p38MAPK inhibitor but not with an ERK1/2 inhibitor undermined the CXCL16 expression induced by Ang-II stimulation by 47% (Figure 49C). Consequently, pretreatment of HUAEC with an NF-κB inhibitor resulted in a significant reduction in the chemokine expression induced by Ang-II (Figure 49C).

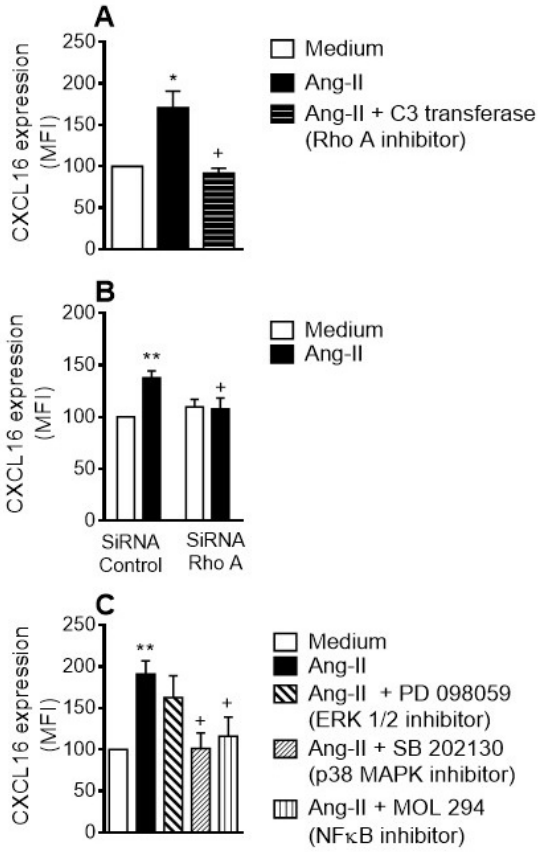

Figure 49: Ang-II-induced CXCL16 overexpression is decreased by Rho A, p38 mitogen-activated protein kinase (MAPK) and nuclear factor (NF)-κB inhibition in HUAEC. (A) CXCL16 expression was determined by flow cytometey in endothelial cells preincubated or not with a RhoA inhibitor (C3 transferase, 2 µg/ml) for 4 h and then stimulated with 1 µM Ang-II for 24h. Results are expressed as mean fluorescence intensity (MFI) (n=5 independent experiments). Values are expressed as mean ± SEM. *$p < 0.05$ relative to values in the medium group; $^{+}p< 0.05$ relative to Ang-II group. (B) HUAEC were transfected with RhoA siRNA or control siRNA. At 48 h post-transfection, cells were stimulated with 1 µM Ang-II for 24h. CXCL16 expression was determined by flow cytometry. Results are expressed as mean fluorescence intensity (MFI) (n=7 independent

experiments). Values are expressed as mean ± SEM. **p < 0.01 relative to values in the medium group; $^{+}$p < 0.05 relative to their respective group in control siRNA transfected cells. (C) HUAEC were stimulated with 1 μM Ang-II for 24 hours. Some cells were pretreated with PD098059 (20 μM), SB202130 (20 μM), or MOL 294 (2.5 μM) for 1 h before Ang-II stimulation. CXCL16 expression was determined by flow cytometry. Results are expressed as mean fluorescence intensity (MFI) (n=4-7 independent experiments). Values are expressed as mean ± SEM. **p < 0.01 relative to values in the medium group; $^{+}$p < 0.05 relative to values in the Ang-II group.

4.4 RESULTS OF THE STUDY: CXCR6/CXCL16 AXIS MEDIATES PLATELET-LEUKOCYTE ARREST IN COPD DYSFUNCTIONAL ARTERIAL ENDOTHELIUM

4.4.1 Platelet activation and expression of CXCL16 and CXCR6 is increased in patients with COPD

Platelet activation was evaluated in COPD patients by flow cytometry. A significant increase in the percentage of platelets expressing PAC-1 was detected in COPD patients compared with control subjects (Figure 50A). Furthermore, P-selectin labeling intensity of platelets, evaluated as mean fluorescence intensity (MFI), was greater in patients with COPD than in control subjects (Figure 50B). Notably, a significant increase in the percentage of circulating platelets expressing CXCL16 and CXCR6 together with a greater mean expression was also detected in COPD patients compared with control subjects (Figures 50C-F).

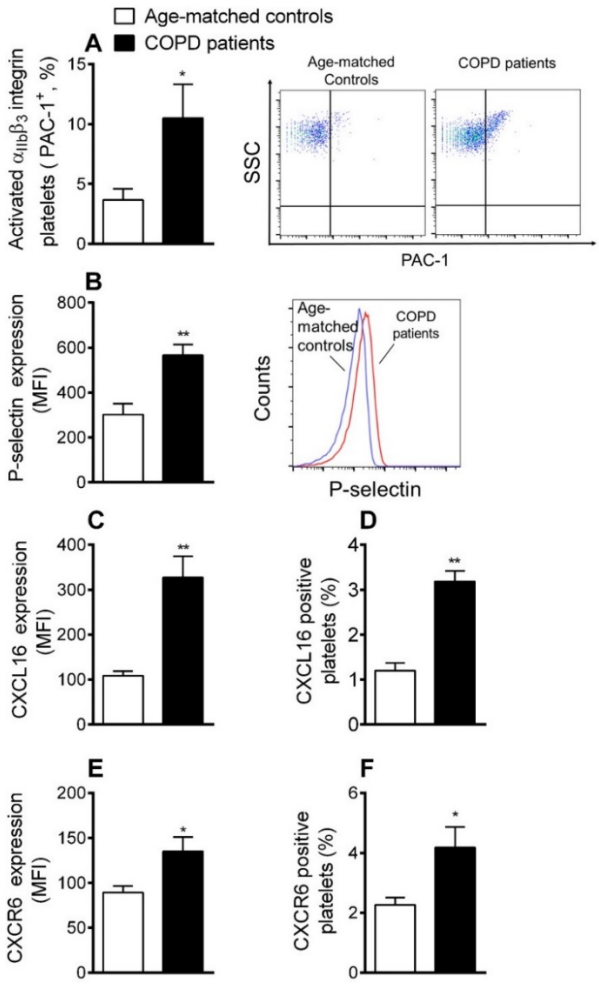

Figure 50. Expression of PAC-1, P-selectin, CXCL16 and CXCR6 in circulating platelets from COPD patients and aged-matched controls by flow cytometry. Platelets were stained with conjugated antibodies against (A) CD41 and PAC-1, (B) CD41 and P-selectin, (C, D) CD41 and CXCL16, and (E, F) CD41 and CXCR6. Results are expressed as (A, D, F) percentage of positive cells and (B, C, E) mean fluorescence intensity (MFI) (n=15 control subjects and n=21 COPD patients). Values are expressed as mean ± SEM. *p<0.05 or **p<0.01 relative to values in the control group.

4.4.2 CXCR6 expression on neutrophils, monocytes and lymphocytes is increased in patients with COPD

Expression of CXCR6 was significantly increased on neutrophils from heparinized whole blood of COPD patients relative to control subjects. In contrast, this increase was eliminated when platelets were dissociated from leukocytes (Figure 51A and B). CXCR6 expression was also greater in monocytes and lymphocytes from COPD patients relative to age-matched control subjects (Figures 51C-F), and this expression was greater when platelets were aggregated to both leukocyte subpopulations.

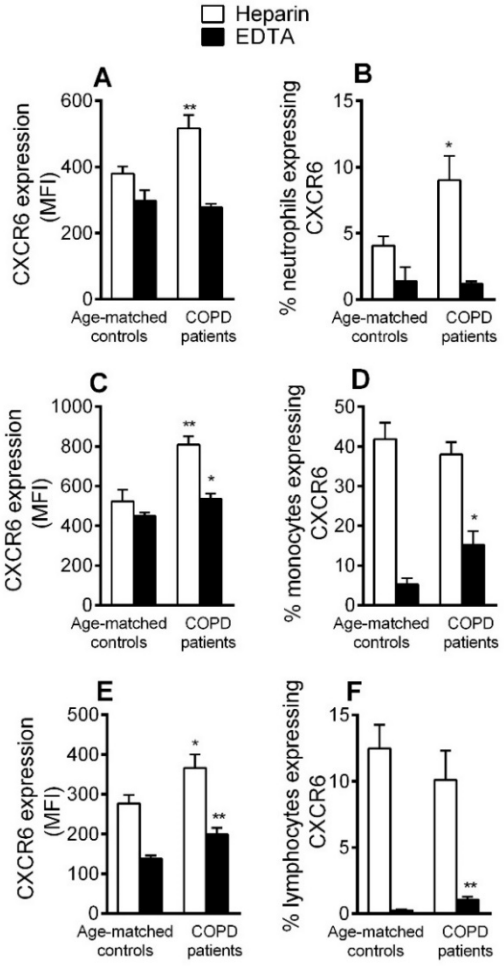

Figure 51: Expression of CXCR6 in different leukocyte subsets from COPD patients and aged-matched controls by flow cytometry. Heparinized whole blood was co-stained with specific markers for (A, B) neutrophils, (C, D) monocytes, and (E, F) lymphocytes and CXCR6. Blood samples were incubated or not with EDTA. Results are expressed as (A, C, E) mean fluorescence intensity (MFI) and (B, D, F) percentage of positive cells (n=15 control subjects and n=21 COPD patients). Values are expressed as mean ± SEM. *p<0.05 or **p<0.01 relative to values in the control group.

Of note, flow cytometry analysis additionally revealed that COPD patients presented augmented numbers of platelet-neutrophil ($CD41^+$, $CD16^+$, $CD14^-$), platelet-monocyte ($CD41^+$, $CD14^+$) and platelet-lymphocyte ($CD41^+$, $CD3^+$) aggregates than age-matched control subjects (Figure 52).

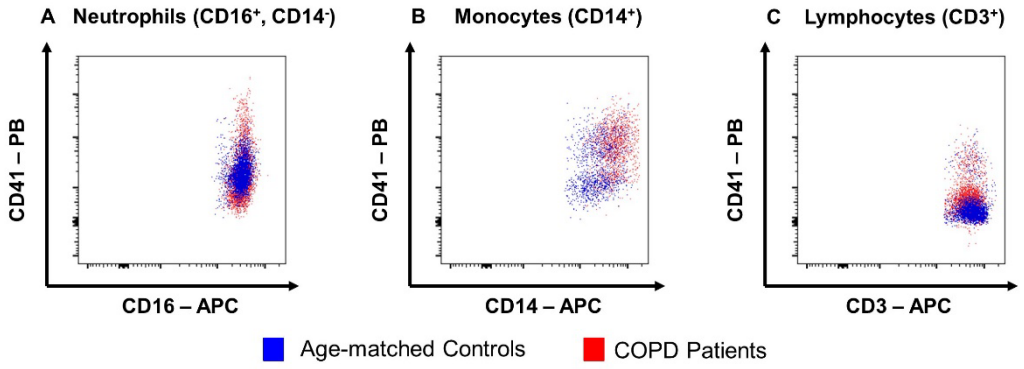

Figure 52: Platelet-neutrophil, monocyte and lymphocyte aggregates are higher in COPD patients than in aged-matched controls. Blood samples from COPD patients (red) and age-matched controls (blue) were double stained with an anti-CD41-PB and anti-CD16-APC (A), anti-CD114-APC (B) or anti-CD3-APC (C) mAbs. Graphs are representative from n=15 control subjects and n=21 COPD patients.

4.4.3 Circulating mononuclear cells from COPD patients show increased adhesiveness to CSE-stimulated HUAEC

To explore the functional consequences of these observations, we examined the involvement of platelet CXCR6 on CXCL16-dependent leukocyte-endothelial cell interactions under dynamic flow conditions. When we perfused heparinized whole blood from COPD patients and their respective aged-matched controls across unstimulated HUAEC, leukocyte adhesiveness was enhanced in the COPD group (Figure 53A). Moreover, these responses were significantly greater after exposure of HUAEC to 1% CSE (Figure 53A). Interestingly, neutralization of CXCL16 activity

on endothelial cells resulted in a significant reduction of CSE-induced platelet-leukocyte endothelial adhesion in both groups (Figure 53A).

Importantly, when platelets were disaggregated from leukocytes, cells from control subjects did not adhere significantly better to CSE-stimulated endothelium than to unstimulated (medium only) HUAEC (Figure 53B). In contrast, a significant increase in leukocyte adhesion was observed in the COPD group (Figure 53B), and neutralization of CXCL16 activity again markedly decreased CSE–induced leukocyte adhesion (Figure 53B). Despite these findings, no significant differences in the circulating levels of soluble CXCL16 were found between the groups (Figure 53C).

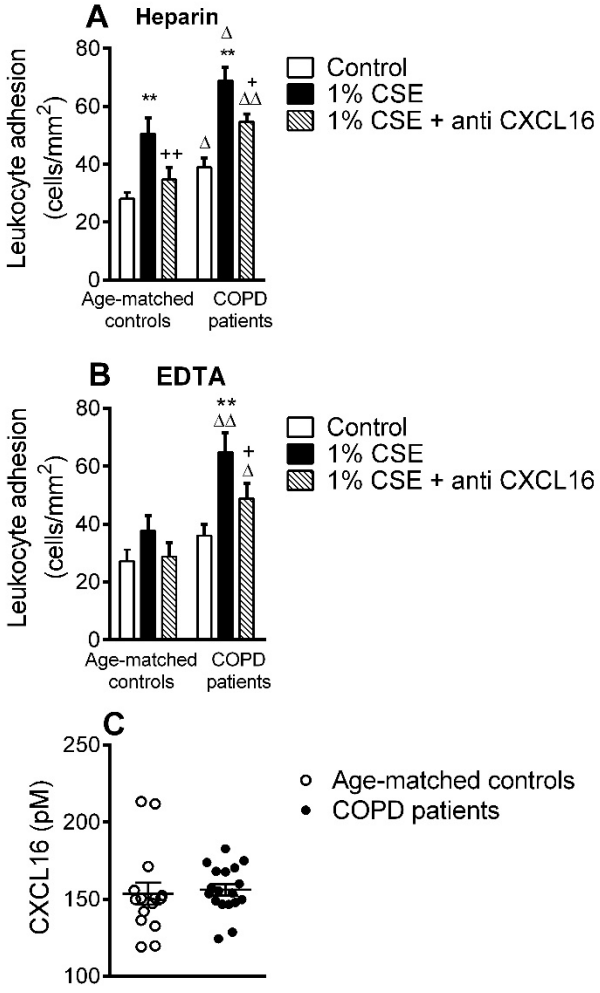

Figure 53: Leukocyte recruitment by CSE-stimulated HUAEC and CXCL16 plasma levels from whole blood of patients with COPD and aged-matched controls. HUAEC were stimulated with 1% CSE for 24 h. Some cells were incubated with a CXCL16 neutralizing antibody (2 µg/ml) or an irrelevant isotype-matched monoclonal antibody

(MOPC21, 2 μg/ml). Subsequently, whole blood from patients with COPD and healthy aged-matched controls incubated (A) without, or (B) with EDTA, was perfused over endothelial monolayers for 5 min at 0.5 dyn/cm2 and leukocyte adhesion quantified (n=15 control subjects and n=21 COPD patients). Values are expressed as the mean ± SEM. **$p<0.01$ relative to values in the medium group; $^{+}p<0.05$ or $^{+\,+}p<0.01$ relative to 1% CSE group; $^{\Delta}p<0.05$ or $^{\Delta\Delta}p<0.01$ relative to the values in the aged-matched control group. (C) CXCL16 plasmatic levels were measured by ELISA (n=15–21 experiments) Values are expressed as the mean ± SEM.

4.4.4 CSE induces functional CXCL16 expression in HUAEC

We examined CXCL16 mRNA expression in HUAEC after stimulation with CSE or INF-γ (20 ng/ml). No changes were observed after 1 h exposure (Figure 54A); however, a significant increase in CXCL16 mRNA was detected after exposure to CSE or INF-γ for 4 h (Figure 54B). Flow cytometry analysis of HUAEC after 24 h exposure to CSE or INF-γ revealed a significant increase in protein levels of CXCL16 (Figure 54C), which was confirmed by immunocytochemistry (Figure 54D).

To investigate the functional role of CSE-induced endothelial CXCL16 expression, freshly isolated human mononuclear cells were perfused across HUAEC monolayers. Compared with unstimulated cells, a significant increase in mononuclear cell arrest was observed in CSE-stimulated HUAEC (Figure 54E). As expected, neutralization of CXCL16 activity on the endothelial cell surface resulted in a significant reduction of CSE-induced mononuclear cell adhesion to HUAEC (62% inhibition, figure 54E).

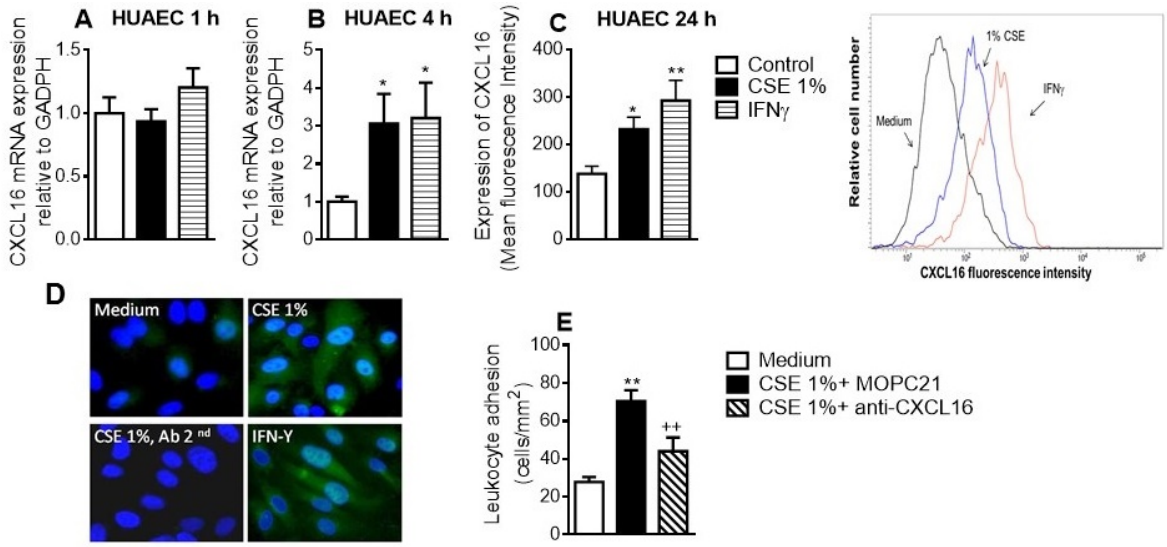

Figure 54: Expression and function of CXCL16 in CSE-stimulated HUAEC and effect of CXCL16 neutralizing antibody on mononuclear leukocyte adhesion. HUAEC were stimulated with CSE 1% or IFNγ (20 ng/ ml) for 1, 4 or 24 h. Relative quantification of mRNA levels for CXCL16 and GAPDH after (A) 1 h and (B) 4 h (n=5–7 independent experiments). Columns show fold increase in CXCL16 mRNA expression relative to control GAPDH. Values are expressed as mean ± SEM of the $2^{-\Delta\Delta Ct}$ values. (C) Protein expression was determined by flow cytometry. Results are expressed as mean fluorescence intensity (MFI) (n=7 independent experiments). Values are expressed as mean ± SEM. *p<0.05 or **p<0.01 relative to values in the medium group. Representative histograms are also shown. (D) Following a similar protocol, CXCL16 was visualized in non-permeabilized HUAEC by immunofluorescence (green). Nuclei were counterstained with 4'6-diamidino-2-phenylindole (DAPI) (n=5 independent experiments). (E) Endothelial cells were stimulated with 1% CSE for 24 h. Some cells were incubated with a CXCL16 neutralizing antibody (2 μg/ml) or an irrelevant isotype-matched monoclonal antibody (MOPC21, 2 μg/ml). Subsequently, human mononuclear cells (1×10^6 cells/ml) were perfused over the monolayers for 5 min at 0.5 dyn/cm^2 and leukocyte accumulation quantified (n=7 independent experiments). Values are expressed as the mean ± SEM. *p<0.05 or **p<0.01 relative to values in the medium group; $^{+}$p<0.05 relative to 1% CSE group.

4.4.5 Gene silencing of Nox5, but not Nox2 or Nox4, inhibits CSE-induced endothelial CXCL16 expression

It is well known that water-soluble components of CS promote reactive oxygen species (ROS) generation, which are involved in mononuclear cell recruitment (Orosz *et al.*, 2007; Rius *et al.*, 2013a). Because NADPH oxidases (Nox) and xanthine oxidase (XO) are important sources of ROS in the vasculature (Rius *et al.*, 2013a), we next evaluated the impact of enzyme inhibition on CXCL16 expression. As anticipated, non-specific inhibition of NADPH oxidases but not XO inhibition diminished CSE-induced CXCL16 expression measured by flow cytometry (Figure 55A).

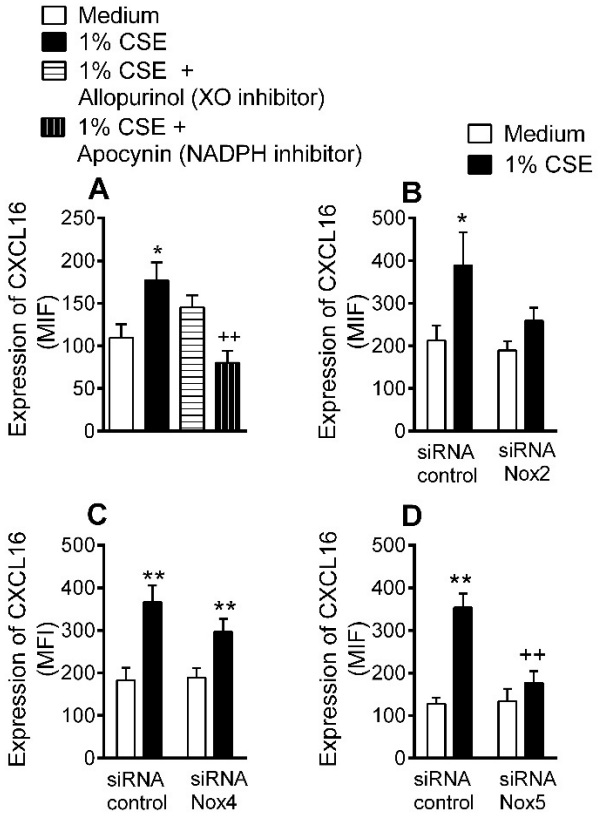

Figure 55: CSE–induced CXCL16 expression are inhibited by apocynin but not by allopurinol. Nox5 but not Nox2 or Nox4 small interfering RNA (siRNA) inhibits CSE–induced CXCL16 expression in HUAEC. (A) CXCL16 expression was determined by flow cytometry in HUAEC preincubated or not with apocynin (30 μM) or allopurinol (100 μM) for 1 h and then stimulated with 1% CSE for 24 h (n=7 independent experiments). Results are expressed as mean fluorescence intensity (MFI). Values are expressed as the mean ± SEM. *$p<0.05$ relative to values in the medium group; $^{++}p<0.01$ relative to 1% CSE group. Endothelial cells were transfected with (B) Nox2, (C) Nox4 or (D) Nox5 siRNA or control siRNA. At 48 h post-transfection, cells were stimulated with 1% CSE for 24 h. CXCL16 expression was determined by flow cytometry. Results are expressed as mean fluorescence intensity (MFI) (n=5-8 independent experiments). Values are expressed as mean ± SEM. *$p<0.05$ or ** $p<0.01$ relative to values in the medium group; $^{++}p<0.01$ relative to 1% CSE group in control siRNA transfected cells.

It is also acknowledged that endothelial cells mainly express the NADPH family members Nox2, Nox4 and Nox5 (BelAiba *et al.*, 2007; Pendyala *et al.*, 2009). To determine the Nox isoform involved in CSE-induced responses, we employed an RNA interference approach to specifically silence individual Nox genes in HUAEC. Significant reduction of Nox2, Nox4 and Nox5 protein expression was evident after 48 h incubation with their respective siRNA (Figure 56).

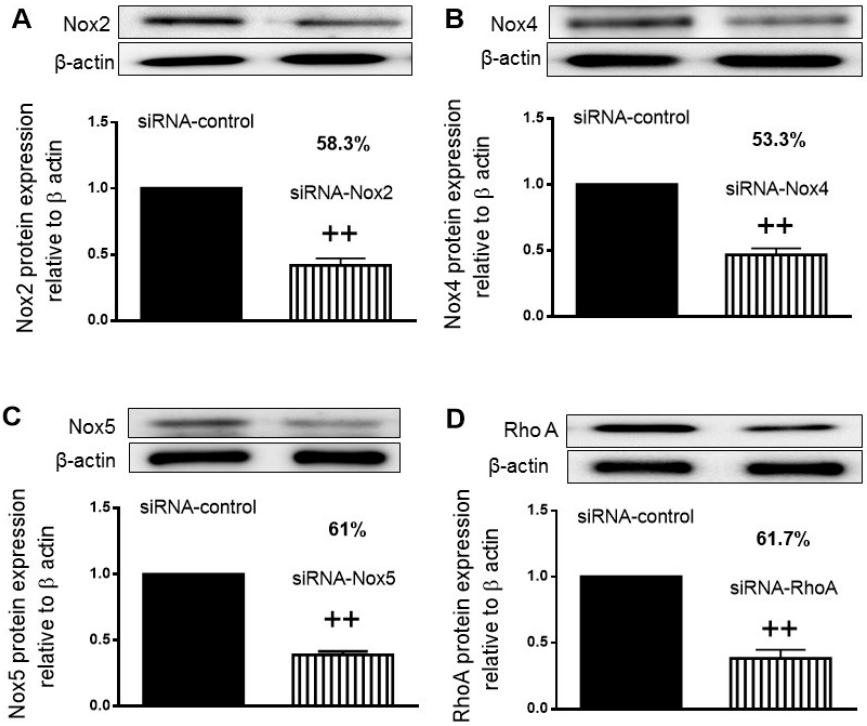

Figure 56: Transfection of HUAEC with Nox 2, Nox 4, Nox 5 or RhoA specific siRNAs. Gene silencing was performed in HUAEC using either control siRNA or specific siRNA to Nox2, Nox4, Nox5 or RhoA. After 48 h, protein expression of Nox2 (A), Nox4 (B), Nox5 (C) or RhoA (D) was determined by western blot to assess silencing efficiency. Results (mean ± SEM of n= 4-5 independent experiments) are expressed relative to β-actin. Representative blots are shown. $^{++}p<0.01$ relative to values in the respective control siRNA group.

Notably, whereas Nox4 silencing had no impact on CSE-induced CXCL16 expression in HUAEC (Figure 55C), a tendency for reduced CXCL16 expression was observed in Nox2-silenced cells (Figure 55B), and silencing of Nox5 resulted in an 81% reduction of CXCL16 in HUAEC (Figure 55D).

4.4.6 RhoA, p38 MAPK, and NF-κB activation are involved in CSE–induced CXCL16 expression in HUAEC

Small GTP-binding proteins (G-proteins), such as RhoA, are activated by CS and are involved in the associated systemic endothelial dysfunction (Duong-Quy *et al.*, 2011). To determine whether RhoA was implicated in CSE-induced CXCL16 expression, we inhibited RhoA activity using C3 transferase and depleted RhoA expression by RNA interference. Both approaches led to a significant reduction of

CXCL16 expression in CSE-treated HUAEC (Figure 57A and Figure 57B, respectively).

RhoA is an upstream regulator of mitogen-activated protein kinase (MAPK) family members including p38 MAPK (Marinissen *et al.*, 2004) and CS can activate endothelial MAPK signaling cascades (Rius *et al.*, 2013a). Because MAPK activation can act on downstream targets, such as NF-κB (Guo *et al.*, 2006; Rius *et al.*, 2010), leading to mononuclear cell recruitment, we next examined the involvement of these redox-signaling pathways on CSE-induced CXCL16 expression. Flow cytometry analysis revealed that pretreatment of arterial endothelial cells with a p38 MAPK inhibitor (SB202130) or with an NF-κB inhibitor (MOL 294), but not with an ERK1/2 inhibitor (PD 098059), significantly decreased surface expression of CXCL6 on CSE-stimulated cells (Figure 57C).

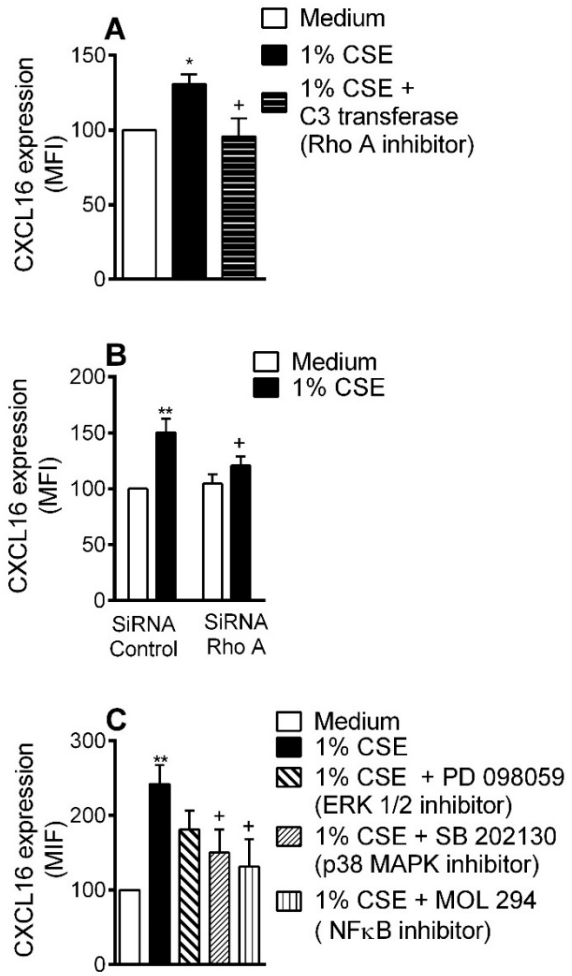

Figure 57: CSE-induced CXCL16 overexpression is decreased by RhoA, p38 mitogen-activated protein kinase (MAPK) and nuclear factor (NF)-κB inhibition in HUAEC.

(A) CXCL16 expression was determined by flow cytometey in endothelial cells preincubated or not with a RhoA inhibitor (C3 transferase, 2 μg/ml) for 4 h and then stimulated with 1% CSE for 24 h. Results are expressed as mean fluorescence intensity (MFI) (n=5 independent experiments). Values are expressed as mean ± SEM. *$p<0.05$ relative to values in the medium group; +$p<0.05$ relative to 1% CSE group. (B) HUAEC were transfected with RhoA siRNA or control siRNA. At 48 h post-transfection, cells were stimulated with 1 % CSE for 24 h. CXCL16 expression was determined by flow cytometry. Results are expressed as mean fluorescence intensity (MFI, n=7 independent experiments). Values are expressed as mean ± SEM.**$p<0.01$ relative to values in the medium group; $^{+}p<0.05$ relative to their respective group in control siRNA transfected cells. (C) HUAEC were stimulated with 1% CSE for 24 h. Some cells were pretreated with PD098059 (20 μM), SB202130 (20 μM), or MOL 294 (2.5 μM) for 1 h before CSE stimulation. CXCL16 expression was determined by flow cytometry. Results are expressed as mean fluorescence intensity (MFI) (n=4-7 independent experiments). Values are expressed as mean ± SEM. **$p<0.01$ relative to values in the medium group; +$p<0.05$ relative to values in the 1% CSE group.

4.4.7 CS-induced leukocyte adhesion to mouse cremasteric arterioles is reduced in CXCR6$^{-/-}$ mice

To explore the potential *in vivo* relevance of these findings, we used a murine model of acute CS exposure in a background of CXCR6 deficiency. Histological analysis of the lungs of animals exposed to CS for 3 days demonstrated a clear inflammatory response in both CXCR6 expressing (CXCR6$^{-/+}$) and CXCR6 deficient (CXCR6$^{-/-}$) mice (Figure 58A), together with a comparable and significant increase in the number of lung leukocytes (Figure 58B).

Systemically, CS exposure induced a significant increase in CD11b-expressing monocytes in both strains compared with unexposed mice; however, the number of CD11b^{+} cells was markedly reduced in CXCR6$^{-/-}$ mice compared with heterozygous animals (Figure 58C). Furthermore, while CS exposure induced a significant increase in arteriolar leukocyte adhesion in the cremaster muscle in both strains as assessed by intravital microscopy, leukocyte adhesion was significantly attenuated in CXCR6$^{-/-}$ mice (39% inhibition, figure 58D). Finally, mRNA and immunohistochemistry analysis of the cremasteric microcirculation demonstrated increased cremasteric expression of CXCL16 in animals exposed to CS (Figure 58E and F).

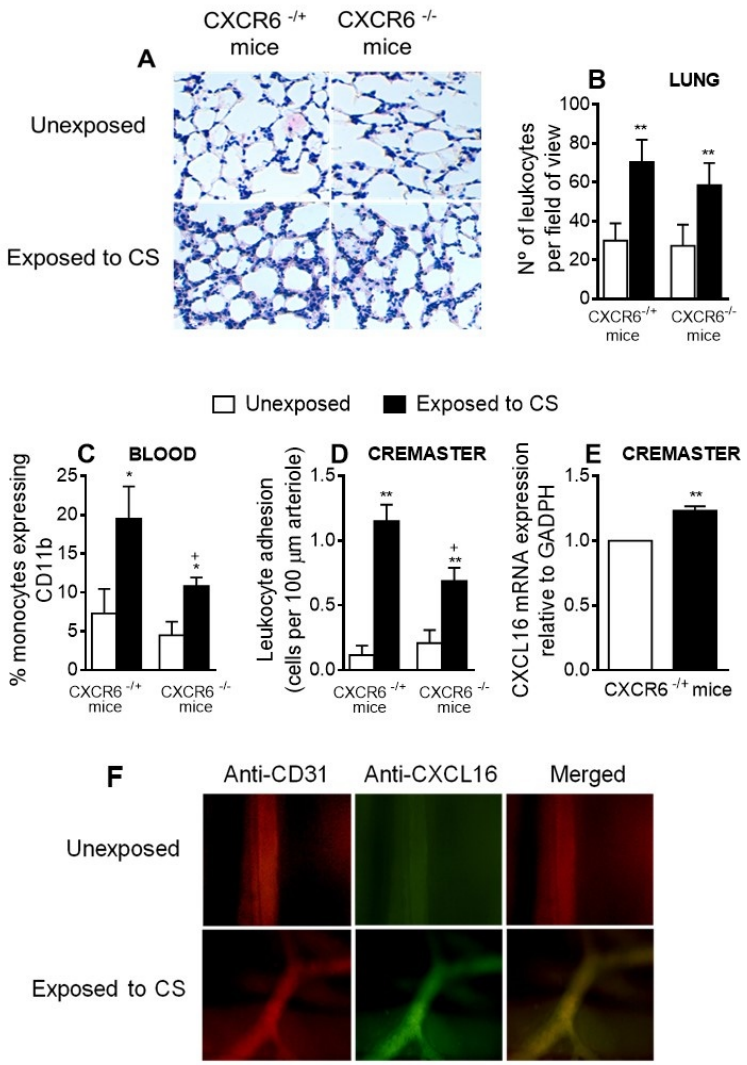

Figure58: Effect of CS exposure in CXCR6 expressing and CXCRC6 knockout mice. Heterozygous ($CXCR6^{-/+}$) and homozygous ($CXCR6^{-/-}$) mice were exposed or not to CS for 3 days and responses were examined 16 h later. Lungs were collected and fixed for staining with (A) hematoxylin/eosin. (B) Number of leukocytes. (C) CD11b expression was determined by flow cytometry of circulating monocytes in heparinized whole blood (D) Leukocyte–arteriolar endothelium interactions was measured by intravital microscopy. In all cases, results are expressed as mean ± SEM (n=5–8 animals per group). $p<0.05$ or $**p<0.01$ relative to non-exposed animals; $^{+}p<0.05$ relative to $CXCR6^{-/+}$ mice. (E) Relative quantification of CXCL16 and β-actin mRNA was determined by RT-PCR. Columns show fold increase in expression of CXCL16 mRNA relative to control GAPDH values (n=5 independent experiments). Values are represented as mean ± SEM of the $2^{-\Delta\Delta Ct}$ values. $**p<0.01$ relative to non-exposed animals. (F) Cremaster muscle was fixed for CXCL16 and endothelium (CD31) staining. CXCL16 expression is shown in green (stained with an Alexa Fluor 488-conjugated donkey anti-rabbit secondary antibody) and vessel endothelium (red) was stained with a PE-conjugated anti-mouse CD31 monoclonal antibody. Overlapping expression of CXCL16 and CD31 is shown in yellow. Results are representative of 5–6 animals per group.

DISCUSSION

5 DISCUSSION

5.1 DISCUSSION OF THE STUDY: COMBINED SUB-OPTIMAL DOSES OF ROSUVASTATIN AND BEXAROTENE IMPAIRS ANGIOTENSIN II-INDUCED ARTERIAL MONONUCLEAR CELL ADHESION THROUGH INHIBITION OF Nox5 SIGNALING PATHWAYS AND INCREASED RXRα/PPARα AND RXRα/PPARɣ INTERACTIONS

Combination therapy that simultaneously addresses multiple mechanisms involved in the pathogenesis of atherosclerosis is an attractive emerging concept for preventing and/or slowing the progression of this disease. Using *in vitro* and *in vivo* approaches, we provide the first demonstration of an anti-inflammatory effect of suboptimal concentrations/doses of two commercially-available drugs, Rosu and Bex, in combination.

Mononuclear leukocyte infiltration into the subendothelial space is a key event in the atherogenic process (Libby, 2002) and treatment with Rosu or Bex has been shown to limit mononuclear cell numbers in atherosclerotic plaques, or their interaction with the arterial endothelium (Kleemann *et al.*, 2003; Sanz *et al.*, 2012). In this study, stimulation of arterial endothelial cells with Ang-II, mimicking a dysfunctional endothelium, promoted the adhesion of mononuclear leukocytes, and this event was clearly reduced by different combined treatments of Rosu and Bex. Remarkably, this reduction was achieved with a suboptimal combination of Rosu (10 nM) and Bex (0.3 μM) since at these concentrations, neither the statin nor the RXR ligand displayed any significant efficacy when assessed individually. To further confirm this striking observation *in vivo*, daily Rosu administration at a dose 4-fold-lower than that required to reduce atherosclerotic lesion formation (Kleemann *et al.*, 2003), or Bex at a dose which was previously found not to inhibit acute TNFα-induced arteriolar leukocyte adhesion (Sanz *et al.*, 2012), were tested individually or in combination in mice subjected to chronic Ang-II infusion (Scalia *et al.*, 2011). In this model of systemic inflammation, arteriolar leukocyte adhesion remained unaltered in Rosu or Bex-treated animals, whereas combined administration of both drugs provoked a synergistic inhibitory effect. Furthermore, atheroma formation and

mononuclear cell infiltration in apoE$^{-/-}$ mice subjected to high fat diet was clearly diminished in animals treated with the drug combination, thus validating our *in vitro* observations in a relevant *in vivo* model.

Leukocyte/arterial interactions require both the expression of several types of CAMs in the endothelium and leukocytes as well as the presence of counter receptor molecules in the leukocyte/endothelial cell (Libby, 2002; Galkina *et al.*, 2009). In addition to adhesion molecules, chemokines also have the potential to recruit specific cell types and are involved in the regulation of leukocyte trafficking (Galkina *et al.*, 2009). The ability of Ang-II to increase the endothelial expression of E-selectin, ICAM-1 and VCAM-1 and also the production of a wide array of leukocyte-recruiting chemokines is well known (Pastore *et al.*, 1999; Tummala *et al.*, 1999; Alvarez *et al.*, 2004; Nabah *et al.*, 2004; Mateo *et al.*, 2006; Rius *et al.*, 2013b). Statins are reported to reduce both the inflammation-induced expression of these endothelial CAMs and the synthesis of numerous chemokines (Mira *et al.*, 2009; Hot *et al.*, 2013). More recently, we have demonstrated decreased expression of E-selectin, ICAM-1 and VCAM-1 and a decrease in the synthesis of CXCL1 or CCL2 by the endothelium with RXR agonists in an inflammatory environment (Sanz *et al.*, 2012). Therefore, it was perhaps not surprising that pretreatment of HUAECs with a Rosu+Bex combination reduced both the expression of CAMs and the synthesis of different chemokines involved in the mononuclear cell arrest evoked by Ang-II. Furthermore, in the *in vivo* setting, the combined administration of suboptimal doses of Rosu+Bex, in addition to attenuating the increased expression of arteriolar E-selectin, ICAM-1, VCAM-1 and fractalkine and the elevated circulating levels of CXCL1, CCL2 and CCL5 induced by chronic Ang-II exposure, also decreased Ang-II-induced CD11b up-regulation on circulating monocytes but not neutrophils. This exciting observation may also suggest that this treatment may result in improved vascular function without compromising other neutrophilic responses required in host defense.

Having established the action of Rosu+Bex on the aforementioned components of the canonical leukocyte recruitment cascade, we sought to determine their effect on some intracellular signaling cascades triggered by activation of the AT_1 Ang-II receptor. The RhoA-Rho kinase pathway has been implicated in leukocyte recruitment (Cernuda-Morollon *et al.*, 2006) and RhoA can be activated by Ang-II,

as shown here and in a previous report (Higuchi *et al.*, 2007). We show that targeted knockdown of RhoA in HUAECs diminished the adhesion of mononuclear cells triggered by Ang-II. Notably, Rosu+Bex abolished Ang-II-induced RhoA activation. Although blockade of the mevalonate pathway by statins can prevent the synthesis of isoprenoid intermediates, such as farnesyl pyrophosphate (FPP) or geranylgeranyl pyrophosphate that are involved in the posttranslational modification of numerous proteins including the γ subunit of heterotrimeric G proteins such as Rho (Cordle *et al.*, 2005; Greenwood *et al.*, 2006), the concentrations of statins required to inhibit Rho-kinase are much greater than those applied here (μM range vs. nM) (Mira *et al.*, 2009; Rashid *et al.*, 2009). Furthermore, to the best of our knowledge, the effect of Bex on RhoA activation has never been addressed. Therefore, additional studies were undertaken to address the inhibitory effect of Rosu+Bex on RhoA activation by Ang-II.

Guided by our initial observations, and given that RhoA is acknowledged as a primary target of oxidative stress upon Ang-II endothelial stimulation (Nguyen Dinh Cat *et al.*, 2013), we explored the effect of the RXR agonist and statin combination on NADPH-oxidase-derived ROS production. Although Nox2, Nox4 and Nox5 are the most abundant NADPH oxidase isoforms in endothelial cells (Lassegue *et al.*, 2010) and are induced by Ang-II (Rius *et al.*, 2013c), only Nox5 appears to play a major role in Ang-II-induced endothelial adhesiveness since both VCAM-1 and fractalkine up-regulation and the subsequent mononuclear cell arrest were found to be Nox5-mediated (Montezano *et al.*, 2010; Rius *et al.*, 2013b). We found that Ang-II-induced production of ROS was attenuated by preincubation of HUAECs with Rosu+Bex. Moreover, Ang-II-dependent Nox2 and Nox5 expression was significantly reduced by the combined treatment and the former in murine aortic endothelial cells, which may account for the reduced arteriolar leukocyte adhesion encountered in animals subjected to chronic Ang-II infusion, as found in other animal models (Fan *et al.*, 2014; Murdoch *et al.*, 2014). Furthermore, since mechanisms through which Ang-II-induced ROS production activate downstream signaling are elusive, we show here that RhoA activation is dependent on Nox5/NADPH oxidase activity. Conversely, knockdown of RhoA in HUAEC or its pharmacological inhibition neither affected Ang-II-induced ROS production nor the

increase in Nox5 expression, indicating that ROS generation by Nox5 is an upstream regulator of RhoA activation in this experimental setting.

PPARs are ligand-activated nuclear hormone receptors that function as transcription factors. The three isoforms of PPAR (PPARα, PPARγ, and PPARβ/δ) are expressed in the endothelium and have been described to curb inflammation in atherosclerosis (Moraes *et al.*, 2006; Balakumar *et al.*, 2012). Ligand binding of PPAR promotes heterodimerization with the RXR receptor, inducing PPAR transactivation of target genes (Moraes *et al.*, 2006; Sanz *et al.*, 2012). In the current study, Rosu+Bex were found to enhance RXR, PPARα and PPARγ protein expression in Ang-II stimulated HUAECs. Importantly, specific knockdown of endothelial RXR, PPARα or PPARγ reversed the inhibitory effects exerted by Rosu+Bex on Ang-II-induced mononuclear leukocyte adhesion. Finally, a clear interaction between RXR/PPARα and RXR/PPARγ was revealed upon co-incubation with Rosu and Bex at suboptimal concentrations. Considering that PPARα or PPARγ agonists can inhibit RhoA activation (Ramirez *et al.*, 2008; Paintlia *et al.*, 2013) and exert antioxidant properties (Moraes *et al.*, 2006), it seems likely that inhibition of Nox5 expression and prevention of ROS generation inhibits RhoA activation via RXR/PPARα and RXR/PPARγ. Indeed, knockdown of RXRα, PPARα or PPARγ abolished the inhibitory action of the drug combination on Ang-II-induced RhoA activation and Nox5 expression. Additionally, RhoA has also been reported to be an upstream regulator of mitogen-activated protein kinase (MAPK) family members, such as p38 MAPK (Marinissen *et al.*, 2004), and the latter can regulate the transcription of many genes through its action on downstream targets such as NF-κB (Guo *et al.*, 2006; Rius *et al.*, 2010); both are involved in inflammatory responses such as the mononuclear cell recruitment induced by Ang-II . Therefore, the inhibition of Ang-II-induced Nox5 activation and expression by Rosu+Bex combination may inhibit the activation of RhoA and different MAPKs that lead to activation of several transcription factors including NFκB and the further regulation of genes encoding different CAMs and chemokines, which actively participate in the mononuclear leukocyte recruitment induced by Ang-II (Figure 59).

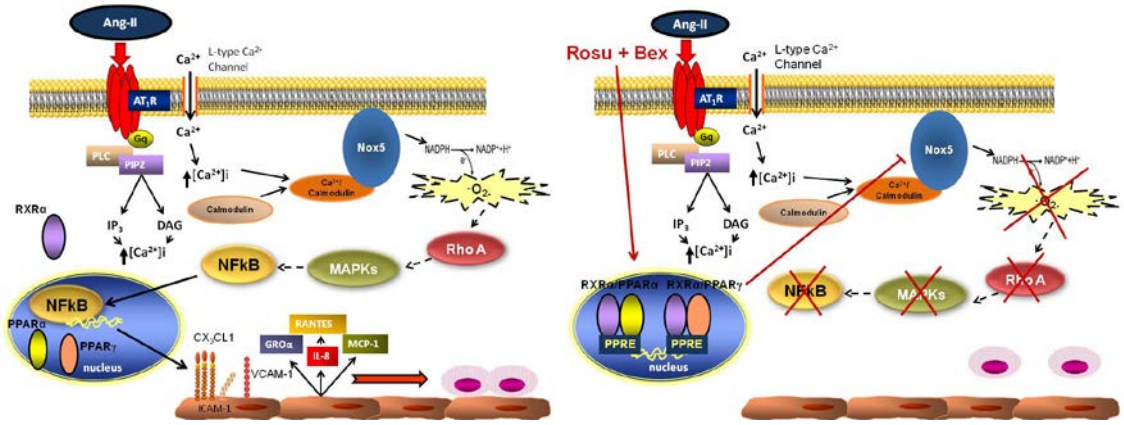

Figure 59: Scheme illustrating the mechanisms of action of the combination of Rosu and Bex at suboptimal concentrations on the signaling pathways involved in Ang-II-induced mononuclear cell recruitment. Binding of Ang-II to its AT_1 receptor (AT_1R) stimulates Ca^{2+} influx through L-type Ca^{2+} channels and activation of calmodulin, which interact with Ca^{2+}/calmodulin binding domains to activate Nox5 as previously described (Montezano *et al.*, 2010). Activated Nox5 results in the generation of superoxide ($O2^{-)}$, activation of RhoA and different MAPKs, which leads to activation of several transcription factors including NFκB, and the further regulation of genes encoding different CAMs (ICAM-1 and VCAM-1) and chemokines (GROα, IL,8, MCP-1, RANTES and CX_3CL1), which actively participate in the mononuclear leukocyte recruitment induced by Ang-II. Preincubation of HUAECs with Rosu+Bex inhibited Nox5 expression and Nox5-induced redox-sensitive pathway activation induced by Ang-II through increased RXRα, PPARα and PPARγ expression as well as RXRα/PPARα and RXRα/PPARγ interactions.

Finally, Ang-II impairs endothelial function through superoxide anion generation and peroxynitrite formation, and eNOS inhibition and uncoupling, reducing NO bioavailability (Loot *et al.*, 2009; Nguyen Dinh Cat *et al.*, 2013), and the anti-adhesive properties of NO are widely recognized (Granger *et al.*, 1996; Hickey *et al.*, 1997). Here we report that Ang-II stimulation reduced NO availability in HUAEC and this reduction was reversed by pretreatment with Rosu+Bex. Additionally, silencing of Nox5 prevented the effects caused by Ang-II and, in the absence of RXRα, PPARα or PPARγ, the combination of Rosu+Bex was unable to fully restore endothelial NO bioavailability. These results suggest that the effects achieved by the drug combination are mainly due to their antioxidant properties.

In conclusion, the present study provides the first evidence that combined therapy with Rosu and Bex at suboptimal concentrations/doses exerts synergistic beneficial effects on endothelial dysfunction produced by Ang-II. This anti-inflammatory activity was found to be mediated through a Nox5-RhoA-RXR/PPAR-

associated mechanism, linking redox-signaling pathways to mononuclear cell recruitment.

5.2 DISCUSSION OF THE STUDY: COMBINED TREATMENT WITH BEXAROTENE AND ROSUVASTATIN REDUCES ANGIOTENSIN-II-INDUCED ABDOMINAL AORTIC ANEURYSM IN apoE$^{-/-}$ MICE AND ANGIOGENESIS.

The search for new strategies to prevent and/or slow down the progression of angiogenesis associated with cardiovascular diseases such as AAA is critical in order to reduce the occurrence of severe complications derived from new vessel formation. This is the first study to report a positive effect of Bex in combination with Rosu on the supression of Ang-II-induced AAA formation in apoE$^{-/-}$ mice. This combined therapy inhibed the proliferation, migration and vessel-network formation induced by Ang-II in *in vitro* and *in vivo* models of angiogenesis.

Experimental and clinical evidence endorses the relevance of the renin-angiotensin system in AAA pathogenesis (Daugherty *et al.*, 2006; Zhang *et al.*, 2009) where increased adventitial neocapillary formation is a key feature (Nishibe *et al.*, 2010). In our study, Bex and Rosu were coadministered at doses that did not exert any significant effects on vascular inflammation *in vivo* (Wang *et al.*, 2011; Sanz *et al.*, 2012). However, we observed that chronic co-administration of Bex with Rosu synergistically reduced aneurysm formation. This effect was accompanied by decreased macrofage and vessel numbers within the lesions, events not detected in untreated animals or in those subjected to a single treatment. Additionally, in our study a clear down-regulation of aortic CXCL1, CCL2 and CCL5 and VEGF mRNA expression was detected in those animals simultanously administered with the drug combination. In this regard, the CCL2/CCR2 axis has been shown to be involved in Ang-II-induced AAA formation (Izhak *et al.*, 2012), and dual blockade of RANTES CCR1/CCR5 receptors markedly limited the accumulation of monocytes within the experimental aortic aneurysm lesion, leading to the inhibition of matrix-degrading protease release, angiogenesis and preservation of the aortic structure (Middleton *et al.*, 2007; Suffee *et al.*, 2012b). Whether these events are linked or not to IL-6

production as found in other human an animal studies (Wojcik *et al.*, 2011; Wang *et al.*, 2013) remains to be determined. Moreover, it is also likely that the decreased VEGF generation could be attributed to the reduced monocyte infiltration elicited by the drug combination, since this angiogenic mediator can be produced by inflammatory monocytes/macrophages recruited during aortic aneurysm development (Nishibe *et al.*, 2010) in addition to endothelial cells.

Inasmuch, increased expression of phospho-AKT and phospho-mTOR in the aortic wall of the AAA induced by Ang-II was markedly attenuated by co-treatment of the animals with the RXR ligand and the statin. In this regard, genetic mutations in the upstream negative regulators of mTOR has been associated with aorta aneurysm formation in experimental animal models and in humans (Cao *et al.*, 2010), and the treatment with mTOR inhibitors has also been found to prevent AAA formation (Lawrence *et al.*, 2004). Thus, the angiopreventive effects reported in the current study suggest that, in vivo, the inhibition of AKT/mTOR pathway seems to play a key role in AAA formation probably limiting the release of inflammatory/proangiogenic molecules.

Recent evidence strongly indicates that inflammation and angiogenesis are interconnected (Mantovani *et al.*, 2008). Indeed, newly formed blood vessels enable the continuous recruitment of inflammatory cells which release a variety of proangiogenic chemokines and growth factors such as VEGF, thereby amplifying the angiogenenic process (Mantovani *et al.*, 2008). The pro-angiogenic effects of Ang-II through its interaction with its AT_1 receptor are well established (Tamarat *et al.*, 2002) and it is known that stimulation of vascular endothelial cells with Ang-II results in the production of a wide array of leukocyte-recruiting chemokines and VEGF (Tamarat *et al.*, 2002; Nabah *et al.*, 2004; Mateo *et al.*, 2006; Willis *et al.*, 2011). Indeed, a subset of these chemotactic cytokines has been implicated in angiogenesis. In this context, ELR^+-CXC chemokines such as CXCL1/GROα, which act mainly on the CXCR2 receptor, are primarily neutrophil chemoattractants, but also display angiogenic activity (Bechara *et al.*, 2007). However, the previous mentioned CC chemokines such as CCL2 and CCL5 have recently been reported to be involved in neovascularization (Izhak *et al.*, 2012; Suffee *et al.*, 2012b). In our study, we have demonstrated that, while the selective blocking of the CXCR2 receptor results in a moderate decrease in Ang-II-induced morphogenesis, the

blockade of CCR2 and simultaneous antagonizing of CCR1, CCR3 and CCR5 receptors or VEGF1/2 drastically reduces the angiogenic response elicited by Ang-II. Thus, CCL2, CCL5 and VEGF seem to be key molecules in the angiogenic activity elicited by this peptide hormone.

On the other hand, RXR agonists (Yen *et al.*, 2006) and statins (Park *et al.*, 2002; Wang *et al.*, 2010) have each been shown to suppress angiogenesis in *in vivo* and *in vitro* models, mainly through VEGF inhibition. In this context, previous data generated by our group have revealed that RXR agonists such as Bex or 9-cis Retinoid Acid reduce the endothelial release of CXCL1 and CCL2 in TNFα-stimulated cells, an effect that is not produced in cells lacking RXRα (Sanz *et al.*, 2012). Furthemore, the production of MCP-1/CCL2, IL-1, IL-6, IL-8/CXCL8 among other cytokines or chemokines by endothelial or different cell types is known to be inhibited by statins (Veillard *et al.*, 2006; Mayer *et al.*, 2007; Jougasaki *et al.*, 2010; Girardi *et al.*, 2011; Patterson *et al.*, 2013; Xiao *et al.*, 2013). Therefore, the anti-angiogenic activity displayed by the Bex/Rosu combination seems to be the consequence of the inhibition of CC angiogenic chemokine (CCL2 and CCL5) generation and release and the inhibition of Ang-II–evoked VEGF production. Since three different RXR isotypes have been described - namely RXRα, RXRβ and RXRγ (Szanto *et al.*, 2004) - we silenced RXRα endothelial expression in an attempt to address whether this isotype was the responsible of the observed effects. Lack of RXRα expression blunted the inhibition of Ang-II-induced neovascularisation exerted by Bex and Rosu co-treatment, indicating that the inhibition of angiogenesis depends on the activation of this nuclear receptor. Moreover, RXRs are common heterodimerization partners of other nuclear receptors, and it is well known that PPARs form permissive RXR heterodimers (Plutzky, 2011). Alternatively, statins activate both PPARα and PPARγ in endothelial cells (Balakumar *et al.*, 2012) and PPARα activation inhibits human dermal endothelial cell proliferation, migration and tube formation *in vitro* through cytoskeleton disruption and inhibition of the critical endothelial cell survival factor AKT (Varet *et al.*, 2003). Similarly, PPARγ agonists also were effective at inhibiting angiogenesis in different experimental models (Xin *et al.*, 1999). In contrast to PPARα and PPARγ, activation of PPARβ resulted in *in vitro* and *in vivo* angiogenesis induction (Piqueras *et al.*, 2007). Given

these evidences, we have additionally demonstrated that knockdown of PPARα or PPARγ, but not of PPARβ, reversed the reduction in Ang-II-induced tube formation produced by the combination of suboptimal concentrations of Bex and Rosu. Furthermore, our results also indicate that RXRα requires both PPARα and PPARγ activation to exert its anti-angiogenic activity. In this regard, while our findings are in accordance with other studies in which Bex did not inhibit tumor invasion and angiogenesis in the absence of PPARγ (Yen *et al.*, 2006), the interaction of RXRα/PPARα as a requirement for combined drug activity has not previously been demonstrated. In light of all this evidence, it is conceivable that the synergism between the RXR ligand and the statin during angiogenesis inhibition was the consequence of RXRα/PPARα and RXRα/PPARγ heterodimerization.

Given that PI3K/AKT/mTOR pathway seems to be involved in Ang-II induced AAA, we next investigated their implication in endothelial cell proliferation induced by Ang-II in human endothelial cells. In fact, phosphorylated mTOR-mediated signalling responses are reported to be relevant in endothelial cell activation, including the induced expression of adhesion molecules or the generation of chemokines and VEGF (Karnoub *et al.*, 2008; Wang *et al.*, 2014). Furthemore, activation of the PI3K/AKT/mTOR pathway is involved in Ang-II-induced cardiac and vascular hypertrophy and remodeling (Hafizi *et al.*, 2004; Stuck *et al.*, 2008) and in the inhibition of nitric oxide release and vasodilatation by insulin stimulation of endothelial cells (Kim *et al.*, 2012). We now show that combined treatment with Bex and Rosu at suboptimal concentrations blocked the phosphorylation of different members of the PI3K/AKT/mTOR/p70S6K signalling pathway in Ang-II-stimulated HUVEC. This effect is probably due to the increased RXRα/PPARα and RXRα/PPARγ interactions elicited by this drug combination. In regard to this, there are several lines of evidence that support this hypothesis. Firstly, previous studies have shown that RXRα/PPARγ activation can lead to mTOR and p70S6K pathway inactivation in hepatocytes (Sharvit *et al.*, 2013). Secondly, combined treatment with RXRα and PPARγ agonists also inhibits this signaling pathway (Lee *et al.*, 2006). Thirdly, this pathway can lead to nuclear factor κB (NFκB) activation (Richmond, 2002), resulting in increased production of angiogenic chemokines (Richmond, 2002) and VEGF (Angelo *et al.*, 2007; Karar *et al.*, 2011), which may account for the

counter interplay between inflammation and angiogenesis. In line with this, we have also provided evidence that PI3K inhibition diminished different angiogenic mediators levels released by the peptide hormone.

In conclusion, this is the first report to demonstrate that a combination of suboptimal doses of Bex and Rosu resulted in a potent inhibition of Ang-II-induced AAA. Additionally, activation of RXRα/PPARα and RXRα/PPARγ interactions seem to be required for the PI3K/AKT/mTOR/P70S6K signaling pathway inhibition that causes the subsequent impairment of endothelial angiogenic chemokines and VEGF release. Therefore, our results suggest that a therapeutic regimen that combines a RXRα ligand with a statin represents a promising pharmaceutical strategy for angiogenesis supression and AAA prevention. Furthermore, the use of low doses of both drugs may reduce the appearance of drug-associated side effects, thus providing a safer therapy.

5.3 DISCUSSION OF THE STUDY: CXCL16/CXCR6 AXIS IS INVOLVED IN ANGIOTENSIN-II-INDUCED ENDOTHELIAL DYSFUNCTION.

In the present study, we report for the first time that CXCL16/CXCR6 axis seemed to play a crucial role in the pro-inflammatory and pro-angiogenic processes induced by Ang-II. In this context, AAA induced by Ang-II was dose-dependently inhibited in those animals treated with an Ang-II AT_1 receptor antagonists, losartan. This effect was accompanied by reduced CXCL16 mARN expression within the lesion and decreased infiltration of cells expressing its cognate receptor, $CXCR6^+$. *In vitro* studies using primary cell cultures of human arterial endothelial cells, revealed that Ang-II was able to promote functional CXCL16 expression. Indeed, mononuclear cell recruitment induced by the peptide hormone was significantly inhibited when chemokine activity was neutralized. Furthermore, increased endothelial expression of CXCL16 caused by Ang-II was found to be dependent on Nox5 expression and subsequent RhoA/p38-MAPK/NFκB activation.

Chronic administration of mice with Ang-II for 15 days caused leukocyte adhesion to cremasteric arterioles together with enhanced arteriolar CXCL16

expression and circulating monocyte and lymphocyte activation. Interestingly, these responses were significantly ameliorated in animals lacking CXCL16 receptor (CXCR6). These initial observations led us to suspect that CXCL16/CXCR6 axis was probably involved in pathologies associated to vascular inflammation in which Ang-II is a key player. Renin-angiotensin system is widely acknowledged to play a role in AAA pathogenesis (Daugherty et al., 2006; Zhang et al., 2009) and Ang-II AT_1 receptor antagonisms, have also been proved to be effective in the treatment of aneurysm formation (Moltzer et al., 2011). Here we have provided evidence that CXCL16/CXCR6 axis is may be involved in Ang-II-induced AAA. Chronic blockade of AT1 receptor decreased both CXCL16 and CXCR6 mARN expression within the aneurismal lesion and these responses correlated with lower numbers of $CXCR6^+$ infiltrated cells. Additionally, both macrophage and lymphocyte numbers were drastically reduced in the lesion of those animals treated with losartan at 30 mg/kg/day. Since both cell types express CXCR6 receptor (Shimaoka *et al.*, 2000; Galkina *et al.*, 2007), it is tempting to speculate that the decreased endothelial expression of CXCL16 is partly responsible of the decreased cellularity. Nevertheless, other chemokines such as CCL2 are likely involved in the aneurismal mononuclear cell infiltration given that Ang-II can promote CCL2 generation and release (Mateo *et al.*, 2006) and neutralization of CCL2 activity or CCR2 antagonisms have been proved to halt AAA development (Izhak *et al.*, 2012).

On the other hand, ameliorated angiogenesis was also detected in the animals subjected to losartan treatment. The interconnection between angiogenesis and inflammation have already been proved (Mantovani et al., 2008). In fact, additional recruitment of inflammatory cells can be driven by newly formed vessels, thus amplifying both the inflammatory and angiogenic processes as these leukocyte subtypes can release pro-angiogenic chemokines and growth factors such as VEGF (Mantovani et al., 2008). Moreover, it is well known that MCP-1/CCL2 through CCR2 receptor interaction, cause leukocyte recruitment (Izhak et al., 2012), angiogenesis (Izhak et al., 2012) and AAA development (de Waard et al., 2010). By contrast, the role of CXCL16 in this pathology has been barely investigated and only recently has been reported increased CXCL16 mRNA expression in CaCl2-induced AAA (Ren et al., 2014).

In this regard, CXCL16 can induce endothelial proliferation, migration and tube formation (Zhuge et al., 2005; Wente et al., 2008). $CXCR6^+$ cells produce angiogenic factors, such as VEGF and IL-8 (Wang et al., 2008) and CXCR6 deficiency resulted in profound reductions in monocyte and T cell infiltration in the arthritic joint which was correlated with impaired vessel formation (Isozaki et al., 2013). Furthermore, a strong correlation between CXCR6 expression and cancer aggressiveness was linked to angiogenic processes (Wang et al., 2008; Gao et al., 2012). In this context, *in vitro* and *in vivo* studies suggest that CXCR6 knockdown inhibits tumorigenicity, cell invasion, angiogenesis, and metastasis of hepatoma cells (Gao et al., 2012). More recently, it has been shown that simultaneous neutralization of MCP-1/CCL2 and CXCL16 activity significantly inhibited tube formation of HUVECs, thus indicating a synergism between both chemokines in neovascularization (Han et al., 2014).

In light of these *in vivo* findings, we tried to translate these results to human cells and here we show that the interaction of Ang-II with its AT_1 receptor increased CXCL16 mRNA and protein expression in human arterial endothelial cells. In agreement with the *in vivo* data, *in vitro* neutralization of CXCL16 activity significantly inhibited human mononuclear cell-arterial endothelium interactions. Taken together all these observations, our *in vivo* and *in vitro* results point a clear functional role of CXCL16 in the inappropriate mononuclear cell recruitment by the Ang-II-induced dysfunctional arterial endothelium.

The activation of redox-sensitive signalling pathways mediates many of the actions of Ang II. In this context, Ang-II can potentiate the induction of the expression of a variety of redox-sensitive factors as well as redox-regulated genes and transcription factors (Das et al., 2004; Higuchi et al., 2007; Montezano et al., 2010; Rius et al., 2013b). In order to investigate the mechanisms involved in Ang-II-induced CXCL16 endothelial expression and since several lines of evidence indicate that the endothelial cell activation that accompanies inflammation generally results in an increase in ROS production, in the current study we observed that a non specific NADPH inhibition blunted the responses to Ang-II while XO inhibition did not. The Nox isoforms Nox2, Nox4 and Nox5 are specially abundant in the endothelium (Lassegue et al., 2010) and previous studies from our group revealed that although Nox2, Nox4 and Nox5 expression rose after Ang-II stimulation in human arterial

endothelial cells, only Nox5 seemed to play a major role in Ang-II-induced mononuclear cell arrest (Rius et al., 2013b). In this regard, endothelial Nox5 was involved in the inflammatory responses induced by Ang-II such as the increased up-regulation of CAMs like VCAM-1 or chemokines like fractalkine (CX3CL1) (Montezano *et al*., 2010; Rius *et al*., 2013b; Escudero *et al*., 2015b). Now we have found that Nox5 was the endothelial Nox isoform responsible of Ang-II-induced increased CXCL16 expression.

Previous studies from our group, showed that RhoA was activated by Nox5-generated superoxide anions (Escudero *et al.*, 2015b), therefore we next sought to investigate the potential involvement of RhoA-Rho kinase pathway in the enhanced expression of CXCL16 evoked by Ang-II. Indeed, either pharmacological inhibition of RhoA or its targeted knockdown in HUAEC diminished CXCL16 expression provoked by Ang-II. Inasmuch, since RhoA is an upstream regulator of MAPK family members, such as p38 MAPK (Marinissen et al., 2004), and the latter can activate transcription factors such as NF-κB (Guo *et al.*, 2006; Rius *et al.*, 2010; Rius *et al.*, 2013b; Escudero *et al.*, 2015b); we then studied the involvement of this pathway. Hence, our findings suggest that Ang-II-induced CXCL16 arterial up-regulation is a consequence of RhoA activation and subsequent p38 MAPK enhanced activity leading to NFκB transactivation and the further regulation of genes including CXCL16, which actively participate in the mononuclear leukocyte recruitment induced by the peptide. Nevertheless, Ang-II signalling other than those explored in the present study cannot be excluded.

In conclusion, we have demonstrated *in vivo* and *in vitro* that CXCL16 seems to be a key molecule in the pro-inflammatory and pro-angiogenic processes in Ang-II-induced aneurysm formation. *In vitro,* Ang-II caused arterial CXCL16-dependent mononuclear cell arrest which appeared to be mediated by ROS generation and the subsequent activation of redox-sensitive signalling pathways. Nevertheless, additional studies in patients prone to AAA development and in animals lacking CXCR6 receptor are required to further confirm whether CXCL16/CXCR6 axis is a potential new biomarker of cardiovascular diseases associated with rennin-angiotensin system activation or an axis susceptible of therapeutic intervention.

5.4 DISCUSSION OF THE STUDY: CXCR6/CXCL16 AXIS MEDIATES PLATELET-LEUKOCYTE ARREST IN COPD DYSFUNCTIONAL ARTERIAL ENDOTHELIUM

Cardiovascular diseases are common co-morbidities in patients with COPD (Sinden et al., 2010), however, the mechanisms by which they develop remain largely unknown. This study provides the first demonstration that COPD patients have greater numbers of activated circulating platelets ($PAC\text{-}1^{+}$) with increased expression of P-selectin, CXCL16 and CXCR6. Moreover, this activation was associated with augmented platelet-leukocyte and leukocyte adhesion to CSE-stimulated human arterial endothelium, which was partly dependent on arterial CXCL16 up-regulation and increased CXCR6 expression on platelet-leukocyte aggregates and mononuclear cells. CSE-induced endothelial CXCL16 expression was dependent on Nox5 expression and on subsequent RhoA and p38-MAPK activation, leading to NFκB translocation to the nucleus and presumably further up-regulation of CXCL16 gene expression. Examination of a mouse model of acute CS exposure demonstrated a mild inflammatory response in the lung that was accompanied by increased CXCL16 expression in the cremasteric arterioles, an organ distant from the lung. CS exposure also caused leukocyte-arteriolar endothelial cell adhesion, which was significantly blunted in animals with a nonfunctional CXCR6 receptor.

Platelet activation is linked to cardiovascular morbidity; indeed, activated platelets can mediate the endothelial adhesion of circulating leukocytes, a feature typical of dysfunctional endothelium that precedes atherogenesis (Landmesser et al., 2004). A recent study has shown that COPD is associated with platelet activation through increased platelet-monocyte aggregates and platelet expression of P-selectin (Maclay et al., 2011). Our results confirm and extend these findings and show that COPD patients have significantly more platelets expressing CXCL16 and CXCR6 compared with age-matched controls, and expression is significantly higher. CXCR6 was recently reported to be highly expressed in platelets (Borst et al., 2012). To investigate the potential role of platelet CXCR6 on CSE-induced leukocyte-arterial endothelium interactions, we first analyzed its expression on different platelet-bound or unbound leukocyte subsets. Surprisingly, we found increased CXCR6 expression

in neutrophils of heparinized whole blood from COPD patients compared with age-matched control subjects. Typically, this subset of leukocytes does not express CXCR6 unless platelet-neutrophil aggregates are present (Wilbanks et al., 2001; Ludwig et al., 2007). In support of such a possibility, we found that when platelets were disaggregated from neutrophils, this increase in neutrophil CXCR6 expression was lost. It seems likely that the increased expression of platelet P-selectin in COPD patients accounts for the increased CXCR6 expression in neutrophils through engagement with granulocyte-expressed-P-selectin glycoprotein ligand (PSGL)-1 present on the surface, resulting in neutrophil-platelet aggregate formation. In parallel, CXCR6 overexpression and increased circulating numbers of $CXCR6^+$ platelet-monocyte/lymphocyte aggregates were found in COPD patients compared with age-matched controls. Furthermore, CXCR6 expression was also significantly increased in these leukocyte subpopulations in the absence of adhered platelets.

To address the functional consequences of these findings, we measured leukocyte/endothelial cell interactions using the dynamic flow chamber assay. We found that platelet-leukocyte adhesion to both unstimulated and CSE-stimulated HUAEC was significantly more potent in the COPD group. The enhanced adhesion of platelet-bound leukocytes from COPD patients to unstimulated endothelium may occur through neutrophil and monocyte CD11b/CD18 integrin interaction with constitutively expressed intercellular cell adhesion molecule-1 (ICAM-1) on the arterial endothelium. Indeed, enhanced CD11b expression on circulating neutrophils and monocytes from COPD patients was previously described (Noguera et al., 2001). Our findings also suggest that platelets are critical for leukocyte adhesion to CSE-stimulated dysfunctional arterial endothelium, because in their absence no significant adhesion was found in aged-matched controls. In this context, it is widely acknowledged that platelets induce leukocyte recruitment in multiple inflammatory disorders and these properties are somehow dissociated from their role in hemostasis (Page et al., 2013). Therefore, it seems that in aged-matched controls, platelet-neutrophil aggregates are likely responsible for the arterial interactions detected since CSE-induced increased adhesiveness was partly dependent on endothelial fractalkine as described previously (Rius et al., 2013a) and on CXCL16 up-regulation (this work), and neutrophils express neither fractalkine receptor (CX_3CR1) (Beck et al., 2003) nor CXCL16 (CXCR6) (Ludwig et al., 2007), but platelets do (Schulz et al.,

2007; Borst et al., 2012). Notably, in a COPD setting, platelet-leukocyte aggregates or platelet unbound leukocytes showed similar adhesion to unstimulated and stimulated arterial endothelium. Moreover, CXCL16 neutralization of CSE-induced leukocyte adhesion exerted a comparable and significant reduction in untreated and EDTA-treated whole blood (48% and 55% with or without bound platelets, respectively). This parity can be attributed to the low shear rate employed (0.5 dyn/cm2), wherein platelet-leukocyte or leukocyte adhesion is platelet independent as described previously for the membrane-bound chemokine fractalkine (CX_3CL1) (Schulz et al., 2007). The same study (Schulz et al., 2007) demonstrated that at higher shear rates, leukocyte-arterial endothelium interactions were platelet-dependent, a possibility not explored in this study. Despite these findings, no differences in the levels of circulating soluble CXCL16 were found in COPD patients compared with aged-matched controls. The clinical impact of these findings are likely relevant. First, patients with metabolic syndrome, who are also prone to atherosclerosis development, showed increased numbers of circulating CXCR6+ cells (Lv et al., 2013). Second, blockade of CXCR6/CXCL16 axis reduces both platelet and leukocyte attachment to the arterial endothelium in COPD regardless of its functionality. It is therefore feasible that increased CXCR6 expression/function in circulating platelets and mononuclear cells may establish a direct link between COPD and the development of cardiovascular disorders.

The reduction in leukocyte adhesion to the inflamed arterial endothelium produced by CXCL16 neutralization led us to investigate the impact of CS on arterial CXCL16 expression in *in vitro* and *in vivo* models. CSE stimulation or acute exposure of mice to CS increased functional CXCL16 on the arterial endothelium or cremasteric arterioles since significantly-enhanced CXCL16-mediated mononuclear cell adhesiveness was observed. To investigate the mechanisms involved in CSE-induced CXCL16 endothelial expression, we used apocynin, a nonspecific NADPH oxidase inhibitor, and found that it decreased chemokine expression. It is well known that smoke-derived free radicals and oxidants form a part of CS and cause a pro-oxidative state in the circulatory system. Indeed, CS exposure induces rapid ROS production and impairs endothelial functions (Michaud et al., 2006). To dissect the endothelial Nox isoforms involved in NADPH oxidase activity, Nox2, Nox4 and Nox5 were silenced by RNA interference, and abrogation of CSE-induced CXCL16

expression was observed only after Nox5 silencing. Of note, mononuclear cell recruitment induced by CS was also found to be Nox5 dependent (Rius et al., 2013a).

The RhoA-Rho kinase pathway has been implicated in leukocyte recruitment (Cernuda-Morollon et al., 2006), and RhoA is acknowledged as a primary target of oxidative stress since it can be activated by Nox5-generated superoxide anions (Escudero *et al.*, 2015a). We show that pharmacological inhibition of RhoA or its targeted knockdown in HUAEC diminished CXCL16 expression provoked by CSE. Additionally, RhoA has been also reported to be an upstream regulator of mitogen-activated protein kinase (MAPK) family members, such as p38 MAPK (Marinissen et al., 2004), and the latter can regulate the transcription of many genes through its action on downstream targets such as NF-κB (Guo et al., 2006; Rius et al., 2010); both are involved in inflammatory responses such as mononuclear cell recruitment induced by CSE (Rius et al., 2013a). Our findings suggest that CSE-induced CXCL16 arterial up-regulation is a consequence of RhoA activation and different MAPKs, such as p38 MAPK, that lead to activation of several transcription factors including NFκB and the further regulation of genes including CXCL16, which actively participate in the mononuclear leukocyte recruitment induced by CSE.

In conclusion, we provide evidence that increased expression of CXCR6 in circulating platelets and mononuclear cells of COPD patients may constitute a prognostic marker for adverse cardiovascular disorders. Moreover, CS induces CXCL16-dependent mononuclear cell arrest by the arterial endothelium through Nox5 expression and RhoA/p38MAPK/NFκB activation, a previously undescribed mechanism. Our study also provides new insights into potential therapeutic use of CXCL16/CXCR6 axis blockade for the prevention and treatment of COPD-associated cardiovascular disease since it dramatically reduces the adherence of platelets and leukocytes from COPD patients to CSE-stimulated arterial endothelium.

CONCLUSIONES

6 CONCLUSIONES

1. La combinación de Bexaroteno y Rosuvastatina a dosis o concentraciones subóptimas inhibió, tanto *in vitro* como *in vivo*, el aumento en la expresión de ICAM-1, VCAM-1 y fractalquina en el endotelio arteriolar, la síntesis de quimiocinas y la adhesión de monocitos al endotelio arteriolar inducido por Angiotensina-II.

2. *In vitro*, los mecanismos implicados en esta sinergia incluyeron la inhibición de la expresión de Nox5 y la subsecuente inactivación de RhoA. Así como el aumento en la expresión de RXRα, PPARα y PPARγ y de las interacciones RXRα/PPARα y RXRα/PPARγ.

3. La combinación de Bexaroteno y Rosuvastatina a dosis subóptimas redujo de manera sinérgica la incidencia y el diámetro del aneurisma aórtico abdominal inducido por Angiotensina-II en ratones $apoE^{-/-}$ sometidos a una dieta rica en grasas. Además, dichos efectos se caracterizados por una inhibición en la infiltración de macrófagos y de la neovascularización en la lesión, así como de una inhibición en la expresión de los mediadores CXCL1, CCL2, CCL5 y VEGF en la aorta

4. La combinación de Bexaroteno y Rosuvastatina a concentraciones subóptimas activó las interacciones RXRα/PPARα y RXRα/PPARγ inhibiendo así la ruta de señalización PI3K/AKT/mTOR/p70S6K, y como consecuencia, la liberación de quimiocinas proangiogenicas y VEGF causada por Angiotensina-II.

5. La combinación de Bexaroteno y Rosuvastatina a dosis subóptimas podría constituir una nueva alternativa terapeutica para el tratamiento la inflamación vascular asociada al sistema renina angiotensina en determinados desórdenes cardiometabólicos, minimizando las reacciones adversas asociadas al tratamiento.

6. La estimulación con Angiotensina-II produjo un aumento funcional de la expresión de CXCL16 tanto en células endoteliales arteriales como en arterias de la circulación cresmastérica de ratón.

7. El bloqueo farmacológico del receptor AT_1 produjo una disminución en la incidencia y el desarrollo del aneurisma aórtico abdominal, además dicho tratamiento redujo la infiltración de macrófagos, linfocitos y células CXCR6

positivas. Estos efectos fueron acompañados por una disminución en la expresión de las quimiocinas CXCL16, MCP-1 y el factor de crecimiento VEGF

8. Tanto la expresión de CXCL16 como la acumulación de leucocitos mononucleares en respuesta a la estimulación del endotelio con Angiotensina-II parecen estar mediadas a través del aumento de expresión de Nox5 y la activación de la vía RhoA/p38MAPK/NFκB.

9. Los pacientes de EPOC mostraron un aumento en la activación plaquetaria, así como en la interacción plaqueta-leucocito y leucocito-endotelio arteriolar estimulado con extracto de humo de tabaco, dicha interacción se debió, en parte, al aumento en la expresión de CXCL16 por parte del endotelio arteriolar y al aumento en la expresión de CXCR6 observado en los agregados plaquetas-leucocito y en las células mononucleares.

10. El humo de tabaco produjo un aumento en la adhesión de células mononucleares al endotelio arteriolar dependiente de CXCL16 mediado a través de la generación de anión superóxido por parte de Nox5 y la subsecuente activación de la vía RhoA/p38MAPK/NFκB.

11. El aumento en la expresión de CXCR6 en plaquetas y células mononucleares circulantes de pacientes de EPOC podría constituir un biomarcador relacionado con la probabilidad de sufrir patologías cardiovasculares asociadas a la EPOC.

12. Fármacos que antagonicen el receptor de CXCL16 o que neutralicen la actividad de esta quimiocina, podrían ser efectivos en la prevención del daño endotelial que se observa en patologías cardiovasculares asociadas a la EPOC y a alteraciones del sistema Renina-Angiotensina.

REFERENCES

7 REFERENCES

Abel S, Hundhausen C, Mentlein R, Schulte A, Berkhout TA, Broadway N, *et al.* (2004). The transmembrane CXC-chemokine ligand 16 is induced by IFN-gamma and TNF-alpha and shed by the activity of the disintegrin-like metalloproteinase ADAM10. *J Immunol* **172**(10)**:** 6362-6372.

Abu Nabah YN, Losada M, Estelles R, Mateo T, Company C, Piqueras L, *et al.* (2007). CXCR2 blockade impairs angiotensin II-induced CC chemokine synthesis and mononuclear leukocyte infiltration. *Arterioscler Thromb Vasc Biol* **27**(11)**:** 2370-2376.

Aghajanian A, Wittchen ES, Campbell SL, Burridge K (2009). Direct activation of RhoA by reactive oxygen species requires a redox-sensitive motif. *PLoS One* **4**(11)**:** e8045.

Agusti A (2007). Systemic effects of chronic obstructive pulmonary disease: what we know and what we don't know (but should). *Proceedings of the American Thoracic Society* **4**(7)**:** 522-525.

Agusti AG (2005). Systemic effects of chronic obstructive pulmonary disease. *Proceedings of the American Thoracic Society* **2**(4)**:** 367-370; discussion 371-362.

Akasu M, Urata H, Kinoshita A, Sasaguri M, Ideishi M, Arakawa K (1998). Differences in tissue angiotensin II-forming pathways by species and organs in vitro. *Hypertension* **32**(3)**:** 514-520.

Alberts AW (1988). Discovery, biochemistry and biology of lovastatin. *Am J Cardiol* **62**(15)**:** 10J-15J.

Alcazar R, Ruiz-Ortega M, Egido J (2003). [Angiotensin II : a key peptide in vascular and renal failure]. *Nefrologia* **23 Suppl 4:** 27-35.

Aldonyte R, Jansson L, Piitulainen E, Janciauskiene S (2003). Circulating monocytes from healthy individuals and COPD patients. *Respir. Res.* **4:** 11.

Alvarez A, Cerda-Nicolas M, Naim Abu Nabah Y, Mata M, Issekutz AC, Panes J, *et al.* (2004). Direct evidence of leukocyte adhesion in arterioles by angiotensin II. *Blood* **104**(2)**:** 402-408.

Alvarez A, Sanz MJ (2001). Reactive oxygen species mediate angiotensin II-induced leukocyte-endothelial cell interactions in vivo. *J. Leukoc. Biol.* **70**(2)**:** 199-206.

Ambrose JA, Barua RS (2004). The pathophysiology of cigarette smoking and cardiovascular disease: an update. *J. Am. Coll. Cardiol.* **43**(10)**:** 1731-1737.

Angelo LS, Kurzrock R (2007). Vascular endothelial growth factor and its relationship to inflammatory mediators. *Clin Cancer Res* **13**(10)**:** 2825-2830.

Angiari S (2015). Selectin-mediated leukocyte trafficking during the development of autoimmune disease. *Autoimmunity reviews* **14**(11)**:** 984-995.

Aplin M, Bonde MM, Hansen JL (2009). Molecular determinants of angiotensin II type 1 receptor functional selectivity. *J. Mol. Cell. Cardiol.* **46**(1)**:** 15-24.

Apostolakis S, Krambovitis E, Vlata Z, Kochiadakis GE, Baritaki S, Spandidos DA (2007). CX3CR1 receptor is up-regulated in monocytes of coronary artery diseased patients: impact of pre-inflammatory stimuli and renin-angiotensin system modulators. *Thromb Res* **121**(3)**:** 387-395.

Ardaillou R (1998). Angiotensin II-complexities beyond AT1 and AT2 receptors. *Nephrol Dial Transplant* **13**(12)**:** 2988-2990.

Aslanian AM, Charo IF (2006). Targeted disruption of the scavenger receptor and chemokine CXCL16 accelerates atherosclerosis. *Circulation* **114**(6)**:** 583-590.

Astrup P, Kjeldsen K (1979). Model studies linking carbon monoxide and/or nicotine to arteriosclerosis and cardiovascular disease. *Prev. Med.* **8**(3)**:** 295-302.

Babelova A, Sedding DG, Brandes RP (2013). Anti-atherosclerotic mechanisms of statin therapy. *Curr Opin Pharmacol* **13**(2)**:** 260-264.

Baggiolini M (1998). Chemokines and leukocyte traffic. *Nature* **392**(6676)**:** 565-568.

Baggiolini M (2001). Chemokines in pathology and medicine. *J Intern Med* **250**(2)**:** 91-104.

Baggiolini M, Dewald B, Moser B (1994). Interleukin-8 and related chemotactic cytokines--CXC and CC chemokines. *Advances in immunology* **55:** 97-179.

Balakumar P, Mahadevan N (2012). Interplay between statins and PPARs in improving cardiovascular outcomes: a double-edged sword? *Br J Pharmacol* **165**(2)**:** 373-379.

Barreiro E, Schols AM, Polkey MI, Galdiz JB, Gosker HR, Swallow EB, *et al.* (2008). Cytokine profile in quadriceps muscles of patients with severe COPD. *Thorax* **63**(2)**:** 100-107.

Bazan JF, Bacon KB, Hardiman G, Wang W, Soo K, Rossi D, *et al.* (1997). A new class of membrane-bound chemokine with a CX3C motif. *Nature* **385**(6617)**:** 640-644.

Beck G, Ludwig F, Schulte J, van Ackern K, van der Woude FJ, Yard BA (2003). Fractalkine is not a major chemoattractant for the migration of neutrophils across microvascular endothelium. *Scand J Immunol* **58**(2)**:** 180-187.

Bechara C, Chai H, Lin PH, Yao Q, Chen C (2007). Growth related oncogene-alpha (GRO-alpha): roles in atherosclerosis, angiogenesis and other inflammatory conditions. *Med Sci Monit* **13**(6)**:** RA87-90.

BelAiba RS, Djordjevic T, Petry A, Diemer K, Bonello S, Banfi B, *et al.* (2007). NOX5 variants are functionally active in endothelial cells. *Free Radic Biol Med* **42**(4)**:** 446-459.

Beltran AE, Briones AM, Garcia-Redondo AB, Rodriguez C, Miguel M, Alvarez Y, *et al.* (2009). p38 MAPK contributes to angiotensin II-induced COX-2 expression in aortic fibroblasts from normotensive and hypertensive rats. *J Hypertens* **27**(1)**:** 142-154.

Benowitz NL (1997). The role of nicotine in smoking-related cardiovascular disease. *Prev. Med.* **26**(4)**:** 412-417.

Berger J, Leibowitz MD, Doebber TW, Elbrecht A, Zhang B, Zhou G, *et al.* (1999). Novel peroxisome proliferator-activated receptor (PPAR) gamma and PPARdelta ligands produce distinct biological effects. *J. Biol. Chem.* **274**(10)**:** 6718-6725.

Berry C, Norrie J, McMurray JJ (2001a). Are angiotensin II receptor blockers more efficacious than placebo in heart failure? Implications of ELITE-2. Evaluation of Losartan In The Elderly. *Am J Cardiol* **87**(5)**:** 606-607, A609.

Berry C, Touyz R, Dominiczak AF, Webb RC, Johns DG (2001b). Angiotensin receptors: signaling, vascular pathophysiology, and interactions with ceramide. *Am J Physiol Heart Circ Physiol* **281**(6)**:** H2337-2365.

Bevilacqua MP, Nelson RM (1993). Selectins. *J Clin Invest* **91**(2)**:** 379-387.

Bishop-Bailey D (2000). Peroxisome proliferator-activated receptors in the cardiovascular system. *British journal of pharmacology* **129**(5)**:** 823-834.

Bishop-Bailey D (2011). PPARs and angiogenesis. *Biochem. Soc. Trans.* **39**(6)**:** 1601-1605.

Bolinder G, Alfredsson L, Englund A, de Faire U (1994). Smokeless tobacco use and increased cardiovascular mortality among Swedish construction workers. *Am. J. Public Health* **84**(3)**:** 399-404.

Borst O, Munzer P, Gatidis S, Schmidt EM, Schonberger T, Schmid E, *et al.* (2012). The inflammatory chemokine CXC motif ligand 16 triggers platelet activation and adhesion via CXC motif receptor 6-dependent phosphatidylinositide 3-kinase/Akt signaling. *Circ Res* **111**(10)**:** 1297-1307.

Brasier AR, Recinos A, 3rd, Eledrisi MS (2002). Vascular inflammation and the renin-angiotensin system. *Arterioscler Thromb Vasc Biol* **22**(8)**:** 1257-1266.

Brewster DC, Cronenwett JL, Hallett Jr JW, Johnston KW, Krupski WC, Matsumura JS (2003). Guidelines for the treatment of abdominal aortic aneurysms: report of a subcommittee of the Joint Council of the American Association for Vascular Surgery and Society for Vascular Surgery. *Journal of vascular surgery* **37**(5)**:** 1106-1117.

Bruemmer D, Blaschke F, Law RE (2005). New targets for PPARgamma in the vessel wall: implications for restenosis. *Int. J. Obes. (Lond.)* **29 Suppl 1:** S26-30.

Bruneau S, Nakayama H, Woda CB, Flynn EA, Briscoe DM (2013). DEPTOR regulates vascular endothelial cell activation and proinflammatory and angiogenic responses. *Blood* **122**(10)**:** 1833-1842.

Calnek DS, Mazzella L, Roser S, Roman J, Hart CM (2003). Peroxisome proliferator-activated receptor gamma ligands increase release of nitric oxide from endothelial cells. *Arterioscler Thromb Vasc Biol* **23**(1)**:** 52-57.

Calzada MJ, del Peso L (2007). Hypoxia-inducible factors and cancer. *Clin. Transl. Oncol.* **9**(5)**:** 278-289.

Cao J, Gong L, Guo DC, Mietzsch U, Kuang SQ, Kwartler CS, *et al.* (2010). Thoracic aortic disease in tuberous sclerosis complex: molecular pathogenesis and potential therapies in Tsc2+/- mice. *Hum Mol Genet* **19**(10)**:** 1908-1920.

Carlos TM, Harlan JM (1994). Leukocyte-endothelial adhesion molecules. *Blood* **84**(7)**:** 2068-2101.

Carlson J, Lyon M, Bishop J, Vaiman A, Cribiu E, Mornex JF, *et al.* (2003). Chromosomal distribution of endogenous Jaagsiekte sheep retrovirus proviral sequences in the sheep genome. *J. Virol.* **77**(17)**:** 9662-9668.

Celi A, Lorenzet R, Furie B, Furie BC (1997). Platelet-leukocyte-endothelial cell interaction on the blood vessel wall. *Seminars in hematology* **34**(4)**:** 327-335.

Cernuda-Morollon E, Ridley AJ (2006). Rho GTPases and leukocyte adhesion receptor expression and function in endothelial cells. *Circ Res* **98**(6)**:** 757-767.

Cimato TR, Palka BA (2014). Fractalkine (CX3CL1), GM-CSF and VEGF-a levels are reduced by statins in adult patients. *Clinical and translational medicine* **3:** 14.

Claudel T, Leibowitz MD, Fievet C, Tailleux A, Wagner B, Repa JJ, *et al.* (2001). Reduction of atherosclerosis in apolipoprotein E knockout mice by activation of the retinoid X receptor. *Proc Natl Acad Sci U S A* **98**(5)**:** 2610-2615.

Clouse WD, Yamaguchi H, Phillips MR, Hurt RD, Fitzpatrick LA, Moyer TP, *et al.* (2000). Effects of transdermal nicotine treatment on structure and function of coronary artery bypass grafts. *J Appl Physiol (1985)* **89**(3)**:** 1213-1223.

Combadiere C, Potteaux S, Gao JL, Esposito B, Casanova S, Lee EJ, *et al.* (2003). Decreased atherosclerotic lesion formation in CX3CR1/apolipoprotein E double knockout mice. *Circulation* **107**(7)**:** 1009-1016.

Combadiere C, Salzwedel K, Smith ED, Tiffany HL, Berger EA, Murphy PM (1998). Identification of CX3CR1. A chemotactic receptor for the human CX3C chemokine fractalkine and a fusion coreceptor for HIV-1. *J. Biol. Chem.* **273**(37)**:** 23799-23804.

Cordle A, Koenigsknecht-Talboo J, Wilkinson B, Limpert A, Landreth G (2005). Mechanisms of statin-mediated inhibition of small G-protein function. *J Biol Chem* **280**(40)**:** 34202-34209.

Cortes V, Quezada N, Rigotti A, Maiz A (2005). [New heterodimeric nuclear receptors: key metabolic regulators with relevance in the pathophysiology and therapy of dyslipidemias and diabetes mellitus]. *Revista medica de Chile* **133**(12)**:** 1483-1492.

Craig WY, Palomaki GE, Haddow JE (1989). Cigarette smoking and serum lipid and lipoprotein concentrations: an analysis of published data. *BMJ* **298**(6676)**:** 784-788.

Cramer PE, Cirrito JR, Wesson DW, Lee CY, Karlo JC, Zinn AE, *et al.* (2012). ApoE-directed therapeutics rapidly clear beta-amyloid and reverse deficits in AD mouse models. *Science* **335**(6075)**:** 1503-1506.

Chai D, Wang B, Shen L, Pu J, Zhang XK, He B (2008). RXR agonists inhibit high-glucose-induced oxidative stress by repressing PKC activity in human endothelial cells. *Free Radic Biol Med* **44**(7)**:** 1334-1347.

Chandrasekar B, Bysani S, Mummidi S (2004). CXCL16 signals via Gi, phosphatidylinositol 3-kinase, Akt, I kappa B kinase, and nuclear factor-kappa B and induces cell-cell adhesion and aortic smooth muscle cell proliferation. *J Biol Chem* **279**(5)**:** 3188-3196.

Chinetti G, Griglio S, Antonucci M, Torra IP, Delerive P, Majd Z, *et al.* (1998). Activation of proliferator-activated receptors alpha and gamma induces apoptosis of human monocyte-derived macrophages. *J. Biol. Chem.* **273**(40)**:** 25573-25580.

Choke E, Thompson MM, Dawson J, Wilson WR, Sayed S, Loftus IM, *et al.* (2006a). Abdominal aortic aneurysm rupture is associated with increased medial neovascularization and overexpression of proangiogenic cytokines. *Arterioscler Thromb Vasc Biol* **26**(9)**:** 2077-2082.

Choke E, Thompson MM, Dawson J, Wilson WRW, Sayed S, Loftus IM, *et al.* (2006b). Abdominal aortic aneurysm rupture is associated with increased medial neovascularization and overexpression of proangiogenic cytokines. *Arteriosclerosis, thrombosis, and vascular biology* **26**(9)**:** 2077-2082.

Chomczynski P, Sacchi N (1987). Single-step method of RNA isolation by acid guanidinium thiocyanate-phenol-chloroform extraction. *Anal Biochem* **162**(1)**:** 156-159.

Choudhury G, Rabinovich R, MacNee W (2014). Comorbidities and systemic effects of chronic obstructive pulmonary disease. *Clin Chest Med* **35**(1)**:** 101-130.

Chung AS, Ferrara N (2011). Developmental and pathological angiogenesis. *Annu Rev Cell Dev Biol* **27:** 563-584.

Das DK, Maulik N, Engelman RM (2004). Redox regulation of angiotensin II signaling in the heart. *J Cell Mol Med* **8**(1)**:** 144-152.

Daugherty A, Cassis LA (2002). Mechanisms of abdominal aortic aneurysm formation. *Current atherosclerosis reports* **4**(3)**:** 222-227.

Daugherty A, Manning MW, Cassis LA (2000). Angiotensin II promotes atherosclerotic lesions and aneurysms in apolipoprotein E-deficient mice. *J Clin Invest* **105**(11)**:** 1605-1612.

Daugherty A, Rateri DL, Cassis LA (2006). Role of the renin-angiotensin system in the development of abdominal aortic aneurysms in animals and humans. *Ann N Y Acad Sci* **1085:** 82-91.

de Gasparo M, Catt KJ, Inagami T, Wright JW, Unger T (2000). International union of pharmacology. XXIII. The angiotensin II receptors. *Pharmacological reviews* **52**(3)**:** 415-472.

de Vries-van der Weij J, de Haan W, Hu L, Kuif M, Oei HL, van der Hoorn JW, *et al.* (2009). Bexarotene induces dyslipidemia by increased very low-density lipoprotein production and cholesteryl ester transfer protein-mediated reduction of high-density lipoprotein. *Endocrinology* **150**(5)**:** 2368-2375.

Decramer M, Janssens W (2013). Chronic obstructive pulmonary disease and comorbidities. *Lancet Respir Med* **1**(1)**:** 73-83.

Delerive P, De Bosscher K, Besnard S, Vanden Berghe W, Peters JM, Gonzalez FJ, *et al.* (1999). Peroxisome proliferator-activated receptor alpha negatively regulates the vascular inflammatory gene response by negative cross-talk with transcription factors NF-kappaB and AP-1. *J. Biol. Chem.* **274**(45)**:** 32048-32054.

Desjardins F, Sekkali B, Verreth W, Pelat M, De Keyzer D, Mertens A, *et al.* (2008). Rosuvastatin increases vascular endothelial PPARgamma expression and corrects blood pressure variability in obese dyslipidaemic mice. *Eur Heart J* **29**(1)**:** 128-137.

Diep QN, El Mabrouk M, Cohn JS, Endemann D, Amiri F, Virdis A, *et al.* (2002). Structure, endothelial function, cell growth, and inflammation in blood vessels of angiotensin II-infused rats: role of peroxisome proliferator-activated receptor-gamma. *Circulation* **105**(19)**:** 2296-2302.

Domazet I, Holleran BJ, Richard A, Vandenberghe C, Lavigne P, Escher E, *et al.* (2015). Characterization of Angiotensin II Molecular Determinants Involved in AT1 Receptor Functional Selectivity. *Mol. Pharmacol.*

Dormuth CR, Hemmelgarn BR, Paterson JM, James MT, Teare GF, Raymond CB, *et al.* (2013). Use of high potency statins and rates of admission for acute kidney injury: multicenter, retrospective observational analysis of administrative databases. *Bmj* **346:** f880.

Douglas G, Bendall JK, Crabtree MJ, Tatham AL, Carter EE, Hale AB, *et al.* (2012). Endothelial-specific Nox2 overexpression increases vascular superoxide and macrophage recruitment in ApoE(-)/(-) mice. *Cardiovascular research* **94**(1)**:** 20-29.

Duong-Quy S, Dao P, Hua-Huy T, Guilluy C, Pacaud P, Dinh-Xuan AT (2011). Increased Rho-kinase expression and activity and pulmonary endothelial dysfunction in smokers with normal lung function. *The European respiratory journal* **37**(2)**:** 349-355.

Duval C, Chinetti G, Trottein F, Fruchart JC, Staels B (2002). The role of PPARs in atherosclerosis. *Trends Mol. Med.* **8**(9)**:** 422-430.

Dworakowski R, Alom-Ruiz SP, Shah AM (2008). NADPH oxidase-derived reactive oxygen species in the regulation of endothelial phenotype. *Pharmacol. Rep.* **60**(1)**:** 21-28.

Dzau VJ (2001). Theodore Cooper Lecture: Tissue angiotensin and pathobiology of vascular disease: a unifying hypothesis. *Hypertension* **37**(4)**:** 1047-1052.

Escudero P, Martinez de Maranon A, Collado A, Gonzalez-Navarro H, Hermenegildo C, Peiro C, *et al.* (2015a). Combined Sub-Optimal Doses of Rosuvastatin and Bexarotene Impair Angiotensin II-Induced Arterial Mononuclear Cell Adhesion Through Inhibition of Nox5 Signaling Pathways and Increased RXR/PPARalpha and RXR/PPARgamma Interactions. *Antioxid Redox Signal* **22**(11)**:** 901-920.

Escudero P, Martinez de Maranon A, Collado A, Gonzalez-Navarro H, Hermenegildo C, Peiro C, *et al.* (2015b). Combined sub-optimal doses of Rosuvastatin and Bexarotene impairs angiotensin II-induced arterial mononuclear cell adhesion through inhibition of Nox5 signaling pathways and increased RXR/PPARalpha and RXR/PPARgamma interactions. *Antioxid Redox Signal*.

Estelles R, Milian L, Nabah YN, Mateo T, Cerda-Nicolas M, Losada M, *et al.* (2005). Effect of boldine, secoboldine, and boldine methine on angiotensin II-induced neutrophil recruitment in vivo. *J Leukoc Biol* **78**(3)**:** 696-704.

Fan LM, Douglas G, Bendall JK, McNeill E, Crabtree MJ, Hale AB, *et al.* (2014). Endothelial cell-specific reactive oxygen species production increases susceptibility to aortic dissection. *Circulation* **129**(25)**:** 2661-2672.

Farol LT, Hymes KB (2004). Bexarotene: a clinical review. *Expert Rev Anticancer Ther* **4**(2)**:** 180-188.

Ferrara N, Gerber H-P, LeCouter J (2003). The biology of VEGF and its receptors. *Nature medicine* **9**(6)**:** 669-676.

Ferrer E, Peinado VI, Diez M, Carrasco JL, Musri MM, Martinez A, *et al.* (2009). Effects of cigarette smoke on endothelial function of pulmonary arteries in the guinea pig. *Respir. Res.* **10:** 76.

Florentin M, Liberopoulos EN, Rizos CV, Kei AA, Liamis G, Kostapanos MS, *et al.* (2013). Colesevelam plus rosuvastatin 5 mg/day versus rosuvastatin 10 mg/day alone on markers of insulin resistance in patients with hypercholesterolemia and impaired fasting glucose. *Metab Syndr Relat Disord* **11**(3)**:** 152-156.

Foschino Barbaro MP, Carpagnano GE, Spanevello A, Cagnazzo MG, Barnes PJ (2007). Inflammation, oxidative stress and systemic effects in mild chronic obstructive pulmonary disease. *Int. J. Immunopathol. Pharmacol.* **20**(4)**:** 753-763.

Fox CS, Massaro JM, Hoffmann U, Pou KM, Maurovich-Horvat P, Liu CY, *et al.* (2007). Abdominal visceral and subcutaneous adipose tissue compartments: association with metabolic risk factors in the Framingham Heart Study. *Circulation* **116**(1)**:** 39-48.

Foxall C, Watson SR, Dowbenko D, Fennie C, Lasky LA, Kiso M, *et al.* (1992). The three members of the selectin receptor family recognize a common carbohydrate epitope, the sialyl Lewis(x) oligosaccharide. *The Journal of cell biology* **117**(4)**:** 895-902.

Fu J, Ding Y, Huang D, Li H, Chen X (2007). The retinoid X receptor-selective ligand, LGD1069, inhibits tumor-induced angiogenesis via suppression of VEGF in human non-small cell lung cancer. *Cancer Lett.* **248**(1)**:** 153-163.

Fu J, Wang W, Liu YH, Lu H, Luo Y (2011). In vitro anti-angiogenic properties of LGD1069, a selective retinoid X-receptor agonist through down-regulating Runx2 expression on Human endothelial cells. *BMC Cancer* **11:** 227.

Galkina E, Harry BL, Ludwig A, Liehn EA, Sanders JM, Bruce A, *et al.* (2007). CXCR6 promotes atherosclerosis by supporting T-cell homing, interferon-gamma production, and macrophage accumulation in the aortic wall. *Circulation* **116**(16)**:** 1801-1811.

Galkina E, Ley K (2009). Immune and inflammatory mechanisms of atherosclerosis (*). *Annu Rev Immunol* **27:** 165-197.

Gan WQ, Man SF, Senthilselvan A, Sin DD (2004). Association between chronic obstructive pulmonary disease and systemic inflammation: a systematic review and a meta-analysis. *Thorax* **59**(7)**:** 574-580.

Garrido AM, Griendling KK (2009). NADPH oxidases and angiotensin II receptor signaling. *Mol. Cell. Endocrinol.* **302**(2)**:** 148-158.

Girardi JM, Farias RE, Ferreira AP, Raposo NR (2011). Rosuvastatin prevents proteinuria and renal inflammation in nitric oxide-deficient rats. *Clinics (Sao Paulo)* **66**(8)**:** 1457-1462.

Gkaliagkousi E, Ferro A (2011). Nitric oxide signalling in the regulation of cardiovascular and platelet function. *Front Biosci (Landmark Ed)* **16:** 1873-1897.

Glass CK, Witztum JL (2001). Atherosclerosis. the road ahead. *Cell* **104**(4)**:** 503-516.

Goebeler M, Kilian K, Gillitzer R, Kunz M, Yoshimura T, Brocker EB, *et al.* (1999). The MKK6/p38 stress kinase cascade is critical for tumor necrosis factor-alpha-induced expression of monocyte-chemoattractant protein-1 in endothelial cells. *Blood* **93**(3)**:** 857-865.

Golomb BA, Evans MA (2008). Statin adverse effects : a review of the literature and evidence for a mitochondrial mechanism. *Am J Cardiovasc Drugs* **8**(6)**:** 373-418.

Gonzalez-Navarro H, Abu Nabah YN, Vinue A, Andres-Manzano MJ, Collado M, Serrano M, *et al.* (2010). p19(ARF) deficiency reduces macrophage and vascular smooth muscle cell apoptosis and aggravates atherosclerosis. *J Am Coll Cardiol* **55**(20)**:** 2258-2268.

Gough PJ, Garton KJ, Wille PT, Rychlewski M, Dempsey PJ, Raines EW (2004). A disintegrin and metalloproteinase 10-mediated cleavage and shedding regulates the cell surface expression of CXC chemokine ligand 16. *J Immunol* **172**(6)**:** 3678-3685.

Goya K, Sumitani S, Xu X, Kitamura T, Yamamoto H, Kurebayashi S, *et al.* (2004). Peroxisome proliferator-activated receptor alpha agonists increase nitric oxide synthase expression in vascular endothelial cells. *Arterioscler Thromb Vasc Biol* **24**(4)**:** 658-663.

Grafe M, Auch-Schwelk W, Zakrzewicz A, Regitz-Zagrosek V, Bartsch P, Graf K, *et al.* (1997). Angiotensin II-induced leukocyte adhesion on human coronary endothelial cells is mediated by E-selectin. *Circ Res* **81**(5)**:** 804-811.

Granger DN, Kubes P (1996). Nitric oxide as antiinflammatory agent. *Methods Enzymol* **269:** 434-442.

Granger DN, Vowinkel T, Petnehazy T (2004). Modulation of the inflammatory response in cardiovascular disease. *Hypertension* **43**(5)**:** 924-931.

Grasso S, Tristante E, Saceda M, Carbonell P, Mayor-Lopez L, Carballo-Santana M, *et al.* (2014). Resistance to Selumetinib (AZD6244) in colorectal cancer cell lines is mediated by p70S6K and RPS6 activation. *Neoplasia* **16**(10)**:** 845-860.

Greenwood J, Steinman L, Zamvil SS (2006). Statin therapy and autoimmune disease: from protein prenylation to immunomodulation. *Nat Rev Immunol* **6**(5)**:** 358-370.

Gunn MD, Ngo VN, Ansel KM, Ekland EH, Cyster JG, Williams LT (1998). A B-cell-homing chemokine made in lymphoid follicles activates Burkitt's lymphoma receptor-1. *Nature* **391**(6669)**:** 799-803.

Guo RW, Yang LX, Li MQ, Liu B, Wang XM (2006). Angiotensin II induces NF-kappa B activation in HUVEC via the p38MAPK pathway. *Peptides* **27**(12)**:** 3269-3275.

Guthikonda S, Sinkey C, Barenz T, Haynes WG (2003). Xanthine oxidase inhibition reverses endothelial dysfunction in heavy smokers. *Circulation* **107**(3)**:** 416-421.

Hackam DG, Thiruchelvam D, Redelmeier DA (2006). Angiotensin-converting enzyme inhibitors and aortic rupture: a population-based case-control study. *Lancet* **368**(9536)**:** 659-665.

Hafizi S, Wang X, Chester AH, Yacoub MH, Proud CG (2004). ANG II activates effectors of mTOR via PI3-K signaling in human coronary smooth muscle cells. *American journal of physiology. Heart and circulatory physiology* **287**(3)**:** H1232-1238.

Hahn AW, Jonas U, Buhler FR, Resink TJ (1994). Activation of human peripheral monocytes by angiotensin II. *FEBS Lett.* **347**(2-3)**:** 178-180.

Hansson GK, Hermansson A (2011). The immune system in atherosclerosis. *Nature immunology* **12**(3)**:** 204-212.

Hansson GK, Libby P, Tabas I (2015). Inflammation and plaque vulnerability. *J Intern Med* **278**(5)**:** 483-493.

Hara T, Katakai T, Lee J-H, Nambu Y, Nakajima-Nagata N, Gonda H, *et al.* (2006). A transmembrane chemokine, CXC chemokine ligand 16, expressed by lymph node fibroblastic reticular cells has the potential to regulate T cell migration and adhesion. *Int Immunol* **18**(2)**:** 301-311.

Hashimoto K, Kataoka N, Nakamura E, Tsujioka K, Kajiya F (2007). Oxidized LDL specifically promotes the initiation of monocyte invasion during transendothelial migration with upregulated PECAM-1 and downregulated VE-cadherin on endothelial junctions. *Atherosclerosis* **194**(2)**:** e9-17.

Heitzer T, Brockhoff C, Mayer B, Warnholtz A, Mollnau H, Henne S, *et al.* (2000). Tetrahydrobiopterin improves endothelium-dependent vasodilation in chronic smokers : evidence for a dysfunctional nitric oxide synthase. *Circ Res* **86**(2)**:** E36-41.

Henderson WR, Chi EY, Teo J-L, Nguyen C, Kahn M (2002). A small molecule inhibitor of redox-regulated NF-kappa B and activator protein-1 transcription blocks allergic airway inflammation in a mouse asthma model. *J Immunol* **169**(9)**:** 5294-5299.

Hennuyer N, Poulain P, Madsen L, Berge RK, Houdebine LM, Branellec D, *et al.* (1999). Beneficial effects of fibrates on apolipoprotein A-I metabolism occur independently of any peroxisome proliferative response. *Circulation* **99**(18)**:** 2445-2451.

Henrion D, Kubis N, Levy BI (2001). Physiological and pathophysiological functions of the AT(2) subtype receptor of angiotensin II: from large arteries to the microcirculation. *Hypertension* **38**(5)**:** 1150-1157.

Hickey MJ, Kubes P (1997). Role of nitric oxide in regulation of leucocyte-endothelial cell interactions. *Exp Physiol* **82**(2)**:** 339-348.

Higuchi S, Ohtsu H, Suzuki H, Shirai H, Frank GD, Eguchi S (2007). Angiotensin II signal transduction through the AT1 receptor: novel insights into mechanisms and pathophysiology. *Clin Sci (Lond)* **112**(8)**:** 417-428.

Hoffman KB, Kraus C, Dimbil M, Golomb BA (2012). A survey of the FDA's AERS database regarding muscle and tendon adverse events linked to the statin drug class. *PLoS One* **7**(8)**:** e42866.

Hofnagel O, Engel T, Severs NJ, Robenek H, Buers I (2011). SR-PSOX at sites predisposed to atherosclerotic lesion formation mediates monocyte-endothelial cell adhesion. *Atherosclerosis* **217**(2)**:** 371-378.

Hofnagel O, Luechtenborg B, Eschert H, Weissen-Plenz G, Severs NJ, Robenek H (2006). Pravastatin inhibits expression of lectin-like oxidized low-density lipoprotein receptor-1 (LOX-1) in Watanabe heritable hyperlipidemic rabbits: a new pleiotropic effect of statins. *Arterioscler Thromb Vasc Biol* **26**(3)**:** 604-610.

Hofnagel O, Luechtenborg B, Plenz G, Robenek H (2002). Expression of the novel scavenger receptor SR-PSOX in cultured aortic smooth muscle cells and umbilical endothelial cells. *Arterioscler Thromb Vasc Biol* **22**(4)**:** 710-711.

Hot A, Lavocat F, Lenief V, Miossec P (2013). Simvastatin inhibits the pro-inflammatory and pro-thrombotic effects of IL-17 and TNF-alpha on endothelial cells. *Ann Rheum Dis* **72**(5)**:** 754-760.

House SD, Lipowsky HH (1987). Leukocyte-endothelium adhesion: microhemodynamics in mesentery of the cat. *Microvasc Res* **34**(3)**:** 363-379.

Hsueh WA, Law RE (2001). PPARgamma and atherosclerosis: effects on cell growth and movement. *Arterioscler Thromb Vasc Biol* **21**(12)**:** 1891-1895.

Huang C-Y, Fong Y-C, Lee C-Y, Chen M-Y, Tsai H-C, Hsu H-C, *et al.* (2009). CCL5 increases lung cancer migration via PI3K, Akt and NF-κB pathways. *Biochemical pharmacology* **77**(5)**:** 794-803.

Hultgren R, Granath F, Swedenborg J (2007). Different disease profiles for women and men with abdominal aortic aneurysms. *European journal of vascular and endovascular surgery* **33**(5)**:** 556-560.

Hundhausen C, Schulte A, Schulz B, Andrzejewski MG, Schwarz N, von Hundelshausen P, *et al.* (2007). Regulated shedding of transmembrane chemokines by the disintegrin and metalloproteinase 10 facilitates detachment of adherent leukocytes. *J Immunol* **178**(12)**:** 8064-8072.

Hurst JR, Perera WR, Wilkinson TM, Donaldson GC, Wedzicha JA (2006). Systemic and upper and lower airway inflammation at exacerbation of chronic obstructive pulmonary disease. *Am. J. Respir. Crit. Care Med.* **173**(1)**:** 71-78.

Hynes RO (1992). Integrins: versatility, modulation, and signaling in cell adhesion. *Cell* **69**(1)**:** 11-25.

Imai T, Hieshima K, Haskell C, Baba M, Nagira M, Nishimura M, *et al.* (1997). Identification and molecular characterization of fractalkine receptor CX3CR1, which mediates both leukocyte migration and adhesion. *Cell* **91**(4)**:** 521-530.

Israelian-Konaraki Z, Reaven PD (2005). Peroxisome proliferator-activated receptor-alpha and atherosclerosis: from basic mechanisms to clinical implications. *Cardiology* **103**(1)**:** 1-9.

Ito H, Takemori K, Suzuki T (2001). Role of angiotensin II type 1 receptor in the leucocytes and endothelial cells of brain microvessels in the pathogenesis of hypertensive cerebral injury. *J Hypertens* **19**(3 Pt 2)**:** 591-597.

Izhak L, Wildbaum G, Jung S, Stein A, Shaked Y, Karin N (2012). Dissecting the autocrine and paracrine roles of the CCR2-CCL2 axis in tumor survival and angiogenesis. *PloS one* **7**(1)**:** e28305.

Izquierdo Alonso JL, Arroyo-Espliguero R (2005). [Chronic obstructive pulmonary disease and cardiovascular risk]. *Arch. Bronconeumol.* **41**(8)**:** 410-412.

Izquierdo MC, Martin-Cleary C, Fernandez-Fernandez B, Elewa U, Sanchez-Nino MD, Carrero JJ, *et al.* (2014). CXCL16 in kidney and cardiovascular injury. *Cytokine Growth Factor Rev* **25**(3)**:** 317-325.

Jaffe EA, Nachman RL, Becker CG, Minick CR (1973). Culture of human endothelial cells derived from umbilical veins. Identification by morphologic and immunologic criteria. *J Clin Invest* **52**(11)**:** 2745-2756.

Jenne CN, Kubes P (2015). Platelets in inflammation and infection. *Platelets* **26**(4)**:** 286-292.

Jeong SH, Park JH, Kim JN, Park YH, Shin SY, Lee YH, *et al.* (2010). Up-regulation of TNF-alpha secretion by cigarette smoke is mediated by Egr-1 in HaCaT human keratinocytes. *Exp. Dermatol.* **19**(8)**:** e206-212.

Johnston KW, Rutherford RB, Tilson MD, Shah DM, Hollier L, Stanley JC (1991). Suggested standards for reporting on arterial aneurysms. *Journal of vascular surgery* **13**(3)**:** 452-458.

Jougasaki M, Ichiki T, Takenoshita Y, Setoguchi M (2010). Statins suppress interleukin-6-induced monocyte chemo-attractant protein-1 by inhibiting Janus kinase/signal transducers and activators of transcription pathways in human vascular endothelial cells. *Br J Pharmacol* **159**(6)**:** 1294-1303.

Kalra VK, Ying Y, Deemer K, Natarajan R, Nadler JL, Coates TD (1994). Mechanism of cigarette smoke condensate induced adhesion of human monocytes to cultured endothelial cells. *J. Cell. Physiol.* **160**(1)**:** 154-162.

Kanwar S, Woodman RC, Poon MC, Murohara T, Lefer AM, Davenpeck KL, *et al.* (1995). Desmopressin induces endothelial P-selectin expression and leukocyte rolling in postcapillary venules. *Blood* **86**(7)**:** 2760-2766.

Karar J, Maity A (2011). PI3K/AKT/mTOR Pathway in Angiogenesis. *Front Mol Neurosci* **4:** 51.

Karnoub AE, Weinberg RA (2008). Ras oncogenes: split personalities. *Nat Rev Mol Cell Biol* **9**(7)**:** 517-531.

Karrowni W, Dughman S, Hajj GP, Miller FJ, Jr. (2011). Statin therapy reduces growth of abdominal aortic aneurysms. *Journal of investigative medicine : the official publication of the American Federation for Clinical Research* **59**(8)**:** 1239-1243.

Kayyali US, Budhiraja R, Pennella CM, Cooray S, Lanzillo JJ, Chalkley R, *et al.* (2003). Upregulation of xanthine oxidase by tobacco smoke condensate in pulmonary endothelial cells. *Toxicol. Appl. Pharmacol.* **188**(1)**:** 59-68.

Keatings VM, Collins PD, Scott DM, Barnes PJ (1996). Differences in interleukin-8 and tumor necrosis factor-alpha in induced sputum from patients with chronic obstructive pulmonary disease or asthma. *Am. J. Respir. Crit. Care Med.* **153**(2)**:** 530-534.

Kennedy J, Kelner GS, Kleyensteuber S, Schall TJ, Weiss MC, Yssel H, *et al.* (1995). Molecular cloning and functional characterization of human lymphotactin. *J Immunol* **155**(1)**:** 203-209.

Kertai MD, Boersma E, Westerhout CM, van Domburg R, Klein J, Bax JJ, *et al.* (2004). Association between long-term statin use and mortality after successful abdominal aortic aneurysm surgery. *The American journal of medicine* **116**(2)**:** 96-103.

Kiefer F, Siekmann AF (2011). The role of chemokines and their receptors in angiogenesis. *Cellular and molecular life sciences* **68**(17)**:** 2811-2830.

Kim CH, Johnston B, Butcher EC (2002). Trafficking machinery of NKT cells: shared and differential chemokine receptor expression among V alpha 24(+)V beta 11(+) NKT cell subsets with distinct cytokine-producing capacity. *Blood* **100**(1)**:** 11-16.

Kim CH, Kunkel EJ, Boisvert J, Johnston B, Campbell JJ, Genovese MC, *et al.* (2001). Bonzo/CXCR6 expression defines type 1-polarized T-cell subsets with extralymphoid tissue homing potential. *J Clin Invest* **107**(5)**:** 595-601.

Kim JA, Jang HJ, Martinez-Lemus LA, Sowers JR (2012). Activation of mTOR/p70S6 kinase by ANG II inhibits insulin-stimulated endothelial nitric oxide synthase and vasodilation. *Am J Physiol Endocrinol Metab* **302**(2)**:** E201-208.

Kim S, Iwao H (2000). Molecular and cellular mechanisms of angiotensin II-mediated cardiovascular and renal diseases. *Pharmacological reviews* **52**(1)**:** 11-34.

Kleemann R, Princen HM, Emeis JJ, Jukema JW, Fontijn RD, Horrevoets AJ, *et al.* (2003). Rosuvastatin reduces atherosclerosis development beyond and independent of its plasma cholesterol-lowering effect in APOE*3-Leiden transgenic mice: evidence for antiinflammatory effects of rosuvastatin. *Circulation* **108**(11)**:** 1368-1374.

Kliewer SA, Forman BM, Blumberg B, Ong ES, Borgmeyer U, Mangelsdorf DJ, *et al.* (1994). Differential expression and activation of a family of murine peroxisome proliferator-activated receptors. *Proc. Natl. Acad. Sci. U. S. A.* **91**(15)**:** 7355-7359.

Klouche M, May AE, Hemmes M, Messner M, Kanse SM, Preissner KT, *et al.* (1999). Enzymatically modified, nonoxidized LDL induces selective adhesion and transmigration of monocytes and T-lymphocytes through human endothelial cell monolayers. *Arterioscler Thromb Vasc Biol* **19**(3)**:** 784-793.

Kojda G, Harrison D (1999). Interactions between NO and reactive oxygen species: pathophysiological importance in atherosclerosis, hypertension, diabetes and heart failure. *Cardiovascular research* **43**(3)**:** 562-571.

Konstantopoulos K, Kukreti S, Smith CW, McIntire LV (1997). Endothelial P-selectin and VCAM-1 each can function as primary adhesive mechanisms for T cells under conditions of flow. *J Leukoc Biol* **61**(2)**:** 179-187.

Krieg T, Cui L, Qin Q, Cohen MV, Downey JM (2004). Mitochondrial ROS generation following acetylcholine-induced EGF receptor transactivation requires metalloproteinase cleavage of proHB-EGF. *J Mol Cell Cardiol* **36**(3)**:** 435-443.

Krieglstein CF, Granger DN (2001). Adhesion molecules and their role in vascular disease. *American journal of hypertension* **14**(6 Pt 2)**:** 44S-54S.

Kubes P, Kanwar S (1994). Histamine induces leukocyte rolling in post-capillary venules. A P-selectin-mediated event. *J Immunol* **152**(7)**:** 3570-3577.

Kume N, Cybulsky MI, Gimbrone MA, Jr. (1992). Lysophosphatidylcholine, a component of atherogenic lipoproteins, induces mononuclear leukocyte adhesion molecules in cultured human and rabbit arterial endothelial cells. *J Clin Invest* **90**(3)**:** 1138-1144.

Kuo P-L, Shen K-H, Hung S-H, Hsu Y-L (2012). CXCL1/GROα increases cell migration and invasion of prostate cancer by decreasing fibulin-1 expression through NF-κB/HDAC1 epigenetic regulation. *Carcinogenesis***:** bgs299.

Kvietys PR, Granger DN (2012). Role of reactive oxygen and nitrogen species in the vascular responses to inflammation. *Free Radic Biol Med* **52**(3)**:** 556-592.

Laemmli UK (1970). Cleavage of structural proteins during the assembly of the head of bacteriophage T4. *Nature* **227**(5259)**:** 680-685.

Lalloyer F, Fievet C, Lestavel S, Torpier G, van der Veen J, Touche V, *et al.* (2006). The RXR agonist bexarotene improves cholesterol homeostasis and inhibits atherosclerosis progression in a mouse model of mixed dyslipidemia. *Arterioscler Thromb Vasc Biol* **26**(12)**:** 2731-2737.

Landmesser U, Hornig B, Drexler H (2004). Endothelial function: a critical determinant in atherosclerosis? *Circulation* **109**(21 Suppl 1)**:** II27-33.

Lassegue B, Griendling KK (2010). NADPH oxidases: functions and pathologies in the vasculature. *Arterioscler Thromb Vasc Biol* **30**(4)**:** 653-661.

Laufs U, La Fata V, Plutzky J, Liao JK (1998). Upregulation of endothelial nitric oxide synthase by HMG CoA reductase inhibitors. *Circulation* **97**(12)**:** 1129-1135.

Laursen JB, Rajagopalan S, Galis Z, Tarpey M, Freeman BA, Harrison DG (1997). Role of superoxide in angiotensin II-induced but not catecholamine-induced hypertension. *Circulation* **95**(3)**:** 588-593.

Law RE, Goetze S, Xi XP, Jackson S, Kawano Y, Demer L, *et al.* (2000). Expression and function of PPARgamma in rat and human vascular smooth muscle cells. *Circulation* **101**(11)**:** 1311-1318.

Lawrence DM, Singh RS, Franklin DP, Carey DJ, Elmore JR (2004). Rapamycin suppresses experimental aortic aneurysm growth. *J Vasc Surg* **40**(2)**:** 334-338.

Lee HJ, Song I-C, Yun H-J, Jo D-Y, Kim S (2014). CXC chemokines and chemokine receptors in gastric cancer: From basic findings towards therapeutic targeting. *World journal of gastroenterology: WJG* **20**(7)**:** 1681.

Lee SJ, Yang EK, Kim SG (2006). Peroxisome proliferator-activated receptor-gamma and retinoic acid X receptor alpha represses the TGFbeta1 gene via PTEN-mediated p70 ribosomal S6 kinase-1 inhibition: role for Zf9 dephosphorylation. *Mol Pharmacol* **70**(1)**:** 415-425.

Lesnik P, Haskell CA, Charo IF (2003). Decreased atherosclerosis in CX3CR1-/- mice reveals a role for fractalkine in atherogenesis. *J Clin Invest* **111**(3)**:** 333-340.

Ley K, Laudanna C, Cybulsky MI, Nourshargh S (2007). Getting to the site of inflammation: the leukocyte adhesion cascade updated. *Nat Rev Immunol* **7**(9)**:** 678-689.

Li M, Liu K, Michalicek J, Angus JA, Hunt JE, Dell'Italia LJ, *et al.* (2004). Involvement of chymase-mediated angiotensin II generation in blood pressure regulation. *J Clin Invest* **114**(1)**:** 112-120.

Libby P (2002). Inflammation in atherosclerosis. *Nature* **420**(6917)**:** 868-874.

Libby P (2012). Inflammation in atherosclerosis. *Arterioscler Thromb Vasc Biol* **32**(9)**:** 2045-2051.

Libby P, Ridker PM, Hansson GK (2011). Progress and challenges in translating the biology of atherosclerosis. *Nature* **473**(7347)**:** 317-325.

Libby P, Sukhova G, Lee RT, Galis ZS (1995). Cytokines regulate vascular functions related to stability of the atherosclerotic plaque. *J. Cardiovasc. Pharmacol.* **25 Suppl 2:** S9-12.

Liu HW, Cheng B, Fu XB, Sun TZ, Li JF (2007). Characterization of AT1 and AT2 receptor expression profiles in human skin during fetal life. *J Dermatol Sci* **46**(3)**:** 221-225.

Loirand G, Guerin P, Pacaud P (2006). Rho kinases in cardiovascular physiology and pathophysiology. *Circ Res* **98**(3)**:** 322-334.

Loot AE, Schreiber JG, Fisslthaler B, Fleming I (2009). Angiotensin II impairs endothelial function via tyrosine phosphorylation of the endothelial nitric oxide synthase. *J Exp Med* **206**(13)**:** 2889-2896.

Lopez AD, Murray CC (1998). The global burden of disease, 1990-2020. *Nat. Med.* **4**(11)**:** 1241-1243.

Lu H, Rateri DL, Cassis LA, Daugherty A (2008). The role of the renin-angiotensin system in aortic aneurysmal diseases. *Curr. Hypertens. Rep.* **10**(2)**:** 99-106.

Ludwig A, Schulte A, Schnack C, Hundhausen C, Reiss K, Brodway N, *et al.* (2005). Enhanced expression and shedding of the transmembrane chemokine CXCL16 by reactive astrocytes and glioma cells. *J. Neurochem.* **93**(5)**:** 1293-1303.

Ludwig A, Weber C (2007). Transmembrane chemokines: versatile 'special agents' in vascular inflammation. *Thromb Haemost* **97**(5)**:** 694-703.

Luscinskas FW, Lawler J (1994). Integrins as dynamic regulators of vascular function. *FASEB journal : official publication of the Federation of American Societies for Experimental Biology* **8**(12)**:** 929-938.

Luster AD (1998). Chemokines--chemotactic cytokines that mediate inflammation. *N Engl J Med* **338**(7)**:** 436-445.

Lv Y, Hou X, Ti Y, Bu P (2013). Associations of CXCL16/CXCR6 with carotid atherosclerosis in patients with metabolic syndrome. *Clinical nutrition* **32**(5)**:** 849-854.

Maclay JD, McAllister DA, Johnston S, Raftis J, McGuinnes C, Deans A, *et al.* (2011). Increased platelet activation in patients with stable and acute exacerbation of COPD. *Thorax* **66**(9)**:** 769-774.

Majzunova M, Dovinova I, Barancik M, Chan JY (2013). Redox signaling in pathophysiology of hypertension. *J. Biomed. Sci.* **20:** 69.

Malerba M, Clini E, Malagola M, Avanzi GC (2013). Platelet activation as a novel mechanism of atherothrombotic risk in chronic obstructive pulmonary disease. *Expert Rev Hematol* **6**(4)**:** 475-483.

Manea A, Tanase LI, Raicu M, Simionescu M (2010). Jak/STAT signaling pathway regulates nox1 and nox4-based NADPH oxidase in human aortic smooth muscle cells. *Arterioscler Thromb Vasc Biol* **30**(1)**:** 105-112.

Manning MW, Cassi LA, Huang J, Szilvassy SJ, Daugherty A (2002). Abdominal aortic aneurysms: fresh insights from a novel animal model of the disease. *Vasc Med* **7**(1)**:** 45-54.

Manriquez J, Diaz O, Borzone G, Lisboa C (2004). [Spirometric reversibility to salbutamol in chronic obstructive pulmonary disease (COPD). Differential effects on FEV1 and on lung volumes]. *Rev. Med. Chil.* **132**(7)**:** 787-793.

Mantovani A, Allavena P, Sica A, Balkwill F (2008). Cancer-related inflammation. *Nature* **454**(7203)**:** 436-444.

Marinissen MJ, Chiariello M, Tanos T, Bernard O, Narumiya S, Gutkind JS (2004). The small GTP-binding protein RhoA regulates c-jun by a ROCK-JNK signaling axis. *Mol Cell* **14**(1)**:** 29-41.

Marinou K, Tousoulis D, Antonopoulos AS, Stefanadi E, Stefanadis C (2010). Obesity and cardiovascular disease: from pathophysiology to risk stratification. *Int J Cardiol* **138**(1)**:** 3-8.

Marx N, Sukhova GK, Collins T, Libby P, Plutzky J (1999). PPARalpha activators inhibit cytokine-induced vascular cell adhesion molecule-1 expression in human endothelial cells. *Circulation* **99**(24)**:** 3125-3131.

Massena S, Christoffersson G, Hjertstrom E, Zcharia E, Vlodavsky I, Ausmees N, *et al.* (2010). A chemotactic gradient sequestered on endothelial heparan sulfate induces directional intraluminal crawling of neutrophils. *Blood* **116**(11)**:** 1924-1931.

Mateo T, Abu Nabah YN, Abu Taha M, Mata M, Cerda-Nicolas M, Proudfoot AE, *et al.* (2006). Angiotensin II-induced mononuclear leukocyte interactions with arteriolar and venular endothelium are mediated by the release of different CC chemokines. *J Immunol* **176**(9)**:** 5577-5586.

Mateo T, Naim Abu Nabah Y, Losada M, Estelles R, Company C, Bedrina B, *et al.* (2007a). A critical role for TNFalpha in the selective attachment of mononuclear leukocytes to angiotensin-II-stimulated arterioles. *Blood* **110**(6)**:** 1895-1902.

Mateo T, Naim Abu Nabah Y, Losada M, Estelles R, Company C, Bedrina B, *et al.* (2007b). A critical role for TNFalpha in the selective attachment of mononuclear leukocytes to angiotensin-II-stimulated arterioles. *Blood* **110**(6)**:** 1895-1902.

Matloubian M, David A, Engel S, Ryan JE, Cyster JG (2000). A transmembrane CXC chemokine is a ligand for HIV-coreceptor Bonzo. *Nat. Immunol.* **1**(4)**:** 298-304.

Mayer C, Gruber HJ, Landl EM, Pailer S, Scharnagl H, Truschnig-Wilders M, *et al.* (2007). Rosuvastatin reduces interleukin-6-induced expression of C-reactive protein in human hepatocytes in a STAT3- and C/EBP-dependent fashion. *Int J Clin Pharmacol Ther* **45**(6)**:** 319-327.

McDermott DH, Fong AM, Yang Q, Sechler JM, Cupples LA, Merrell MN, *et al.* (2003). Chemokine receptor mutant CX3CR1-M280 has impaired adhesive function and correlates with protection from cardiovascular disease in humans. *J Clin Invest* **111**(8)**:** 1241-1250.

McDermott DH, Halcox JP, Schenke WH, Waclawiw MA, Merrell MN, Epstein N, *et al.* (2001). Association between polymorphism in the chemokine receptor CX3CR1 and coronary vascular endothelial dysfunction and atherosclerosis. *Circ Res* **89**(5)**:** 401-407.

McEver RP (2010). Rolling back neutrophil adhesion. *Nature immunology* **11**(4)**:** 282-284.

McEver RP, Zhu C (2010). Rolling cell adhesion. *Annual review of cell and developmental biology* **26:** 363-396.

McFarland K, Spalding TA, Hubbard D, Ma J-N, Olsson R, Burstein ES (2013). Low Dose Bexarotene Treatment Rescues Dopamine Neurons and Restores Behavioral Function in Models of Parkinson's Disease. *ACS chemical neuroscience* **4**(11)**:** 1430-1438.

Mehta PK, Griendling KK (2007). Angiotensin II cell signaling: physiological and pathological effects in the cardiovascular system. *Am J Physiol Cell Physiol* **292**(1)**:** C82-97.

Michaud SE, Dussault S, Groleau J, Haddad P, Rivard A (2006). Cigarette smoke exposure impairs VEGF-induced endothelial cell migration: role of NO and reactive oxygen species. *J Mol Cell Cardiol* **41**(2)**:** 275-284.

Michel J-B (2001). Contrasting outcomes of atheroma evolution intimal accumulation versus medial destruction. *Arteriosclerosis, thrombosis, and vascular biology* **21**(9)**:** 1389-1392.

Michel J-B, Martin-Ventura J-L, Egido J, Sakalihasan N, Treska V, Lindholt J, *et al.* (2010). Novel aspects of the pathogenesis of aneurysms of the abdominal aorta in humans. *Cardiovasc. Res.***:** cvq337.

Michel O, Dentener M, Corazza F, Buurman W, Rylander R (2001). Healthy subjects express differences in clinical responses to inhaled lipopolysaccharide that are related with inflammation and with atopy. *J. Allergy Clin. Immunol.* **107**(5)**:** 797-804.

Middleton RK, Lloyd GM, Bown MJ, Cooper NJ, London NJ, Sayers RD (2007). The pro-inflammatory and chemotactic cytokine microenvironment of the abdominal aortic aneurysm wall: a protein array study. *J Vasc Surg* **45**(3)**:** 574-580.

Mignatti P, Tsuboi R, Robbins E, Rifkin DB (1989). In vitro angiogenesis on the human amniotic membrane: requirement for basic fibroblast growth factor-induced proteinases. *The Journal of cell biology* **108**(2)**:** 671-682.

Mihos CG, Pineda AM, Santana O (2014). Cardiovascular effects of statins, beyond lipid-lowering properties. *Pharmacol. Res.* **88:** 12-19.

Mira E, Manes S (2009). Immunomodulatory and anti-inflammatory activities of statins. *Endocr Metab Immune Disord Drug Targets* **9**(3)**:** 237-247.

Mizutani K, Roca H, Varsos Z, Pienta KJ (2009). Possible mechanism of CCL2-induced Akt activation in prostate cancer cells. *Anticancer research* **29**(8)**:** 3109-3113.

Moatti D, Faure S, Fumeron F, Amara Mel W, Seknadji P, McDermott DH, *et al.* (2001). Polymorphism in the fractalkine receptor CX3CR1 as a genetic risk factor for coronary artery disease. *Blood* **97**(7)**:** 1925-1928.

Mombouli JV, Vanhoutte PM (1999). Endothelial dysfunction: from physiology to therapy. *J. Mol. Cell. Cardiol.* **31**(1)**:** 61-74.

Montezano AC, Burger D, Paravicini TM, Chignalia AZ, Yusuf H, Almasri M, *et al.* (2010). Nicotinamide adenine dinucleotide phosphate reduced oxidase 5 (Nox5) regulation by angiotensin II and endothelin-1 is mediated via calcium/calmodulin-dependent, rac-1-independent pathways in human endothelial cells. *Circ Res* **106**(8)**:** 1363-1373.

Montezano AC, Nguyen Dinh Cat A, Rios FJ, Touyz RM (2014). Angiotensin II and vascular injury. *Curr. Hypertens. Rep.* **16**(6)**:** 431.

Moore KJ, Tabas I (2011). Macrophages in the pathogenesis of atherosclerosis. *Cell* **145**(3)**:** 341-355.

Moraes LA, Piqueras L, Bishop-Bailey D (2006). Peroxisome proliferator-activated receptors and inflammation. *Pharmacol Ther* **110**(3)**:** 371-385.

Mortaz E, Lazar Z, Koenderman L, Kraneveld AD, Nijkamp FP, Folkerts G (2009). Cigarette smoke attenuates the production of cytokines by human plasmacytoid dendritic cells and enhances the release of IL-8 in response to TLR-9 stimulation. *Respir. Res.* **10:** 47.

Moser B, Wolf M, Walz A, Loetscher P (2004). Chemokines: multiple levels of leukocyte migration control. *Trends Immunol* **25**(2)**:** 75-84.

Mozaffarian D, Benjamin EJ, Go AS, Arnett DK, Blaha MJ, Cushman M, *et al.* (2016). Executive Summary: Heart Disease and Stroke Statistics-2016 Update: A Report From the American Heart Association. *Circulation* **133**(4)**:** 447-454.

Mueller R, Chanez P, Campbell AM, Bousquet J, Heusser C, Bullock GR (1996). Different cytokine patterns in bronchial biopsies in asthma and chronic bronchitis. *Respir. Med.* **90**(2)**:** 79-85.

Murdoch CE, Chaubey S, Zeng L, Yu B, Ivetic A, Walker SJ, *et al.* (2014). Endothelial NADPH oxidase-2 promotes interstitial cardiac fibrosis and diastolic dysfunction through proinflammatory effects and endothelial-mesenchymal transition. *J Am Coll Cardiol* **63**(24)**:** 2734-2741.

Nabah YN, Mateo T, Estelles R, Mata M, Zagorski J, Sarau H, *et al.* (2004). Angiotensin II induces neutrophil accumulation in vivo through generation and release of CXC chemokines. *Circulation* **110**(23)**:** 3581-3586.

Nakayama T, Hieshima K, Izawa D, Tatsumi Y, Kanamaru A, Yoshie O (2003). Cutting edge: profile of chemokine receptor expression on human plasma cells accounts for their efficient recruitment to target tissues. *J Immunol* **170**(3)**:** 1136-1140.

Nedeljkovic ZS, Gokce N, Loscalzo J (2003). Mechanisms of oxidative stress and vascular dysfunction. *Postgrad. Med. J.* **79**(930)**:** 195-199; quiz 198-200.

Nguyen Dinh Cat A, Montezano AC, Burger D, Touyz RM (2013). Angiotensin II, NADPH oxidase, and redox signaling in the vasculature. *Antioxid Redox Signal* **19**(10)**:** 1110-1120.

Nickenig G, Murphy TJ (1996). Enhanced angiotensin receptor type 1 mRNA degradation and induction of polyribosomal mRNA binding proteins by angiotensin II in vascular smooth muscle cells. *Mol Pharmacol* **50**(4)**:** 743-751.

Nishibe T, Dardik A, Kondo Y, Kudo F, Muto A, Nishi M, *et al.* (2010). Expression and localization of vascular endothelial growth factor in normal abdominal aorta and abdominal aortic aneurysm. *Int Angiol* **29**(3)**:** 260-265.

Niu J, Azfer A, Zhelyabovska O, Fatma S, Kolattukudy PE (2008). Monocyte chemotactic protein (MCP)-1 promotes angiogenesis via a novel transcription factor, MCP-1-induced protein (MCPIP). *Journal of Biological Chemistry* **283**(21)**:** 14542-14551.

Noel AA, Gloviczki P, Cherry Jr KJ, Bower TC, Panneton JM, Mozes GI, *et al.* (2001). Ruptured abdominal aortic aneurysms: the excessive mortality rate of conventional repair. *Journal of vascular surgery* **34**(1)**:** 41-46.

Noguera A, Batle S, Miralles C, Iglesias J, Busquets X, MacNee W, *et al.* (2001). Enhanced neutrophil response in chronic obstructive pulmonary disease. *Thorax* **56**(6)**:** 432-437.

Oro C, Qian H, Thomas WG (2007). Type 1 angiotensin receptor pharmacology: signaling beyond G proteins. *Pharmacol Ther* **113**(1)**:** 210-226.

Orosz Z, Csiszar A, Labinskyy N, Smith K, Kaminski PM, Ferdinandy P, *et al.* (2007). Cigarette smoke-induced proinflammatory alterations in the endothelial phenotype: role

of NAD(P)H oxidase activation. *American journal of physiology. Heart and circulatory physiology* **292**(1)**:** H130-139.

Oyekan A (2011). PPARs and their effects on the cardiovascular system. *Clin. Exp. Hypertens.* **33**(5)**:** 287-293.

Page C, Pitchford S (2013). Neutrophil and platelet complexes and their relevance to neutrophil recruitment and activation. *International immunopharmacology* **17**(4)**:** 1176-1184.

Paintlia AS, Paintlia MK, Singh AK, Singh I (2013). Modulation of Rho-Rock signaling pathway protects oligodendrocytes against cytokine toxicity via PPAR-alpha-dependent mechanism. *Glia* **61**(9)**:** 1500-1517.

Panigrahy D, Kaipainen A, Huang S, Butterfield CE, Barnes CM, Fannon M, *et al.* (2008). PPARalpha agonist fenofibrate suppresses tumor growth through direct and indirect angiogenesis inhibition. *Proc. Natl. Acad. Sci. U. S. A.* **105**(3)**:** 985-990.

Paoletti R, Gotto AM, Jr., Hajjar DP (2004). Inflammation in atherosclerosis and implications for therapy. *Circulation* **109**(23 Suppl 1)**:** III20-26.

Park HJ, Kong D, Iruela-Arispe L, Begley U, Tang D, Galper JB (2002). 3-hydroxy-3-methylglutaryl coenzyme A reductase inhibitors interfere with angiogenesis by inhibiting the geranylgeranylation of RhoA. *Circ Res* **91**(2)**:** 143-150.

Pastore L, Tessitore A, Martinotti S, Toniato E, Alesse E, Bravi MC, *et al.* (1999). Angiotensin II stimulates intercellular adhesion molecule-1 (ICAM-1) expression by human vascular endothelial cells and increases soluble ICAM-1 release in vivo. *Circulation* **100**(15)**:** 1646-1652.

Patterson KA, Zhang X, Wrobleski SK, Hawley AE, Lawrence DA, Wakefield TW, *et al.* (2013). Rosuvastatin reduced deep vein thrombosis in ApoE gene deleted mice with hyperlipidemia through non-lipid lowering effects. *Thromb Res* **131**(3)**:** 268-276.

Peiro C, Vallejo S, Gembardt F, Palacios E, Novella S, Azcutia V, *et al.* (2013). Complete blockade of the vasorelaxant effects of angiotensin-(1-7) and bradykinin in murine microvessels by antagonists of the receptor Mas. *J Physiol.* **591(Pt 9):** 2275-2285.

Pellegrini MP, Newby DE, Maxwell S, Webb DJ (2001). Short-term effects of transdermal nicotine on acute tissue plasminogen activator release in vivo in man. *Cardiovascular research* **52**(2)**:** 321-327.

Pendyala S, Usatyuk PV, Gorshkova IA, Garcia JGN, Natarajan V (2009). Regulation of NADPH oxidase in vascular endothelium: the role of phospholipases, protein kinases, and cytoskeletal proteins. *Antioxid Redox Signal* **11**(4)**:** 841-860.

Peng SX, Rockafellow BA, Skedzielewski TM, Huebert ND, Hageman W (2009). Improved pharmacokinetic and bioavailability support of drug discovery using serial blood sampling in mice. *J Pharm Sci* **98**(5)**:** 1877-1884.

Penn A, Snyder C (1988). Arteriosclerotic plaque development is 'promoted' by polynuclear aromatic hydrocarbons. *Carcinogenesis* **9**(12)**:** 2185-2189.

Perez-Amodio S, Tra WM, Rakhorst HA, Hovius SE, van Neck JW (2011). Hypoxia preconditioning of tissue-engineered mucosa enhances its angiogenic capacity in vitro. *Tissue engineering. Part A* **17**(11-12)**:** 1583-1593.

Petrescu F, Voican SC, Silosi I (2010). Tumor necrosis factor-alpha serum levels in healthy smokers and nonsmokers. *Int. J. Chron. Obstruct. Pulmon. Dis.* **5:** 217-222.

Phillipson M, Kubes P (2011). The neutrophil in vascular inflammation. *Nature medicine* **17**(11)**:** 1381-1390.

Piqueras L, Kubes P, Alvarez A, O'Connor E, Issekutz AC, Esplugues JV, *et al.* (2000). Angiotensin II induces leukocyte-endothelial cell interactions in vivo via AT(1) and AT(2) receptor-mediated P-selectin upregulation. *Circulation* **102**(17)**:** 2118-2123.

Piqueras L, Reynolds AR, Hodivala-Dilke KM, Alfranca A, Redondo JM, Hatae T, *et al.* (2007). Activation of PPARbeta/delta induces endothelial cell proliferation and angiogenesis. *Arterioscler Thromb Vasc Biol* **27**(1)**:** 63-69.

Piqueras L, Sanz MJ, Perretti M, Morcillo E, Norling L, Mitchell JA, *et al.* (2009). Activation of PPARbeta/delta inhibits leukocyte recruitment, cell adhesion molecule expression, and chemokine release. *J Leukoc Biol* **86**(1)**:** 115-122.

Plutzky J (2011). The PPAR-RXR transcriptional complex in the vasculature: energy in the balance. *Circ Res* **108**(8)**:** 1002-1016.

Polianova MT, Ruscetti FW, Pert CB, Ruff MR (2005). Chemokine receptor-5 (CCR5) is a receptor for the HIV entry inhibitor peptide T (DAPTA). *Antiviral Res* **67**(2)**:** 83-92.

Pozzi A, Ibanez MR, Gatica AE, Yang S, Wei S, Mei S, *et al.* (2007). Peroxisomal proliferator-activated receptor-alpha-dependent inhibition of endothelial cell proliferation and tumorigenesis. *J. Biol. Chem.* **282**(24)**:** 17685-17695.

Pratheeshkumar P, Budhraja A, Son Y-O, Wang X, Zhang Z, Ding S, *et al.* (2012). Quercetin inhibits angiogenesis mediated human prostate tumor growth by targeting VEGFR-2 regulated AKT/mTOR/P70S6K signaling pathways. *PloS one* **7**(10)**:** e47516.

Pueyo ME, Gonzalez W, Nicoletti A, Savoie F, Arnal JF, Michel JB (2000). Angiotensin II stimulates endothelial vascular cell adhesion molecule-1 via nuclear factor-kappaB activation induced by intracellular oxidative stress. *Arterioscler Thromb Vasc Biol* **20**(3)**:** 645-651.

Ramirez SH, Heilman D, Morsey B, Potula R, Haorah J, Persidsky Y (2008). Activation of peroxisome proliferator-activated receptor gamma (PPARgamma) suppresses Rho GTPases in human brain microvascular endothelial cells and inhibits adhesion and transendothelial migration of HIV-1 infected monocytes. *J Immunol* **180**(3)**:** 1854-1865.

Rashid M, Tawara S, Fukumoto Y, Seto M, Yano K, Shimokawa H (2009). Importance of Rac1 signaling pathway inhibition in the pleiotropic effects of HMG-CoA reductase inhibitors. *Circ J* **73**(2)**:** 361-370.

Ray R, Shah AM (2005). NADPH oxidase and endothelial cell function. *Clin Sci (Lond)* **109**(3)**:** 217-226.

Rezaie-Majd A, Maca T, Bucek RA, Valent P, Muller MR, Husslein P, *et al.* (2002). Simvastatin reduces expression of cytokines interleukin-6, interleukin-8, and monocyte chemoattractant protein-1 in circulating monocytes from hypercholesterolemic patients. *Arterioscler Thromb Vasc Biol* **22**(7)**:** 1194-1199.

Riambau V, Guerrero F, Montañá X, Gilabert R (2007). Aneurisma de aorta abdominal y enfermedad vascular renal. *Revista Española de Cardiología* **60**(6)**:** 639-654.

Richmond A (2002). Nf-kappa B, chemokine gene transcription and tumour growth. *Nat Rev Immunol* **2**(9)**:** 664-674.

Ridker PM, Danielson E, Fonseca FA, Genest J, Gotto AM, Jr., Kastelein JJ, *et al.* (2008). Rosuvastatin to prevent vascular events in men and women with elevated C-reactive protein. *N Engl J Med* **359**(21)**:** 2195-2207.

Rikitake Y, Kawashima S, Takeshita S, Yamashita T, Azumi H, Yasuhara M, *et al.* (2001). Anti-oxidative properties of fluvastatin, an HMG-CoA reductase inhibitor, contribute to prevention of atherosclerosis in cholesterol-fed rabbits. *Atherosclerosis* **154**(1)**:** 87-96.

Rius C, Abu-Taha M, Hermenegildo C, Piqueras L, Cerda-Nicolas JM, Issekutz AC, *et al.* (2010). Trans- but not cis-resveratrol impairs angiotensin-II-mediated vascular inflammation through inhibition of NF-kappaB activation and peroxisome proliferator-activated receptor-gamma upregulation. *J Immunol* **185**(6)**:** 3718-3727.

Rius C, Company C, Piqueras L, Cerda-Nicolas JM, Gonzalez C, Servera E, *et al.* (2013a). Critical role of fractalkine (CX3CL1) in cigarette smoke-induced mononuclear cell adhesion to the arterial endothelium. *Thorax* **68**(2)**:** 177-186.

Rius C, Piqueras L, Gonzalez-Navarro H, Albertos F, Company C, Lopez-Gines C, *et al.* (2013b). Arterial and venous endothelia display differential functional fractalkine (CX3CL1) expression by angiotensin-II. *Arterioscler Thromb Vasc Biol* **33**(1)**:** 96-9104.

Ross R (1993). The pathogenesis of atherosclerosis: a perspective for the 1990s. *Nature* **362**(6423)**:** 801-809.

Ross R (1999). Atherosclerosis--an inflammatory disease. *N Engl J Med* **340**(2)**:** 115-126.

Ruberg FL, Loscalzo J (2002). Prothrombotic determinants of coronary atherothrombosis. *Vasc. Med.* **7**(4)**:** 289-299.

Ruiz-Ortega M, Lorenzo O, Suzuki Y, Ruperez M, Egido J (2001). Proinflammatory actions of angiotensins. *Curr. Opin. Nephrol. Hypertens.* **10**(3)**:** 321-329.

Sabroe I, Peck MJ, Van Keulen BJ, Jorritsma A, Simmons G, Clapham PR, *et al.* (2000). A small molecule antagonist of chemokine receptors CCR1 and CCR3. Potent inhibition of eosinophil function and CCR3-mediated HIV-1 entry. *J Biol Chem* **275**(34)**:** 25985-25992.

Sakalihasan N, Limet R, Defawe O (2005). Abdominal aortic aneurysm. *The Lancet* **365**(9470)**:** 1577-1589.

Sallusto F, Baggiolini M (2008). Chemokines and leukocyte traffic. *Nature immunology* **9**(9)**:** 949-952.

Sanz MJ, Albertos F, Otero E, Juez M, Morcillo EJ, Piqueras L (2012). Retinoid X receptor agonists impair arterial mononuclear cell recruitment through peroxisome proliferator-activated receptor-gamma activation. *J Immunol* **189**(1)**:** 411-424.

Satou R, Gonzalez-Villalobos RA, Miyata K, Ohashi N, Katsurada A, Navar LG, *et al.* (2008). Costimulation with angiotensin II and interleukin 6 augments angiotensinogen expression in cultured human renal proximal tubular cells. *Am. J. Physiol. Renal Physiol.* **295**(1)**:** F283-289.

Scalia R, Gong Y, Berzins B, Freund B, Feather D, Landesberg G, *et al.* (2011). A novel role for calpain in the endothelial dysfunction induced by activation of angiotensin II type 1 receptor signaling. *Circ Res* **108**(9)**:** 1102-1111.

Scarisbrick JJ, Morris S, Azurdia R, Illidge T, Parry E, Graham-Brown R, *et al.* (2013). U.K. consensus statement on safe clinical prescribing of bexarotene for patients with cutaneous T-cell lymphoma. *Br J Dermatol* **168**(1)**:** 192-200.

Schnell CR, Stauffer F, Allegrini PR, O'Reilly T, McSheehy PM, Dartois C, *et al.* (2008). Effects of the dual phosphatidylinositol 3-kinase/mammalian target of rapamycin inhibitor NVP-BEZ235 on the tumor vasculature: implications for clinical imaging. *Cancer research* **68**(16)**:** 6598-6607.

Schouten O, van Laanen JH, Boersma E, Vidakovic R, Feringa HH, Dunkelgrun M, *et al.* (2006). Statins are associated with a reduced infrarenal abdominal aortic aneurysm growth. *European journal of vascular and endovascular surgery : the official journal of the European Society for Vascular Surgery* **32**(1)**:** 21-26.

Schulte A, Schulz B, Andrzejewski MG, Hundhausen C, Mletzko S, Achilles J, *et al.* (2007). Sequential processing of the transmembrane chemokines CX3CL1 and CXCL16 by alpha- and gamma-secretases. *Biochem. Biophys. Res. Commun.* **358**(1)**:** 233-240.

Schulz C, Schafer A, Stolla M, Kerstan S, Lorenz M, von Bruhl ML, *et al.* (2007). Chemokine fractalkine mediates leukocyte recruitment to inflammatory endothelial cells in flowing whole blood: a critical role for P-selectin expressed on activated platelets. *Circulation* **116**(7)**:** 764-773.

Schwarz MK, Wells TN (2002). New therapeutics that modulate chemokine networks. *Nat Rev Drug Discov* **1**(5)**:** 347-358.

Seizer P, Stellos K, Selhorst G, Kramer BF, Lang MR, Gawaz M, *et al.* (2011). CXCL16 is a novel scavenger receptor on platelets and is associated with acute coronary syndrome. *Thromb Haemost* **105**(6)**:** 1112-1114.

Sharvit E, Abramovitch S, Reif S, Bruck R (2013). Amplified inhibition of stellate cell activation pathways by PPAR-gamma, RAR and RXR agonists. *PLoS One* **8**(10)**:** e76541.

Shatanawi A, Romero MJ, Iddings JA, Chandra S, Umapathy NS, Verin AD, *et al.* (2011). Angiotensin II-induced vascular endothelial dysfunction through RhoA/Rho kinase/p38 mitogen-activated protein kinase/arginase pathway. *Am J Physiol Cell Physiol* **300**(5)**:** C1181-1192.

Shen Y, Rattan V, Sultana C, Kalra VK (1996). Cigarette smoke condensate-induced adhesion molecule expression and transendothelial migration of monocytes. *Am. J. Physiol.* **270**(5 Pt 2)**:** H1624-1633.

Shimada K, Yazaki Y (1978). Binding sites for angiotensin II in human mononuclear leucocytes. *Journal of biochemistry* **84**(4)**:** 1013-1015.

Shimaoka T, Kume N, Minami M, Hayashida K, Kataoka H, Kita T, *et al.* (2000). Molecular cloning of a novel scavenger receptor for oxidized low density lipoprotein, SR-PSOX, on macrophages. *J. Biol. Chem.* **275**(52)**:** 40663-40666.

Shimaoka T, Nakayama T, Fukumoto N, Kume N, Takahashi S, Yamaguchi J, *et al.* (2004). Cell surface-anchored SR-PSOX/CXC chemokine ligand 16 mediates firm adhesion of CXC chemokine receptor 6-expressing cells. *J Leukoc Biol* **75**(2)**:** 267-274.

Sin DD, Leung R, Gan WQ, Man SP (2007). Circulating surfactant protein D as a potential lung-specific biomarker of health outcomes in COPD: a pilot study. *BMC Pulm. Med.* **7:** 13.

Sinden NJ, Stockley RA (2010). Systemic inflammation and comorbidity in COPD: a result of 'overspill' of inflammatory mediators from the lungs? Review of the evidence. *Thorax* **65**(10)**:** 930-936.

Singh RB, Mengi SA, Xu YJ, Arneja AS, Dhalla NS (2002). Pathogenesis of atherosclerosis: A multifactorial process. *Exp. Clin. Cardiol.* **7**(1)**:** 40-53.

Smith CJ, Fischer TH (2001). Particulate and vapor phase constituents of cigarette mainstream smoke and risk of myocardial infarction. *Atherosclerosis* **158**(2)**:** 257-267.

Smith MC, Wrobel JP (2014). Epidemiology and clinical impact of major comorbidities in patients with COPD. *Int J Chron Obstruct Pulmon Dis* **9:** 871-888.

Soran H, Durrington P (2008). Rosuvastatin: efficacy, safety and clinical effectiveness. *Expert Opin Pharmacother* **9**(12)**:** 2145-2160.

Springer TA (1990). Adhesion receptors of the immune system. *Nature* **346**(6283)**:** 425-434.

Springer TA (1994). Traffic signals for lymphocyte recirculation and leukocyte emigration: the multistep paradigm. *Cell* **76**(2)**:** 301-314.

Staels B, Koenig W, Habib A, Merval R, Lebret M, Torra IP, *et al.* (1998). Activation of human aortic smooth-muscle cells is inhibited by PPARalpha but not by PPARgamma activators. *Nature* **393**(6687)**:** 790-793.

Stalker TJ, Lefer AM, Scalia R (2001). A new HMG-CoA reductase inhibitor, rosuvastatin, exerts anti-inflammatory effects on the microvascular endothelium: the role of mevalonic acid. *Br J Pharmacol* **133**(3)**:** 406-412.

Stolle K, Berges A, Lietz M, Lebrun S, Wallerath T (2010). Cigarette smoke enhances abdominal aortic aneurysm formation in angiotensin II-treated apolipoprotein E-deficient mice. *Toxicol. Lett.* **199**(3)**:** 403-409.

Streb JW, Miano JM (2003). Retinoids: pleiotropic agents of therapy for vascular diseases? *Curr Drug Targets Cardiovasc Haematol Disord* **3**(1)**:** 31-57.

Stuck BJ, Lenski M, Bohm M, Laufs U (2008). Metabolic switch and hypertrophy of cardiomyocytes following treatment with angiotensin II are prevented by AMP-activated protein kinase. *J Biol Chem* **283**(47)**:** 32562-32569.

Suffee N, Hlawaty H, Meddahi-Pelle A, Maillard L, Louedec L, Haddad O, *et al.* (2012a). RANTES/CCL5-induced pro-angiogenic effects depend on CCR1, CCR5 and glycosaminoglycans. *Angiogenesis* **15**(4)**:** 727-744.

Suffee N, Hlawaty H, Meddahi-Pelle A, Maillard L, Louedec L, Haddad O, *et al.* (2012b). RANTES/CCL5-induced pro-angiogenic effects depend on CCR1, CCR5 and glycosaminoglycans. *Angiogenesis* **15**(4)**:** 727-744.

Sullivan GW, Lee DD, Ross WG, DiVietro JA, Lappas CM, Lawrence MB, *et al.* (2004). Activation of A2A adenosine receptors inhibits expression of alpha 4/beta 1 integrin (very late antigen-4) on stimulated human neutrophils. *J Leukoc Biol* **75**(1)**:** 127-134.

Sun YP, Zhu BQ, Browne AE, Sievers RE, Bekker JM, Chatterjee K, *et al.* (2001). Nicotine does not influence arterial lipid deposits in rabbits exposed to second-hand smoke. *Circulation* **104**(7)**:** 810-814.

Sunderkötter C, Steinbrink K, Goebeler M, Bhardwaj R, Sorg C (1994). Macrophages and angiogenesis. *Journal of leukocyte biology* **55**(3)**:** 410-422.

Swirski FK, Nahrendorf M (2013). Leukocyte behavior in atherosclerosis, myocardial infarction, and heart failure. *Science* **339**(6116)**:** 161-166.

Szanto A, Narkar V, Shen Q, Uray IP, Davies PJ, Nagy L (2004). Retinoid X receptors: X-ploring their (patho)physiological functions. *Cell Death Differ* **11 Suppl 2:** S126-143.

Tabas I (2007). Apoptosis and efferocytosis in mouse models of atherosclerosis. *Curr. Drug Targets* **8**(12)**:** 1288-1296.

Tahergorabi Z, Khazaei M (2012). A review on angiogenesis and its assays. *Iranian journal of basic medical sciences* **15**(6)**:** 1110.

Takahashi H, Ogata H, Nishigaki R, Broide DH, Karin M (2010). Tobacco smoke promotes lung tumorigenesis by triggering IKKbeta- and JNK1-dependent inflammation. *Cancer cell* **17**(1)**:** 89-97.

Takemoto M, Liao JK (2001). Pleiotropic effects of 3-hydroxy-3-methylglutaryl coenzyme a reductase inhibitors. *Arterioscler Thromb Vasc Biol* **21**(11)**:** 1712-1719.

Tamarat R, Silvestre JS, Durie M, Levy BI (2002). Angiotensin II angiogenic effect in vivo involves vascular endothelial growth factor- and inflammation-related pathways. *Lab Invest* **82**(6)**:** 747-756.

Taniyama Y, Ushio-Fukai M, Hitomi H, Rocic P, Kingsley MJ, Pfahnl C, *et al.* (2004). Role of p38 MAPK and MAPKAPK-2 in angiotensin II-induced Akt activation in vascular smooth muscle cells. *Am. J. Physiol. Cell Physiol.* **287**(2)**:** C494-499.

Teoh CM, Tan SS, Tran T (2015). Integrins as Therapeutic Targets for Respiratory Diseases. *Current molecular medicine* **15**(8)**:** 714-734.

Teupser D, Pavlides S, Tan M, Gutierrez-Ramos JC, Kolbeck R, Breslow JL (2004). Major reduction of atherosclerosis in fractalkine (CX3CL1)-deficient mice is at the brachiocephalic artery, not the aortic root. *Proceedings of the National Academy of Sciences of the United States of America* **101**(51)**:** 17795-17800.

Thompson M, Jones L, Nasim A, Sayers R, Bell P (1996). Angiogenesis in abdominal aortic aneurysms. *European journal of vascular and endovascular surgery* **11**(4)**:** 464-469.

Tousoulis D, Andreou I, Tsiatas M, Miliou A, Tentolouris C, Siasos G, *et al.* (2011). Effects of rosuvastatin and allopurinol on circulating endothelial progenitor cells in patients with congestive heart failure: the impact of inflammatory process and oxidative stress. *Atherosclerosis* **214**(1)**:** 151-157.

Touyz RM, Briones AM, Sedeek M, Burger D, Montezano AC (2011). NOX isoforms and reactive oxygen species in vascular health. *Mol Interv* **11**(1)**:** 27-35.

Touyz RM, Schiffrin EL (2000). Signal transduction mechanisms mediating the physiological and pathophysiological actions of angiotensin II in vascular smooth muscle cells. *Pharmacol. Rev.* **52**(4)**:** 639-672.

Tracy RP, Psaty BM, Macy E, Bovill EG, Cushman M, Cornell ES, *et al.* (1997). Lifetime smoking exposure affects the association of C-reactive protein with cardiovascular disease risk factors and subclinical disease in healthy elderly subjects. *Arterioscler Thromb Vasc Biol* **17**(10)**:** 2167-2176.

Trivedi HK, Patel MC (2012). Development and Validation of a Stability-Indicating RP-UPLC Method for Determination of Rosuvastatin and Related Substances in Pharmaceutical Dosage Form. *Sci Pharm* **80**(2)**:** 393-406.

Tummala PE, Chen XL, Sundell CL, Laursen JB, Hammes CP, Alexander RW, *et al.* (1999). Angiotensin II induces vascular cell adhesion molecule-1 expression in rat vasculature: A potential link between the renin-angiotensin system and atherosclerosis. *Circulation* **100**(11)**:** 1223-1229.

Ulbrich H, Eriksson EE, Lindbom L (2003). Leukocyte and endothelial cell adhesion molecules as targets for therapeutic interventions in inflammatory disease. *Trends Pharmacol Sci* **24**(12)**:** 640-647.

Unger T, Chung O, Csikos T, Culman J, Gallinat S, Gohlke P, *et al.* (1996). Angiotensin receptors. *J Hypertens Suppl* **14**(5)**:** S95-103.

Vakeva L, Ranki A, Hahtola S (2012). Ten-year experience of bexarotene therapy for cutaneous T-cell lymphoma in Finland. *Acta Derm Venereol* **92**(3)**:** 258-263.

van der Voort R, Verweij V, de Witte TM, Lasonder E, Adema GJ, Dolstra H (2010). An alternatively spliced CXCL16 isoform expressed by dendritic cells is a secreted chemoattractant for CXCR6+ cells. *J. Leukoc. Biol.* **87**(6)**:** 1029-1039.

Varet J, Vincent L, Mirshahi P, Pille JV, Legrand E, Opolon P, *et al.* (2003). Fenofibrate inhibits angiogenesis in vitro and in vivo. *Cell Mol Life Sci* **60**(4)**:** 810-819.

Veillard NR, Braunersreuther V, Arnaud C, Burger F, Pelli G, Steffens S, *et al.* (2006). Simvastatin modulates chemokine and chemokine receptor expression by geranylgeranyl isoprenoid pathway in human endothelial cells and macrophages. *Atherosclerosis* **188**(1)**:** 51-58.

Vernooy JH, Kucukaycan M, Jacobs JA, Chavannes NH, Buurman WA, Dentener MA, *et al.* (2002). Local and systemic inflammation in patients with chronic obstructive pulmonary disease: soluble tumor necrosis factor receptors are increased in sputum. *Am. J. Respir. Crit. Care Med.* **166**(9)**:** 1218-1224.

Victorino GP, Newton CR, Curran B (2002). Effect of angiotensin II on microvascular permeability. *The Journal of surgical research* **104**(2)**:** 77-81.

Vidal-Puig AJ, Considine RV, Jimenez-Linan M, Werman A, Pories WJ, Caro JF, *et al.* (1997). Peroxisome proliferator-activated receptor gene expression in human tissues. Effects of obesity, weight loss, and regulation by insulin and glucocorticoids. *J Clin Invest* **99**(10)**:** 2416-2422.

Vijaynagar B, Bown MJ, Sayers RD, Choke E (2013). Potential role for anti-angiogenic therapy in abdominal aortic aneurysms. *European journal of clinical investigation* **43**(7)**:** 758-765.

Villar F, Pedro-Botet J, Vila R, Lahoz C (2013). Aneurisma aórtico. *Clínica e Investigación en Arteriosclerosis* **25**(5)**:** 224-230.

Volpe M, Savoia C, De Paolis P, Ostrowska B, Tarasi D, Rubattu S (2002). The renin-angiotensin system as a risk factor and therapeutic target for cardiovascular and renal disease. *J Am Soc Nephrol* **13 Suppl 3:** S173-178.

Wagner DD, Frenette PS (2008). The vessel wall and its interactions. *Blood* **111**(11)**:** 5271-5281.

Wagner JG, Roth RA (2000). Neutrophil migration mechanisms, with an emphasis on the pulmonary vasculature. *Pharmacological reviews* **52**(3)**:** 349-374.

Wang C, Qin L, Manes TD, Kirkiles-Smith NC, Tellides G, Pober JS (2014). Rapamycin antagonizes TNF induction of VCAM-1 on endothelial cells by inhibiting mTORC2. *J Exp Med* **211**(3)**:** 395-404.

Wang C, Tao W, Wang Y, Bikow J, Lu B, Keating A, *et al.* (2010). Rosuvastatin, identified from a zebrafish chemical genetic screen for antiangiogenic compounds, suppresses the growth of prostate cancer. *Eur Urol* **58**(3)**:** 418-426.

Wang D, Wang H, Guo Y, Ning W, Katkuri S, Wahli W, *et al.* (2006). Crosstalk between peroxisome proliferator-activated receptor delta and VEGF stimulates cancer progression. *Proc. Natl. Acad. Sci. U. S. A.* **103**(50)**:** 19069-19074.

Wang HB, Wang JT, Zhang L, Geng ZH, Xu WL, Xu T, *et al.* (2007). P-selectin primes leukocyte integrin activation during inflammation. *Nature immunology* **8**(8)**:** 882-892.

Wang JA, Chen WA, Wang Y, Zhang S, Bi H, Hong B, *et al.* (2011). Statins exert differential effects on angiotensin II-induced atherosclerosis, but no benefit for abdominal aortic aneurysms. *Atherosclerosis* **217**(1)**:** 90-96.

Wang Z, Dai H, Xing M, Yu Z, Lin X, Wang S, *et al.* (2013). Effect of a single high loading dose of rosuvastatin on percutaneous coronary intervention for acute coronary syndromes. *J Cardiovasc Pharmacol Ther* **18**(4)**:** 327-333.

Warnholtz A, Nickenig G, Schulz E, Macharzina R, Brasen JH, Skatchkov M, *et al.* (1999). Increased NADH-oxidase-mediated superoxide production in the early stages of atherosclerosis: evidence for involvement of the renin-angiotensin system. *Circulation* **99**(15)**:** 2027-2033.

Watanabe T, Barker TA, Berk BC (2005). Angiotensin II and the endothelium: diverse signals and effects. *Hypertension* **45**(2)**:** 163-169.

Weber C, Erl W, Weber K, Weber PC (1996). Increased adhesiveness of isolated monocytes to endothelium is prevented by vitamin C intake in smokers. *Circulation* **93**(8)**:** 1488-1492.

Weber C, Erl W, Weber KS, Weber PC (1997). HMG-CoA reductase inhibitors decrease CD11b expression and CD11b-dependent adhesion of monocytes to endothelium and reduce increased adhesiveness of monocytes isolated from patients with hypercholesterolemia. *J Am Coll Cardiol* **30**(5)**:** 1212-1217.

Weitz-Schmidt G, Welzenbach K, Brinkmann V, Kamata T, Kallen J, Bruns C, *et al.* (2001). Statins selectively inhibit leukocyte function antigen-1 by binding to a novel regulatory integrin site. *Nature medicine* **7**(6)**:** 687-692.

White JR, Lee JM, Young PR, Hertzberg RP, Jurewicz AJ, Chaikin MA, *et al.* (1998). Identification of a potent, selective non-peptide CXCR2 antagonist that inhibits interleukin-8-induced neutrophil migration. *J Biol Chem* **273**(17)**:** 10095-10098.

Wilbanks A, Zondlo SC, Murphy K, Mak S, Soler D, Langdon P, *et al.* (2001). Expression cloning of the STRL33/BONZO/TYMSTRligand reveals elements of CC, CXC, and CX3C chemokines. *J Immunol* **166**(8)**:** 5145-5154.

Willis LM, El-Remessy AB, Somanath PR, Deremer DL, Fagan SC (2011). Angiotensin receptor blockers and angiogenesis: clinical and experimental evidence. *Clin Sci (Lond)* **120**(8)**:** 307-319.

Wojcik BM, Wrobleski SK, Hawley AE, Wakefield TW, Myers DD, Jr., Diaz JA (2011). Interleukin-6: a potential target for post-thrombotic syndrome. *Ann Vasc Surg* **25**(2)**:** 229-239.

Wolf G, Ziyadeh FN, Thaiss F, Tomaszewski J, Caron RJ, Wenzel U, *et al.* (1997). Angiotensin II stimulates expression of the chemokine RANTES in rat glomerular endothelial cells. Role of the angiotensin type 2 receptor. *J Clin Invest* **100**(5)**:** 1047-1058.

Wuttge DM, Zhou X, Sheikine Y, Wagsater D, Stemme V, Hedin U, *et al.* (2004). CXCL16/SR-PSOX is an interferon-gamma-regulated chemokine and scavenger receptor expressed in atherosclerotic lesions. *Arterioscler Thromb Vasc Biol* **24**(4)**:** 750-755.

Xia Y, Entman ML, Wang Y (2013). Critical role of CXCL16 in hypertensive kidney injury and fibrosis. *Hypertension* **62**(6)**:** 1129-1137.

Xiao H, Qin X, Ping D, Zuo K (2013). Inhibition of Rho and Rac geranylgeranylation by atorvastatin is critical for preservation of endothelial junction integrity. *PLoS One* **8**(3)**:** e59233.

Xin X, Yang S, Kowalski J, Gerritsen ME (1999). Peroxisome proliferator-activated receptor gamma ligands are potent inhibitors of angiogenesis in vitro and in vivo. *J Biol Chem* **274**(13)**:** 9116-9121.

Yao L, Pan J, Setiadi H, Patel KD, McEver RP (1996). Interleukin 4 or oncostatin M induces a prolonged increase in P-selectin mRNA and protein in human endothelial cells. *J Exp Med* **184**(1)**:** 81-92.

Yen WC, Prudente RY, Corpuz MR, Negro-Vilar A, Lamph WW (2006). A selective retinoid X receptor agonist bexarotene (LGD1069, targretin) inhibits angiogenesis and metastasis in solid tumours. *Br J Cancer* **94**(5)**:** 654-660.

Yi G-w, Zeng Q-t, Mao X-b, Cheng M, Yang X-f, Liu H-t, *et al.* (2011). Overexpression of CXCL16 promotes a vulnerable plaque phenotype in Apolipoprotein E-Knockout Mice. *Cytokine* **53**(3)**:** 320-326.

Yoshizumi M, Abe J, Tsuchiya K, Berk BC, Tamaki T (2003). Stress and vascular responses: atheroprotective effect of laminar fluid shear stress in endothelial cells: possible role of mitogen-activated protein kinases. *J. Pharmacol. Sci.* **91**(3)**:** 172-176.

Zeng M, Yan H, Chen Y, Zhao H-J, Lv Y, Liu C, *et al.* (2012). Suppression of NF-κB reduces myocardial no-reflow. *PloS one* **7**(10).

Zernecke A, Weber C Chemokines in the vascular inflammatory response of atherosclerosis. *Cardiovasc Res* **86**(2)**:** 192-201.

Zhang Y, Naggar JC, Welzig CM, Beasley D, Moulton KS, Park HJ, *et al.* (2009). Simvastatin inhibits angiotensin II-induced abdominal aortic aneurysm formation in apolipoprotein E-knockout mice: possible role of ERK. *Arterioscler Thromb Vasc Biol* **29**(11)**:** 1764-1771.

Zhuge X, Murayama T, Arai H, Yamauchi R, Tanaka M, Shimaoka T, *et al.* (2005). CXCL16 is a novel angiogenic factor for human umbilical vein endothelial cells. *Biochemical and biophysical research communications* **331**(4)**:** 1295-1300.